

NATIONAL CENTRE FOR NUCLEAR RESEARCH

DOCTORAL THESIS

Relativistic Hydrodynamics Beyond the Second Order

Author:

Viktor SVENSSON 

Supervisor:

dr hab. Michał P. HELLER 

*A thesis submitted in fulfillment of the requirements
for the degree of Doctor of Physical Sciences*

at the

National Centre for Nuclear Research



NATIONAL
CENTRE
FOR NUCLEAR
RESEARCH
ŚWIERK

June 14, 2021

NATIONAL CENTRE FOR NUCLEAR RESEARCH

Abstract

Relativistic Hydrodynamics Beyond the Second Order

VIKTOR SVENSSON

Relativistic hydrodynamics is a theory of close to equilibrium dynamics, but exactly what sets the limit of its applicability is not known. In both experiment and theoretical modeling of heavy-ion collisions it has been observed that a hydrodynamic description can work surprisingly far from equilibrium. This thesis concerns two different approaches towards understanding the limits of hydrodynamics: constitutive relations at large order and far from equilibrium. Gradient expanded constitutive relations often diverge, and we contribute towards understanding how and why they do so. The interplay between hydrodynamic and nonhydrodynamic modes plays a central role. Far from equilibrium, constitutive relations can emerge in the form of hydrodynamic attractors. We present a novel perspective on attractors, based on quantifying the associated information loss and universality.

NATIONAL CENTRE FOR NUCLEAR RESEARCH

Streszczenie

Relativistic Hydrodynamics Beyond the Second Order

Hydrodynamika Relatywistyczna w Rzędach Wyższych niż Drugi

Viktor SVENSSON

Hydrodynamika relatywistyczna ma za zadanie opisać dynamikę klasy układów fizycznych lokalnie bliskich równowadze, ale dokładne warunki jej stosowalności pozostają otwartym problemem. W badaniach nad zderzeniami jąder atomowych przy ultrarelatywistycznych energiach zaobserwowano, że opis w języku hydrodynamiki relatywistycznej może po krótkim czasie zaskakująco dobrze opisywać wynik zderzenia, mimo, że układ fizyczny jest ciągle bardzo daleki od lokalnej równowagi termodynamicznej. Niniejsza praca doktorska rozwija dwa komplementarne podejścia do zrozumienia co ogranicza stosowalność opisu hydrodynamicznego. Pierwsze podejście dotyczy zachowania hydrodynamicznego rozwinięcia gradientowego w wysokich rzędach, które w znaczącej większości znanych do tej pory przypadków jest rozbieżne. Badania zawarte w pracy doktorskiej dostarczają lepszego zrozumienia tego zachowania, do czego kluczowy okazał się związek między hydrodynamicznymi i niehydrodynamicznymi stopniami swobody. Drugie rozwinięte podejście dotyczy atraktorów hydrodynamicznych, które są aktualnym tematem badawczym dotyczącym nierównowagowej definicji hydrodynamiki. Niniejsza praca doktorska dostarcza nowego spojrzenia na atraktory hydrodynamiczne, które bazuje na ilościowym ujęciu efektywnej utraty informacji o stanie początkowym i wynikających z tego uniwersalnych własnościach dynamiki układu.

Acknowledgements

First I would like to thank my supervisor, Michał Heller, for continuously encouraging me to take on new challenges and without whom this thesis would not have been possible. Thanks to the National Centre for Nuclear Research, and in particular Michał Spaliński, for this opportunity and for support during this research. The research in this thesis is a highly collaborative effort, and I'm indebted to all my coauthors for their knowledge, hard work and insightful discussions. Thanks to Albin and Artur for making the office a great place to be.

I want to thank the Albert Einstein Institute, especially Anika, for their hospitality during my frequent visits to Potsdam. Thanks to the whole Gravity, Quantum Fields and Information group for all the stimulating discussions, and special thanks to my fellow PhD students Hugo and Johannes.

My gratitude to everyone, including friends and family, who have helped me along the way. Special thanks to Ellen for her invaluable support. Lastly I would like to thank budget airlines for keeping us connected.

Contents

Abstract	i
Streszczenie	ii
Acknowledgements	iii
List of Figures	vi
List of Abbreviations	vii
Conventions	vii
1 Introduction	1
2 QGP and its descriptions	3
2.1 Bjorken flow	4
2.2 Kinetic theory	5
2.3 AdS/CFT	6
3 Hydrodynamics and the gradient expansion	7
3.1 When do constitutive relations emerge?	8
4 Linear response and modes	9
4.1 Modes in different theories	10
4.2 Analytic structure of modes	11
4.3 Back to coordinate space	12
5 Dealing with asymptotic series	14
5.1 Borel summation	14
5.2 Transseries and resurgence	15
5.3 Spacetime transseries	16
6 Gradient expansion beyond linearity	18
6.1 Subtleties in RTA	18
7 The hydrodynamic attractor	21
7.1 Information loss and slow roll	22
7.2 Towards more complicated flows	22
8 Summary	24
8.1 Article summaries	24
8.2 Open questions	26
Bibliography	27

A Hydrodynamization in kinetic theory: Transient modes and the gradient expansion	40
B How does relativistic kinetic theory remember about initial conditions?	46
C Hydrodynamic Attractors in Phase Space	57
D Transseries for causal diffusive systems	67
E Convergence of hydrodynamic modes: insights from kinetic theory and holography	105
F The hydrodynamic gradient expansion in linear response theory	129

List of Figures

2.1	Schematic diagram of a heavy-ion collision, see [41] for a review. Several different frameworks are used to model the evolution, covering different parameter regimes. The main focus of this thesis is how hydrodynamics emerges from kinetic theory or holography.	4
4.1	The structure of hydrodynamic and nonhydrodynamic modes in the sound channel in BRSSS [90], $\mathcal{N} = 4$ SYM [112] and RTA kinetic theory [11, 110]. The hydrodynamic sector is universal, but the nonhydrodynamic sector is not. They play an important role in the large order behaviour of the gradient expansion, both at the linear and nonlinear level.	11
6.1	The singularities of the Borel plane of the gradient expansion in conformal RTA. The singularities of the Padé approximant arrange to form branch cuts. The branch cut starting at $\xi = 3/2$ can be interpreted as coming from the nonhydrodynamic branch cut seen in linear response in Fig. 4.1. This follows the pattern of other models analyzed in a similar manner. However, the singularities which are not located on $\text{Im } \xi = 0$ are unphysical. This is an important cautionary lesson when studying the large order gradient expansion. Figure adapted from Article A.	19
7.1	Numerical solutions (blue) of BRSSS in Bjorken flow quickly converge to each other, implying a loss of information. In addition, the solutions end up in a region that can be characterized by the pullback attractor or slow roll approximation [14]. The mechanism controlling the convergence is different at early (expansion) and late times (interactions) [109].	21
7.2	The same model as in Fig 7.1, but viewed from the full phase space. The attractor shows up as a dimensional reduction from two to one dimension. It can be quantified by imposing a metric and using algorithms such as PCA. Figures from Article C.	23

List of Abbreviations

AdS	Anti de-Sitter
aHydro	anisotropic Hydrodynamics
BRSSS	Baier-Romatschke-Son-Starinets-Stephanov
CFT	Conformal Field Theory
CGC	Color Glass Condensate
HJSW	Heller-Janik-Spaliński-Witaszczyk
LHC	Large Hadron Collider
MIS	Müller-Israel-Stewart
ODE	Ordinary Differential Equation
PCA	Principal Component Analysis
PDE	Partial Differential Equation
QCD	Quantum Chromodynamics
QFT	Quantum Field Theory
QGP	Quark-Gluon Plasma
QNM	Quasinormal Mode
RHIC	Relativistic Heavy Ion Collider
RTA	Relaxation Time Approximation
SYM	Super Yang-Mills

Conventions

Throughout this thesis, natural units where $c = \hbar = G = k_B = 1$ are used as well as a mostly plus metric signature.

1 Introduction

Relativistic hydrodynamics was formulated a long time ago [8, 9] but remains at the forefront of several research areas today. It plays an important role in heavy-ion collisions, where it is used to describe the expanding quark-gluon plasma (QGP) [10, 11]. These experiments have inspired new developments in hydrodynamics [12], such as anisotropic hydrodynamics [13], attractors [14], and the incorporation of spin [15, 16]. There are applications in astrophysics [17, 18] and cosmology [19], which are stimulated by the advent of gravitational wave astronomy [20]. In condensed matter, electron flow in graphene can be modelled with relativistic hydrodynamics [21, 22].

At the same time as the applications of relativistic hydrodynamics continue to widen, a deeper understanding of its foundations is also being pursued. Other foundational questions currently being pursued and which are not covered in this thesis are hydrodynamical frames [23, 24], inclusion of fluctuations [25, 26], pole skipping [27–29], generalized hydrodynamics [30].

In this thesis, the main focus is on constitutive relations. These are central to a hydrodynamic formulation and they relate different components of the energy-momentum tensor to reduce the number of degrees of freedom. To understand where hydrodynamics applies, we need to understand the properties of constitutive relations and when they emerge. Close to equilibrium, these can be described with a perturbative expansion, the *gradient expansion*. Several of the papers in this thesis are devoted to the convergence properties of this series, which gives insights into when the expansion gives an accurate description of the underlying physics. In many cases, it is a divergent series and requires extra mathematical tools to make sense. Effective constitutive relations that reduce the number of degrees of freedom can also emerge without being described by a gradient expansion, which we refer to as a hydrodynamic attractor.

This is a cumulative thesis based on five published papers and one under review.

Published

- [1] Michal P. Heller, Aleksi Kurkela, Michał Spaliński, and Viktor Svensson. Hydrodynamization in Kinetic Theory: Transient Modes and the Gradient Expansion. In: *Physical Review D* 97.9 (May 31, 2018), p. 091503. DOI: [10.1103/PhysRevD.97.091503](https://doi.org/10.1103/PhysRevD.97.091503).
- [2] Michal P. Heller and Viktor Svensson. How Does Relativistic Kinetic Theory Remember about Initial Conditions? In: *Physical Review D* 98.5 (Sept. 17, 2018), p. 054016. DOI: [10.1103/PhysRevD.98.054016](https://doi.org/10.1103/PhysRevD.98.054016).
- [3] Michal P. Heller, Ro Jefferson, Michał Spaliński, and Viktor Svensson. Hydrodynamic Attractors in Phase Space. In: *Physical Review Letters* 125.13 (Sept. 22, 2020), p. 132301. DOI: [10.1103/PhysRevLett.125.132301](https://doi.org/10.1103/PhysRevLett.125.132301).
- [4] Michal P. Heller, Alexandre Serantes, Michał Spaliński, Viktor Svensson, and Benjamin Withers. Transseries for Causal Diffusive Systems. In: *Journal of High Energy Physics* 2021.4 (Apr. 20, 2021), p. 192. DOI: [10.1007/JHEP04\(2021\)192](https://doi.org/10.1007/JHEP04(2021)192).

- [5] Michal P. Heller, Alexandre Serantes, Michał Spaliński, Viktor Svensson, and Benjamin Withers. Convergence of Hydrodynamic Modes: Insights from Kinetic Theory and Holography. In: *SciPost Physics* 10.6 (June 1, 2021), p. 123. DOI: [10.21468/SciPostPhys.10.6.123](https://doi.org/10.21468/SciPostPhys.10.6.123).

Unpublished

- [6] Michal P. Heller, Alexandre Serantes, Michał Spaliński, Viktor Svensson, and Benjamin Withers. The Hydrodynamic Gradient Expansion in Linear Response Theory. July 10, 2020. URL: <https://arxiv.org/abs/2007.05524v1>.

These are reprinted in Sections [A](#), [B](#), [C](#), [D](#), [E](#) and [F](#). This guide is written in logical rather than chronological order and the lessons from the above papers are interspersed throughout the text. I have also been involved in studies of nonequilibrium physics with tensor networks [\[7\]](#), but it is outside the scope of this thesis.

In [Sec. 2](#), we describe some of the ingredients in the modeling of heavy-ion collisions, with an emphasis on those relevant for hydrodynamics. In [Sec. 3](#), we present the basics of relativistic hydrodynamics and the role of the gradient expansion. Linearized dynamics around thermal equilibrium is covered in [Sec. 4](#). We put a particular emphasis on the distinction and relation between hydrodynamic and nonhydrodynamic modes. The importance of the latter in regards to the applicability of hydrodynamics is one of the key lessons of the past decade. [Sec. 5](#) presents the mathematical tools for analyzing asymptotic series. [Sec. 6](#), concerns the gradient expansion beyond linear response, which shares some qualitative features with the linear case. The hydrodynamic attractor, a different approach to constitutive relations, is described in [Sec. 7](#). With the background material and context presented, [Sec. 8](#) contains summaries of this thesis, the articles included in it, as well as some open questions.

Throughout this thesis, we use natural units where $c = \hbar = G = k_B = 1$ and a mostly plus metric signature.

2 QGP and its descriptions

In the early 2000s, the Relativistic Heavy Ion Collider (RHIC) began colliding heavy ions at energies high enough to produce a QGP [31–34], whose evolution can be described with hydrodynamics [35, 36]. Understanding this form of matter is then essential to interpret the result of such experiments which are now also being performed at the Large Hadron Collider (LHC) [37, 38]. Similar conditions occurred in the early universe, and these experiments further a better understanding of quantum chromodynamics (QCD) and its phase diagram [39]. Heavy-ion collisions and the QGP should in principle be described by the standard model. However, studying non-equilibrium dynamics in an interacting quantum field theory (QFT) is far too complicated, so it is necessary to employ simplified models. There are many different techniques and frameworks employed, such as perturbative QCD, lattice QCD, kinetic theory, the Anti-de Sitter/conformal field theory (AdS/CFT) correspondence and relativistic hydrodynamics.

The different models apply at different stages of a heavy-ion collision, see [40, 41] for reviews and Fig. 2.1 for a schematic diagram. Before the collision, since the heavy ions are very close to the light cone, the initial state is approximately boost invariant, which inspires the boost invariance assumption of Bjorken flow. The structure of the Lorentz contracted nuclei can be described in the framework of Color Glass Condensate (CGC) [42] where strong color fields dominate. Shortly after the collision, the evolution can be modeled by kinetic theory or AdS/CFT. After a sufficient amount of thermalization, the QGP is formed and can be described by relativistic viscous hydrodynamics [11]. As the plasma expands and cools down, it condenses into hadrons, whose evolution is then described by kinetic theory. The questions studied in this thesis relate to the transition from the microscopic theories of kinetic theory and AdS/CFT to the macroscopic theory of hydrodynamics.

Exactly how close to equilibrium a system must be for a hydrodynamic description to hold is not clear at this point. Heuristically, hydrodynamics should work at length scales much larger than microscopic scales. This can be diagnosed by various dimensionless numbers, such as the Knudsen number which is the ratio between the microscopic mean free path and a macroscopic scale set by the size of gradients. Based on comparison to experimental data from heavy-ion collisions, and to simulations in microscopic models, hydrodynamics has been seen to apply surprisingly far away from equilibrium, in the sense that the pressure anisotropy is large [43–47]. This has inspired an alternative formulation: anisotropic hydrodynamics (aHydro) [13, 48, 49], where the hydrodynamic expansion is constructed around an anisotropic state. Hydrodynamics is also being used for smaller and smaller systems, describing collisions involving smaller nuclei [50–58]. In this thesis we seek to better understand the standard hydrodynamic formulation, see Sec. 3. To gain deeper insights, it is useful to study simplified models, such as relaxation time approximation kinetic theory (RTA) and $\mathcal{N} = 4$ Super Yang-Mills (SYM) in the holographic regime, covering weak and strong coupling respectively. Considering simple flows with many symmetries, such as Bjorken flow [59], is also very helpful.

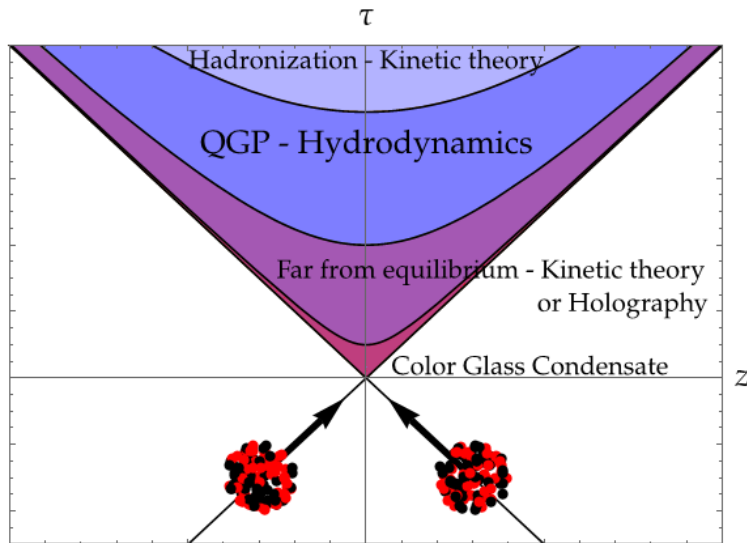


FIGURE 2.1: Schematic diagram of a heavy-ion collision, see [41] for a review. Several different frameworks are used to model the evolution, covering different parameter regimes. The main focus of this thesis is how hydrodynamics emerges from kinetic theory or holography.

2.1 Bjorken flow

Imposing the symmetries of Bjorken flow results in a dramatic simplification. Bjorken flow is characterized by boost invariance in the beam direction and homogeneity and isotropy in the transverse plane [59]. Studying flows with many symmetries makes it possible to find analytical solutions [60], calculate large orders in perturbative expansions [61] and test how hydrodynamics compares to microscopic theories [62]. This is conveniently described in Milne coordinates, using the proper time $\tau = \sqrt{t^2 - z^2}$ and spacetime rapidity $\eta = \arctan z/t$. The metric in these coordinates is

$$ds^2 = -d\tau^2 + \tau^2 d\eta^2 + dx_{\perp}^2. \quad (2.1)$$

The energy momentum tensor takes the form

$$T_{\nu}^{\mu} = \text{Diagonal}(-\varepsilon, p_L, p_T, p_T, p_T), \quad (2.2)$$

where each of the variables depend only on τ . As a measure for how far the system is from equilibrium, one may use the dimensionless pressure anisotropy

$$\mathcal{A} \equiv \frac{p_T - p_L}{\varepsilon/3}, \quad (2.3)$$

which vanishes at equilibrium. The dynamics in Bjorken flow is controlled by two effects. There is the expansion, characterized by a time scale τ , which dilutes the system along the longitudinal direction and pushes the system to an anisotropic state. Then there is interactions, characterized by a time scale τ_{π} , which tries to establish equilibrium and isotropy. If the interactions are strong enough, the system approaches equilibrium with zero temperature at asymptotically late times.

It is convenient to use a dimensionless time variable $w \equiv \tau/\tau_{\pi}$, so that interactions

start to dominate at around $w = 1$. The inverse of w can be interpreted as measuring the size of gradients. Thus, the late time limit and the gradient expansion are very tightly related in Bjorken flow. The ability to measure gradients with a single parameter is one of the key simplifications provided by Bjorken flow.

Another simple flow is Gubser flow [63, 64], which incorporates some transverse dynamics. It is also simple to characterize gradients in this flow [65], and many of the studies made in Bjorken flow are often soon after repeated for Gubser flow.

2.2 Kinetic theory

Kinetic theory describes systems of particles whose dominant interactions come from two-particle scattering [66]. The state of the system is described by the distribution function

$$f(x, p), \quad (2.4)$$

which describes the density of particles with a certain momentum at a certain location. Its evolution is described by the (here relativistic) Boltzmann equation

$$p^\mu \partial_\mu f = C[f], \quad (2.5)$$

where the left hand side represents propagation of particles and $C[f]$ is a collision kernel which describes interactions. The collision kernel is often of considerable complexity, resulting in a nonlinear, integro-differential equation.

An important class of observables is given by the moments of the distribution function. Here, the most relevant one is the energy-momentum tensor

$$T^{\mu\nu} = \int \frac{d^3 p}{p^0} p^\mu p^\nu f(x, p). \quad (2.6)$$

Hydrodynamical models can be constructed by formulating equations of motion directly for a set of moments, though the procedure is not unique [67–76].

We will use a simplified version of the collision kernel [77, 78]

$$C[f] = -p^\mu u_\mu \frac{f - f_{\text{eq}}}{\tau_{\text{rel}}}, \quad (2.7)$$

where f_{eq} has the standard equilibrium form

$$f_{\text{eq}} = e^{\frac{p^\mu u_\mu}{T}}. \quad (2.8)$$

The fluid velocity u^μ and the temperature are defined by the Landau matching condition

$$T^{\mu\nu} u_\mu = -\varepsilon u^\nu, \quad (2.9)$$

and the equilibrium equation of state is used to relate the energy density and temperature. While the collision kernel is linear, the definition of temperature makes the equations nonlinear. This theory is known as the relaxation time approximation (RTA). The relaxation time τ_π may be a functional of f and the momentum p^μ . A simple class of models, studied in Article B, is where $\tau_\pi \propto T^{-\Delta}$.

2.3 AdS/CFT

The Anti-de Sitter/conformal field theory (AdS/CFT) correspondence [79–81], is a correspondence between a strongly coupled quantum field theory and a weakly coupled gravitational theory. The gravitational theory has one more dimension, so the correspondence is often referred to as holography. One of the most useful aspects is that difficult problems on one side of the duality may become much simpler on the other. This is the case for non-equilibrium dynamics, which is much easier on the gravitational side.

Not all QFTs have gravitational duals. The original proposal of Maldacena used string theory to relate strongly coupled $\mathcal{N} = 4$ SYM and a gravitational theory in AdS. In the 't Hooft limit, the gravitational side is classical. In this thesis, by $\mathcal{N} = 4$ SYM we will always take it to be in the holographic regime. The duality has been extended to cover other situations [82, 83]. QCD has $N = 3$, and is weakly coupled at high energy, so if it has a dual it must be based on string theory rather than classical gravity. However, one can construct duals that mimic at least some features of QCD [84], which at least allows for qualitative insights into the behaviour of QCD at strong coupling. For applications in heavy-ion collisions, see [85–87]. There are numerous applications of holography outside of heavy-ion collisions, such as for condensed matter systems [88].

Holographic techniques allows one to derive the hydrodynamic limit of strongly coupled QFT, using the framework of fluid/gravity duality [89]. A famous result of this framework is that for a large class of models the ratio of shear viscosity to entropy density is $\frac{\eta}{s} = \frac{1}{4\pi}$.

3 Hydrodynamics and the gradient expansion

This section describes the basics of hydrodynamics, with a focus on constitutive relations and the gradient expansion. The universality of hydrodynamics comes from symmetry. Symmetries give conservation laws which serve as the equations of motion. In relativistic theories, the conservation of the energy-momentum tensor reads

$$\nabla_\mu T^{\mu\nu} = 0. \quad (3.1)$$

There may be additional symmetries, with their associated conservation laws, but we do not consider it here. In 3 + 1 dimensions, the number of independent components of $T^{\mu\nu}$ is 10. With only four conservation laws, the system is under-determined. We can either introduce additional equations of motion, or reduce the number of degrees of freedom. In both of these strategies, the gradient expansion plays a central role.

First, we define a set of fundamental hydrodynamic fields, often taken to be the temperature T and the fluid velocity u^μ satisfying $u^\mu u_\mu = -1$. There is no unique way to define these off equilibrium [23]. As in Sec. 2.2, we use the Landau frame where

$$T^{\mu\nu} u_\nu = -\varepsilon u^\mu, \quad (3.2)$$

and the energy density ε is related to the temperature using the equation of state. We then express $T^{\mu\nu}$ in terms of these fields and all possible terms constructed from their gradients

$$T^{\mu\nu} = \sum_{k=0}^{\infty} T_{(k)}^{\mu\nu}, \quad (3.3)$$

where $T_{(k)}^{\mu\nu}$ involves k derivatives of the fundamental fields. The first term is the perfect fluid contribution which in the Landau frame takes the form

$$T_{(0)}^{\mu\nu} = \varepsilon(T) u^\mu u^\nu + p(T) \Delta^{\mu\nu}, \quad (3.4)$$

where $\Delta^{\mu\nu} = g^{\mu\nu} + u^\mu u^\nu$ is the transverse projector to the fluid velocity. The first order terms are

$$T_{(1)}^{\mu\nu} = -\eta \sigma^{\mu\nu} - \zeta \Delta^{\mu\nu} \nabla_\lambda u^\lambda, \quad (3.5)$$

where η and ζ are the shear and bulk¹ viscosity transport coefficients. $\sigma^{\mu\nu}$ is the transverse and traceless combination formed from $\nabla^\mu u^\nu$. Each order in the gradient expansion introduces additional tensor structures, each with their own transport coefficient. The number of terms grows very fast. In a conformal theory, at first order there is 1, at second order there are 5 [90] and at third order there are 19 [91, 92]. Due to the fast growth of the number of terms and of their complexity, characterizing the large order behaviour of the gradient expansion in general is not an easy problem. By

¹We consider mostly conformal theories, so the bulk viscosity will not be relevant.

imposing the symmetries of Bjorken flow, these calculations become feasible [61]. Another strategy is to calculate the resummed gradient expansion numerically [93–96].

The gradient expansion is not unique. It depends on the choice of hydrodynamic frame, and the equations of motion can be used to convert between time and spatial derivatives. One can use a truncated gradient expansion to construct models of hydrodynamics, and the choices made influences the number of degrees of freedom as well as properties like well-posedness, causality and stability [23, 24]. The early first order theories [8, 9] suffer from acausality or instability [97, 98]. Better behaved is the second order model of Müller-Israel-Stewart (MIS) [68, 69, 99–102] and its modern completion Baier-Romatschke-Son-Starinets-Stephanov (BRSSS) [90]. Recently, there has been an effort to construct well-behaved first order theories through different frame choices [23, 24, 103–108]. All well-behaved theories include additional nonhydrodynamic modes, which act as a regulator enforcing causality at large momentum [54].

The picture presented here is in the spirit of effective field theory, where the most general construction consistent with the symmetries is derived [90]. On the other hand, given a particular microscopic theory, one can consider its hydrodynamic limit. The gradient expansion derived from a microscopic theory must match the construction above, but such calculation fixes the transport coefficients. Kinetic theory and AdS/CFT provide two complementary frameworks, covering weakly and strongly coupled theories respectively. These theories have an infinite number of degrees of freedom, most of which are irrelevant for the hydrodynamic limit.

3.1 When do constitutive relations emerge?

How does an infinite number of degrees of freedom reduce to only a few? When constitutive relations do emerge and are characterized by the gradient expansion, what determines the large order behaviour? Is the expansion convergent or divergent? To explore these questions, we will start with linear response in Sec. 4 before we tackle the nonlinear case.

Close to equilibrium, linear response theory gives insight into how this happens. There, the dynamics of the system can be decomposed into long-lived hydrodynamic modes, and short-lived nonhydrodynamic modes. After some time, only the hydrodynamic modes are relevant, and these give constitutive relations that can be described by the gradient expansion. While this may be a sufficient criterion, it is not obvious how to generalize it to the full nonlinear response. However, studies of the gradient expansion suggests that a similar story can be told there, see Sec. 6. But there can also be other mechanisms at play, not relying on the distinction between hydrodynamic and nonhydrodynamic modes. One mechanism, described in Sec. 7, is the Bjorken flow attractor [14], which emerges due to the fast expansion at early times [109].

One of the key lessons is that the gradient-expanded constitutive relations are usually divergent. This does not mean that the constitutive relations are useless, as there are methods to meaningfully convert the series into definite and accurate numbers, see Sec. 5. In addition, the precise way in which the series diverges is related to nonhydrodynamic excitations. However, without supplying information about those excitations, the constitutive relations always possess an (often small) ambiguity.

4 Linear response and modes

It is instructive to consider linear response around a thermal state. The emergence of constitutive relations can be understood through the decomposition of the response into hydrodynamic and nonhydrodynamic modes. These modes are characterized in momentum space by dispersion relations $\omega(k)$. Hydrodynamic modes are universal, while the nonhydrodynamic modes differ between theories. Nevertheless, these modes are connected by analytic continuation, which has consequences for the convergence radius. Translating from momentum space to real space is nontrivial, and may convert a convergent hydrodynamic dispersion relation to a divergent real space gradient expansion.

The source for the energy-momentum tensor $T^{\mu\nu}$ is the metric $g^{\mu\nu}$. Given a perturbation in the metric, the response is

$$\delta T^{\mu\nu} = \int d\omega d^3k e^{-i\omega t + \vec{k}\cdot\vec{x}} G_{\alpha\beta}^{\mu\nu}(\omega, \vec{k}) \delta g^{\alpha\beta}(\omega, \vec{k}), \quad (4.1)$$

where $G_{\alpha\beta}^{\mu\nu}$ is a retarded Green's function. The index structure can be split into five independent pieces [83], and we are interested in the sound and shear channel which are described by two functions $G^{\parallel}(\omega, \vec{k})$ and $G^{\perp}(\omega, \vec{k})$. These determine the modes of the theory. We can take the integral over ω in Eq. 4.1 by sending the contour out to infinity. Assuming that the arcs at infinity are negligible, the only contribution comes from various singularities of the Green's functions, such as poles, branch points or even essential singularities. For a fixed \vec{k} , such a contribution behaves as

$$\delta T^{\mu\nu}(t, \vec{x}) \sim e^{-i\omega(k)t + i\vec{k}\cdot\vec{x}}, \quad (4.2)$$

although branch points may introduce additional power laws. In some cases, we characterize the singularities by a simple equation. For example, take the shear channel and suppose that it can be written as

$$G_{\alpha\beta}^{\perp}(\omega, \vec{k}) = \frac{D(\omega, \vec{k})}{P(\omega, \vec{k})}, \quad (4.3)$$

where $D(\omega, \vec{k})$ and $P(\omega, \vec{k})$ are analytic.¹ Then the non-analyticities of G^{\perp} are given by $P = 0$. Solutions to $P = 0$ are classified as hydrodynamic or non-hydrodynamic. Hydrodynamic modes are those modes where

$$\lim_{k \rightarrow 0} \omega(k) = 0, \quad (4.4)$$

¹We should note that this assumption does not hold in all models. In RTA, the Green's function involves logarithms [110, 111], but a similar analysis applies in that case, see Article E.

which implies that they correspond to conserved quantities. The rest are nonhydrodynamic. Often², such modes satisfy

$$\Im[\omega(0)] \neq 0, \quad (4.5)$$

in which case they decay exponentially fast. They are not conserved. In this way, linear response theory around equilibrium provides an explanation for how constitutive relations emerge. When k is small, the gradients are small and the hydrodynamic modes are necessarily long-lived due to conservation laws. Nonhydrodynamic modes have no such constraint and tend to decay fast. The system is well-described by purely hydrodynamic contributions at late times.

If k is small, we can do a perturbative expansion around $k = 0$. This is the gradient expansion in momentum space. The hydrodynamic modes are further constrained by consistency with the gradient expansion in real space. Assuming a conformal theory, the shear and sound channel modes satisfy

$$\omega_{\perp}(\vec{k}) = -i \frac{3\eta}{4\epsilon} \vec{k}^2 + \dots \quad (4.6a)$$

$$\omega_{\parallel}(\vec{k}) = \pm \frac{|\vec{k}|}{\sqrt{3}} + \dots, \quad (4.6b)$$

This structure is common to any theory with these symmetries. Different theories have different values of the transport coefficients. The nonhydrodynamic modes have no such structural constraint, and differ in both form and physical interpretation between theories, see Fig 4.1.

4.1 Modes in different theories

Nonhydrodynamic modes have naturally not been in the spotlight of research into hydrodynamics. Determining the structure of modes in different theories is something that only recently has become a topic of interest. In holographic models, the nonhydrodynamic modes come from poles in the Green function [112]. In the dual gravity theory, these are known as quasinormal modes (QNMs), and they correspond to the ringdown of black holes [113]. These poles are arranged in a characteristic "Christmas tree" structure, see Fig. 4.1.

On the other hand, in RTA kinetic theory, nonhydrodynamic modes come from logarithmic branch points [110, 111]. The branch cut can be interpreted as the effect from propagation of individual microscopic particles. Branch points can also be found in free Yang-Mills theory [114]. How the transition between the weakly and strongly coupled cases may occur has been studied in [115].

The hydrodynamic models, such as MIS and BRSSS, also have a nonhydrodynamic sector [90]. There are usually just a few of them, as these theories are only designed to capture the hydrodynamic sector faithfully. However, it is possible to also arrange the nonhydrodynamic sector in such a way as to mimic another microscopic theory. BRSSS has similarities to kinetic theory when k is small, as then the nonhydrodynamic

²But not always, see [111].

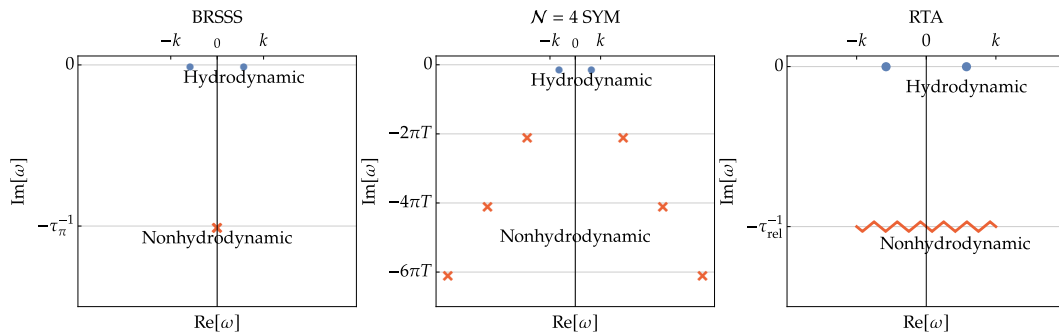


FIGURE 4.1: The structure of hydrodynamic and nonhydrodynamic modes in the sound channel in BRSSS [90], $\mathcal{N} = 4$ SYM [112] and RTA kinetic theory [11, 110]. The hydrodynamic sector is universal, but the nonhydrodynamic sector is not. They play an important role in the large order behaviour of the gradient expansion, both at the linear and nonlinear level.

sector is purely decaying. There are also theories that aim to capture the oscillatory structure of nonhydrodynamic modes at small k in AdS/CFT [116, 117].

4.2 Analytic structure of modes

The different solutions $\omega(k)$ are not necessarily independent. The solutions to $P(\omega, k) = 0$ may be different branches of a single function defined on the same Riemann surface [118]. The simplest example comes from BRSSS, where the solutions are [90]

$$\omega_{\perp}(k) = i \frac{-1 \pm \sqrt{1 - 4D\tau_{\pi}k^2}}{2\tau_{\pi}}. \quad (4.7)$$

Two solutions differ only by the branch chosen for the square root. For a certain momentum, they collide, and this collision sets the radius of convergence for $\omega(k)$. The modes may be transformed into each other by following certain paths in k .

How generic is this behaviour? To make general statements, one strategy is to exploit properties of the equation

$$P(\omega, \vec{k}) = 0 \quad (4.8)$$

directly to constrain the singularities of $\omega(k)$ [119, 120]. In Article E we showed how to make this rigorous. The result is that singularities of $\omega(k)$ can only occur at points where either P is non-analytic or where it satisfies

$$\partial_{\omega}P(\omega, k) = 0. \quad (4.9)$$

Note that singularities *may* occur at these points, but they do not necessarily do so.

If P is analytic, which is the case in BRSSS, we can say more about the nature of these singularities. The singularities can only come from locations where $\partial_{\omega}P$ vanishes. By the Weierstrass preparation theorem [121], the only possible singularities are branch points. At such points, there is a mode collision. Around these singularities,

ω can be expanded in a Puiseux series - a series in fractional powers of k with a finite radius of convergence. This is the case in BRSSS, where P is a simple analytic function. This is also observed in holography [118–120, 122], but it is not known if P is analytic.

In RTA, P is not analytic everywhere, due to the logarithmic functions present in the Green's function [110]. This makes the structure of the singularities much more involved. We showed in Article E that in RTA kinetic theory, there are logarithmic singularities, as well as singularities that are accumulation points of poles. This has not been observed in other models. None of these can be described by a local Puiseux series, and it is not known what the radius of convergence is around such singularities.

To summarize, the radius of convergence of hydrodynamic modes has in all cases considered (except for a perfect fluid) found to be finite, and set by collisions with other modes. Assuming analyticity of P around $\omega = k = 0$, it follows that the radius is non-zero, although it could be infinite. In Article F, we argued based on causality that the radius of convergence should be finite. The coefficients of the dispersion relation will then grow geometrically with a rate set by some inverse momentum k_*^{-1} . This has nontrivial consequences for transport coefficients.

4.3 Back to coordinate space

To translate this story to coordinate space, one has to do the Fourier transform. However, this is not so trivial. While the distinction between different modes is well-defined when considering a single value of k , they can be transformed into each other by analytic continuation along a path in k . In the Fourier transform, the integral over k can be deformed along such paths, which makes the identification of the hydrodynamic contribution subtle. We have employed two different strategies in Articles F and D.

In Article F, we determine the values of the transport coefficients (in the purely spatial gradient expansion) in terms of the hydrodynamic dispersion relation. The geometric growth of the latter implies the same for the former. This is one half of the information required to determine the convergence of the gradient expansion, with the other half coming from the tensor structures constructed from repeated derivatives acting on the hydrodynamic fields. This latter contribution is tightly linked to the support of hydrodynamic fields in momentum space. In particular, if the support in momentum space is only up to k_{\max} , the derivatives feature a geometric growth set by that value. As a result, convergence of the gradient expansion is determined by whether the ratio

$$\left| \frac{k_{\max}}{k_*} \right| \quad (4.10)$$

is above or below one.

Saddle point integration is used in Article D. This requires introducing a perturbative parameter ϵ (not to be confused with the energy density ε). Inspired by results in Bjorken flow, see Sec. 6, where nonhydrodynamic modes are nonperturbative, we seek for a parameter that does the same here. The solution is to scale time and space as

$$t \rightarrow t/\epsilon^z, \quad x \rightarrow x/\epsilon, \quad (4.11)$$

with the value of z depending on the sound or shear channel. The saddles may be localized anywhere in the complex \vec{k} plane, and where they end up depends on initial data. For slowly varying solutions, where hydrodynamics is expected to apply, it is natural to expect saddles at $\vec{k} = 0$. In that case, the saddle point expansion results in a series of the form

$$\delta T^{\mu\nu} \sim \sum_n e^{i\omega_n(0)/\epsilon} \sum_{k=0}^{\infty} \epsilon^k c_{nk}^{\mu\nu}. \quad (4.12)$$

These are explicit expressions for the hydrodynamic and nonhydrodynamic contributions. The expansions around each saddle point is generically an asymptotic series [123, 124]. Their large order behaviour can be explicitly related to the presence of other saddles that live on the same Riemann surface [125] which, as we have seen, the different modes often do.

For data with infinite support in momentum space, this suggests that the hydrodynamic contribution at large order behaves as

$$T_n \sim \frac{\Gamma(n + \beta)}{\chi^{n+\beta}}, \quad (4.13)$$

where $\chi = |\omega_{\min}(0)|$, although if the saddle is located at some finite k , χ may be different. The arguments for this depend on techniques applicable only for linear response but very similar conclusions have been observed for the full gradient expansion in nonlinear theories, see Sec. 6.

5 Dealing with asymptotic series

As we have seen, the gradient expansion does not necessarily converge. Divergent series may satisfy a weaker property: that of being asymptotic. Asymptotic series are series where, for a fixed finite truncation, it becomes increasingly accurate as the perturbative parameter goes to zero. In this section, we cover how to turn asymptotic series into numbers, how to mine them for nonperturbative information and how to improve the accuracy. These methods are studied in the theory of resurgence, which generalizes the connections between saddles in saddle point integration. Resurgent methods operate directly on the series and can be applied beyond linear response, see Sec. 6.

There are two main strategies for converting an asymptotic series into useful numbers. The simplest is optimal truncation, where the series is truncated at an optimal location, before the coefficients start to diverge. This can achieve exponential accuracy [126], outperforming convergent series. The other strategy is to use a resummation procedure. We use Borel summation here. This method gives rise to ambiguities that can be interpreted as nonperturbative contributions. In particular, the saddle point techniques can be mapped to Borel summation with a simple change of variables [127], and the different saddles map to the ambiguities in Borel summation.

The nonperturbative contributions can be included on top of the perturbative series, resulting in a transseries. If one has access to the nonperturbative information required to resolve the ambiguities, the transseries can represent an exact solution.

5.1 Borel summation

Borel summation is based on the identity

$$n! = \int_0^\infty d\xi e^{-\xi} \xi^n, \quad (5.1)$$

which is used to remove the factorial growth of a series. Given a formal sum¹

$$\mathcal{A}(w) = \sum_{n=0}^{\infty} \frac{a_n}{w^n}, \quad (5.2)$$

we define the Borel sum as

$$\mathcal{A}_c(w) = w \int_c^\infty d\xi e^{-\xi w} \mathcal{A}_B(\xi) \quad (5.3)$$

where

$$\mathcal{A}_B(\xi) \equiv \sum_{n=0}^{\infty} \frac{a_n}{n!} \xi^n, \quad (5.4)$$

¹We use notation that matches that used for the gradient expansion in Bjorken flow used in Articles A and B, but the methods apply more generally.

and c denotes the contour that connects $\xi = 0$ and $\xi = \infty$. Any choice of contour is fine, but since $\mathcal{A}_{\mathcal{B}}(w)$ may have singularities, the answer will in general depend on this choice. A pole or branch point at ξ_* in the Borel plane gives rise to an exponential term of the form

$$e^{-\xi_* w} w^\beta, \quad (5.5)$$

with β depending on the order of the singularity. The ambiguities imply a limit for the accuracy of the resummation, unless additional nonperturbative information is provided to resolve them.

The location of singularities is set by the large order behaviour. In particular, for a series where $a_n \sim n!/\xi_*^n$, the singularity is located at ξ_* . For series obtained through saddle point techniques, the location of singularities is set by the other saddles. This is an example of resurgence, where information about nonperturbative sectors is reconstructed through the large order behaviour of the perturbative series.

In practice, it is rare to know the coefficients to all orders, in which case the analytic structure of the Borel transform must be inferred. One way to do this is by Padé approximants, which is an approximation by a rational function. A Padé approximant of order $[m/n]$ is a function

$$R(\xi) = \frac{P(\xi)}{Q(\xi)}, \quad (5.6)$$

where Q and P are polynomials of order m and n . Their coefficients are uniquely specified by matching the Taylor expansion of $R(\xi)$ to the first $m+n$ coefficients of $\mathcal{A}_{\mathcal{B}}(\xi)$. The Padé approximant has poles at the roots of the denominator, which means that unlike a truncated Taylor series, it has singularities. It can represent poles very well, but branch cuts can also show up. In that case, the poles align themselves along a curve starting at the branch point. The larger the order, the denser the poles. See Fig. 6.1 for an example.

5.2 Transseries and resurgence

To improve on the perturbative series and resolve the ambiguity in the summation, nonperturbative terms must be included. The nonperturbative terms may take the form of exponentials, logarithms or iterated versions of those. Usually, only the exponential terms arise and the result is a transseries of the form

$$\mathcal{A}(w) = \sum_{n=0} a_n w^{-n} + \sigma e^{-S w} w^\beta \sum_{n=0} b_n w^{-n} + \dots, \quad (5.7)$$

where w is large. As exemplified by saddle point techniques, or Borel summation, there are relations between the large order behaviour of the coefficients in one sector and the low order coefficients in other sectors. These relations are formalized and studied in the theory of resurgence [128], which offers practical tools to analyze asymptotic series.

1. The resurgent relations can be used to extract the nonperturbative sectors from the perturbative series (and the other way around).
2. Transseries can be truncated to achieve great accuracy [129], often exceeding that of convergent series.

The transseries can represent an exact solution to a problem, while the perturbative series is incomplete. The prize to pay is that the transseries requires nonperturbative information to be specified. This is the prefactor σ in Eq. 5.7. Transseries occur in many fields, as they arise naturally in differential equations [124]. They play an important role in quantum mechanics, where the different sectors arise as different saddle points in the path integral and are interpreted as instantons or tunneling effects [130].

One important concept is that of Stokes lines. If the transseries depends on some parameters, then as those parameters are varied, at certain points different sectors may be turned on or off. This manifests itself in the Borel plane by singularities crossing the resummation contour, and in the saddle point analysis as a change in which saddle points are relevant. The prefactor σ in the series jumps.

5.3 Spacetime transseries

The studies in Bjorken and Gubser flow are greatly simplified since the equations of motions are ordinary differential equations. Transseries for ordinary differential equations (ODEs) is a well-studied topic [124]. Going beyond these simple flows, the hydrodynamic equations become partial differential equations (PDEs), for which transseries are less studied. In Article D, we investigated transseries in BRSSS, without restriction to highly symmetric flows such as Bjorken or Gubser flow. In this case, the transseries will depend on x and t , so it is important to pay attention to Stokes phenomena. For a PDE, there can be effects that turn on and off in different regions of spacetime [127, 131, 132].

We considered linear perturbations away from equilibrium, which simplifies the analysis considerably. Shear channel fluctuations in BRSSS can be described by the telegraphers equation

$$\tau \partial_t^2 \rho + \partial_t \rho - D \partial_x^2 \rho = 0. \quad (5.8)$$

This is the simplest equation describing relativistic diffusion and occurs in many contexts, as discussed in Article D.

To construct a transseries, we must define a perturbative parameter. Differently from Bjorken flow, the size of gradients cannot be characterized by a single parameter. The basic criterion we use to introduce a small parameter is the following: the (non)hydrodynamic modes should be (non)perturbative. This corresponds to a large time and large distance limit, although time and space may be scaled differently depending on the behaviour of the modes. We find transseries solutions to the equation of motion, rather than the gradient expanded constitutive relations themselves.

Due to linearity, solutions can be found through Fourier transforming. The real space result is then expressed as an integral over momentum, which lends itself to a saddle point analysis. Complementary to this, we also solve it using a direct ansatz in position space. While the first method requires linearity, the second method can in principle be extended to nonlinear theories.

As observed before in PDEs, we find Stokes lines at certain locations in space time. The location depends on the initial data, which enables an equivalent interpretation - there are Stokes lines in the space of initial data. This is different from Bjorken flow, where there are no Stokes lines. The interpretation of the nonperturbative sector

depends on initial data. If the saddle point analysis localizes at small k , it is diffusive, but if it localizes at large k , it represents a propagating wave packet.

6 Gradient expansion beyond linearity

We now go beyond linear response theory, and consider cases where the gradient expansion has been determined at the nonlinear level. This is much more complicated, so these studies are usually confined to specific, simple models. The number of tensor structures and transport coefficients is much higher although it is explicitly known only at few orders. Fourier transforming is not appropriate, so we cannot use it to identify different modes, nor for saddle point integration. The main tool in this case is resurgence, and in particular Borel. Many of the lessons from linear response continue to hold. The gradient expansion tends to diverge and the way in which it does so is again related to nonhydrodynamic modes. There are cases where it converges [133, 134], but these are probably exceptions to the rule.

In the context of heavy ion collisions¹, the computation of the gradient expansion to large orders was initiated in $\mathcal{N} = 4$ SYM in Bjorken flow [61]. The gradient expansion was found to diverge factorially as in Eq. 4.13. The geometric growth turned out to be $\chi = |3\omega/2|$, where ω is the frequency of the most long-lived nonhydrodynamic mode at zero momentum. The factor of $3/2$ can be understood as an effect of the evolving background [138]. This suggests that in order to improve the gradient expansion, one should construct a transseries where the nonperturbative sectors are related to nonhydrodynamic modes.

The same conclusion was reached in BRSSS [14]. In Bjorken flow, the theory has only more degree of freedom apart from the hydrodynamic one. This degree of freedom can be represented by the nonperturbative sector in the transseries [139]. In $\mathcal{N} = 4$ SYM and other holographic models, there are an infinite number of degrees of freedom, corresponding to the metric in the gravitational dual. Accordingly, there are an infinite tower of nonhydrodynamic modes, which is also reflected in the Borel plane [140]. Another case where such a counting has been verified is a second order hydrodynamical model [141]. In RTA there are also an infinite number of degrees of freedom, corresponding to states of the distribution function.

6.1 Subtleties in RTA

In Article A we probed the gradient expansion in conformal RTA, shown to be divergent in a similar model in [142]. Two features could be seen in the Borel plane, see Fig 6.1, one of which corresponds to the branch point in linear response, but the other one had no clear interpretation. Two things were mysterious about this result - one would have expected an infinite number of ambiguities, as in $\mathcal{N} = 4$ SYM, and what is the interpretation of additional singularity in the Borel plane? The latter feature could ultimately be related to analytic continuation of the time variable along a path in the complex plane. In addition, we found no trace of these singularities in solutions we

¹There has been earlier work on the convergence properties of the Chapman-Enskog expansion in nonrelativistic kinetic theory [135–137], but we focus here on the recent literature.

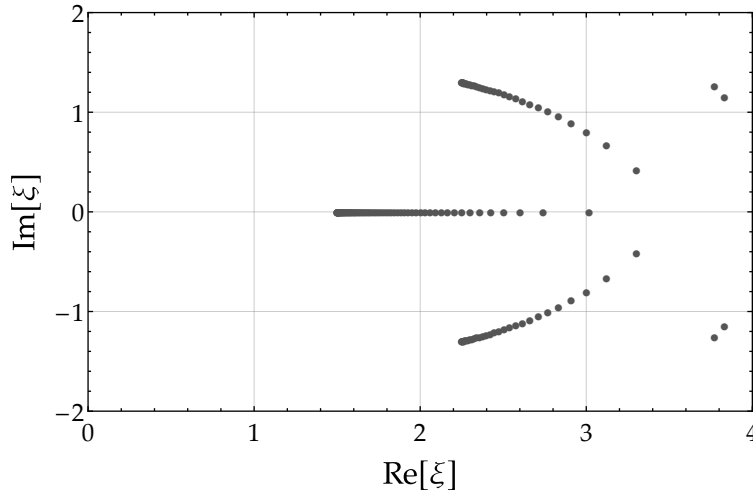


FIGURE 6.1: The singularities of the Borel plane of the gradient expansion in conformal RTA. The singularities of the Padé approximant arrange to form branch cuts. The branch cut starting at $\xi = 3/2$ can be interpreted as coming from the nonhydrodynamic branch cut seen in linear response in Fig. 4.1. This follows the pattern of other models analyzed in a similar manner. However, the singularities which are not located on $\text{Im}\xi = 0$ are unphysical. This is an important cautionary lesson when studying the large order gradient expansion. Figure adapted from Article A.

calculated numerically. Thus, these ambiguities do not seem to represent any physical nonhydrodynamic modes.

As for the number of ambiguities, in the follow-up Article B, we showed that the physical ambiguity in the Borel plane is degenerate. There are in fact an infinite number of singularities stacked on top of each other. They are distinguished by subleading power law corrections. These two results present two cautionary lessons when using Borel summation. Singularities in the Borel plane may be degenerate, and they may be unphysical.

In Article B we also considered a more general RTA model by modifying the relaxation time. This class of models is parametrized by the parameter Δ . We considered $\Delta < 3$, where the interactions are strong enough that the system thermalizes. The conclusions are qualitatively the same for all these models, however, for $\Delta > 2$, the unphysical singularities actually give the dominant contribution to the large order behaviour of the gradient expansion. Thus, while they may be unphysical, they leave an unavoidable imprint on the gradient expansion.

The cases that we did not consider were later investigated by others. The case $\Delta > 3$ was used in [143] to construct models that mimic more closely the behaviour of the expanding QGP, which at first seem to thermalize but eventually decouple. The marginal case $\Delta = 3$ was studied in [134], in which case the gradient expansion actually converges.

The divergent gradient expansion has also been confirmed for other theories and flows. For BRSSS in Gubser flow [65], anisotropic hydrodynamics [144], Gauss-Bonnet holography [145], cosmological flows [146], hydrodynamics in general frames [147]. Transseries in RTA in Bjorken flow has been studied in [148, 149].

Transseries solutions have been studied in Gubser flow for different theories [150, 151].

7 The hydrodynamic attractor

The hydrodynamic attractor was suggested in [14] as a way to explain far from equilibrium hydrodynamics. In BRSSS in Bjorken flow, when different solutions for the pressure anisotropy \mathcal{A} is plotted against $w = \tau T$, they quickly collapse and become indistinguishable, see Fig. 7.1. This fact by itself is not particularly surprising. From linear response we expect that the nonhydrodynamic contribution decays exponentially close to equilibrium. The two surprises are: 1. The collapse happens at large pressure anisotropy. 2. The collapse can happen at large gradients/early time.

Many studies have reproduced this in other models in Bjorken and Gubser flow, confirming that similar behavior can be seen in other phenomenological models [65, 133, 134, 141, 143, 147, 152–154], in kinetic theory [155–163] as well as in holography [140, 145, 164, 165]. Phenomenological implications are explored in [166, 167].

There are several strategies to explain and describe the attractor. Various kinds of attractors are known in the mathematical theory of dynamical systems, and the BRSSS attractor is of a particular type called a pullback attractor [168]. Ideas from this field are explored in [148–151]. In [161], a connection is made to adiabatic notions familiar from quantum mechanics.

The expansion in Bjorken flow plays an important role, at least for BRSSS and kinetic theory [109]. These theories feature an early time attractor, coming from the expansion. This is in addition to the nonhydrodynamic collapse operational at late times. No such distinction was found for $\mathcal{N} = 4$ SYM .

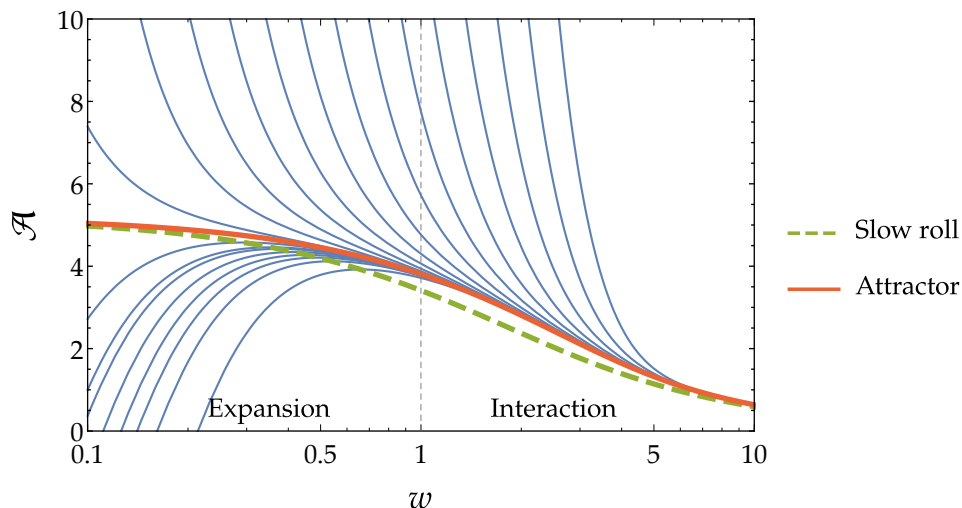


FIGURE 7.1: Numerical solutions (blue) of BRSSS in Bjorken flow quickly converge to each other, implying a loss of information. In addition, the solutions end up in a region that can be characterized by the pullback attractor or slow roll approximation [14]. The mechanism controlling the convergence is different at early (expansion) and late times (interactions) [109].

7.1 Information loss and slow roll

In BRSSS, the attractor \mathcal{A}_* can be defined as the unique solution that is bounded as $w \rightarrow 0$. Supposing that the limit $w \rightarrow 0$ was inaccessible to us, how could we quantify and identify the attractor? In Fig 7.1, the point $w = 0$ is in fact not included, so everything one can conclude from it must be independent of that point. There are two things happening that we want to quantify. The solutions are converging to each other, and when they converge they end up in a certain region. The first is a kind of information loss, where different solutions become indistinguishable, while the second represents a universality. We use these concepts to characterize attractors in Article C.

These two phenomena are not the same. Consider an analogy to the expansion of the universe. Following the trajectories of galaxies back in time, as the universe contracts the trajectories converge. However, they do not converge to a particular region in the universe, because there is no point that is singled out as the center. In Fig 7.1, the solutions are also converging but here they do end up *somewhere*.

Plots like Fig 7.1 appeal to an intuitive sense of closeness. To quantify it, a natural choice to compare two solutions at some w is then to consider $|\mathcal{A}_1(w) - \mathcal{A}_2(w)|$. Based on such a metric, one can diagnose the information loss as the solutions converge.

As to where they end up, the slow roll approximation can explain it. The zeroth order slow roll is defined as the union of points where $\mathcal{A}'(w) = 0$ [14]. This is not a solution, but it approximates the attractor and it predicts the region that the solutions end up in. Thus, the slow roll can be used as a proxy for universality. One way to understand why slow roll is related to universality is the following heuristic argument. Solutions spend more time in slow regions than in fast regions, so thus they are more likely to be found in the former.

Neither slow roll nor information loss can be used to identify the pullback attractor, or to otherwise define a unique solution to call the hydrodynamic attractor. However, they characterize the properties that are usually associated with the hydrodynamic attractor in Fig 7.1. Another advantage of this formulation is that it is easy to generalize to more complicated flows.

7.2 Towards more complicated flows

One of the main challenges is to investigate attractors in cases with less symmetry, breaking the conformal or boost invariance or including transverse dynamics. This has been studied in [169–171], which indicated that the attractor persists at least for moderate breakings. Slow roll for general flows in BRSSS has been studied in [172].

One difficulty with less restricted flows is how to choose which variables to study. In [14], the attractor is detected by studying the pressure anisotropy as a function of τT . It is not apparent by studying the temperature as a function of τ . To make it apparent without requiring a fine-tuning of the choice of variables, one needs to enlarge the space of variables e.g. by using the full two dimensional phase space of (T, T') . The loss of information from the attractor is then represented by the contraction of the two-dimensional space into one dimension. Then information loss and universality can be characterized as in the previous section.

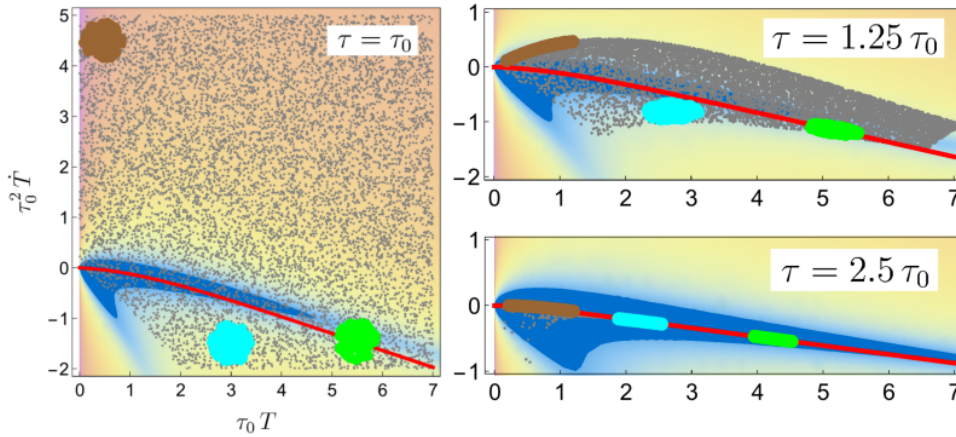


FIGURE 7.2: The same model as in Fig 7.1, but viewed from the full phase space. The attractor shows up as a dimensional reduction from two to one dimension. It can be quantified by imposing a metric and using algorithms such as PCA. Figures from Article C.

This is the basis of Article C. We present a phase space perspective on the attractor, where it shows up as a reduction of dimensionality. This generalizes the standard view, which only considers $1 \rightarrow 0$ dimensional reduction. Higher dimensional spaces are more difficult to study visually, so we provide quantitative methods to measure what is usually left implicit in plots of the attractor. We use Principal Component Analysis (PCA), the simplest machine learning algorithm, to estimate the dimensionality of a set of solutions. PCA is able to characterize linear manifolds, and we find that it works quite well for the theories we consider (BRSSS, HJSW, RTA).

The information loss that comes with the attractor can be viewed as an emergent constitutive relation. It reduces the degrees of freedom, which suggests that the model can be simplified. In cases where the attractor is not governed by near equilibrium physics, such as at early times where the expansion dominates, these relations arise from far from equilibrium effects. Another example of this behaviour is the phenomena of prescaling seen in kinetic theory [173].

8 Summary

The transition between microscopic theories and a hydrodynamic description has come under increased scrutiny from heavy ion collisions, as described in Sec. 2. One of the essential elements of hydrodynamics are the constitutive relations. These relations can be described with the gradient expansion, Sec. 3, or by hydrodynamic attractors, Sec. 7.

The convergence properties of the gradient expansion must be understood in order to understand how well hydrodynamics approximates the underlying microscopic theory. Sec. 4 describes what can be learned from linear response. Nonhydrodynamic modes and the support of initial data in momentum space play a crucial role. If the initial data has large gradients, the gradient expansion will diverge.

Sec. 5 describes how to handle divergent asymptotic series. The Borel transform of the series contains information on nonperturbative corrections coming from nonhydrodynamic modes. These corrections represent a limit for the accuracy of the gradient expansion.

These methods have been applied to the full nonlinear gradient expansion where the Fourier transform and saddle point techniques cannot be used, see Sec. 6. The key simplification in this case comes from assuming highly symmetric flows such as Bjorken flow. We focus on RTA kinetic theory, since this case presents some cautionary lessons where Borel analysis can include unphysical singularities.

Finally, the hydrodynamic attractor represents constitutive relations far from equilibrium. Sec. 7 describes our work on how to characterize and measure attractors. We suggest a data driven approach, which can be used to search for attractors in less symmetric flows.

8.1 Article summaries

In previous sections, we have presented necessary background material and put the papers into context. Here we summarize the main contributions of the papers.

A Hydrodynamization in kinetic theory: Transient modes and the gradient expansion The gradient expansion in Bjorken flow was known to diverge in some strongly coupled theories as well as BRSSS. To understand how generic it is, it was important to also cover the weakly coupled case. In conformal RTA kinetic theory, we showed that it diverges, and that the divergence is controlled by the nonhydrodynamic mode. However, differently from the cases analyzed before, there were also unphysical singularities in the Borel plane which do not correspond to nonhydrodynamic modes. This is important to keep in mind in a Borel analysis of the large order behaviour.

B How does relativistic kinetic theory remember about initial conditions? One of the main puzzles remaining after Article A, was in what way the infinite number of degrees of freedom of kinetic theory manifests itself in the Borel plane.

We determined that the physical singularity in the Borel plane is degenerate. The nonhydrodynamic contributions behave to leading order as

$$\sigma_i e^{-3/2w} w^{\beta_i}, \quad (8.1)$$

where different modes are distinguished by having different power laws β_i . The number of allowed β 's is infinite, which one would expect from a microscopic theory involving infinite degrees of freedom. σ_i depends on initial data and is how nonhydrodynamic information is encoded as the system expands and approaches equilibrium. We considered a one parameter family of models, which all had qualitatively the same features in the Borel plane.

C Hydrodynamic Attractors in Phase Space We introduced new methods to enable the search for attractors in less restricted models and flows. We showed that by taking a higher dimensional phase space perspective, one can avoid the necessity for a fine-tuned choice of variables. The attractor is viewed as reduction in dimensionality, and we used PCA to quantify this notion. We also generalize slow roll to this perspective, arguing that it is a good proxy to characterize universality. We applied these techniques to BRSSS, HJSW and RTA.

F The hydrodynamic gradient expansion in linear response theory Most studies of the large order gradient expansion were done for simple models in Bjorken flow. The mechanism behind divergence was not completely understood. Does the factorial growth result from the growth of the number of transport coefficients, their value, or the values of the tensor structures? In this paper, by considering linear response, we disentangled these mechanisms and were able to make statements about more general flows.

In linear response, neither the number of transport coefficients nor their value feature a geometric growth. The factorial growth came in this case from the repeated spatial derivatives, which in turn is related to the support of hydrodynamic fields in momentum space.

In addition, dispersion relations in momentum space had come under increased scrutiny, with observations and arguments implying they have a finite radius of convergence. In this paper we showed how the convergence properties of the dispersion relations are related to the convergence properties of the real space gradient expansion.

D Transseries for causal diffusive systems Transseries solutions had been constructed for 1-dimensional flows like Bjorken flow. How this could be generalized to other flows was an open question. In this paper, we used linear response to study this. We proposed introducing a perturbative parameter that separates the hydrodynamic and nonhydrodynamic contributions into different transseries sectors. We apply this to the telegraphers equation, which among other things describes shear channel fluctuations in BRSSS. An interesting outcome was how the nonhydrodynamic sector depends on initial conditions and regions in spacetime. In some cases they are diffusive and in other they represent propagating effects.

E Convergence of hydrodynamic modes: insights from kinetic theory and holography In $\mathcal{N} = 4$ SYM and BRSSS, the convergence radius of the dispersion relations of hydrodynamic modes was set by mode collisions. To understand how general this is, it was important to cover the weakly coupled case as well. RTA has a more complicated structure of modes, see Fig. 4.1 so it differed in some ways as compared to the other cases. There is a richer set of singularities as well as possible mode collisions with what is most likely unphysical modes. Nevertheless, we show that there is a general criteria for where the singularities are allowed to be, that applies to all of these theories.

8.2 Open questions

The work in this thesis answers questions about the gradient expansion and hydrodynamic attractors, but at the same time opens up new questions and directions. We formulate some of these here.

In this work, we have considered the applicability of hydrodynamics from the perspective of how well the gradient expansion encodes the dissipative effects of the underlying microscopic theory. The answer to this is set by nonhydrodynamic modes. Something that deserves further exploration is optimal truncation. Where should the gradient expansion be truncated to achieve the greatest accuracy?

There are different choices one can make when constructing the gradient expansion, by converting between spatial and time derivatives. In Article F, we studied two cases. One with only spatial derivatives and one with only time derivatives. These have slightly different convergence properties. The spatial expansion is governed by $\omega(k)$, while the other expansion by $k(\omega)$. Is there a deeper understanding that puts different choices of the gradient expansion and different combinations of ω and k on an equal footing? Related to this, one can consider modes around a boosted equilibrium, which also mixes ω and k in a non-trivial way.

Several assumptions and choices in this thesis can be reconsidered. These include choosing other hydrodynamic frame than the Landau frame, breaking conformality or including the effects of fluctuations. The first two would certainly modify some technical details of the calculations, but it's hard to see why it would lead to any qualitative change in the conclusions. However, the inclusion of fluctuations changes the character of the gradient expansion considerably, allowing for new non-analytic terms. How such terms affect the large order behaviour is unknown.

There are questions remaining about RTA. The Borel analysis gave rise to unphysical singularities in Articles A and B. At the same time, the mode structure in the linearized analysis in Article E features mysterious modes living on non-principal sheets of the retarded Green's functions. Whether there is a link between these, or what the latter modes really mean is not known.

RTA is a toy model, with some serious deficiencies [174], but has been essential for getting analytic control of the weakly coupled case. An important question is what of the analysis in RTA applies to more realistic models in kinetic theory.

While in most cases the gradient expansion diverges, there are some exceptions. The exceptions in the linear case are understood, see Article F, but how should the nonlinear exceptions [133, 134] be understood?

Bibliography

- [1] Michal P. Heller et al. Hydrodynamization in Kinetic Theory: Transient Modes and the Gradient Expansion. In: *Physical Review D* 97.9 (May 31, 2018), p. 091503. DOI: [10.1103/PhysRevD.97.091503](https://doi.org/10.1103/PhysRevD.97.091503).
- [2] Michal P. Heller and Viktor Svensson. How Does Relativistic Kinetic Theory Remember about Initial Conditions? In: *Physical Review D* 98.5 (Sept. 17, 2018), p. 054016. DOI: [10.1103/PhysRevD.98.054016](https://doi.org/10.1103/PhysRevD.98.054016).
- [3] Michal P. Heller et al. Hydrodynamic Attractors in Phase Space. In: *Physical Review Letters* 125.13 (Sept. 22, 2020), p. 132301. DOI: [10.1103/PhysRevLett.125.132301](https://doi.org/10.1103/PhysRevLett.125.132301).
- [4] Michal P. Heller et al. Transseries for Causal Diffusive Systems. In: *Journal of High Energy Physics* 2021.4 (Apr. 20, 2021), p. 192. DOI: [10.1007/JHEP04\(2021\)192](https://doi.org/10.1007/JHEP04(2021)192).
- [5] Michal P. Heller et al. Convergence of Hydrodynamic Modes: Insights from Kinetic Theory and Holography. In: *SciPost Physics* 10.6 (June 1, 2021), p. 123. DOI: [10.21468/SciPostPhys.10.6.123](https://doi.org/10.21468/SciPostPhys.10.6.123).
- [6] Michal P. Heller et al. The Hydrodynamic Gradient Expansion in Linear Response Theory. July 10, 2020. URL: <https://arxiv.org/abs/2007.05524v1>.
- [7] Mari Carmen Bañuls et al. From Spin Chains to Real-Time Thermal Field Theory Using Tensor Networks. In: *Physical Review Research* 2.3 (Aug. 25, 2020), p. 033301. DOI: [10.1103/PhysRevResearch.2.033301](https://doi.org/10.1103/PhysRevResearch.2.033301).
- [8] Carl Eckart. The Thermodynamics of Irreversible Processes. III. Relativistic Theory of the Simple Fluid. In: *Physical Review* 58.10 (Nov. 15, 1940), pp. 919–924. DOI: [10.1103/PhysRev.58.919](https://doi.org/10.1103/PhysRev.58.919).
- [9] L. D. Landau and E. M. Lifshitz. *Fluid Mechanics*. 2nd ed. Vol. 6. Landau and Lifshitz: Course of Theoretical Physics. Pergamon, 1987. 554 pp.
- [10] Ulrich Heinz and Raimond Snellings. Collective Flow and Viscosity in Relativistic Heavy-Ion Collisions. In: *Annual Review of Nuclear and Particle Science* 63.1 (Oct. 19, 2013), pp. 123–151. DOI: [10.1146/annurev-nucl-102212-170540](https://doi.org/10.1146/annurev-nucl-102212-170540).
- [11] Paul Romatschke and Ulrike Romatschke. *Relativistic Fluid Dynamics In and Out of Equilibrium – Ten Years of Progress in Theory and Numerical Simulations of Nuclear Collisions*. May 17, 2019. arXiv: [1712.05815](https://arxiv.org/abs/1712.05815) [[astro-ph](#), [physics:cond-mat](#), [physics:hep-th](#), [physics:nucl-th](#)]. URL: <http://arxiv.org/abs/1712.05815>.
- [12] Wojciech Florkowski, Michal P. Heller, and Michał Spaliński. New Theories of Relativistic Hydrodynamics in the LHC Era. In: *Reports on Progress in Physics* 81.4 (Feb. 2018), p. 046001. DOI: [10.1088/1361-6633/aaa091](https://doi.org/10.1088/1361-6633/aaa091).
- [13] Mubarak Alqahtani, Mohammad Nopoush, and Michael Strickland. Relativistic Anisotropic Hydrodynamics. In: *Progress in Particle and Nuclear Physics* 101 (July 1, 2018), pp. 204–248. DOI: [10.1016/j.pnpnp.2018.05.004](https://doi.org/10.1016/j.pnpnp.2018.05.004).

- [14] Michał P. Heller and Michał Spaliński. Hydrodynamics Beyond the Gradient Expansion: Resurgence and Resummation. In: *Physical Review Letters* 115.7 (Aug. 14, 2015), p. 072501. doi: [10.1103/PhysRevLett.115.072501](https://doi.org/10.1103/PhysRevLett.115.072501).
- [15] L. Adamczyk et al. Global Λ Hyperon Polarization in Nuclear Collisions. In: *Nature* 548.7665 (7665 Aug. 2017), pp. 62–65. doi: [10.1038/nature23004](https://doi.org/10.1038/nature23004).
- [16] Samapan Bhadury et al. *New Developments in Relativistic Fluid Dynamics with Spin*. Jan. 28, 2021. arXiv: [2101.11964](https://arxiv.org/abs/2101.11964) [hep-ph, physics:nucl-th]. URL: <http://arxiv.org/abs/2101.11964>.
- [17] N. Andersson and G. L. C. Comer. *Relativistic Fluid Dynamics: Physics for Many Different Scales*. Aug. 27, 2020. arXiv: [2008.12069](https://arxiv.org/abs/2008.12069) [gr-qc]. URL: <http://arxiv.org/abs/2008.12069>.
- [18] Luca Baiotti and Luciano Rezzolla. *Binary Neutron-Star Mergers: A Review of Einstein’s Richest Laboratory*. Mar. 22, 2017. doi: [10.1088/1361-6633/aa67bb](https://doi.org/10.1088/1361-6633/aa67bb). arXiv: [1607.03540](https://arxiv.org/abs/1607.03540) [astro-ph, physics:gr-qc].
- [19] Iver Brevik et al. Viscous Cosmology for Early- and Late-Time Universe. In: *International Journal of Modern Physics D* 26.14 (July 17, 2017), p. 1730024. doi: [10.1142/S0218271817300245](https://doi.org/10.1142/S0218271817300245).
- [20] LIGO Scientific Collaboration and Virgo Collaboration et al. Observation of Gravitational Waves from a Binary Black Hole Merger. In: *Physical Review Letters* 116.6 (Feb. 11, 2016), p. 061102. doi: [10.1103/PhysRevLett.116.061102](https://doi.org/10.1103/PhysRevLett.116.061102).
- [21] Boris N. Narozhny et al. Hydrodynamic Approach to Electronic Transport in Graphene. In: *Annalen der Physik* 529.11 (2017), p. 1700043. doi: [10.1002/andp.201700043](https://doi.org/10.1002/andp.201700043).
- [22] Andrew Lucas and Kin Chung Fong. Hydrodynamics of Electrons in Graphene. In: *Journal of Physics: Condensed Matter* 30.5 (Feb. 7, 2018), p. 053001. doi: [10.1088/1361-648X/aaa274](https://doi.org/10.1088/1361-648X/aaa274). arXiv: [1710.08425](https://arxiv.org/abs/1710.08425).
- [23] Pavel Kovtun. Lectures on Hydrodynamic Fluctuations in Relativistic Theories. In: *Journal of Physics A: Mathematical and Theoretical* 45.47 (Nov. 2012), p. 473001. doi: [10.1088/1751-8113/45/47/473001](https://doi.org/10.1088/1751-8113/45/47/473001).
- [24] Fábio S. Bemfica, Marcelo M. Disconzi, and Jorge Noronha. Nonlinear Causality of General First-Order Relativistic Viscous Hydrodynamics. In: *Physical Review D* 100.10 (Nov. 11, 2019), p. 104020. doi: [10.1103/PhysRevD.100.104020](https://doi.org/10.1103/PhysRevD.100.104020). arXiv: [1907.12695](https://arxiv.org/abs/1907.12695).
- [25] Paolo Glorioso and Hong Liu. *Lectures on Non-Equilibrium Effective Field Theories and Fluctuating Hydrodynamics*. May 23, 2018. arXiv: [1805.09331](https://arxiv.org/abs/1805.09331) [cond-mat, physics:gr-qc, physics:hep-th, physics:nucl-th]. URL: <http://arxiv.org/abs/1805.09331>.
- [26] Marcus Bluhm et al. Dynamics of Critical Fluctuations: Theory – Phenomenology – Heavy-Ion Collisions. In: *Nuclear Physics A* 1003 (Nov. 1, 2020), p. 122016. doi: [10.1016/j.nuclphysa.2020.122016](https://doi.org/10.1016/j.nuclphysa.2020.122016).
- [27] Sašo Grozdanov, Koenraad Schalm, and Vincenzo Scopelliti. Black Hole Scrambling from Hydrodynamics. In: *Physical Review Letters* 120.23 (June 7, 2018), p. 231601. doi: [10.1103/PhysRevLett.120.231601](https://doi.org/10.1103/PhysRevLett.120.231601).
- [28] Mike Blake, Hyunseok Lee, and Hong Liu. A Quantum Hydrodynamical Description for Scrambling and Many-Body Chaos. In: *Journal of High Energy Physics* 2018.10 (Oct. 19, 2018), p. 127. doi: [10.1007/JHEP10\(2018\)127](https://doi.org/10.1007/JHEP10(2018)127).

- [29] Changha Choi, Márk Mezei, and Gábor Sárosi. Pole Skipping Away from Maximal Chaos. In: *Journal of High Energy Physics* 2021.2 (Feb. 24, 2021), p. 207. DOI: [10.1007/JHEP02\(2021\)207](https://doi.org/10.1007/JHEP02(2021)207).
- [30] Benjamin Doyon. Lecture Notes on Generalised Hydrodynamics. In: *SciPost Physics Lecture Notes* (Aug. 28, 2020), p. 018. DOI: [10.21468/SciPostPhysLectNotes.18](https://doi.org/10.21468/SciPostPhysLectNotes.18).
- [31] J. Adams et al. Experimental and Theoretical Challenges in the Search for the Quark–Gluon Plasma: The STAR Collaboration’s Critical Assessment of the Evidence from RHIC Collisions. In: *Nuclear Physics A. First Three Years of Operation of RHIC 757.1* (Aug. 8, 2005), pp. 102–183. DOI: [10.1016/j.nuclphysa.2005.03.085](https://doi.org/10.1016/j.nuclphysa.2005.03.085).
- [32] K. Adcox et al. Formation of Dense Partonic Matter in Relativistic Nucleus–Nucleus Collisions at RHIC: Experimental Evaluation by the PHENIX Collaboration. In: *Nuclear Physics A. First Three Years of Operation of RHIC 757.1* (Aug. 8, 2005), pp. 184–283. DOI: [10.1016/j.nuclphysa.2005.03.086](https://doi.org/10.1016/j.nuclphysa.2005.03.086).
- [33] I. Arsene et al. Quark–Gluon Plasma and Color Glass Condensate at RHIC? The Perspective from the BRAHMS Experiment. In: *Nuclear Physics A. First Three Years of Operation of RHIC 757.1* (Aug. 8, 2005), pp. 1–27. DOI: [10.1016/j.nuclphysa.2005.02.130](https://doi.org/10.1016/j.nuclphysa.2005.02.130).
- [34] B. B. Back et al. The PHOBOS Perspective on Discoveries at RHIC. In: *Nuclear Physics A. First Three Years of Operation of RHIC 757.1* (Aug. 8, 2005), pp. 28–101. DOI: [10.1016/j.nuclphysa.2005.03.084](https://doi.org/10.1016/j.nuclphysa.2005.03.084).
- [35] Miklos Gyulassy and Larry McLerran. New Forms of QCD Matter Discovered at RHIC. In: *Nuclear Physics A. Quark-Gluon Plasma. New Discoveries at RHIC: Case for the Strongly Interacting Quark-Gluon Plasma. Contributions from the RBRC Workshop Held May 14-15, 2004 750.1* (Mar. 21, 2005), pp. 30–63. DOI: [10.1016/j.nuclphysa.2004.10.034](https://doi.org/10.1016/j.nuclphysa.2004.10.034).
- [36] Edward Shuryak. What RHIC Experiments and Theory Tell Us about Properties of Quark–Gluon Plasma? In: *Nuclear Physics A. Quark-Gluon Plasma. New Discoveries at RHIC: Case for the Strongly Interacting Quark-Gluon Plasma. Contributions from the RBRC Workshop Held May 14-15, 2004 750.1* (Mar. 21, 2005), pp. 64–83. DOI: [10.1016/j.nuclphysa.2004.10.022](https://doi.org/10.1016/j.nuclphysa.2004.10.022).
- [37] Peter Braun-Munzinger et al. Properties of Hot and Dense Matter from Relativistic Heavy Ion Collisions. In: *Physics Reports. Memorial Volume in Honor of Gerald E. Brown 621* (Mar. 21, 2016), pp. 76–126. DOI: [10.1016/j.physrep.2015.12.003](https://doi.org/10.1016/j.physrep.2015.12.003).
- [38] Panagiota Foka and Malgorzata Anna Janik. An Overview of Experimental Results from Ultra-Relativistic Heavy-Ion Collisions at the CERN LHC: Bulk Properties and Dynamical Evolution. In: *Reviews in Physics* 1 (Nov. 2016), pp. 154–171. DOI: [10.1016/j.revip.2016.11.002](https://doi.org/10.1016/j.revip.2016.11.002). arXiv: [1702.07233](https://arxiv.org/abs/1702.07233).
- [39] Wit Busza, Krishna Rajagopal, and Wilke van der Schee. Heavy Ion Collisions: The Big Picture and the Big Questions. In: *Annual Review of Nuclear and Particle Science* 68.1 (2018), pp. 339–376. DOI: [10.1146/annurev-nucl-101917-020852](https://doi.org/10.1146/annurev-nucl-101917-020852).

- [40] S. Schlichting and D. Teaney. The First Fm/c of Heavy-Ion Collisions. In: *Annual Review of Nuclear and Particle Science* 69.1 (Oct. 19, 2019), pp. 447–476. DOI: [10.1146/annurev-nucl-101918-023825](https://doi.org/10.1146/annurev-nucl-101918-023825).
- [41] Jürgen Berges et al. *Thermalization in QCD: Theoretical Approaches, Phenomenological Applications, and Interdisciplinary Connections*. June 3, 2020. arXiv: [2005.12299](https://arxiv.org/abs/2005.12299) [cond-mat, physics:hep-ph, physics:hep-th, physics:nucl-th, physics:quant-ph]. URL: <http://arxiv.org/abs/2005.12299>.
- [42] Francois Gelis et al. The Color Glass Condensate. In: *Annual Review of Nuclear and Particle Science* 60.1 (2010), pp. 463–489. DOI: [10.1146/annurev.nucl.010909.083629](https://doi.org/10.1146/annurev.nucl.010909.083629).
- [43] Paul M. Chesler and Laurence G. Yaffe. Boost Invariant Flow, Black Hole Formation, and Far-from-Equilibrium Dynamics in $\mathcal{N}=4$ Supersymmetric Yang-Mills Theory. In: *Physical Review D* 82.2 (July 19, 2010), p. 026006. DOI: [10.1103/PhysRevD.82.026006](https://doi.org/10.1103/PhysRevD.82.026006).
- [44] Michal P. Heller, Romuald A. Janik, and Przemysław Witaszczyk. Characteristics of Thermalization of Boost-Invariant Plasma from Holography. In: *Physical Review Letters* 108.20 (May 18, 2012), p. 201602. DOI: [10.1103/PhysRevLett.108.201602](https://doi.org/10.1103/PhysRevLett.108.201602).
- [45] Jorge Casalderrey-Solana et al. From Full Stopping to Transparency in a Holographic Model of Heavy Ion Collisions. In: *Physical Review Letters* 111.18 (Oct. 29, 2013), p. 181601. DOI: [10.1103/PhysRevLett.111.181601](https://doi.org/10.1103/PhysRevLett.111.181601).
- [46] Aleksi Kurkela and Yan Zhu. Isotropization and Hydrodynamization in Weakly Coupled Heavy-Ion Collisions. In: *Physical Review Letters* 115.18 (Oct. 27, 2015), p. 182301. DOI: [10.1103/PhysRevLett.115.182301](https://doi.org/10.1103/PhysRevLett.115.182301).
- [47] P. Romatschke. Do Nuclear Collisions Create a Locally Equilibrated Quark–Gluon Plasma? In: *The European Physical Journal C* 77.1 (Jan. 10, 2017), p. 21. DOI: [10.1140/epjc/s10052-016-4567-x](https://doi.org/10.1140/epjc/s10052-016-4567-x).
- [48] Mauricio Martinez and Michael Strickland. Dissipative Dynamics of Highly Anisotropic Systems. In: *Nuclear Physics A* 848.1 (Dec. 15, 2010), pp. 183–197. DOI: [10.1016/j.nuclphysa.2010.08.011](https://doi.org/10.1016/j.nuclphysa.2010.08.011).
- [49] Wojciech Florkowski and Radosław Ryblewski. Highly Anisotropic and Strongly Dissipative Hydrodynamics for Early Stages of Relativistic Heavy-Ion Collisions. In: *Physical Review C* 83.3 (Mar. 21, 2011), p. 034907. DOI: [10.1103/PhysRevC.83.034907](https://doi.org/10.1103/PhysRevC.83.034907).
- [50] Piotr Bożek. Collective Flow in \sqrt{s} -Pb and \sqrt{s} -Pb Collisions at TeV Energies. In: *Physical Review C* 85.1 (Jan. 30, 2012), p. 014911. DOI: [10.1103/PhysRevC.85.014911](https://doi.org/10.1103/PhysRevC.85.014911).
- [51] Piotr Bożek and Wojciech Broniowski. Correlations from Hydrodynamic Flow in pPb Collisions. In: *Physics Letters B* 718.4 (Jan. 29, 2013), pp. 1557–1561. DOI: [10.1016/j.physletb.2012.12.051](https://doi.org/10.1016/j.physletb.2012.12.051).
- [52] Piotr Bożek and Wojciech Broniowski. Collective Dynamics in High-Energy Proton-Nucleus Collisions. In: *Physical Review C* 88.1 (July 8, 2013), p. 014903. DOI: [10.1103/PhysRevC.88.014903](https://doi.org/10.1103/PhysRevC.88.014903).
- [53] M. Habich et al. Testing Hydrodynamic Descriptions of P+p Collisions at $\sqrt{s}=7\sqrt{s}$ TeV. In: *The European Physical Journal C* 76.7 (July 19, 2016), p. 408. DOI: [10.1140/epjc/s10052-016-4237-z](https://doi.org/10.1140/epjc/s10052-016-4237-z).

- [54] Michał Spaliński. Small Systems and Regulator Dependence in Relativistic Hydrodynamics. In: *Physical Review D* 94.8 (Oct. 3, 2016), p. 085002. DOI: [10.1103/PhysRevD.94.085002](https://doi.org/10.1103/PhysRevD.94.085002).
- [55] Ryan D. Weller and Paul Romatschke. *One Fluid to Rule Them All: Viscous Hydrodynamic Description of Event-by-Event Central P+p, P+Pb and Pb+Pb Collisions at $\sqrt{s}=5.02$ TeV*. Jan. 24, 2017. DOI: [10.1016/j.physletb.2017.09.077](https://doi.org/10.1016/j.physletb.2017.09.077). arXiv: [1701.07145](https://arxiv.org/abs/1701.07145) [hep-ph, physics:nucl-ex, physics:nucl-th].
- [56] V. Khachatryan et al. Evidence for Collectivity in Pp Collisions at the LHC. In: *Physics Letters B* 765 (Feb. 10, 2017), pp. 193–220. DOI: [10.1016/j.physletb.2016.12.009](https://doi.org/10.1016/j.physletb.2016.12.009).
- [57] J. L. Nagle and W. A. Zajc. Small System Collectivity in Relativistic Hadron and Nuclear Collisions. In: *Annual Review of Nuclear and Particle Science* 68.1 (Oct. 19, 2018), pp. 211–235. DOI: [10.1146/annurev-nucl-101916-123209](https://doi.org/10.1146/annurev-nucl-101916-123209). arXiv: [1801.03477](https://arxiv.org/abs/1801.03477).
- [58] Ulrich Heinz and J. Scott Moreland. Hydrodynamic Flow in Small Systems or: “How the Heck Is It Possible That a System Emitting Only a Dozen Particles Can Be Described by Fluid Dynamics?” In: *Journal of Physics: Conference Series* 1271.1 (July 1, 2019), p. 012018. DOI: [10.1088/1742-6596/1271/1/012018](https://doi.org/10.1088/1742-6596/1271/1/012018).
- [59] J. D. Bjorken. Highly Relativistic Nucleus-Nucleus Collisions: The Central Rapidity Region. In: *Physical Review D* 27.1 (Jan. 1, 1983), pp. 140–151. DOI: [10.1103/PhysRevD.27.140](https://doi.org/10.1103/PhysRevD.27.140).
- [60] Yoshitaka Hatta, Jorge Noronha, and Bo-Wen Xiao. Systematic Study of Exact Solutions in Second-Order Conformal Hydrodynamics. In: *Physical Review D* 89.11 (June 9, 2014), p. 114011. DOI: [10.1103/PhysRevD.89.114011](https://doi.org/10.1103/PhysRevD.89.114011).
- [61] Michał P. Heller, Romuald A. Janik, and Przemysław Witaszczyk. Hydrodynamic Gradient Expansion in Gauge Theory Plasmas. In: *Physical Review Letters* 110.21 (May 22, 2013), p. 211602. DOI: [10.1103/PhysRevLett.110.211602](https://doi.org/10.1103/PhysRevLett.110.211602).
- [62] Wojciech Florkowski, Radosław Ryblewski, and Michael Strickland. Testing Viscous and Anisotropic Hydrodynamics in an Exactly Solvable Case. In: *Physical Review C* 88.2 (Aug. 7, 2013), p. 024903. DOI: [10.1103/PhysRevC.88.024903](https://doi.org/10.1103/PhysRevC.88.024903).
- [63] Steven S. Gubser. Symmetry Constraints on Generalizations of Bjorken Flow. In: *Physical Review D* 82.8 (Oct. 26, 2010), p. 085027. DOI: [10.1103/PhysRevD.82.085027](https://doi.org/10.1103/PhysRevD.82.085027).
- [64] Steven S. Gubser and Amos Yarom. Conformal Hydrodynamics in Minkowski and de Sitter Spacetimes. In: *Nuclear Physics B* 846.3 (May 21, 2011), pp. 469–511. DOI: [10.1016/j.nuclphysb.2011.01.012](https://doi.org/10.1016/j.nuclphysb.2011.01.012).
- [65] Gabriel S. Denicol and Jorge Noronha. Hydrodynamic Attractor and the Fate of Perturbative Expansions in Gubser Flow. In: *Physical Review D* 99.11 (June 10, 2019), p. 116004. DOI: [10.1103/PhysRevD.99.116004](https://doi.org/10.1103/PhysRevD.99.116004).
- [66] Sybren Ruurds Groot et al. *Relativistic Kinetic Theory: Principles and Applications*. North-Holland Publishing Company, 1980. 444 pp.
- [67] Harold Grad. On the Kinetic Theory of Rarefied Gases. In: *Communications on Pure and Applied Mathematics* 2.4 (1949), pp. 331–407. DOI: [10.1002/cpa.3160020403](https://doi.org/10.1002/cpa.3160020403).

- [68] Werner Israel. Nonstationary Irreversible Thermodynamics: A Causal Relativistic Theory. In: *Annals of Physics* 100.1 (Sept. 10, 1976), pp. 310–331. DOI: [10.1016/0003-4916\(76\)90064-6](https://doi.org/10.1016/0003-4916(76)90064-6).
- [69] W. Israel and J. M. Stewart. Thermodynamics of Nonstationary and Transient Effects in a Relativistic Gas. In: *Physics Letters A* 58.4 (Sept. 6, 1976), pp. 213–215. DOI: [10.1016/0375-9601\(76\)90075-X](https://doi.org/10.1016/0375-9601(76)90075-X).
- [70] B. Betz, D. Henkel, and D. H. Rischke. From Kinetic Theory to Dissipative Fluid Dynamics. In: *Progress in Particle and Nuclear Physics*. Heavy-Ion Collisions from the Coulomb Barrier to the Quark-Gluon Plasma 62.2 (Apr. 1, 2009), pp. 556–561. DOI: [10.1016/j.pnpnp.2008.12.018](https://doi.org/10.1016/j.pnpnp.2008.12.018).
- [71] Andrej El, Zhe Xu, and Carsten Greiner. Extension of Relativistic Dissipative Hydrodynamics to Third Order. In: *Physical Review C* 81.4 (Apr. 6, 2010), p. 041901. DOI: [10.1103/PhysRevC.81.041901](https://doi.org/10.1103/PhysRevC.81.041901).
- [72] G. S. Denicol, T. Koide, and D. H. Rischke. Dissipative Relativistic Fluid Dynamics: A New Way to Derive the Equations of Motion from Kinetic Theory. In: *Physical Review Letters* 105.16 (Oct. 12, 2010), p. 162501. DOI: [10.1103/PhysRevLett.105.162501](https://doi.org/10.1103/PhysRevLett.105.162501).
- [73] G. S. Denicol et al. Derivation of Fluid Dynamics from Kinetic Theory with the 14-Moment Approximation. In: *The European Physical Journal A* 48.11 (Nov. 28, 2012), p. 170. DOI: [10.1140/epja/i2012-12170-x](https://doi.org/10.1140/epja/i2012-12170-x).
- [74] G. S. Denicol et al. Derivation of Transient Relativistic Fluid Dynamics from the Boltzmann Equation. In: *Physical Review D* 85.11 (June 26, 2012), p. 114047. DOI: [10.1103/PhysRevD.85.114047](https://doi.org/10.1103/PhysRevD.85.114047).
- [75] Amaresh Jaiswal. Relativistic Third-Order Dissipative Fluid Dynamics from Kinetic Theory. In: *Physical Review C* 88.2 (Aug. 30, 2013), p. 021903. DOI: [10.1103/PhysRevC.88.021903](https://doi.org/10.1103/PhysRevC.88.021903).
- [76] G. S. Denicol. Kinetic Foundations of Relativistic Dissipative Fluid Dynamics. In: *Journal of Physics G: Nuclear and Particle Physics* 41.12 (Nov. 2014), p. 124004. DOI: [10.1088/0954-3899/41/12/124004](https://doi.org/10.1088/0954-3899/41/12/124004).
- [77] P. L. Bhatnagar, E. P. Gross, and M. Krook. A Model for Collision Processes in Gases. I. Small Amplitude Processes in Charged and Neutral One-Component Systems. In: *Physical Review* 94.3 (May 1, 1954), pp. 511–525. DOI: [10.1103/PhysRev.94.511](https://doi.org/10.1103/PhysRev.94.511).
- [78] J. L. Anderson and H. R. Witting. A Relativistic Relaxation-Time Model for the Boltzmann Equation. In: *Physica* 74.3 (June 15, 1974), pp. 466–488. DOI: [10.1016/0031-8914\(74\)90355-3](https://doi.org/10.1016/0031-8914(74)90355-3).
- [79] Juan Maldacena. The Large-N Limit of Superconformal Field Theories and Supergravity. In: *International Journal of Theoretical Physics* 38.4 (Apr. 1, 1999), pp. 1113–1133. DOI: [10.1023/A:1026654312961](https://doi.org/10.1023/A:1026654312961).
- [80] S. S. Gubser, I. R. Klebanov, and A. M. Polyakov. Gauge Theory Correlators from Non-Critical String Theory. In: *Physics Letters B* 428.1 (May 28, 1998), pp. 105–114. DOI: [10.1016/S0370-2693\(98\)00377-3](https://doi.org/10.1016/S0370-2693(98)00377-3).
- [81] Edward Witten. Anti de Sitter Space and Holography. In: *Advances in Theoretical and Mathematical Physics* 2.2 (Mar. 1998), pp. 253–291. DOI: [10.4310/ATMP.1998.v2.n2.a2](https://doi.org/10.4310/ATMP.1998.v2.n2.a2).

- [82] Ofer Aharony et al. Large N Field Theories, String Theory and Gravity. In: *Physics Reports* 323.3 (Jan. 1, 2000), pp. 183–386. DOI: [10.1016/S0370-1573\(99\)00083-6](https://doi.org/10.1016/S0370-1573(99)00083-6).
- [83] Martin Ammon and Johanna Erdmenger. *Gauge/Gravity Duality: Foundations and Applications*. Cambridge University Press, 2015. URL: <https://www.cambridge.org/us/academic/subjects/physics/theoretical-physics-and-mathematical-physics/gaugegravity-duality-foundations-and-applications>, %20https://www.cambridge.org/us/academic/subjects/physics/theoretical-physics-and-mathematical-physics.
- [84] Alberto Güijosa. QCD, with Strings Attached. In: *International Journal of Modern Physics E* 25.10 (Oct. 1, 2016), p. 1630006. DOI: [10.1142/S021830131630006X](https://doi.org/10.1142/S021830131630006X).
- [85] Jorge Casalderrey-Solana et al. *Gauge/String Duality, Hot QCD and Heavy Ion Collisions*. Aug. 8, 2012. arXiv: [1101.0618](https://arxiv.org/abs/1101.0618) [cond-mat, physics:hep-ph, physics:hep-th, physics:nucl-th]. URL: <http://arxiv.org/abs/1101.0618>.
- [86] Paul M. Chesler and Wilke van der Schee. Early Thermalization, Hydrodynamics and Energy Loss in AdS/CFT. In: *International Journal of Modern Physics E* 24.10 (Sept. 22, 2015), p. 1530011. DOI: [10.1142/S0218301315300118](https://doi.org/10.1142/S0218301315300118).
- [87] Michal P. Heller. Holography, Hydrodynamization and Heavy-Ion Collisions. In: *Acta Physica Polonica B* 47.12 (2016), p. 2581. DOI: [10.5506/APhysPolB.47.2581](https://doi.org/10.5506/APhysPolB.47.2581). arXiv: [1610.02023](https://arxiv.org/abs/1610.02023).
- [88] Sean A. Hartnoll, Andrew Lucas, and Subir Sachdev. *Holographic Quantum Matter*. Mar. 20, 2018. arXiv: [1612.07324](https://arxiv.org/abs/1612.07324) [cond-mat, physics:hep-th]. URL: <http://arxiv.org/abs/1612.07324>.
- [89] Sayantani Bhattacharyya et al. Nonlinear Fluid Dynamics from Gravity. In: *Journal of High Energy Physics* 2008.02 (Feb. 2008), pp. 045–045. DOI: [10.1088/1126-6708/2008/02/045](https://doi.org/10.1088/1126-6708/2008/02/045).
- [90] Rudolf Baier et al. Relativistic Viscous Hydrodynamics, Conformal Invariance, and Holography. In: *Journal of High Energy Physics* 2008.04 (Apr. 2008), pp. 100–100. DOI: [10.1088/1126-6708/2008/04/100](https://doi.org/10.1088/1126-6708/2008/04/100).
- [91] Sašo Grozdanov and Nikolaos Kaplis. Constructing Higher-Order Hydrodynamics: The Third Order. In: *Physical Review D* 93.6 (Mar. 25, 2016), p. 066012. DOI: [10.1103/PhysRevD.93.066012](https://doi.org/10.1103/PhysRevD.93.066012).
- [92] Saulo M. Diles et al. Third-Order Relativistic Hydrodynamics: Dispersion Relations and Transport Coefficients of a Dual Plasma. In: *Journal of High Energy Physics* 2020.5 (5 May 1, 2020), pp. 1–40. DOI: [10.1007/JHEP05\(2020\)019](https://doi.org/10.1007/JHEP05(2020)019).
- [93] M. Lublinsky and E. Shuryak. How Much Entropy Is Produced in Strongly Coupled Quark-Gluon Plasma (sQGP) by Dissipative Effects? In: *Physical Review C* 76.2 (Aug. 2, 2007), p. 021901. DOI: [10.1103/PhysRevC.76.021901](https://doi.org/10.1103/PhysRevC.76.021901).
- [94] M. Lublinsky and E. Shuryak. Improved Hydrodynamics from the AdS/CFT Duality. In: *Physical Review D* 80.6 (Sept. 24, 2009), p. 065026. DOI: [10.1103/PhysRevD.80.065026](https://doi.org/10.1103/PhysRevD.80.065026).

- [95] Yanyan Bu and Michael Lublinsky. All Order Linearized Hydrodynamics from Fluid-Gravity Correspondence. In: *Physical Review D* 90.8 (Oct. 3, 2014), p. 086003. DOI: [10.1103/PhysRevD.90.086003](https://doi.org/10.1103/PhysRevD.90.086003).
- [96] Yanyan Bu and Michael Lublinsky. Linearized Fluid/Gravity Correspondence: From Shear Viscosity to All Order Hydrodynamics. In: *Journal of High Energy Physics* 2014.11 (11 Nov. 1, 2014), pp. 1–33. DOI: [10.1007/JHEP11\(2014\)064](https://doi.org/10.1007/JHEP11(2014)064).
- [97] William A. Hiscock and Lee Lindblom. Generic Instabilities in First-Order Dissipative Relativistic Fluid Theories. In: *Physical Review D* 31.4 (Feb. 15, 1985), pp. 725–733. DOI: [10.1103/PhysRevD.31.725](https://doi.org/10.1103/PhysRevD.31.725).
- [98] William A. Hiscock and Lee Lindblom. Linear Plane Waves in Dissipative Relativistic Fluids. In: *Physical Review D* 35.12 (June 15, 1987), pp. 3723–3732. DOI: [10.1103/PhysRevD.35.3723](https://doi.org/10.1103/PhysRevD.35.3723).
- [99] Ingo Müller. Zum Paradoxon der Wärmeleitungstheorie. In: *Zeitschrift für Physik* 198.4 (Aug. 1, 1967), pp. 329–344. DOI: [10.1007/BF01326412](https://doi.org/10.1007/BF01326412).
- [100] J. M. Stewart and Stephen William Hawking. On Transient Relativistic Thermodynamics and Kinetic Theory. In: *Proceedings of the Royal Society of London. A. Mathematical and Physical Sciences* 357.1688 (Oct. 10, 1977), pp. 59–75. DOI: [10.1098/rspa.1977.0155](https://doi.org/10.1098/rspa.1977.0155).
- [101] W. Israel and J. M. Stewart. Transient Relativistic Thermodynamics and Kinetic Theory. In: *Annals of Physics* 118.2 (Apr. 1, 1979), pp. 341–372. DOI: [10.1016/0003-4916\(79\)90130-1](https://doi.org/10.1016/0003-4916(79)90130-1).
- [102] William A Hiscock and Lee Lindblom. Stability and Causality in Dissipative Relativistic Fluids. In: *Annals of Physics* 151.2 (Dec. 1, 1983), pp. 466–496. DOI: [10.1016/0003-4916\(83\)90288-9](https://doi.org/10.1016/0003-4916(83)90288-9).
- [103] P. Ván and T. S. Biró. First Order and Stable Relativistic Dissipative Hydrodynamics. In: *Physics Letters B* 709.1 (Mar. 13, 2012), pp. 106–110. DOI: [10.1016/j.physletb.2012.02.006](https://doi.org/10.1016/j.physletb.2012.02.006).
- [104] Pavel Kovtun. First-Order Relativistic Hydrodynamics Is Stable. In: *Journal of High Energy Physics* 2019.10 (Oct. 2019). DOI: [10.1007/JHEP10\(2019\)034](https://doi.org/10.1007/JHEP10(2019)034).
- [105] Fabio S. Bemfica, Marcelo M. Disconzi, and Jorge Noronha. Causality and Existence of Solutions of Relativistic Viscous Fluid Dynamics with Gravity. In: *Physical Review D* 98.10 (Nov. 30, 2018), p. 104064. DOI: [10.1103/PhysRevD.98.104064](https://doi.org/10.1103/PhysRevD.98.104064). arXiv: [1708.06255](https://arxiv.org/abs/1708.06255).
- [106] Fabio S. Bemfica, Marcelo M. Disconzi, and Jorge Noronha. *General-Relativistic Viscous Fluid Dynamics*. Sept. 23, 2020. arXiv: [2009.11388](https://arxiv.org/abs/2009.11388) [gr-qc, physics:hep-ph, physics:hep-th, physics:nucl-th]. URL: <http://arxiv.org/abs/2009.11388>.
- [107] Lorenzo Gavassino, Marco Antonelli, and Brynmor Haskell. When the Entropy Has No Maximum: A New Perspective on the Instability of the First-Order Theories of Dissipation. In: *Phys.Rev.D* 102.4 (2020). DOI: [10.1103/PhysRevD.102.043018](https://doi.org/10.1103/PhysRevD.102.043018).
- [108] Raphael E. Hoult and Pavel Kovtun. Stable and Causal Relativistic Navier-Stokes Equations. In: *Journal of High Energy Physics* 2020.6 (June 9, 2020), p. 67. DOI: [10.1007/JHEP06\(2020\)067](https://doi.org/10.1007/JHEP06(2020)067).

- [109] Aleksi Kurkela et al. Early- and Late-Time Behavior of Attractors in Heavy-Ion Collisions. In: *Physical Review Letters* 124.10 (Mar. 10, 2020), p. 102301. DOI: [10.1103/PhysRevLett.124.102301](https://doi.org/10.1103/PhysRevLett.124.102301).
- [110] Paul Romatschke. Retarded Correlators in Kinetic Theory: Branch Cuts, Poles and Hydrodynamic Onset Transitions. In: *The European Physical Journal C* 76.6 (June 24, 2016), p. 352. DOI: [10.1140/epjc/s10052-016-4169-7](https://doi.org/10.1140/epjc/s10052-016-4169-7).
- [111] Aleksi Kurkela and Urs Achim Wiedemann. Analytic Structure of Nonhydrodynamic Modes in Kinetic Theory. In: *The European Physical Journal C* 79.9 (Sept. 19, 2019), p. 776. DOI: [10.1140/epjc/s10052-019-7271-9](https://doi.org/10.1140/epjc/s10052-019-7271-9).
- [112] Pavel K. Kovtun and Andrei O. Starinets. Quasinormal Modes and Holography. In: *Physical Review D* 72.8 (Oct. 14, 2005), p. 086009. DOI: [10.1103/PhysRevD.72.086009](https://doi.org/10.1103/PhysRevD.72.086009).
- [113] Emanuele Berti, Vitor Cardoso, and Andrei O. Starinets. Quasinormal Modes of Black Holes and Black Branes. In: *Classical and Quantum Gravity* 26.16 (July 24, 2009), p. 163001. DOI: [10.1088/0264-9381/26/16/163001](https://doi.org/10.1088/0264-9381/26/16/163001).
- [114] Sean A. Hartnoll and S. Prem Kumar. AdS Black Holes and Thermal Yang-Mills Correlators. In: *Journal of High Energy Physics* 2005.12 (Dec. 2005), pp. 036–036. DOI: [10.1088/1126-6708/2005/12/036](https://doi.org/10.1088/1126-6708/2005/12/036).
- [115] Sašo Grozdanov, Nikolaos Kaplis, and Andrei O. Starinets. From Strong to Weak Coupling in Holographic Models of Thermalization. In: *Journal of High Energy Physics* 2016.7 (July 29, 2016), p. 151. DOI: [10.1007/JHEP07\(2016\)151](https://doi.org/10.1007/JHEP07(2016)151).
- [116] Jorge Noronha and Gabriel S. Denicol. *Transient Fluid Dynamics of the Quark-Gluon Plasma According to AdS/CFT*. Feb. 5, 2013. arXiv: [1104.2415](https://arxiv.org/abs/1104.2415) [hep-ph, physics:hep-th, physics:nucl-th]. URL: <http://arxiv.org/abs/1104.2415>.
- [117] Michal P. Heller et al. Coupling Hydrodynamics to Nonequilibrium Degrees of Freedom in Strongly Interacting Quark-Gluon Plasma. In: *Physical Review Letters* 113.26 (Dec. 24, 2014), p. 261601. DOI: [10.1103/PhysRevLett.113.261601](https://doi.org/10.1103/PhysRevLett.113.261601).
- [118] Benjamin Withers. Short-Lived Modes from Hydrodynamic Dispersion Relations. In: *Journal of High Energy Physics* 2018.6 (June 11, 2018), p. 59. DOI: [10.1007/JHEP06\(2018\)059](https://doi.org/10.1007/JHEP06(2018)059).
- [119] Sašo Grozdanov et al. The Complex Life of Hydrodynamic Modes. In: *Journal of High Energy Physics* 2019.11 (Nov. 18, 2019), p. 97. DOI: [10.1007/JHEP11\(2019\)097](https://doi.org/10.1007/JHEP11(2019)097).
- [120] Sašo Grozdanov et al. Convergence of the Gradient Expansion in Hydrodynamics. In: *Physical Review Letters* 122.25 (June 28, 2019), p. 251601. DOI: [10.1103/PhysRevLett.122.251601](https://doi.org/10.1103/PhysRevLett.122.251601).
- [121] Philippe Flajolet and Robert Sedgewick. *Analytic Combinatorics*. Cambridge University Press, Jan. 15, 2009. 825 pp.
- [122] Aron Jansen and Christiana Pantelidou. Quasinormal Modes in Charged Fluids at Complex Momentum. In: *Journal of High Energy Physics* 2020.10 (Oct. 19, 2020), p. 121. DOI: [10.1007/JHEP10\(2020\)121](https://doi.org/10.1007/JHEP10(2020)121).
- [123] Frank Olver et al. *NIST Digital Library of Mathematical Functions*. URL: <https://dlmf.nist.gov/>.

- [124] Ovidiu Costin. *Asymptotics and Borel Summability*. 1st ed. Chapman and Hall/CRC, Dec. 4, 2008. DOI: [10.1201/9781420070323](https://doi.org/10.1201/9781420070323).
- [125] Michael Victor Berry and C. J. Howls. Hyperasymptotics for Integrals with Saddles. In: *Proceedings of the Royal Society of London. Series A: Mathematical and Physical Sciences* 434.1892 (Sept. 9, 1991), pp. 657–675. DOI: [10.1098/rspa.1991.0119](https://doi.org/10.1098/rspa.1991.0119).
- [126] Ovidiu Costin and Martin D. Kruskal. On Optimal Truncation of Divergent Series Solutions of Nonlinear Differential Systems. In: *Proceedings of the Royal Society of London. Series A: Mathematical, Physical and Engineering Sciences* 455.1985 (May 8, 1999), pp. 1931–1956. DOI: [10.1098/rspa.1999.0387](https://doi.org/10.1098/rspa.1999.0387).
- [127] C. J. Howls, P. J. Langman, and A. B. Olde Daalhuis. On the Higher-Order Stokes Phenomenon. In: *Proceedings of the Royal Society of London. Series A: Mathematical, Physical and Engineering Sciences* 460.2048 (Aug. 8, 2004), pp. 2285–2303. DOI: [10.1098/rspa.2004.1299](https://doi.org/10.1098/rspa.2004.1299).
- [128] Inês Aniceto, Gökçe Başar, and Ricardo Schiappa. A Primer on Resurgent Transseries and Their Asymptotics. In: *Physics Reports. A Primer on Resurgent Transseries and Their Asymptotics* 809 (May 25, 2019), pp. 1–135. DOI: [10.1016/j.physrep.2019.02.003](https://doi.org/10.1016/j.physrep.2019.02.003).
- [129] John P. Boyd. The Devil’s Invention: Asymptotic, Superasymptotic and Hyperasymptotic Series. In: *Acta Applicandae Mathematica* 56.1 (Mar. 1, 1999), pp. 1–98. DOI: [10.1023/A:1006145903624](https://doi.org/10.1023/A:1006145903624).
- [130] M. Mariño. Lectures on Non-Perturbative Effects in Large N Gauge Theories, Matrix Models and Strings. In: *Fortschritte der Physik* 62.5-6 (2014), pp. 455–540. DOI: [10.1002/prop.201400005](https://doi.org/10.1002/prop.201400005).
- [131] S. Jonathan Chapman and David B Mortimer. Exponential Asymptotics and Stokes Lines in a Partial Differential Equation. In: *Proceedings of the Royal Society A: Mathematical, Physical and Engineering Sciences* 461.2060 (Aug. 8, 2005), pp. 2385–2421. DOI: [10.1098/rspa.2005.1475](https://doi.org/10.1098/rspa.2005.1475).
- [132] S. J. Chapman et al. Why Is a Shock Not a Caustic? The Higher-Order Stokes Phenomenon and Smoothed Shock Formation. In: *Nonlinearity* 20.10 (Sept. 2007), pp. 2425–2452. DOI: [10.1088/0951-7715/20/10/009](https://doi.org/10.1088/0951-7715/20/10/009).
- [133] Gabriel S. Denicol and Jorge Noronha. Analytical Attractor and the Divergence of the Slow-Roll Expansion in Relativistic Hydrodynamics. In: *Physical Review D* 97.5 (Mar. 26, 2018), p. 056021. DOI: [10.1103/PhysRevD.97.056021](https://doi.org/10.1103/PhysRevD.97.056021).
- [134] Gabriel S. Denicol and Jorge Noronha. Exact Hydrodynamic Attractor of an Ultrarelativistic Gas of Hard Spheres. In: *Physical Review Letters* 124.15 (Apr. 13, 2020), p. 152301. DOI: [10.1103/PhysRevLett.124.152301](https://doi.org/10.1103/PhysRevLett.124.152301).
- [135] Harold Grad. Asymptotic Theory of the Boltzmann Equation. In: *The Physics of Fluids* 6.2 (Feb. 1, 1963), pp. 147–181. DOI: [10.1063/1.1706716](https://doi.org/10.1063/1.1706716).
- [136] James A. McLennan. Convergence of the Chapman-Enskog Expansion for the Linearized Boltzmann Equation. In: *The Physics of Fluids* 8.9 (Sept. 1, 1965), pp. 1580–1584. DOI: [10.1063/1.1761467](https://doi.org/10.1063/1.1761467).
- [137] Andres Santos, J. Javier Brey, and James W. Dufty. Divergence of the Chapman-Enskog Expansion. In: *Physical Review Letters* 56.15 (Apr. 14, 1986), pp. 1571–1574. DOI: [10.1103/PhysRevLett.56.1571](https://doi.org/10.1103/PhysRevLett.56.1571).

- [138] Romuald A. Janik and Robi Peschanski. Gauge-Gravity Duality and Thermalization of a Boost-Invariant Perfect Fluid. In: *Physical Review D* 74.4 (Aug. 24, 2006), p. 046007. DOI: [10.1103/PhysRevD.74.046007](https://doi.org/10.1103/PhysRevD.74.046007).
- [139] Gökçe Başar and Gerald V. Dunne. Hydrodynamics, Resurgence, and Transasymptotics. In: *Physical Review D* 92.12 (Dec. 15, 2015), p. 125011. DOI: [10.1103/PhysRevD.92.125011](https://doi.org/10.1103/PhysRevD.92.125011).
- [140] Inês Aniceto et al. The Large Proper-Time Expansion of Yang-Mills Plasma as a Resurgent Transseries. In: *Journal of High Energy Physics* 2019.2 (Feb. 13, 2019), p. 73. DOI: [10.1007/JHEP02\(2019\)073](https://doi.org/10.1007/JHEP02(2019)073).
- [141] Inês Aniceto and Michał Spaliński. *Resurgence in Extended Hydrodynamics*. Mar. 26, 2016. DOI: [10.1103/PhysRevD.93.085008](https://doi.org/10.1103/PhysRevD.93.085008). arXiv: [1511.06358](https://arxiv.org/abs/1511.06358) [hep-th, physics:math-ph].
- [142] Gabriel S. Denicol and Jorge Noronha. *Divergence of the Chapman-Enskog Expansion in Relativistic Kinetic Theory*. Aug. 28, 2016. arXiv: [1608.07869](https://arxiv.org/abs/1608.07869) [hep-ph, physics:hep-th, physics:nucl-th]. URL: <http://arxiv.org/abs/1608.07869>.
- [143] Chandrodoy Chattopadhyay and Ulrich Heinz. Hydrodynamics from Free-Streaming to Thermalization and Back Again. In: *Physics Letters B* 801 (Feb. 10, 2020), p. 135158. DOI: [10.1016/j.physletb.2019.135158](https://doi.org/10.1016/j.physletb.2019.135158).
- [144] Wojciech Florkowski, Radosław Ryblewski, and Michał Spaliński. Gradient Expansion for Anisotropic Hydrodynamics. In: *Physical Review D* 94.11 (Dec. 21, 2016), p. 114025. DOI: [10.1103/PhysRevD.94.114025](https://doi.org/10.1103/PhysRevD.94.114025).
- [145] Jorge Casalderrey-Solana, Nikola I. Gushterov, and Ben Meiring. Resurgence and Hydrodynamic Attractors in Gauss-Bonnet Holography. In: *Journal of High Energy Physics* 2018.4 (Apr. 9, 2018), p. 42. DOI: [10.1007/JHEP04\(2018\)042](https://doi.org/10.1007/JHEP04(2018)042).
- [146] Alex Buchel, Michal P. Heller, and Jorge Noronha. Entropy Production, Hydrodynamics, and Resurgence in the Primordial Quark-Gluon Plasma from Holography. In: *Physical Review D* 94.10 (Nov. 23, 2016), p. 106011. DOI: [10.1103/PhysRevD.94.106011](https://doi.org/10.1103/PhysRevD.94.106011).
- [147] M. Shokri and F. Taghinavaz. Conformal Bjorken Flow in the General Frame and Its Attractor: Similarities and Discrepancies with the Müller-Israel-Stewart Formalism. In: *Physical Review D* 102.3 (Aug. 26, 2020), p. 036022. DOI: [10.1103/PhysRevD.102.036022](https://doi.org/10.1103/PhysRevD.102.036022).
- [148] Alireza Behtash et al. Dynamical Systems and Nonlinear Transient Rheology of the Far-from-Equilibrium Bjorken Flow. In: *Physical Review D* 99.11 (June 14, 2019), p. 116012. DOI: [10.1103/PhysRevD.99.116012](https://doi.org/10.1103/PhysRevD.99.116012).
- [149] Alireza Behtash et al. Non-Perturbative Rheological Behavior of a Far-from-Equilibrium Expanding Plasma. In: *Physics Letters B* 797 (Oct. 10, 2019), p. 134914. DOI: [10.1016/j.physletb.2019.134914](https://doi.org/10.1016/j.physletb.2019.134914).
- [150] Alireza Behtash, C. N. Cruz-Camacho, and M. Martinez. Far-from-Equilibrium Attractors and Nonlinear Dynamical Systems Approach to the Gubser Flow. In: *Physical Review D* 97.4 (Feb. 26, 2018), p. 044041. DOI: [10.1103/PhysRevD.97.044041](https://doi.org/10.1103/PhysRevD.97.044041).
- [151] Alireza Behtash et al. Global Flow Structure and Exact Formal Transseries of the Gubser Flow in Kinetic Theory. In: *Journal of High Energy Physics* 2020.7 (July 30, 2020), p. 226. DOI: [10.1007/JHEP07\(2020\)226](https://doi.org/10.1007/JHEP07(2020)226).

- [152] Sunil Jaiswal et al. Exact Solutions and Attractors of Higher-Order Viscous Fluid Dynamics for Bjorken Flow. In: *Physical Review C* 100.3 (Sept. 3, 2019), p. 034901. DOI: [10.1103/PhysRevC.100.034901](https://doi.org/10.1103/PhysRevC.100.034901).
- [153] Toshali Mitra et al. Hydrodynamic Attractor of a Hybrid Viscous Fluid in Bjorken Flow. In: *Physical Review Research* 2.4 (Dec. 4, 2020), p. 043320. DOI: [10.1103/PhysRevResearch.2.043320](https://doi.org/10.1103/PhysRevResearch.2.043320).
- [154] Toshali Mitra, Ayan Mukhopadhyay, and Alexander Soloviev. Hydrodynamic Attractor and Novel Fixed Points in Superfluid Bjorken Flow. In: (Dec. 31, 2020). URL: <https://arxiv.org/abs/2012.15644v1>.
- [155] Jean-Paul Blaizot and Li Yan. Fluid Dynamics of out of Equilibrium Boost Invariant Plasmas. In: *Physics Letters B* 780 (May 10, 2018), pp. 283–286. DOI: [10.1016/j.physletb.2018.02.058](https://doi.org/10.1016/j.physletb.2018.02.058).
- [156] Jean-Paul Blaizot and Li Yan. Emergence of Hydrodynamical Behavior in Expanding Ultra-Relativistic Plasmas. In: *Annals of Physics* 412 (Jan. 1, 2020), p. 167993. DOI: [10.1016/j.aop.2019.167993](https://doi.org/10.1016/j.aop.2019.167993).
- [157] Jean-Paul Blaizot and Li Yan. Analytical Attractor for Bjorken Expansion. In: (June 15, 2020). URL: <https://arxiv.org/abs/2006.08815v1>.
- [158] Michael Strickland, Jorge Noronha, and Gabriel S. Denicol. Anisotropic Nonequilibrium Hydrodynamic Attractor. In: *Physical Review D* 97.3 (Feb. 22, 2018), p. 036020. DOI: [10.1103/PhysRevD.97.036020](https://doi.org/10.1103/PhysRevD.97.036020).
- [159] M. Strickland. The Non-Equilibrium Attractor for Kinetic Theory in Relaxation Time Approximation. In: *Journal of High Energy Physics* 2018.12 (Dec. 21, 2018), p. 128. DOI: [10.1007/JHEP12\(2018\)128](https://doi.org/10.1007/JHEP12(2018)128).
- [160] Michael Strickland and Ubaid Tantiary. Exact Solution for the Non-Equilibrium Attractor in Number-Conserving Relaxation Time Approximation. In: *Journal of High Energy Physics* 2019.10 (Oct. 7, 2019), p. 69. DOI: [10.1007/JHEP10\(2019\)069](https://doi.org/10.1007/JHEP10(2019)069).
- [161] Jasmine Brewer, Li Yan, and Yi Yin. Adiabatic Hydrodynamization in Rapidly-Expanding Quark-Gluon Plasma. In: (Sept. 30, 2019). URL: <https://arxiv.org/abs/1910.00021v1>.
- [162] Ashutosh Dash and Victor Roy. Hydrodynamic Attractors for Gubser Flow. In: *Physics Letters B* 806 (July 10, 2020), p. 135481. DOI: [10.1016/j.physletb.2020.135481](https://doi.org/10.1016/j.physletb.2020.135481).
- [163] Dekrayat Almaalol, Alekski Kurkela, and Michael Strickland. Nonequilibrium Attractor in High-Temperature QCD Plasmas. In: *Physical Review Letters* 125.12 (Sept. 17, 2020), p. 122302. DOI: [10.1103/PhysRevLett.125.122302](https://doi.org/10.1103/PhysRevLett.125.122302).
- [164] Paul Romatschke. Relativistic Fluid Dynamics Far From Local Equilibrium. In: *Physical Review Letters* 120.1 (Jan. 5, 2018), p. 012301. DOI: [10.1103/PhysRevLett.120.012301](https://doi.org/10.1103/PhysRevLett.120.012301).
- [165] Michał Spaliński. Universal Behaviour, Transients and Attractors in Supersymmetric Yang–Mills Plasma. In: *Physics Letters B* 784 (Sept. 10, 2018), pp. 21–25. DOI: [10.1016/j.physletb.2018.07.003](https://doi.org/10.1016/j.physletb.2018.07.003).
- [166] Giuliano Giacalone, Aleksas Mazeliauskas, and Sören Schlichting. Hydrodynamic Attractors, Initial State Energy, and Particle Production in Relativistic Nuclear Collisions. In: *Physical Review Letters* 123.26 (Dec. 30, 2019), p. 262301. DOI: [10.1103/PhysRevLett.123.262301](https://doi.org/10.1103/PhysRevLett.123.262301).

- [167] A. Behtash et al. Transasymptotics and Hydrodynamization of the Fokker-Planck Equation for Gluons. In: (Nov. 16, 2020). URL: <https://arxiv.org/abs/2011.08235v1>.
- [168] Peter E. Kloeden and Martin Rasmussen. *Nonautonomous Dynamical Systems*. American Mathematical Soc., Aug. 17, 2011. 274 pp. Google Books: [ByCCAwwAAQBAJ](#).
- [169] Paul Romatschke. Relativistic Hydrodynamic Attractors with Broken Symmetries: Non-Conformal and Non-Homogeneous. In: *Journal of High Energy Physics* 2017.12 (Dec. 14, 2017), p. 79. DOI: [10.1007/JHEP12\(2017\)079](https://doi.org/10.1007/JHEP12(2017)079).
- [170] Aleksi Kurkela et al. Hydrodynamization in Systems with Detailed Transverse Profiles. In: *Physics Letters B* 811 (Dec. 10, 2020), p. 135901. DOI: [10.1016/j.physletb.2020.135901](https://doi.org/10.1016/j.physletb.2020.135901).
- [171] Victor E. Ambrus et al. Bjorken Flow Attractors with Transverse Dynamics. In: (Feb. 23, 2021). URL: <https://arxiv.org/abs/2102.11785v1>.
- [172] Gabriel S. Denicol and Jorge Noronha. Connecting Far-from-Equilibrium Hydrodynamics to Resummed Transport Coefficients and Attractors. In: *Nuclear Physics A*. The 28th International Conference on Ultra-Relativistic Nucleus-Nucleus Collisions: Quark Matter 2019 1005 (Jan. 1, 2021), p. 121748. DOI: [10.1016/j.nuclphysa.2020.121748](https://doi.org/10.1016/j.nuclphysa.2020.121748).
- [173] Aleksas Mazeliauskas and Jürgen Berges. Prescaling and Far-from-Equilibrium Hydrodynamics in the Quark-Gluon Plasma. In: *Physical Review Letters* 122.12 (Mar. 26, 2019), p. 122301. DOI: [10.1103/PhysRevLett.122.122301](https://doi.org/10.1103/PhysRevLett.122.122301).
- [174] Gabriel S. Rocha, Gabriel S. Denicol, and Jorge Noronha. *Novel Relaxation Time Approximation to the Relativistic Boltzmann Equation*. Mar. 20, 2021. arXiv: [2103.07489](https://arxiv.org/abs/2103.07489) [[hep-ph](#), [physics:hep-th](#), [physics:nucl-th](#)]. URL: <http://arxiv.org/abs/2103.07489>.

Hydrodynamization in kinetic theory: Transient modes and the gradient expansion

Michał P. Heller,^{1,2,3,*} Alekski Kurkela,^{4,5,†} Michał Spaliński,^{3,6,‡} and Viktor Svensson^{3,1,§}

¹Max Planck Institute for Gravitational Physics, Potsdam-Golm D-14476, Germany

²Perimeter Institute for Theoretical Physics, Waterloo, Ontario N2L 2Y5, Canada

³National Centre for Nuclear Research, 00-681 Warsaw, Poland

⁴Theoretical Physics Department, CERN, CH-1211 Geneva, Switzerland

⁵Faculty of Science and Technology, University of Stavanger, 4036 Stavanger, Norway

⁶Physics Department, University of Białystok, 15-245 Białystok, Poland

 (Received 17 November 2016; revised manuscript received 16 March 2018; published 31 May 2018)

We explore the transition to hydrodynamics in a weakly coupled model of quark-gluon plasma given by kinetic theory in the relaxation-time approximation with conformal symmetry. We demonstrate that the gradient expansion in this model has a vanishing radius of convergence due to the presence of a transient (nonhydrodynamic) mode, in a way similar to results obtained earlier in strongly coupled gauge theories. This suggests that the mechanism by which hydrodynamic behavior emerges is the same, which we further corroborate by a novel comparison between solutions of different weakly and strongly coupled models. However, in contrast with other known cases, we find that not all the singularities of the analytic continuation of the Borel transform of the gradient expansion correspond to transient excitations of the microscopic system; some of them reflect analytic properties of the kinetic equation when the proper time is continued to complex values.

DOI: [10.1103/PhysRevD.97.091503](https://doi.org/10.1103/PhysRevD.97.091503)

I. INTRODUCTION AND SUMMARY

Heavy-ion collisions at the Relativistic Heavy Ion Collider and LHC provide an outstanding opportunity to test our understanding of QCD. Perhaps unsurprisingly, a fully *ab initio* theoretical description has turned out to be very challenging. This has led to the exploration of models of increasing complexity and often nonoverlapping domains of validity—see, e.g., Refs. [1,2] for a review of such models in the context of the hydrodynamic description in ultrarelativistic heavy-ion collisions.

In this paper, we focus on the poorly understood transient far-from-equilibrium regime, which precedes viscous hydrodynamic evolution of quark-gluon plasma (QGP). There are two approaches to the study of the transition to hydrodynamics (hydrodynamization) in non-Abelian gauge theories like QCD: a weakly coupled description based on effective kinetic theory (EKT) [3] (see also Refs. [4–9]) and a strongly coupled plasma paradigm based on

holography [10] (see Refs. [11–14] for sample results). They involve very different physical pictures and mathematical frameworks; the first relies on the Boltzmann equation, while the second makes use of higher-dimensional Einstein equations. Since under experimental conditions the QCD coupling is neither parametrically small nor large, it is crucial to understand which implications of these approaches can be viewed as universal.

Our aim is to shed light on equilibration in weakly coupled systems by examining large-order behavior of the hydrodynamic gradient expansion [15] in the framework of the kinetic theory model given by the Boltzmann equation in the relaxation-time approximation (RTA) [16]. We also assume conformal symmetry, as its breaking at strong coupling does not significantly alter equilibration processes [17,18], whereas at weak coupling at vanishing quark masses, it is a next-to-leading-order effect (see, e.g., Ref. [5]). The key result of this paper is demonstrating the vanishing radius of convergence of the gradient expansion in this kinetic theory model (see also Ref. [19] which studied in this context the RTA kinetic theory with constant relaxation time) and understanding some puzzling features revealed by these studies. The reason for the divergence turns out to be the same as in the case of holographic plasma: the presence of fast-decaying (nonhydrodynamic) modes [20–23] of which the relaxation controls the emergence of hydrodynamic behavior (and, in particular, its applicability to the physics of heavy-ion collisions [24–26]). This is connected with the existence of

*michal.p.heller@aei.mpg.de

†aleksi.kurkela@cern.ch

‡michal.spalinski@ncbj.gov.pl

§viktor.svensson@aei.mpg.de

Published by the American Physical Society under the terms of the Creative Commons Attribution 4.0 International license. Further distribution of this work must maintain attribution to the author(s) and the published article's title, journal citation, and DOI.

attractors that govern the evolution far from equilibrium [21,27–35]. In this context, see also Refs. [36,37] for studies of possible manifestations of analogous fast-decaying modes in trapped Fermi gases close to unitarity as well as Ref. [38], in which various features of transient modes are analyzed as a function of the microscopic interaction strength in a holographic toy model.

Quite remarkably, our analysis of the Borel transform of the gradient expansion in the RTA kinetic theory reveals not only the expected purely decaying mode [22] but also singularities that could naively be interpreted as transient contributions to the energy-momentum tensor exhibiting damped oscillatory behavior, similar to the findings of Ref. [39]. This would, however, be surprising, since the mechanism described there does not apply to the RTA theory [40]. In fact, we demonstrate below that these singularities are instead a manifestation of analytic properties of the evolution equations in complexified time. This feature is related to what has been observed in other contexts where large-order behavior of perturbative series expansions is used to draw conclusions about nonperturbative effects (see, e.g., Refs. [41–44]).

Our conclusions concerning hydrodynamization provide strong motivation for comparing numerical solutions of the RTA evolution equations with the EKT results at intermediate coupling reported in Refs. [8,9] and with the AdS/CFT-based simulations of Ref. [45]. We uncover semi-quantitative agreement, and as a byproduct of this analysis, we present a new and effective way of visualizing (see Fig. 2) the correlation between the hydrodynamization time and the value of the η/s ratio noted in Ref. [46].

II. KINETIC THEORY

We address the issues discussed above in the context of Bjorken flow [47], which is conveniently formulated in (proper-time) rapidity coordinates τ - y . They are related to Minkowski lab-frame coordinates t - z by $t = \tau \cosh y$ and $z = \tau \sinh y$, where z is the collision axis. Assuming translation symmetry in the transverse plane \mathbf{x}_T , the on-shell distribution function f depends only on the proper time τ , the modulus of the transverse momentum $p \equiv |\mathbf{p}_T|$ and the boost-invariant variable $u = \tau^2 p^y$.

In the RTA, the collision kernel appearing in the Boltzmann equation is linearized around the equilibrium distribution, which for simplicity we take to be Boltzmann,

$$f_0(\tau, u, p) = \frac{1}{(2\pi)^3} \exp \left[-\frac{\sqrt{u^2 + p^2 \tau^2}}{\tau T(\tau)} \right]. \quad (1)$$

The RTA Boltzmann equation takes the form

$$\frac{\partial f(\tau, u, p)}{\partial \tau} = \frac{1}{\tau_{\text{rel}}} \{f_0(\tau, u, p) - f(\tau, u, p)\}. \quad (2)$$

To ensure conformal symmetry, we assume that the relaxation time is of the form

$$\tau_{\text{rel}} = \frac{\gamma}{T(\tau)}, \quad (3)$$

where γ is dimensionless and is the only parameter of this model. The dependence of temperature on the proper time is determined dynamically by imposing the Landau matching condition [48,49]

$$\mathcal{E}(\tau) = \frac{3}{\pi^2} T^4(\tau), \quad (4)$$

where

$$\mathcal{E}(\tau) = 2 \int d^4 p \delta(p^2) \theta(p^0) \frac{u^2 + p^2 \tau^2}{\tau^2} f(\tau, u, p) \quad (5)$$

is the energy density (per particle species).

III. HYDRODYNAMIC GRADIENT EXPANSION

In a conformal theory, the eigenvalues of the expectation value of the energy-momentum tensor in a boost-invariant state are functions of the proper time τ alone. They are given by the energy density \mathcal{E} and the longitudinal and transverse pressures \mathcal{P}_L and \mathcal{P}_T :

$$\mathcal{P}_L = -\mathcal{E} - \tau \dot{\mathcal{E}}, \quad \mathcal{P}_T = \mathcal{E} + \frac{1}{2} \tau \dot{\mathcal{E}}. \quad (6)$$

Away from equilibrium, \mathcal{P}_L and \mathcal{P}_T differ from the equilibrium pressure at the same energy density $\mathcal{P} \equiv \mathcal{E}/3$. It is convenient to study the approach to equilibrium by examining the behavior of the pressure anisotropy

$$\mathcal{A} \equiv \frac{\mathcal{P}_T - \mathcal{P}_L}{\mathcal{P}} \quad (7)$$

as a function of the dimensionless variable $w \equiv T\tau$. The gradient expansion of \mathcal{A} takes the form

$$\mathcal{A}(w) = \sum_{n=1}^{\infty} a_n w^{-n}. \quad (8)$$

This follows directly from Eq. (6) and (7) if we use the fact that in conformal theories near equilibrium $\mathcal{E} \sim T^4$ and for boost-invariant flow $T \sim \tau^{-1/3} + O(\tau^{-1})$ [47] (up to exponentially suppressed corrections).

To determine the coefficients a_n , we look for a solution of the Boltzmann equation (2) in the form

$$f(\tau, u, p) = f_0(\tau, u, p) \left(1 + \sum_{n=1}^{\infty} w^{-n} h_n \left(\frac{u}{w}, \frac{p}{T} \right) \right). \quad (9)$$

Inserting Eq. (9) into the Boltzmann equation (2), one can algebraically determine the functions h_n in terms of the unknown coefficients a_n . A key step in doing this is to eliminate proper-time derivatives of temperature in favor of \mathcal{A} and then using Eq. (8).

The Landau matching condition Eq. (4) implies that at each order $n > 0$

$$\int d^4 p \delta(p^2) \theta(p^0) \frac{v^2}{\tau^2} f_0(\tau, u, p) h_n \left(\frac{u}{w}, \frac{p}{T} \right) = 0. \quad (10)$$

This condition amounts to a linear, algebraic equation that determines the expansion coefficient a_{n-1} .

Proceeding this way, we have calculated the expansion coefficients analytically up to order 426 (we include the result of this calculation in the Supplemental Material [50]). As a cross-check, we have also calculated the first ten terms using two independent, albeit slower, methods from Refs. [48,49,51], noting perfect agreement.

The leading expansion coefficients read

$$a_1 = 8/5\gamma, \quad a_2 = 32/105\gamma^2, \quad a_3 = -416/525\gamma^3. \quad (11)$$

They can be used to match the transport coefficients of Baier-Romatschke-Son-Starinets-Stephanov hydrodynamics [20] to the RTA model. In particular, one finds

$$\eta/s = \gamma/5. \quad (12)$$

At large orders, the expansion coefficients in Eq. (8) exhibit factorial growth. This demonstrates the vanishing radius of convergence of the hydrodynamic series, which parallels similar findings obtained numerically in $\mathcal{N} = 4$ super symmetric Yang-Mills theory using holography [15,52] as well as in hydrodynamics [21,53,54]. This is to be expected on general grounds, since the RTA theory contains, apart from hydrodynamic excitations, also a short-lived mode [22] of which the physics is not captured by the truncated gradient expansion, as shown in Refs. [15,21].

IV. BOREL TRANSFORM AND SHORT-LIVED MODES

In this section, we explore the Borel transform technique as a way to map out the excitations of expanding QGP.

The Borel transform removes the leading-order factorial growth of the coefficients,

$$\mathcal{A}_B(\xi) = \sum_{n=1}^{\infty} \frac{a_n}{n!} \xi^n. \quad (13)$$

The inverse transform is given by the Borel summation formula

$$\mathcal{A}_{\text{resummed}}(w) = \frac{1}{w} \int_0^{\infty} d\xi e^{-\xi/w} \mathcal{A}_B(\xi) \quad (14)$$

and is not uniquely defined since the analytic continuation of $\mathcal{A}_B(\xi)$ necessarily contains singularities that are responsible for the vanishing radius of convergence of the original series. We analytically continue the series from Eq. (13) truncated at 426 terms by means of Padé approximants. Figure 1 shows the poles of the Padé approximant, which condense in a way known to signify a branch-point singularity [55].

In Ref. [21] (see also Refs. [15,52–54,56]), the ambiguity in the Borel summation associated with singularities

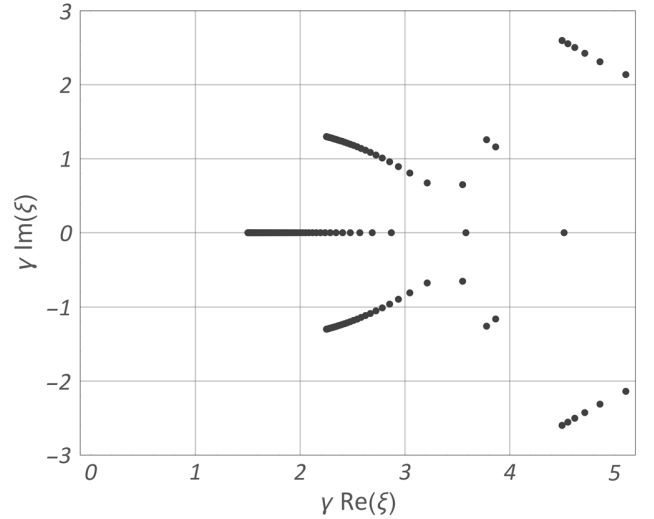


FIG. 1. Poles of the Padé approximant to the Borel transform of the gradient expansion. We have checked that the structure of singularities remains stable as the number of terms kept in the series is varied. We have also checked that the residues of the pictured poles lie well above what was set as the numerical accuracy, i.e., that they are not numerical artifacts. The depicted singularities are discretizations of branch cuts with branch points at values of ξ given in Eqs. (16) and (20) as well as at $\xi_0 + \xi_{\pm}$ and $2\xi_{\pm}$ (see also Ref. [34] for a related statement based on a smaller data set from the previous version of the present manuscript).

of the analytic continuation of the Borel transform has been argued to disappear once the gradient expansion is supplemented with exponentially decaying terms,

$$\delta\mathcal{A} \sim e^{-\xi_0 w}, \quad (15)$$

where ξ_0 denotes the beginning of a cut in the complex Borel plane. In the case under consideration, the cut closest to the origin starts, up to five decimal places, at

$$\xi_0 = 1.5000/\gamma. \quad (16)$$

The constants ξ_0 appearing in Eq. (15) can in general be complex (they then come in conjugate pairs), and in the examples analyzed so far in the literature, they appear in positive integer multiples. Each such term comes with an infinite gradient expansion of its own, and the term with the lowest ξ_0 in a given family comes with an independent complex integration constant. In all known cases [15,21,52–54] (see Ref. [1] for a review), those least-damped modes within a given family coincide with singularities of retarded equilibrium two-point functions of the energy-momentum tensor at vanishing momentum.

In the context of the RTA kinetic theory, the studies of Ref. [22] reveal the presence of a zero-momentum fast-evolving mode in the isotropization of the energy-momentum tensor to its equilibrium form:

$$\delta\langle T^{\mu\nu} \rangle \sim e^{-\omega_0 T t}, \quad \omega_0 = 1/\gamma. \quad (17)$$

The nontrivial background flow is known to modify the above equation to the form [15,57,58]

$$\delta\langle T^{\mu\nu}\rangle \sim e^{-\omega_0 \int T(x) u_\mu dx^\mu}, \quad (18)$$

which for the case of Bjorken flow, neglecting subleading terms at large values of w , reduces to

$$\delta\mathcal{A} \sim e^{-\frac{3}{2}\omega_0 w}. \quad (19)$$

This, together with Eq. (17), reproduces Eq. (16). Let us also note here that the analysis in Ref. [59] reveals that the cut along the real axis seen in Fig. 1 must be, in fact, an infinite collection of independent cuts. They all start at the same branch point, i.e., $\xi = \xi_0$, but are characterized by different discontinuities and are interpreted as an infinite set of modes carrying information about the initial distribution function to late times w .

Importantly, Fig. 1 contains also a pair of singularities characterized by

$$\xi_\pm \approx (2.25016 \pm 1.29898i)/\gamma. \quad (20)$$

If one were to apply straightforwardly the lessons from earlier studies of other models of expanding plasmas, these complex values of ξ_0 would be interpreted as oscillatory-type transient contributions to the pressure anisotropy. As shown in the next section, in which we argue that these are unphysical, this natural-looking conclusion is premature. This is an important point, since such singularities appear also in other kinetic theory models, such as those with $\tau_{\text{rel}} \sim T^{-\Delta}$, for $0 < \Delta < 3$. Notably, for $\Delta > 2$, the unphysical modes are actually closest to the origin, so naively they would correspond to the dominant nonhydrodynamic corrections [59].

V. ANALYTIC PROPERTIES OF RTA KINETIC THEORY

To explain the singularities of the Borel transform at ξ_\pm , see Eq. (20) and Fig. 1, we use the integral equation [49], which follows from the Boltzmann equation [48] and directly determines the local energy density $\mathcal{E}(\tau)$:

$$g(\tau) = \mathcal{E}_0(\tau) + \frac{1}{2} \int_{\tau_0}^{\tau} \frac{d\tau'}{\tau_{\text{rel}}(\tau')} H\left(\frac{\tau'}{\tau}\right) g(\tau'). \quad (21)$$

In the expression above, $\mathcal{E}_0(\tau)$ carries information about initial conditions but will not be relevant in the following analysis. The object of interest is the energy density $\mathcal{E}(\tau)$, which appears in

$$g(\tau) = \mathcal{E}(\tau) e^{\int_{\tau_0}^{\tau} \frac{d\tau'}{\tau_{\text{rel}}(\tau')}} \quad (22)$$

as well as in $\tau_{\text{rel}}(\tau)$ through Eqs. (3) and (4). The function $H(q)$ originates from the second moment of the equilibrium distribution function, Eq. (1), and reads

$$H(q) = q^2 + \frac{\arctan \sqrt{\frac{1}{q^2} - 1}}{\sqrt{\frac{1}{q^2} - 1}}. \quad (23)$$

What will be crucial in the following is the analytic structure of H . Since the natural variable in our considerations is w and at late times $w \sim \tau^{2/3}$, we shall write the argument of H as $q = (w'/w)^{3/2} \equiv \zeta^{3/2}$.

Among the singularities of $H(\zeta^{3/2})$, the one of interest is the branch point stemming from the square root in the denominator. It appears as a singularity when the arctan function in the numerator is taken in a nonprincipal branch. As a result, one finds

$$H(\zeta^{3/2}) \sim (1 - \zeta^3)^{-1/2}, \quad (24)$$

which has branch points at third roots of unity. We will be interested in the ones located at

$$\zeta_\pm = e^{\pm i\frac{2}{3}\pi}. \quad (25)$$

The key observation is that the presence of singularities in the complex ζ plane leads to inequivalent choices of integration contours in Eq. (21), the only physical choice being homologous to the integration along the real axis. If one uses the late-time solution for $g(\tau(w))$ obtained from Eq. (11) under the integral in Eq. (21) and considers two inequivalent contours around ζ_- (or, similarly, ζ_+), denoted \mathcal{C}_1 and \mathcal{C}_2 , one finds

$$\delta g(w) \sim \left[\int_{\mathcal{C}_1} d\zeta - \int_{\mathcal{C}_2} d\zeta \right] e^{\frac{3w}{2\gamma}} H(\zeta^{3/2}) \times \dots, \quad (26)$$

where the ellipsis denotes terms subleading at large w . Similarly to the analysis around Eq. (14), the branch cuts lead to contributions to δg of the form

$$\delta g \sim e^{-\frac{3\zeta_\pm}{2\gamma} w}, \quad (27)$$

where we truncated subleading terms at large values of w . Finally, note that δg and $\delta\mathcal{E}$ are related through Eq. (22) with, at late times/large values of w , $e^{\int_{\tau_0}^{\tau} \frac{d\tau'}{\tau_{\text{rel}}(\tau')}} \sim e^{\frac{3}{2\gamma} w}$, which ultimately gives

$$\delta\mathcal{E}_\pm \sim e^{-\frac{3}{2\gamma}(\zeta_\pm - 1)w}. \quad (28)$$

Comparing the exponent in the equation above with Eq. (20), one observes a remarkable agreement up to four decimal places. As a further way of corroborating this result, one can use the techniques utilized earlier in this context in Refs. [15,21] to match the square root character of the branch cut in Eq. (24) with the leading power-law correction in w to contributions from the ξ_\pm singularities in the Borel plane, with very good agreement.

All this taken together gives us confidence that the correct interpretation of the singularities given in Eq. (20) is that they correspond not to physical excitations but

rather to analytic properties of kinetic theory for complexified values of the w variable. The physical integration contour in Eq. (21) along real values of τ' does not pick up these contributions (and, no wonder, they are not seen in solutions of the initial value problem discussed in Ref. [59]). The gradient expansion itself does not preclude unphysical choices of contour, and this is reflected in its large-order behavior. Similar phenomena can be seen in the integral equation considered in Ref. [60] or in the ghost-instanton story of Ref. [43]. Their origin goes back to the fundamental point of resurgence: all nonperturbative information is encoded in the large-order behavior of the perturbative sector.

VI. HYDRODYNAMIZATION COMPARED

In previous sections, we have demonstrated that hydrodynamization in the RTA takes place through the decay of transient nonhydrodynamical modes in complete analogy to the situation at strong coupling. On the other hand, the RTA shares structural similarities with EKT—while the collision kernels of the QCD effective kinetic theory have much richer structure than the RTA, many qualitative features at the level of kinetic theory coincide. In this section, we further strengthen the connection between RTA and EKT by noting that the similarity between these two theories goes beyond abstract structural similarity and that they agree semiquantitatively when the values of η/s are matched between the two theories.

To demonstrate the extent of quantitative agreement between different models, inspired by Ref. [46], we introduce a new, rescaled variable $\tilde{w} \equiv \frac{w}{4\pi\eta/s}$. This is useful for such comparisons, since the late-time behavior of the pressure anisotropy \mathcal{A} is given by

$$\mathcal{A}_H(\tilde{w}) = \frac{2}{\pi\tilde{w}} + \mathcal{O}\left(\frac{1}{\tilde{w}^2}\right).$$

The leading behavior is completely universal and does not depend on the value of η/s . Deviations from the asymptotic form characterize contributions arising beyond first-order hydrodynamics, and, indeed, we say that the system has reached the hydrodynamic regime when for a given state the relative difference between \mathcal{A} and \mathcal{A}_H remains smaller than some threshold value. Figure 2 shows a comparison of the time evolution of the system evolved in the EKT from Ref. [9], RTA using the methodology of Refs. [48,49], and numerical AdS/CFT calculation of Refs. [13,45,61]. For the EKT and RTA simulations, we took the initial condition used in Ref. [9], whereas for the AdS/CFT simulation, we took typical initial conditions from Ref. [45]. We evolved the systems using EKT with $\lambda = 10$ corresponding to $\eta/s \approx 0.642$, holography with $\eta/s = 1/4\pi$, and RTA with γ fixed to reproduce the value of η/s of either model. Note that every kinetic theory curve in Fig. 2 corresponds to a different initial distribution function. In all these models,

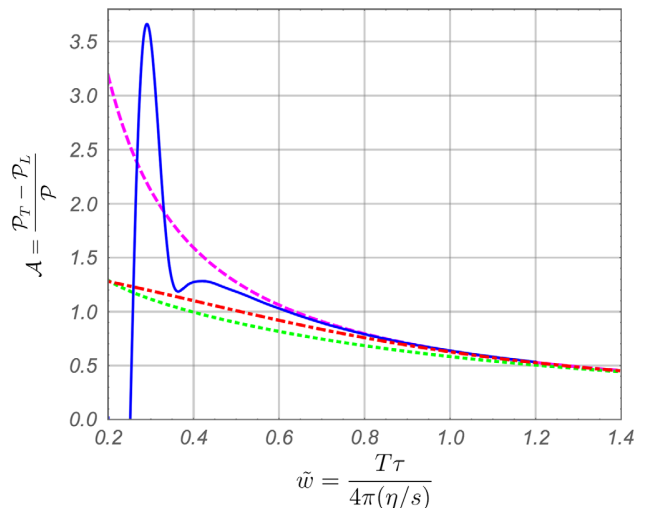


FIG. 2. The dashed magenta curve represents first-order hydrodynamics, the blue line is the holographic result, and the red dashed-dotted line is from EKT. The green dotted curve stands for a solution of RTA starting from initial distribution similar to EKT and with the same shear viscosity, $\eta/s = 0.624$. Despite differences in microscopic dynamics, one sees significant qualitative and some quantitative similarities between different theories.

the evolution is similar but distinct. Remarkably, in each case—despite vastly differing microphysics—the evolution converges to first-order viscous hydrodynamics roughly at the same value of \tilde{w} variable, i.e. $\tilde{w} \approx 1$. It is striking that in all these cases the pressure anisotropy at the time of hydrodynamization is as high as $\mathcal{A} \approx 0.6$ – 0.8 .

The structural and quantitative similarities of EKT and RTA suggest that the gradient expansion in EKT also exhibits a zero radius of convergence and that the weak coupling hydrodynamization is driven by the same qualitative process. This is connected with the notion of attractors that have been explored in both RTA and holography [28,29]. To what extent these insights translate to EKT is an important problem.

ACKNOWLEDGMENTS

We would like to thank the authors of Ref. [39] as well as I. Aniceto, G. Dunne, W. Florkowski, R. Janik, P. Romatschke, W. van der Schee, M. Martinez, and M. Strickland for valuable discussions and correspondence. Research at Perimeter Institute is supported by the Government of Canada through Industry Canada and by the Province of Ontario through the Ministry of Research & Innovation. M.P.H. acknowledges support from the Alexander von Humboldt Foundation and the Federal Ministry for Education and Research through the Sofja Kovalevskaja Award. M.S. and V.S. were supported by the Polish National Science Centre Grant No. 2015/19/B/ST2/02824.

- [1] W. Florkowski, M. P. Heller, and M. Spalinski, *Rep. Prog. Phys.* **81**, 046001 (2018).
- [2] P. Romatschke and U. Romatschke, [arXiv:1712.05815](https://arxiv.org/abs/1712.05815).
- [3] P. B. Arnold, G. D. Moore, and L. G. Yaffe, *J. High Energy Phys.* **01** (2003) 030.
- [4] R. Baier, A. H. Mueller, D. Schiff, and D. T. Son, *Phys. Lett. B* **502**, 51 (2001).
- [5] P. B. Arnold, C. Dogan, and G. D. Moore, *Phys. Rev. D* **74**, 085021 (2006).
- [6] A. Kurkela and G. D. Moore, *J. High Energy Phys.* **12** (2011) 044.
- [7] A. Kurkela and G. D. Moore, *J. High Energy Phys.* **11** (2011) 120.
- [8] A. Kurkela and E. Lu, *Phys. Rev. Lett.* **113**, 182301 (2014).
- [9] A. Kurkela and Y. Zhu, *Phys. Rev. Lett.* **115**, 182301 (2015).
- [10] J. M. Maldacena, *Adv. Theor. Math. Phys.* **2**, 231 (1998).
- [11] P. M. Chesler and L. G. Yaffe, *Phys. Rev. D* **82**, 026006 (2010).
- [12] P. M. Chesler and L. G. Yaffe, *Phys. Rev. Lett.* **106**, 021601 (2011), [arXiv:1011.3562](https://arxiv.org/abs/1011.3562).
- [13] M. P. Heller, R. A. Janik, and P. Witaszczyk, *Phys. Rev. Lett.* **108**, 201602 (2012).
- [14] J. Casalderrey-Solana, H. Liu, D. Mateos, K. Rajagopal, and U. A. Wiedemann, *Gauge/String Duality, Hot QCD and Heavy Ion Collisions* (Cambridge University Press, Cambridge, England, 2011).
- [15] M. P. Heller, R. A. Janik, and P. Witaszczyk, *Phys. Rev. Lett.* **110**, 211602 (2013).
- [16] J. Anderson and H. Witting, *Physica (Amsterdam)* **74**, 466 (1974).
- [17] A. Buchel, M. P. Heller, and R. C. Myers, *Phys. Rev. Lett.* **114**, 251601 (2015).
- [18] R. A. Janik, G. Plewa, H. Soltanpanahi, and M. Spalinski, *Phys. Rev. D* **91**, 126013 (2015).
- [19] G. S. Denicol and J. Noronha, [arXiv:1608.07869](https://arxiv.org/abs/1608.07869).
- [20] R. Baier, P. Romatschke, D. T. Son, A. O. Starinets, and M. A. Stephanov, *J. High Energy Phys.* **04** (2008) 100.
- [21] M. P. Heller and M. Spalinski, *Phys. Rev. Lett.* **115**, 072501 (2015).
- [22] P. Romatschke, *Eur. Phys. J. C* **76**, 352 (2016).
- [23] A. Kurkela and U. A. Wiedemann, [arXiv:1712.04376](https://arxiv.org/abs/1712.04376).
- [24] P. Romatschke, *Eur. Phys. J. C* **75**, 305 (2015).
- [25] M. Habich, G. A. Miller, P. Romatschke, and W. Xiang, *Eur. Phys. J. C* **76**, 408 (2016).
- [26] M. Spalinski, *Phys. Rev. D* **94**, 085002 (2016).
- [27] P. Romatschke, *Eur. Phys. J. C* **77**, 21 (2017).
- [28] P. Romatschke, *Phys. Rev. Lett.* **120**, 012301 (2018).
- [29] M. Spaliński, *Phys. Lett. B* **776**, 468 (2018).
- [30] P. Romatschke, *J. High Energy Phys.* **12** (2017) 079.
- [31] M. Strickland, J. Noronha, and G. Denicol, *Phys. Rev. D* **97**, 036020 (2018).
- [32] W. Florkowski, E. Maksymiuk, and R. Ryblewski, *Phys. Rev. C* **97**, 024915 (2018).
- [33] G. S. Denicol and J. Noronha, *Phys. Rev. D* **97**, 056021 (2018).
- [34] J. Casalderrey-Solana, N. I. Gushterov, and B. Meiring, [arXiv:1712.02772](https://arxiv.org/abs/1712.02772).
- [35] J.-P. Blaizot and L. Yan, *Phys. Lett. B* **780**, 283 (2018).
- [36] J. Brewer and P. Romatschke, *Phys. Rev. Lett.* **115**, 190404 (2015).
- [37] H. Bantilan, J. T. Brewer, T. Ishii, W. E. Lewis, and P. Romatschke, *Phys. Rev. A* **94**, 033621 (2016).
- [38] S. Grozdanov, N. Kaplis, and A. O. Starinets, *J. High Energy Phys.* **07** (2016) 151.
- [39] D. Bazow, M. Martinez, and U. W. Heinz, *Phys. Rev. D* **93**, 034002 (2016); **93**, 034002 (2016).
- [40] M. Martinez and U. Heinz (private communication).
- [41] G. V. Dunne, Lectures given at the Schladming Winter School 2015, Schladming, Austria (unpublished).
- [42] G. V. Dunne and M. Ünsal, *Proc. Sci.*, LATTICE2015, (2016) 010.
- [43] G. Basar, G. V. Dunne, and M. Unsal, *J. High Energy Phys.* **10** (2013) 041.
- [44] I. Aniceto, G. Başar, and R. Schiappa, [arXiv:1802.10441](https://arxiv.org/abs/1802.10441).
- [45] J. Jankowski, G. Plewa, and M. Spalinski, *J. High Energy Phys.* **12** (2014) 105.
- [46] L. Keegan, A. Kurkela, P. Romatschke, W. van der Schee, and Y. Zhu, [arXiv:1512.05347](https://arxiv.org/abs/1512.05347).
- [47] J. Bjorken, *Phys. Rev. D* **27**, 140 (1983).
- [48] G. Baym, *Phys. Lett.* **138B**, 18 (1984).
- [49] W. Florkowski, R. Ryblewski, and M. Strickland, *Phys. Rev. C* **88**, 024903 (2013).
- [50] See Supplemental Material at <http://link.aps.org/supplemental/10.1103/PhysRevD.97.091503> for details about 425 lowest terms in the hydrodynamic gradient expansion, as defined by Eq. (8).
- [51] A. Jaiswal, *Phys. Rev. C* **87**, 051901 (2013).
- [52] A. Buchel, M. P. Heller, and J. Noronha, *Phys. Rev. D* **94**, 106011 (2016).
- [53] G. Basar and G. V. Dunne, *Phys. Rev. D* **92**, 125011 (2015).
- [54] I. Aniceto and M. Spaliński, *Phys. Rev. D* **93**, 085008 (2016).
- [55] H. S. Yamada and K. S. Ikeda, [arXiv:1308.4453](https://arxiv.org/abs/1308.4453).
- [56] W. Florkowski, R. Ryblewski, and M. Spalinski, *Phys. Rev. D* **94**, 114025 (2016).
- [57] R. A. Janik and R. B. Peschanski, *Phys. Rev. D* **74**, 046007 (2006).
- [58] M. P. Heller, R. A. Janik, M. Spaliński, and P. Witaszczyk, *Phys. Rev. Lett.* **113**, 261601 (2014).
- [59] M. P. Heller and V. Svensson, [arXiv:1802.08225](https://arxiv.org/abs/1802.08225).
- [60] I. Aniceto, *J. Phys. A* **49**, 065403 (2016).
- [61] M. P. Heller, R. A. Janik, and P. Witaszczyk, *Phys. Rev. D* **85**, 126002 (2012).

How does relativistic kinetic theory remember about initial conditions?

Michal P. Heller^{1,2,*} and Viktor Svensson^{2,1,†}

¹Max Planck Institute for Gravitational Physics, Potsdam-Golm D-14476, Germany

²National Centre for Nuclear Research, 00-681 Warsaw, Poland



(Received 10 April 2018; published 17 September 2018)

Understanding hydrodynamization in microscopic models of heavy-ion collisions has been an important topic in current research. Many lessons obtained within the strongly coupled (holographic) models originate from the properties of transient excitations of equilibrium encapsulated by short-lived quasinormal modes of black holes. This paper aims to develop similar intuition for expanding plasma systems described by a simple model from the weakly coupled domain: the Boltzmann equation in the relaxation time approximation. We show that in this kinetic theory setup there are infinitely many transient modes carrying information about the initial distribution function. They all have the same exponential damping set by the relaxation time but are distinguished by different power-law suppressions and different frequencies of oscillations, logarithmic in proper time. Finally, we also analyze the resurgent interplay between the hydrodynamics and transients in this setup.

DOI: 10.1103/PhysRevD.98.054016

I. INTRODUCTION

The success of hydrodynamics as a part of the phenomenological description of data obtained in ultra-relativistic heavy-ion collision experiments at RHIC and LHC has triggered significant theoretical interest in understanding the transition to the hydrodynamic regime—hydrodynamization—from a microscopic standpoint [1–3]. There are two kinds of setups in which this outstanding problem has been addressed to date: strongly coupled models based on holography (also known as the AdS/CFT correspondence or gauge-gravity duality) [4–6] and weakly coupled setups based on kinetic theory (the Boltzmann equation); see, e.g., Refs. [7,8] for a review of some of these developments. The aim of the present paper is to apply intuitions developed using holographic methods to expanding plasma setups described within kinetic theory and in this way compare the two microscopic mechanisms for hydrodynamization.

We will be studying longitudinally expanding plasma systems in 1 + 3 dimensions with the assumption of boost invariance along the expansion axis z (see Ref. [9]) and a conformal equation of state relating the matter energy density \mathcal{E} and its equilibrium pressure \mathcal{P} as $\mathcal{E} = 3\mathcal{P}$. Assuming local thermalization at late proper time $\tau = \sqrt{t^2 - z^2}$, the energy-momentum tensor of matter is fully characterized by one dimensionful number Λ that sets the prefactor in the asymptotic scaling of the energy density with proper time [10]

$$\mathcal{E}|_{\tau \rightarrow \infty} = \frac{\Lambda^4}{(\Lambda\tau)^{4/3}}. \quad (1)$$

As reviewed in Sec. III, power-law corrections to the above equation are interpreted as a hydrodynamic gradient expansion and, at least superficially, do not require new information about initial conditions. This raises the puzzle encapsulated by the title of our paper. The microscopic dynamics in the setup of interest is captured by the distribution function $f(x, p)$, which is a non-negative function of spacetime position x^μ (in the present setup only τ will matter) and the on-shell particle 4-momentum p^μ (we are assuming here for simplicity massless microscopic constituents). The energy-momentum tensor of the underlying matter is given by the second moment of the distribution function

$$T^{\mu\nu} = \int dP p^\mu p^\nu f(x, p), \quad (2)$$

where dP stands for the phase space measure defined in Eq. (16). The local energy density $\mathcal{E}(\tau)$ in Eq. (1) is simply equal to $-T^\tau_\tau$. The distribution function itself solves a first-order partial differential equation (the Boltzmann equation) of the form

$$p^\mu \partial_\mu f(x, p) = \mathcal{C}[f], \quad (3)$$

where the collisional kernel \mathcal{C} depends only on the distribution function f at a given spacetime point x^μ . As a result, in order to solve the initial value problem one needs to know the distribution on some timelike hypersurface (here taken to

*michal.p.heller@aei.mpg.de

†viktor.svensson@aei.mpg.de

be a hypersurface of constant τ) as a function of 4-momentum p^μ . Such an initial condition contains an infinite amount of data (dimensionful parameters), which is in stark contrast with the late-time behavior captured by Eq. (1). Even with the simplifying assumption of rotational invariance in the transversal plane, the initial distribution function is an arbitrary non-negative function of two variables. To rephrase our title: what kind of corrections to Eq. (1) carry the vast majority of information about initial conditions set by the initial distribution function?

As already anticipated, we will be interested in answering this question using intuitions developed in the holographic studies of heavy-ion collisions. In fact, holography shares one key feature with the present setup: the microscopic description is naturally formulated using variables that live in a greater number of dimensions than the observables (there: correlation functions of operators; here: moments of the distribution function). In holography, if one neglects nonlinear effects, one finds that Eq. (1) is supplemented by a discrete set of infinitely many corrections of the form

$$\delta\mathcal{E}_j|_{\tau\rightarrow\infty} = b_j \tau^{\alpha_j} e^{-\gamma_j(\Lambda\tau)^{2/3}} \cos(\omega_j(\Lambda\tau)^{2/3} + \phi_j), \quad (4)$$

which encapsulate transient excitations undergoing exponential decay with oscillations [11,12]. Then, at least superficially, an infinite set of amplitudes b_j and phases ϕ_j offers a possibility of encoding information about initial conditions set in the higher-dimensional gravitational description. Furthermore, the decay rates γ_j and oscillation frequencies ω_j are related to positions of single-pole singularities in complexified frequency and at zero momentum in the Fourier-transformed retarded two-point function of the energy-momentum tensor in global thermal equilibrium [11]. That these singularities are single poles has been understood as the hallmark feature of strongly coupled setups; see, e.g., Ref. [13]. On the gravity side, these singularities are the aforementioned transient quasinormal modes of dual black holes [14].

Preliminary results from Ref. [15] (see also the recent Ref. [16]) confirm general expectations that the relevant singularities of the energy-momentum tensor in kinetic theory are of branch-cut type, whereas Eq. (4) holds for simple poles. Our paper, therefore, is all about understanding how Eq. (4) gets modified in the simplest kinetic theory model, considered e.g., in Ref. [15]. The only “microscopic” parameter in the collisional kernel—the relaxation time—is considered to exhibit a general power-law dependence on temperature (but not on the quasiparticles’ momenta, as in Ref. [16]); see Eq. (9). Therefore, our study includes some of the results of Refs. [17–20] as special cases.

We believe the issue we are raising and the setup we are using to address it are interesting for a number of reasons. First and foremost, on the motivational front, if one were to

search for transient phenomena in heavy-ion collisions or other setups, one would naturally search for excitations of a type given by Eq. (4) rather than perturbations of global equilibrium. Furthermore, the interplay between hydrodynamics and transients has become a topic of significant interest in the past decade. This includes formulating effective theories of hydrodynamics with a view towards a better phenomenological description of experimental data [12,21–26], applications of resurgence techniques to non-equilibrium setups in which transient modes act as analogues of nonperturbative effects and hydrodynamics represents an asymptotic perturbative expansion [17,18,27–31], as well as viewing hydrodynamics beyond the gradient expansion as a set of special attractor solutions [8,20,28,31–35]. Our work is also motivated by ongoing efforts to bridge weak- and strong-coupling approaches using holography with higher-derivative corrections [36–40] and extrapolating kinetic theory predictions from weak to realistic/larger couplings [18,41]. Last but not least, our studies are also relevant for attempts to use kinetic theory to map early-time dynamics in heavy-ion collisions to hydrodynamics [42]. The interested reader is invited to consult recent review articles [7,43,44] for an extended discussion of some of these developments.

II. KINETIC THEORY MODELS OF INTEREST

Following earlier studies in Refs. [15,17–20,34,45,46] we consider expanding plasma systems governed by kinetic theory with the collisional kernel $\mathcal{C}[f]$ in the so-called relaxation time approximation (RTA). In our presentation we will follow the conventions of Ref. [46].

The RTA ansatz was introduced originally in Refs. [47,48] and constitutes perhaps the simplest kinetic theory model with hydrodynamic behavior. Within this ansatz, the collisional kernel is linear in the distribution function and vanishes when the latter takes the equilibrium form $f_0(x, p)$:

$$\mathcal{C}[f] = p \cdot U(x) \frac{f(x, p) - f_0(x, p)}{\tau_{\text{rel}}}. \quad (5)$$

This theory contains one adjustable “microscopic” variable—the relaxation time τ_{rel} —and requires specifying the relevant equilibrium distribution function $f_0(x, p)$. We take the latter to be of the Boltzmann form, i.e.,

$$f_0(x, p) = \frac{1}{(2\pi)^3} \exp\left[-\frac{p \cdot U(x)}{T(x)}\right]. \quad (6)$$

Generalizations to Dirac-Fermi and Bose-Einstein distributions are straightforward. In Eq. (6), and also in Eq. (5), $T(x)$ is the effective temperature, i.e., the temperature of the equilibrium state with the same local energy density \mathcal{E} . In the present case they are related by

$$\mathcal{E} = \frac{3}{\pi^2} T^4. \quad (7)$$

Furthermore, the unit timelike four-vector $U(x)$ is the flow velocity defined by the Landau frame (Landau matching) condition for the energy-momentum tensor given by Eq. (2):

$$T^\mu{}_\nu U^\nu = -\mathcal{E} U^\mu. \quad (8)$$

The last part in specifying the model is defining the relaxation time. We will specialize to models with the relaxation time τ_{rel} exhibiting power-law dependence on the effective temperature

$$\tau_{\text{rel}} = \gamma T(\tau)^{-\Delta}, \quad (9)$$

where the overall constant γ , dimensionful for $\Delta \neq 1$, will be set to unity and can always be restored based on dimensional analysis/physical grounds. Two values of Δ stand out: $\Delta = 0$ for which the relaxation time is constant and the theory significantly simplifies and $\Delta = 1$ for which the theory is conformally invariant. Gradient expansions (at large orders) in such RTA models were considered earlier, respectively, in Refs. [17,18].

Let us now specialize to the boost-invariant case [9]. This flow is easiest to study by using the proper time (τ) and spacetime rapidity (y) as coordinates, defined by

$$t = \tau \cosh y \quad \text{and} \quad z = \tau \sinh y. \quad (10)$$

Under longitudinal boosts, τ stays invariant and y gets shifted by a constant. In proper time–rapidity coordinates, components of tensors (e.g., p^μ , U^μ or $T^{\mu\nu}$) are boost invariant as long as they do not depend on y .

The kinematics of this simple flow dictates that

$$U = \partial_\tau \quad (11)$$

and that T be a function of τ only. The symmetries of the problem lead to an energy-momentum tensor $T^{\mu\nu}$ with three different components, $T^\tau{}_\tau$, $T^y{}_y$ and $T^1{}_1 = T^2{}_2$ defining (minus) the local energy density $\mathcal{E}(\tau)$, longitudinal pressure $\mathcal{P}_L(\tau)$ and transversal pressure $\mathcal{P}_T(\tau)$ respectively. They are further related by tracelessness (since we assume massless particles) and conservation equations of the energy-momentum tensor, implying

$$\mathcal{P}_L(\tau) = -\mathcal{E}(\tau) - \tau \dot{\mathcal{E}}(\tau) \quad \text{and} \quad \mathcal{P}_T(\tau) = \mathcal{E}(\tau) + \frac{1}{2} \tau \dot{\mathcal{E}}(\tau). \quad (12)$$

The natural observable, and a measure of deviations from local thermal equilibrium, is the pressure anisotropy normalized to what would be the equilibrium pressure at the same energy density [7,49], i.e.,

$$\mathcal{A}(\tau) = \frac{\mathcal{P}_T(\tau) - \mathcal{P}_L(\tau)}{\mathcal{P}(\tau)}, \quad (13)$$

where $\mathcal{P}(\tau) = \mathcal{E}(\tau)/3$. Moving on to the microscopic level, one can take the distribution function to be a function of proper time τ , the dimensionless combination $\tau p^y \equiv \hat{p}^y$ and the magnitude of the transversal momentum p_T . In this parametrization, the Boltzmann equation takes a particularly simple form

$$\partial_\tau f(\tau, \hat{p}^y, p_T) = \frac{f_0(\tau, \hat{p}^y, p_T) - f(\tau, \hat{p}^y, p_T)}{\tau_{\text{rel}}(\tau)}, \quad (14)$$

where we remind the reader that the relaxation time in the general case will be time dependent and

$$f_0(\tau, \hat{p}^y, p_T) = \frac{1}{(2\pi)^3} \exp\left(-\frac{\sqrt{(\hat{p}^y)^2 + \tau^2 p_T^2}}{\tau T(\tau)}\right). \quad (15)$$

Last, let us remark that the measure factor in the phase space integration dP reads

$$dP = \frac{2\pi p_T}{\tau p^\tau} d\hat{p}^y dp_T, \quad (16)$$

where

$$p^\tau = \frac{1}{\tau} \sqrt{(\hat{p}^y)^2 + \tau^2 p_T^2} \quad (17)$$

and, as a result, the energy density takes the form

$$\begin{aligned} \mathcal{E}(\tau) &= \int dP (p^\tau)^2 f(\tau, \hat{p}^y, p_T) \\ &= \frac{2\pi}{\tau^2} \int_0^\infty dp_T \int_{-\infty}^\infty d\hat{p}^y p_T \sqrt{(\hat{p}^y)^2 + \tau^2 p_T^2} f(\tau, \hat{p}^y, p_T). \end{aligned} \quad (18)$$

Let us now move on to the initial value problem. As anticipated in the introduction, solving Eq. (14) requires knowing f as a function of two variables, \hat{p}^y and p_T , at some initial time τ_0 . One can see it in two steps. First, one can write a formal integral solution for the distribution function of the form

$$\begin{aligned} f(\tau, \hat{p}^y, p_T) &= D(\tau, \tau_0) f(\tau_0, \hat{p}^y, p_T) \\ &\quad + \int_{\tau_0}^\tau \frac{d\tau'}{\tau_{\text{rel}}(\tau')} D(\tau, \tau') f_0(\tau', \hat{p}^y, p_T), \end{aligned} \quad (19)$$

where

$$D(\tau_2, \tau_1) = \exp\left[-\int_{\tau_1}^{\tau_2} \frac{d\tau'}{\tau_{\text{rel}}(\tau')}\right]. \quad (20)$$

Note that the above expression is exponentially suppressed for $\tau_2 \gg \tau_1$.

In Eq. (19), one should bear in mind that the relaxation time can depend on the effective temperature [see Eq. (9)] and, through Eqs. (7) and (18) on the distribution function at a given instance of proper time. This is resolved by taking the second moment of both sides of Eq. (19) with respect to p^x , as in Eq. (18), since this leads to an expression depending only on the effective temperature $T(\tau)$. Indeed, one then obtains the following integral equation [45,46]:

$$\mathcal{E}(\tau)D(\tau, \tau_0)^{-1} = \mathcal{E}_0(\tau) + \frac{1}{2} \int_{\tau_0}^{\tau} \frac{d\tau'}{\tau_{\text{rel}}(\tau')} \mathcal{E}(\tau')D(\tau', \tau_0)^{-1} H\left(\frac{\tau'}{\tau}\right), \quad (21)$$

where

$$H(q) = q^2 + \frac{\arctan \sqrt{\frac{1}{q^2} - 1}}{\sqrt{\frac{1}{q^2} - 1}} \quad (22)$$

and

$$\mathcal{E}_0(\tau) = \frac{2\pi}{\tau^2} \int_0^{\infty} dp_T \int_{-\infty}^{\infty} d\hat{p}^y \times p_T \sqrt{(\hat{p}^y)^2 + \tau^2 p_T^2} f(\tau_0, \hat{p}^y, p_T). \quad (23)$$

Equation (21) will play the central role in the analysis here. Before we move on to describing new results, a few remarks are in order. First, Eq. (21) is an integral equation, i.e., the effective temperature at a given instance of proper time depends on the whole temperature history until that moment. Second, $\mathcal{E}_0(\tau)$ feeds information about the initial distribution function into the temperature profile as a function of proper time. The definition of $\mathcal{E}_0(\tau)$ implies the symmetry $\mathcal{E}_0(\tau) = \mathcal{E}_0(-\tau)$ and a late-time expansion of the form

$$\mathcal{E}_0(\tau) = \frac{1}{|\tau|} \left(\epsilon_1 + \frac{\epsilon_3}{\tau^2} + \frac{\epsilon_5}{\tau^4} + \dots \right), \quad (24)$$

i.e., with only even powers in the parentheses and, in general, with infinitely many independent coefficients ϵ_j . Third, the function $H(q)$ under the integral is evaluated only for $q \in (0, 1]$, but as we showed with our collaborators in Ref. [18], its analytic properties in the complex q plane are, in fact, important. The coarse features of $H(q)$ make it similar to a simple linear function, i.e., $2q$, but, as we will see in Secs. III and IV, its fine details directly translate into the values of hydrodynamic transport coefficients and transient modes. Finally, Eq. (21) is in general a strongly nonlinear equation for the effective temperature $T(\tau)$ or,

equivalently, local energy density $\mathcal{E}(\tau)$ because of the temperature-dependent relaxation time $\tau_{\text{rel}}(\tau)$. However, for constant relaxation time, i.e., for $\Delta = 0$ in Eqs. (9) and (21) becomes a linear equation for $\mathcal{E}(\tau)$. This significant simplification will allow us in Sec. V to see some beautiful resurgent relations between the hydrodynamic and the transient parts of $\mathcal{E}(\tau)$. Otherwise, Eq. (21) can be solved numerically, which we do in Sec. VI using a refinement of the method from Ref. [46].

III. GRADIENT EXPANSION

In the boost-invariant flow, the hydrodynamic gradient expansion (i.e., expansion in the Knudsen number) is a power series in the ratio of the microscopic dissipation scale, here set by τ_{rel} , and the size of the gradient which is set by the kinematics to be $\frac{1}{\tau}$. We will call this dimensionless ratio w :

$$w \equiv \frac{\tau}{\tau_{\text{rel}}}. \quad (25)$$

If we use our ansatz for the relaxation time, then w reads

$$w = \tau T(\tau)^\Delta. \quad (26)$$

In the conformally invariant case, $\Delta = 1$, we recover the w variable introduced in Ref. [49], which justifies the name. In particular, when comparing different solutions of Eq. (21) we will be looking at the normalized pressure anisotropy \mathcal{A} defined in Eq. (13) as a function of w . Of course, one can still treat w as a function of proper time, i.e., $w(\tau)$, as we will often do below.

The energy density can therefore be formally expanded as

$$\mathcal{E}(\tau) = \frac{\Lambda^4}{(\Lambda\tau)^{4/3}} \left(1 + \frac{e_1}{w(\tau)} + \frac{e_2}{w(\tau)^2} + \dots \right) \quad (27)$$

where the coefficients e_j are fixed by Δ and independent of the initial condition. Alternatively, one can represent the energy density in the equivalent late-time expansion as

$$\mathcal{E}(\tau) = \frac{\Lambda^4}{(\Lambda\tau)^{4/3}} \left(1 + \frac{\tilde{e}_1}{(\Lambda\tau)^{1-\Delta/3}} + \frac{\tilde{e}_2}{(\Lambda\tau)^{2-2\Delta/3}} + \dots \right), \quad (28)$$

where comparison with Eq. (27) allows one to relate \tilde{e}_j 's and e_j 's. One can deduce from Eq. (28) that the allowed range of the parameter Δ is

$$\Delta < 3, \quad (29)$$

as otherwise the relaxation time at late times gets too large to allow for a depletion of gradients. Such an effect was seen in Refs. [50,51], in RTA kinetic theory undergoing Gubser flow. The rapid expansion in that setup drives the

system away from thermal equilibrium. The case $\Delta > 3$ is not explored in this paper, but we note that the eremitic expansion of Ref. [52] may be more appropriate in that case.

Expansions in Eqs. (27) and (28) translate directly into the large- w expansion of the normalized pressure anisotropy \mathcal{A} :

$$\mathcal{A} = \frac{a_1}{w} + \frac{a_2}{w^2} + \dots \quad (30)$$

Again, it should be noted that the gradient expansion in Eq. (30) does not contain any information about an initial state and in Eqs. (27) and (28) the only information sits in the asymptotic scaling set by Λ . Regarding its relation to the transport coefficients, the term a_1 is related to the ratio of the shear viscosity η to the entropy density and the term a_2 is related to a combination of second-order transport coefficients τ_π and λ_1 ; see, e.g., Ref. [7] for details.

As noted in Ref. [18], the gradient expansion in RTA kinetic theory can be generated using integration by parts of the integral in Eq. (21). First, let us observe that

$$D(\tau', \tau_0)^{-1} = \tau_{\text{rel}}(\tau') \frac{d}{d\tau'} D(\tau', \tau_0)^{-1}. \quad (31)$$

The appearance of a derivative allows for repeated application of integration by parts in Eq. (21). Focusing only on the relevant integral one gets

$$\begin{aligned} & \int_{\tau_0}^{\tau} \frac{d\tau'}{\tau_{\text{rel}}(\tau')} H\left(\frac{\tau'}{\tau}\right) \mathcal{E}(\tau') D(\tau', \tau_0)^{-1} \\ &= \int_{\tau_0}^{\tau} d\tau' H\left(\frac{\tau'}{\tau}\right) \mathcal{E}(\tau') \frac{d}{d\tau'} D(\tau', \tau_0)^{-1} \\ &= H(1) \mathcal{E}(\tau) D(\tau, \tau_0)^{-1} - H\left(\frac{\tau_0}{\tau}\right) \mathcal{E}(\tau_0) \\ &\quad - \int_{\tau_0}^{\tau} d\tau' \frac{d}{d\tau'} \left[H\left(\frac{\tau'}{\tau}\right) \mathcal{E}(\tau') \right] D(\tau', \tau_0)^{-1}. \end{aligned} \quad (32)$$

Exactly the same logic can be applied to the final integral appearing in the above equation, which leads to an iterative scheme that can be executed indefinitely. Every subsequent integration by parts is going to generate a term proportional to $D(\tau, \tau_0)^{-1}$ which at late times is exponentially enhanced over the other term. Gathering such dominant terms and neglecting others in the iterated version of Eq. (21) leads to a differential relation involving derivatives of $H(q)$ at $q=1$ and derivatives of $\mathcal{E}(\tau)$ measured in units of relaxation time. As a result one obtains

$$\sum_{j=1}^{\infty} \left(-\tau_{\text{rel}}(\tau') \frac{d}{d\tau'} \right)^j H\left(\frac{\tau'}{\tau}\right) \mathcal{E}(\tau') \Big|_{\tau'=\tau} = 0, \quad (33)$$

which needs to vanish up to exponentially small corrections (hence the equality in the equation above). Using this expression with the sum truncated at, say, $j=3$ and $\mathcal{E}(\tau)$ given by the gradient expansion allows us to determine, in this case, e_1 and e_2 in Eq. (27) and, as a result, a_1 and a_2 in Eq. (30). The result reads

$$a_1 = \frac{8}{5} \quad \text{and} \quad a_2 = \frac{88}{105} - \frac{8}{15} \Delta. \quad (34)$$

Iterating this scheme further allows one to get higher-order transport. This approach works best for a constant relaxation time in which case one can get the lowest 1500 coefficients. We did this by first using Eq. (33) to derive a recursive relation for the coefficients e_j from Eq. (27), which, for $\Delta=0$, happen to be the same as the coefficients \tilde{e}_j appearing in Eq. (28), and solving this relation. Unfortunately, the number of terms generated in Eq. (33) gets significantly bigger and the whole approach becomes slower for generic values of Δ . However, in all the cases we checked it was sufficient to demonstrate that the gradient expansion has a vanishing radius of convergence, as expected on general grounds [7]. For a temperature-dependent relaxation time the methods from Refs. [7,18] and, perhaps, also Ref. [17] are better suited to get a significant number of terms, e.g., 425 terms in the conformal case ($\Delta=1$) considered in Ref. [18].

A standard way of dealing with asymptotic series is the Borel transform, which takes $a_n w^{-n}$ to $a_n \zeta^n / n!$, and Borel summation which at the level of a series inverts the former operation; see e.g., Ref. [7]. In Fig. 1 we show the structure of singularities of the Borel transform of the truncated hydrodynamic gradient expansion for six representative values of Δ . As a way of analytically continuing the Borel transform away from the origin we use the standard symmetric Padé approximation. In Fig. 1 we always see poles on the real axis and for $\Delta > 0$ we also see singularities further in the complex plane. As argued in Ref. [18], the latter are not physical excitations, but rather represent analytic properties of Eq. (21) with contours of integration over τ' extended away from the real axis. To see this, note that the gradient expansion, computed using Eq. (33), does not know about the choice of contour between τ_0 and τ in Eq. (21). Different choices of contour will differ by terms coming from singularities of the integrand. By the analytic properties of $H(x)$, such terms will behave as

$$\delta \mathcal{E} \sim e^{-\frac{1+(-1)^{\pm\Delta/3}}{1-\Delta/3} w}. \quad (35)$$

While these terms are not to be interpreted as transients, they are nevertheless important. For $\Delta > 2$, these will in fact represent the dominant large-order behavior of the gradient expansion. This has similarities with the ghost instantons studied in quantum mechanics in Ref. [53]. Last, the movement of the off-axis poles as $\Delta \rightarrow 3$ signals a

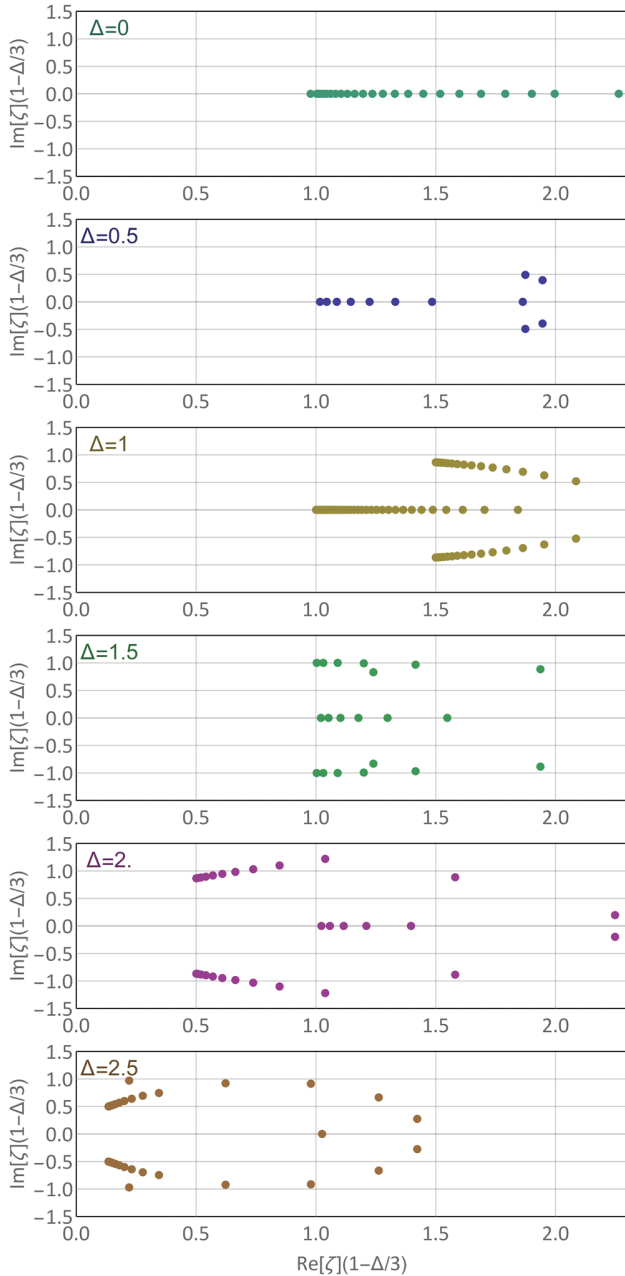


FIG. 1. Singularities of the Borel transform of the hydrodynamic gradient expansion of \mathcal{A} for sample values of allowed Δ ; see Eq. (29). As a method of analytic continuation we use Padé approximants. The cases of $\Delta = 0$ and $\Delta = 1$ were studied before in, respectively, Refs. [17,18]. In the plots sequences of poles represent branch cuts, a known feature of the Padé approximation; see, e.g., Ref. [54]. The singularities on the real axis are physical and give rise to transients of the form dictated by Eq. (36). The arguments in Sec. IV make it clear that this singularity is an infinite set of branch cuts with the same branch point, but of a different order. The singularities off the real axis are unphysical and follow from contour deformations in the integral in Eq. (21), as explained for $\Delta = 1$ in Ref. [18]. Surprisingly, the unphysical singularities, whose location is at $1 + (-1)^{\pm\Delta/3}$, start controlling the radius of convergence of the hydrodynamic series for $\Delta > 2$.

breakdown of this analysis, as anticipated in the discussion around Eq. (29).

In the present manuscript we will be concerned with singularities lying on the real axis and their relation to transient modes (Sec. IV) and resurgence (Sec. V).

IV. TRANSIENT MODES

We have seen that the gradient expansion is universal, independent of initial conditions. In this section, we describe transient corrections to the universal late-time behavior. These transient modes come with an overall amplitude and phase that offer the possibility to encode initial information. To this end, we discard \mathcal{E}_0 and set the lower limit of integration τ_0/τ to 0. This may seem contradictory, as this removes all initial data. We do this as here we are only concerned with demonstrating how data *can* be stored rather than the particular way a given initial condition *is* stored. We will say more about the matching of initial data to late-time modes in Sec. V. We present here the $\Delta = 0$ case as the general case introduces mainly notational (not technical) difficulties.

Since Eq. (21) contains exponential suppression in the form of $D(\tau, \tau_0)$, a natural ansatz for the energy density is

$$\mathcal{E}(\tau) = \mathcal{E}_{ge}(\tau) + \sigma D(\tau, \tau_0) \mathcal{E}_\beta(\tau), \quad (36)$$

where $\mathcal{E}_{ge}(\tau)$ is the gradient expansion and $\mathcal{E}_\beta(\tau)$ is a power series with leading power β (which, as we will soon see, is in general a complex number), i.e.,

$$\mathcal{E}_\beta(\tau) = w^\beta \left(1 + \frac{e_{\beta,1}}{w} + \frac{e_{\beta,2}}{w^2} + \dots \right). \quad (37)$$

Inserting this into Eq. (21) and matching powers of w leads to equations for β and $e_{\beta,k}$. In this section, β is the object of interest. As described in Sec. V, for a given β , the rest of the coefficients $e_{\beta,k}$ are uniquely determined. However, the equations leave σ undetermined. Hence, each allowed value of β supplies one free parameter where initial data can be stored. Also, it is implicitly assumed in Eq. (36) that we sum over all allowed (as we will soon see, infinitely many) values of β , each with an independent value of σ .

One finds that the β 's are given by zeros of the function

$$M(z) \equiv \int_0^1 dx H(x) x^z. \quad (38)$$

Note that the integral converges only for $z > -1$ and that for such z , $M(z) > 0$. One must analytically continue $M(z)$ to complex z to find any solutions. This can be done by using a series expansion for H or the representation

$$M(z) = \frac{{}_3F_2(1, \frac{z}{2} + 2, \frac{z}{2} + 2; \frac{z}{2} + \frac{5}{2}, \frac{z}{2} + 3; 1)}{2z^2 + 14z + 24} + \frac{1}{2(z+4)}. \quad (39)$$

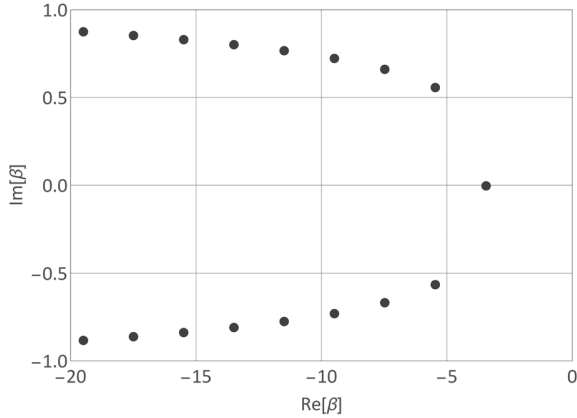


FIG. 2. Points in the figure shows roots of the function $M(\beta)$. For $\Delta = 0$, each root gives rise to a transient mode of the form $e^{-\tau\beta}$. For other Δ , the modes behave as in Eq. (41). The roots with the largest real part will be the dominant ones. The first three are $\beta_1 \approx -3.4313$, $\beta_{\pm 2} \approx -5.4584 \pm 0.5614i$, $\beta_{\pm 3} \approx -7.4746 \pm 0.6648i$.

Solutions to $M(z) = 0$ are shown in Fig. 2. The string of zeros seems to continue indefinitely, leading us to believe that there are an infinite number of allowed β 's. One is purely real and the rest come in conjugate pairs with successively smaller real parts.

Let us stress the difference between these solutions and the Borel plane depicted in Fig. 1. The Borel analysis reveals the exponential dependence i.e., the decay rate (for an exponential decay in w) and oscillation frequency (for oscillation in w). This analysis gives the subleading power-law correction. For the transients, the exponential dependence is purely real, and one would be tempted to conclude that there is no oscillation. However, the imaginary parts of these solutions give rise to logarithmic oscillations as

$$\Re(\sigma\tau^\beta) \propto \tau^{\Re(\beta)} \cos(\theta + \Im(\beta) \log(\tau)), \quad (40)$$

for some phase θ . We were unable to find other transients in the present setup and the fact that we nevertheless found an infinite set of modes, in principle capable of capturing all of the information about the initial conditions, leads us to believe that there are none. Let us repeat what was said in the caption of Fig. 1. A generalization of the argument from Ref. [18] shows that the other exponents that can be read off from Fig. 1 are not physical modes.

Finally, we note that the argument presented above generalizes in a simple manner to the case of arbitrary Δ . In such a situation, the power law also gets contributions from $D(\tau, \tau_0)$. To leading order in $w = \tau/\tau_{\text{rel}}$, transient contributions to $\mathcal{E}(\tau)$ behave as

$$e^{-\frac{w}{1-\Delta/3}} w^{\beta + \frac{4\Delta}{45(1-\Delta/3)^2}}, \quad (41)$$

where β satisfies $M(\beta(1 - \Delta/3) - \Delta/3) = 0$. This is the main result of this paper. It should be compared with what is found in holographic setups, where transients behave as in Eq. (4). There are three main differences. The first is the appearance of singularities in the Borel plane that do not represent transients on top of the hydro part. Second, the transients that do carry information are all stacked on top of each other in the Borel plane. This corresponds to identical exponential decay but with different power laws. Last, while in holography the transients generically oscillate in proper time, in this kinetic theory they do so in logarithmic time.

In Sec. VI we corroborate these results with numerical solutions.

V. RESURGENCE AND INITIAL CONDITIONS FOR CONSTANT τ_{rel}

When τ_{rel} is constant, Eq. (21) is linear. This is a great simplification, allowing us to investigate resurgent relations between the hydrodynamic and the nonhydrodynamic modes, as well as describe how to match initial data to amplitudes of transients.

We start the resurgent analysis by calculating the coefficients in the power series \mathcal{E}_β . It satisfies

$$\mathcal{E}_\beta(\tau) = \frac{\tau}{2\tau_{\text{rel}}} \int_0^1 H(x) \mathcal{E}_\beta(\tau x) dx. \quad (42)$$

With a power-series ansatz as in Eq. (37), we can match powers and solve for the coefficients in the series. They satisfy the recursive equation

$$e_{\beta,k+1} = \frac{e_{\beta,k}}{M(\beta - k - 1)}. \quad (43)$$

An immediate question arises: what is the large-order behavior of $e_{\beta,k}$? Is it divergent and if so, will it tell us about additional transient modes? For large k ,

$$\frac{e_{\beta,k+1}}{e_{\beta,k}} = -k + \left(\beta + \frac{4}{3}\right) + \frac{16}{45k} + \dots \quad (44)$$

This can be turned into a differential equation and a solution of this equation is a function that at large w behaves as

$$e^w w^{-\beta-4/3} \left(1 - \frac{16}{45w} - \frac{424}{14175w^2} \dots\right). \quad (45)$$

To find the contribution to $\mathcal{E}(\tau)$ we must take into account $D(\tau, \tau_0)$ and w^β in Eqs. (36) and (37). These cancel out the exponential and the $w^{-\beta}$ respectively, leaving us with a series whose leading power is $-4/3$. Given that in the current case of $\Delta = 0$, $w \sim \tau$, one immediately recognizes in it the famous Bjorken perfect fluid solution [9]. By the

use of Eqs. (12) and (13), one can calculate the corresponding series for \mathcal{A} . This turns out to be

$$\frac{8}{5w} + \frac{88}{105w^2} + \dots \quad (46)$$

Comparing with Eq. (34), and setting there Δ to 0, we see that this is in fact the hydrodynamic gradient expansion. Note that this argument holds for every value of allowed β .

This is an explicit demonstration of resurgent properties of these solutions; see Refs. [55,56] for introductions to resurgence and Ref. [57] for another example of resurgent phenomena in the context of integral equations. The gradient expansion can be reconstructed from the large-order behavior of the transient, since in the constant relaxation case the only exponential contribution to $\mathcal{E}(\tau)$ with respect to each transient is the hydrodynamic series itself.

Now we describe how to map between initial conditions, described by \mathcal{E}_0 , and transient modes. This procedure only works for $\Delta = 0$, i.e., when the problem is linear. Given a solution $\mathcal{E}(\tau)$, one can trivially solve for $\mathcal{E}_0(\tau)$ in Eq. (21). Knowing the form of transients, one can calculate the corresponding \mathcal{E}_0 to each transient. Thus, a decomposition of a solution \mathcal{E} into transients can be translated into a decomposition of \mathcal{E}_0 .

As a check of this, we have numerically calculated the \mathcal{E}_0 's corresponding to the first two transients and compared these with the late-time expansion of \mathcal{E}_0 in Eq. (24). The characteristic features of this expansion, namely the leading power of $1/\tau$ and a vanishing quadratic term, can be verified for these solutions.

VI. COMPARISON WITH NUMERICAL SOLUTIONS

In previous sections, we have calculated a family of transient modes, each exponentially decaying with the same rate but with different power laws. These powers were determined from a rather high-level argument and additional checks are required to be confident that they are physical modes. Indeed, as observed in Ref. [18], the analytic structure of H can give rise to unphysical modes. This section presents numerical evidence that they are physical.

Our interest in looking at transients prompts the need for very precise numerics. We need a time interval long enough so that they are clearly separated from each other in magnitude. In holographic setups, the ratio of the magnitudes of the transients is exponentially large. In this case, there is only a power-law suppression. Thus, this setup requires a longer interval of time compared to what a similar calculation in holography would need. Since the transients decay exponentially fast compared to the hydrodynamic contribution, this presents an obvious numerical challenge. Finite difference methods have an error that

scales polynomially in the grid spacing which makes them unsuitable for studying exponentially small effects. More appropriate are spectral and pseudospectral methods which have an error that (for smooth functions) scales exponentially in the grid spacing. See, e.g., Refs. [58,59] for introductions to these methods.

Given an initial distribution function, the integral equation (21) can be solved by iteration. We choose the initial distribution function so that $\mathcal{E}_0(\tau)$ can be calculated analytically. For $\Delta = 0$, we calculated solutions on an interval from $w = 5$ to $w = 170$. This means we need an accuracy of at least $e^{-170} \approx 10^{-74}$. We achieved this by performing calculations in MATHEMATICA with 1350 grid points and precision 900, iterating the equation until the maximal relative error between subsequent iterations was less than 10^{-150} . For this process to converge, spectral filtering was used; see Ref. [59]. For each initial condition we required several hours of computations on a powerful desktop computer. By a process of subtracting solutions of different initial conditions, we are able to study transients.

Independent of initial conditions, \mathcal{A} behaves universally at late times, corresponding to the hydrodynamic gradient expansion; see Eq. (34). Subtracting two solutions will remove the universal behavior and leave only the transient behavior. Taking also a logarithmic derivative will remove the overall amplitude and we are left with a universal late-time behavior corresponding to the transient mode. By taking into account the phase θ in Eq. (40), this subtraction can be repeated to get a sequence of functions whose behavior is universal at late times. Here, we consider the first two functions so obtained. These subtractions do not involve a phase, and so we define

$$\mathcal{A}_0 = \mathcal{A}, \quad (47)$$

$$\mathcal{A}_1 = \frac{d}{dw} \log(\mathcal{A}_0 - \mathcal{A}'_0), \quad (48)$$

$$\mathcal{A}_2 = \frac{d}{dw} \log(\mathcal{A}_1 - \mathcal{A}'_1), \quad (49)$$

where the prime denotes solutions obtained using different initial conditions. \mathcal{A}_k will be related to the transient corresponding to β_k . Analytic calculation implies

$$\mathcal{A}_1(w) = -1 + \frac{\beta_1 + 7/3}{w} + \dots, \quad (50)$$

where the -1 comes from the exponential decay rate. As seen in Fig. 3, both the decay rate and β_1 approach their predicted analytic values (red dashed line).

The next transient is supposed to exhibit oscillations in logarithmic time. To leading order, \mathcal{A}_2 satisfies

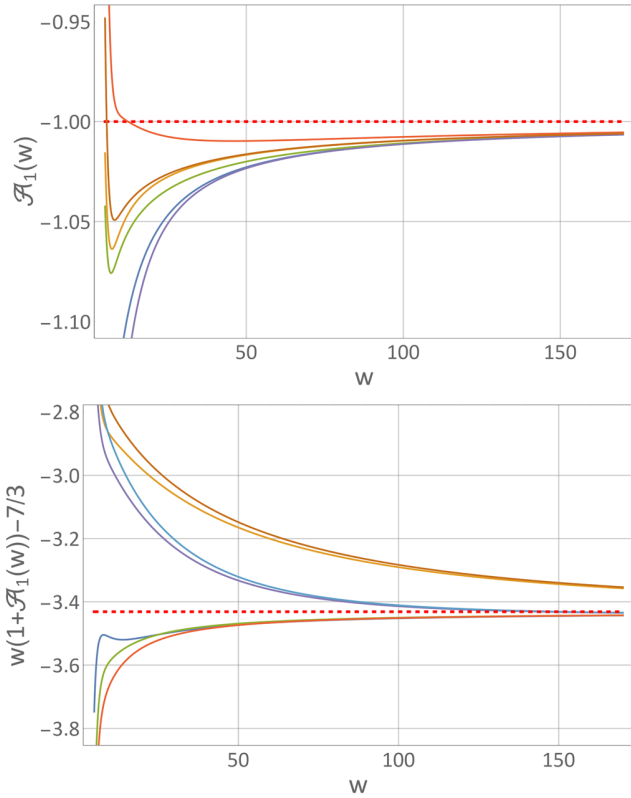


FIG. 3. Shown here is $\mathcal{A}_1(w)$ defined in Eq. (47). The plots provide overwhelming evidence that Eq. (50) accurately describes the first transient mode. Note that $\Delta = 0$. (Top) All curves approach the exponential decay rate of the transient modes -1 . (Bottom) All curves approach the power-law decay rate of the first transient mode β_1 .

$$w\mathcal{A}_2(w) = \Re(\beta_2) - \beta_1 - 1 - \Im(\beta_2) \tan(\theta + \Im(\beta_2) \log(w)) \\ \approx -3.0271 - 0.5614 \tan(\theta + 0.5614 \log(w)), \quad (51)$$

where numerical values for β_1 and β_2 have been used. This has characteristic singularities that should have clear signals in the numerical solutions. However, corrections coming from subleading transients could spoil this if their amplitudes are large enough. Indeed, as Fig. 4 shows, some solutions are not well described by Eq. (51) while others are. With only one adjustable parameter and fitting only to a small interval at late times, one finds a remarkable agreement; see Fig. 4. This is striking confirmation of the multiplicity of cuts stacked on top of each other in the Borel plane and demonstrates the physicality of oscillations in logarithmic time.

In addition, one can also fit β_2 to the data. The result matches the analytic value to better than 1%.

VII. SUMMARY AND OUTLOOK

In the present article we analyzed the nonhydrodynamic sector of kinetic theory in the relaxation time approximation.

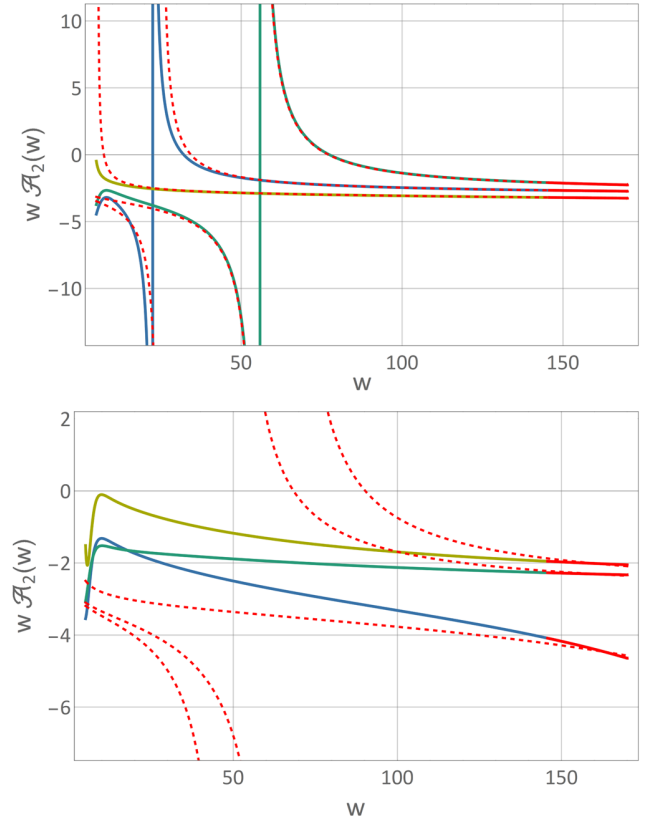


FIG. 4. This figure compares the numerically evaluated \mathcal{A}_2 , i.e., the second transient, with theoretical predictions for $\Delta = 0$. Dashed red lines are of the form of Eq. (40), where θ is fitted using data in the continuous red colored region at late times. (Top) Equation (40) describes the curves very well. Fitting also the value of β_2 , it differs from the analytical value by less than 1%. The vertical segments represent a singularity of the tangent function appearing in Eq. (51). (Bottom) Likely due to interference from subleading transients with large amplitudes, the fit does not work well.

Using a three-pronged approach involving asymptotic series, analytic solutions of an integral equation and high-precision numerical solutions of the initial value problem, we showed how each of these methods allow us to probe this sector. The relaxation time was taken to exhibit general power-law dependence on the effective temperature; see Eq. (9). Such a theory was regarded here as a toy model of weakly coupled gauge theory dynamics. Moreover, we focused on expanding plasma systems undergoing rapid longitudinal expansion, similarly to ultrarelativistic heavy-ion collisions. We simplified our treatment by further assuming boost invariance along the expansion axis and no transversal dynamics. Our chief motivation, inspired by similar analyses in holography, was to understand what imprint weakly coupled transient effects will have on the energy-momentum tensor of expanding plasma. The fact that the Boltzmann equation requires specifying a function not only of spacetime coordinates but also of momenta in order to solve the initial

value problem indicated that there should be infinitely many transient effects carrying information about a given initial condition to late times. This intuition turned out to be correct and we discovered that in the expanding plasma system in RTA kinetic theory there are infinitely many exponentially suppressed contributions to the energy-momentum tensor, decaying on a time scale $\tau_{\text{decay}} = (1 - \Delta/3)\tau_{\text{rel}}$; see Sec. IV and Eq. (41). What differentiates these transients from each other is the subleading behavior. We showed that it consists of different power-law decays and oscillations in logarithmic time; see Eqs. (40) and (41), as well as Fig. 2. We corroborated both findings with the analysis of large orders of the hydrodynamic gradient expansion (see Sec. III and Fig. 1) and an explicit solution of the initial value problem (see Sec. VI and Figs. 3 and 4), noting very good agreement. The latter was achieved by a very accurate method of implementing the initial value problem given by the pseudospectral methods and use of the iterative scheme from Ref. [46].

Furthermore, similarly to the studies reported in Ref. [18], we saw singularities of the Borel transform of the hydrodynamic gradient expansion that do not correspond to modes of the expanding plasma; see Fig. 1. For $\Delta > 3/2$, these would represent the dominant contribution to transient behavior in the initial value problem, something which we did not see. What is also interesting is that for $\Delta > 2$, these singularities become the dominant effects controlling the divergence of the hydrodynamic gradient expansion, as opposed to the least-damped transients in all the other known setups dealing with hydrodynamics; see, e.g., Ref [7] for a review. However, there are intriguing similarities with the so-called ghost instantons explored in a quantum-mechanical setting in Ref. [53].

We note that for constant relaxation time ($\Delta = 0$) the integral equation for the energy density becomes linear; see Eq. (21). Here we find beautiful resurgent relations in which large orders of the hydrodynamic gradient expansion carry information about the transient modes and the large-order gradient expansion accompanying each transient mode is controlled by the hydrodynamic series; see Eq. (45). As a result, the trans-series ansatz in this case consists only of two types of contributions: the hydrodynamic series and a sum over transient modes without any further nonlinear effects. For $\Delta \neq 0$, we expect nonlinear effects. The question of what happens when $\Delta > 3$ or at the point of breakdown, $\Delta = 3$, is left open.

Our work raises several interesting questions. Perhaps the most important one is what kind of transients in expanding plasma systems (or other setups undergoing macroscopic motion) exist for other collisional kernels and are their decay rates comparable/the same? This is of relevance in the search for transient effects in heavy-ion collision or cold-atom experiments; see, e.g., Refs. [60,61].

Another interesting question is if it is possible to derive the properties of the transients directly from singularities of the retarded two-point function of the energy-momentum tensor studied in Ref. [15]. The reason why we expect such a link to exist is, first, that similar analysis works out in holography (see Ref. [11]), and, second, that the properties of transients are related to the properties of the function $H(q)$ given by Eq. (22) and the latter is related to properties of equilibrium, i.e., the equilibrium distribution function given by Eq. (15). Furthermore, the Green's function analysis in Ref. [15] revealed branch cut singularities with the imaginary part of branch points (which are responsible for dissipation) being given by the inverse of the relaxation time and this is precisely what we observed here. Such a method of translating from the singularities of the energy-momentum tensor Green's functions to expanding plasma systems may shed light on how transients manifest themselves both for kinetic theories with more complicated collisional kernels, (see the recent Ref. [16]) and for more general flows.

On the latter front, it would be very interesting to generalize the present analysis to other flows, starting from the most symmetric ones such as cosmological expansion addressed in Refs. [62,63] or (perturbations of) the so-called Gubser flow [64] studied in the RTA kinetic theory in Refs. [50,51]. An interesting aspect for such a comparison is the question of what happens when the relaxation time from the present setup scales with the effective temperature faster than $\frac{1}{T}$. For such relaxation times, we do not expect local equilibrium in the energy-momentum tensor at asymptotically late times and a similar phenomenon was indeed seen in Refs. [50,51]. It would be, therefore, interesting to understand if in such cases hydrodynamics becomes a good description of the boost-invariant plasma for a window of intermediate times and how the system exits the hydrodynamic regime.

ACKNOWLEDGMENTS

We are grateful to our collaborators from Ref. [18], A. Kurkela and M. Spalinski, and friends and colleagues, in particular I. Aniceto, G. Basar, J. Casalderrey-Solana, G. Dunne, W. Florkowski, U. Heinz, R. Janik, P. Kovtun, H. Marrochio, M. Martinez, J. Noronha, P. Romatschke, M. Strickland, L. Yaffe, and P. Witaszczyk and for useful discussions, correspondence and comments on the draft. The Gravity, Quantum Fields and Information group at Albert Einstein Institute that we are part of is generously supported by the Alexander von Humboldt Foundation and the Federal Ministry for Education and Research through the Sofja Kovalevskaja Award. V.S. also acknowledges partial support from the National Science Centre through Grant No. 2015/19/B/ST2/02824.

- [1] U. W. Heinz, *AIP Conf. Proc.* **739**, 163 (2005).
- [2] J. Casalderrey-Solana, H. Liu, D. Mateos, K. Rajagopal, and U. A. Wiedemann, *Gauge/String Duality, Hot QCD and Heavy Ion Collisions* (Cambridge University Press, Cambridge, England, 2014).
- [3] W. Busza, K. Rajagopal, and W. van der Schee, *arXiv:1802.04801*.
- [4] J. M. Maldacena, *Adv. Theor. Math. Phys.* **2**, 231 (1998).
- [5] E. Witten, *Adv. Theor. Math. Phys.* **2**, 253 (1998).
- [6] S. Gubser, I. R. Klebanov, and A. M. Polyakov, *Phys. Lett. B* **428**, 105 (1998).
- [7] W. Florkowski, M. P. Heller, and M. Spalinski, *Rep. Prog. Phys.* **81**, 046001 (2018).
- [8] P. Romatschke, *Phys. Rev. Lett.* **120**, 012301 (2018).
- [9] J. Bjorken, *Phys. Rev. D* **27**, 140 (1983).
- [10] P. M. Chesler and L. G. Yaffe, *Phys. Rev. D* **82**, 026006 (2010).
- [11] R. A. Janik and R. B. Peschanski, *Phys. Rev. D* **74**, 046007 (2006).
- [12] M. P. Heller, R. A. Janik, M. Spaliński, and P. Witaszczyk, *Phys. Rev. Lett.* **113**, 261601 (2014).
- [13] S. A. Hartnoll, A. Lucas, and S. Sachdev, *arXiv:1612.07324*.
- [14] P. K. Kovtun and A. O. Starinets, *Phys. Rev. D* **72**, 086009 (2005).
- [15] P. Romatschke, *Eur. Phys. J. C* **76**, 352 (2016).
- [16] A. Kurkela and U. A. Wiedemann, *arXiv:1712.04376*.
- [17] G. S. Denicol and J. Noronha, *arXiv:1608.07869*.
- [18] M. P. Heller, A. Kurkela, M. Spalinski, and V. Svensson, *Phys. Rev. D* **97**, 091503 (2018).
- [19] J.-P. Blaizot and L. Yan, *J. High Energy Phys.* **11** (2017) 161.
- [20] J.-P. Blaizot and L. Yan, *Phys. Lett. B* **780**, 283 (2018).
- [21] R. Baier, P. Romatschke, D. T. Son, A. O. Starinets, and M. A. Stephanov, *J. High Energy Phys.* **04** (2008) 100.
- [22] W. Florkowski and R. Ryblewski, *Phys. Rev. C* **83**, 034907 (2011).
- [23] M. Martinez and M. Strickland, *Nucl. Phys.* **A848**, 183 (2010).
- [24] G. S. Denicol, H. Niemi, E. Molnar, and D. H. Rischke, *Phys. Rev. D* **85**, 114047 (2012); **91**, 039902(E) (2015).
- [25] G. Denicol, E. Molnar, H. Niemi, and D. Rischke, *Eur. Phys. J. A* **48**, 170 (2012).
- [26] M. Stephanov and Y. Yin, *Phys. Rev. D* **98**, 036006 (2018).
- [27] M. P. Heller, R. A. Janik, and P. Witaszczyk, *Phys. Rev. Lett.* **110**, 211602 (2013).
- [28] M. P. Heller and M. Spalinski, *Phys. Rev. Lett.* **115**, 072501 (2015).
- [29] G. Basar and G. V. Dunne, *Phys. Rev. D* **92**, 125011 (2015).
- [30] I. Aniceto and M. Spalinski, *Phys. Rev. D* **93**, 085008 (2016).
- [31] M. Spalinski, *Phys. Lett. B* **776**, 468 (2018).
- [32] M. Strickland, J. Noronha, and G. Denicol, *Phys. Rev. D* **97**, 036020 (2018).
- [33] P. Romatschke, *J. High Energy Phys.* **12** (2017) 079.
- [34] G. S. Denicol and J. Noronha, *Phys. Rev. D* **97**, 056021 (2018).
- [35] A. Behtash, C. N. Cruz-Camacho, and M. Martinez, *Phys. Rev. D* **97**, 044041 (2018).
- [36] S. Grozdanov, N. Kaplis, and A. O. Starinets, *J. High Energy Phys.* **07** (2016) 151.
- [37] T. Andrade, J. Casalderrey-Solana, and A. Ficnar, *J. High Energy Phys.* **02** (2017) 016.
- [38] S. Grozdanov and W. van der Schee, *Phys. Rev. Lett.* **119**, 011601 (2017).
- [39] S. Grozdanov and A. O. Starinets, *J. High Energy Phys.* **03** (2017) 166.
- [40] J. Casalderrey-Solana, N. I. Gushterov, and B. Meiring, *J. High Energy Phys.* **04** (2018) 042.
- [41] L. Keegan, A. Kurkela, P. Romatschke, W. van der Schee, and Y. Zhu, *J. High Energy Phys.* **04** (2016) 031.
- [42] L. Keegan, A. Kurkela, A. Mazeliauskas, and D. Teaney, *J. High Energy Phys.* **08** (2016) 171.
- [43] P. Romatschke and U. Romatschke, *arXiv:1712.05815*.
- [44] M. Alqahtani, M. Nopoush, and M. Strickland, *Prog. Part. Nucl. Phys.* **101**, 204 (2018).
- [45] G. Baym, *Phys. Lett. B* **138**, 18 (1984).
- [46] W. Florkowski, R. Ryblewski, and M. Strickland, *Phys. Rev. C* **88**, 024903 (2013).
- [47] P. L. Bhatnagar, E. P. Gross, and M. Krook, *Phys. Rev.* **94**, 511 (1954).
- [48] J. L. Anderson and H. R. Witting, *Physica* **74**, 466 (1974).
- [49] M. P. Heller, R. A. Janik, and P. Witaszczyk, *Phys. Rev. Lett.* **108**, 201602 (2012).
- [50] G. S. Denicol, U. W. Heinz, M. Martinez, J. Noronha, and M. Strickland, *Phys. Rev. D* **90**, 125026 (2014).
- [51] G. S. Denicol, U. W. Heinz, M. Martinez, J. Noronha, and M. Strickland, *Phys. Rev. Lett.* **113**, 202301 (2014).
- [52] P. Romatschke, *Eur. Phys. J. C* **78**, 636 (2018).
- [53] G. Basar, G. V. Dunne, and M. Unsal, *J. High Energy Phys.* **10** (2013) 041.
- [54] H. S. Yamada and K. S. Ikeda, *arXiv:1308.4453*.
- [55] G. V. Dunne, in *Proceedings of the Schladming Winter School 2015, Schladming, Styria, Austria, 2015* (to be published), <http://physik.uni-graz.at/schladming2015/LectureNotes/Dunne.pdf>.
- [56] I. Aniceto, G. Basar, and R. Schiappa, *arXiv:1802.10441*.
- [57] I. Aniceto, *J. Phys. A* **49**, 065403 (2016).
- [58] D. Dutykh, *arXiv:1606.05432*.
- [59] J. P. Boyd, *Chebyshev and Fourier Spectral Methods* (Dover, New York, 2001).
- [60] J. Liu, C. Shen, and U. Heinz, *Phys. Rev. C* **91**, 064906 (2015); **92**, 049904(E) (2015).
- [61] J. Brewer and P. Romatschke, *Phys. Rev. Lett.* **115**, 190404 (2015).
- [62] D. Bazow, G. S. Denicol, U. Heinz, M. Martinez, and J. Noronha, *Phys. Rev. Lett.* **116**, 022301 (2016).
- [63] A. Buchel, M. P. Heller, and J. Noronha, *Phys. Rev. D* **94**, 106011 (2016).
- [64] S. S. Gubser, *Phys. Rev. D* **82**, 085027 (2010).

Hydrodynamic Attractors in Phase Space

Michał P. Heller^{1,2,*}, Ro Jefferson^{1,†}, Michał Spaliński^{2,3,‡} and Viktor Svensson^{2,1,§}

¹Max Planck Institute for Gravitational Physics, Potsdam-Golm 14476, Germany

²National Centre for Nuclear Research, 02-093 Warsaw, Poland

³Physics Department, University of Białystok, 15-245 Białystok, Poland

 (Received 27 March 2020; revised 3 July 2020; accepted 27 August 2020; published 22 September 2020)

Hydrodynamic attractors have recently gained prominence in the context of early stages of ultra-relativistic heavy-ion collisions at the RHIC and LHC. We critically examine the existing ideas on this subject from a phase space point of view. In this picture the hydrodynamic attractor can be seen as a special case of the more general phenomenon of dynamical dimensionality reduction of phase space regions. We quantify this using principal component analysis. Furthermore, we adapt the well known slow-roll approximation to this setting. These techniques generalize easily to higher dimensional phase spaces, which we illustrate by a preliminary analysis of a dataset describing the evolution of a five-dimensional manifold of initial conditions immersed in a 16-dimensional representation of the phase space of the Boltzmann kinetic equation in the relaxation time approximation.

DOI: [10.1103/PhysRevLett.125.132301](https://doi.org/10.1103/PhysRevLett.125.132301)

Introduction.—The physics of strong interactions studied in heavy-ion collisions at the RHIC and LHC (see, e.g., Ref. [1] for a concise contemporary review) has been a remarkable source of inspiration for the study of complex systems far from equilibrium. The phenomenological success of relativistic hydrodynamics, together with calculations in microscopic models based on holography and kinetic theory, have inspired several novel research directions. One such direction is centered on the notion of hydrodynamic attractors. These were introduced in Ref. [2] with the aim of capturing universal features of non-equilibrium physics beyond the limitations of the gradient expansion and were subsequently explored in many works, including Refs. [3–32].

In the context of reproducing the spectra of soft particles in ultrarelativistic heavy-ion collisions, the underlying observable of interest is the expectation value of the energy-momentum tensor $\langle T^{\mu\nu} \rangle$. Ideally, one would like to have a way of predicting its behavior as a function of time directly in QCD. Such calculations remain beyond reach, but have been pursued in quantum field theories possessing a gravity dual [33–35] in a number of works, see Refs. [36,37] for a review. Another line of development replaces QCD by its effective kinetic theory description [38], as reviewed in Refs. [37,39]. The evolution of $\langle T^{\mu\nu} \rangle$ depends on the initial state, captured by the bulk metric in

holography, or by the initial distribution function in the kinetic theory. After some time, the vast majority of this information is effectively lost, and $\langle T^{\mu\nu} \rangle$ evolves hydrodynamically. These explorations have led to the idea of a hydrodynamic attractor, identified in Ref. [2] in a class of hydrodynamic theories [40–42] as a specific solution which is approached by generic solutions initialized at arbitrarily small times. It was also observed there that a “slow-roll” condition akin to what is used in inflationary cosmology [43,44] leads to an accurate approximation of this attractor. Subsequent works have led to many interesting phenomenological applications [2,5,16,45,46].

Despite these developments, there are three important yet largely unexplored issues. The first addresses the different concepts of attractor, the second concerns their relevance for the dynamics of initial states of interest and the third is the question of their existence beyond highly symmetric settings. We address these points with the goal of clearing the ground for new developments, in particular for generalizations to more realistic flows with less symmetry. Our approach is based on the phase space picture, i.e., the space of variables needed to parametrize the dynamics underlying $\langle T^{\mu\nu} \rangle$, which was introduced in this context in Refs. [11,47].

Dissipation of initial state information.—There are two key features of the dynamics following an ultrarelativistic heavy-ion collision: the expansion that drives the system away from equilibrium and interactions that favor equilibration [13]. The simplest model of this is Bjorken flow which assumes one-dimensional expansion and boost-invariance along the expansion axis, conveniently described in terms of proper time τ and spacetime rapidity y . In interacting conformal theories, at asymptotically late

Published by the American Physical Society under the terms of the Creative Commons Attribution 4.0 International license. Further distribution of this work must maintain attribution to the author(s) and the published article's title, journal citation, and DOI. Funded by SCOAP³.

times the system follows a scaling solution for the (effective) temperature [48]

$$T(\tau) = \frac{\Lambda}{(\Lambda\tau)^{1/3}} + \dots \quad (1)$$

In this equation, the dimensionful constant Λ is the only trace of initial conditions. Corrections to this come in two forms: higher-order power-law terms which are sensitive only to Λ , and exponential corrections which encode information about the initial conditions and describe its dissipation [2,4,12,49–51]. This asymptotic form is usually referred to as a transseries [52]. The simplest models where this can be observed explicitly are formulated in the language of hydrodynamics.

Models of hydrodynamics.—We primarily focus on hydrodynamic theories (see Ref. [53] for a review), which despite their name include transient nonhydrodynamic excitations needed to avoid acausality. In such models, $\langle T^{\mu\nu} \rangle$ is decomposed into a perfect fluid term and a “dissipative” part denoted by $\pi^{\mu\nu}$:

$$\langle T^{\mu\nu} \rangle = (\mathcal{E} + \mathcal{P})u^\mu u^\nu + \mathcal{P}g^{\mu\nu} + \pi^{\mu\nu}, \quad (2)$$

where $u_\mu u^\mu = -1$, $u_\mu \pi^{\mu\nu} = 0$, and the energy density \mathcal{E} and pressure \mathcal{P} are related by the thermodynamic equation of state. In the conformal case considered here, $\mathcal{P} = \mathcal{E}/3$. Conservation equations of $\langle T^{\mu\nu} \rangle$ provide the four equations of motion for \mathcal{E} and u^μ . Hydrodynamic models, building on the original ideas of Refs. [40,41], provide the remaining equations for $\pi^{\mu\nu}$ in terms of relaxation-type dynamics that ensure matching to the hydrodynamic gradient expansion of any microscopic model.

In this Letter, we consider two classes of models. The first one is the Müller-Israel-Stewart (MIS) model [40,41]

$$\tau_\pi \mathcal{D}\pi^{\mu\nu} = -\pi^{\mu\nu} + \eta\sigma^{\mu\nu}, \quad (3)$$

where $\mathcal{D}\pi^{\mu\nu} \equiv u^\alpha \nabla_\alpha \pi^{\mu\nu} + \dots$, is the Weyl-covariant derivative in the comoving direction [54,55] and $\sigma^{\mu\nu} = 2\mathcal{D}^{(\mu} u^{\nu)}$ is the shear tensor. One can supplement Eq. (3) with additional terms defining the so-called Baier-Romatschke-Son-Starinets-Stephanov (BRSSS) model [42] and in the following we will refer to it as MIS-BRSSS models. Conformal symmetry requires that

$$\eta = C_\eta \frac{\mathcal{E} + \mathcal{P}}{T} \quad \text{and} \quad \tau_\pi = \frac{C_{\tau_\pi}}{T} \quad \text{with} \quad \mathcal{E} \sim T^4, \quad (4)$$

where C_η , C_{τ_π} are dimensionless constants and T is defined as the temperature of an equilibrium state at the same energy density \mathcal{E} . Equation (3) implies relaxation phenomena on a time scale defined by the relaxation time τ_π .

For the Bjorken flow, the combined equations reduce to a second order ordinary differential equation (ODE) for the effective temperature $T(\tau)$, see Eq. (7.17) in Ref. [53].

The hydrodynamic attractor was originally observed in this model in Ref. [2] using a special scale-invariant parametrization involving pressure anisotropy (note $\pi_2^2 = \pi_3^3$)

$$\mathcal{A} = \frac{\pi_2^2 - \pi_y^y}{\mathcal{P}} = 6 + 18\tau \frac{\dot{T}(\tau)}{T(\tau)}, \quad (5)$$

which is understood as a function of time measured by

$$w = \tau T(\tau). \quad (6)$$

We denote derivatives with respect to τ with a dot and derivatives with respect to w with a prime. In contrast with $T(\tau)$, $\mathcal{A}(w)$ satisfies a first order ODE, see Eq. (7.18) in Ref. [53].

The second hydrodynamic theory of interest here is the Heller-Janik-Spalinski-Witaszczyk (HJSW) model [55] (see also Ref. [56]), in which Eq. (3) is replaced by

$$\left\{ \left(\frac{1}{T} \mathcal{D} \right)^2 + \frac{2}{T^2 \tau_\pi} \mathcal{D} \right\} \pi^{\mu\nu} = -\frac{\tau_\pi^{-2} + \omega^2}{T^2} \{ \pi^{\mu\nu} + \eta\sigma^{\mu\nu} \}. \quad (7)$$

This structure again ensures relaxation phenomena on a timescale τ_π , but here they occur in an oscillatory manner as in $\mathcal{N} = 4$ supersymmetric Yang-Mills theory [57], with frequency $\omega = C_\omega T$. This model leads to a third order ODE for the effective temperature $T(\tau)$ or a second order ODE for $\mathcal{A}(w)$, see Eq. (7.26) in Ref. [53], and provides a workable setting with a richer set of initial conditions than offered by MIS-BRSSS models.

Hydrodynamic attractors.—The hydrodynamic attractor in MIS-BRSSS models arose through studying a range of solutions for $\mathcal{A}(w)$ that converge and then evolve toward local thermal equilibrium [2]. This behavior is known in the mathematical literature [58] as a forward attractor. Intuitively, forward attractors are solutions that attract nearby sets as $w \rightarrow \infty$. In MIS-BRSSS models, every solution is a forward attractor. Conversely, by considering solutions initialized at earlier and earlier times we observe that generic solutions (which diverge at $w = 0$) decay to a specific solution which is regular there. Such behavior is known as a pullback attractor.

These two notions of attractors, introduced in this context in [47] are concerned with different regimes: the forward attractor describes asymptotically late times while the pullback attractor is a statement about early times. In MIS-BRSSS models, there is a unique solution which is both a pullback attractor and a forward attractor; we denote this solution by $\mathcal{A}_*(w)$.

Attractors and phase space.—The above discussion raises two concerns. The first is that were one to visualize a range of solutions $T(\tau)$, the hydrodynamic attractor would not be apparent, and yet it is encoded there since $\mathcal{A}(w)$ can be clearly derived from $T(\tau)$. If a different observable showed attractor behavior how would one find

it? This issue must be clarified if one aims to identify attractors in more complicated settings. We address it by considering the full phase space parametrized by (τ, T, \dot{T}) for MIS-BRSSS models and $(\tau, T, \dot{T}, \ddot{T})$ for the HJSW model. We include proper time as one of the phase space variables because we are dealing with a nonautonomous system.

The second concern stems from the fact that forward and pullback attractors strongly depend on either asymptotically late or asymptotically early time dynamics. Such asymptotic regimes may be inaccessible or unphysical. We address this by focusing on the *local dynamics* on families of constant- τ slices of phase space, on which solutions of the equations of motion appear as points (see Figs. 1 and 3). However, any particular solution $\mathcal{A}(w)$ corresponds to a different curve on each slice, as dictated by Eq. (5). On the basis of earlier studies, one expects that, as τ increases, different solutions (points on constant- τ slices) will collapse to the curves representing the attractor $\mathcal{A}_*(w)$. This is what one *eventually* sees in Figs. 1 (bottom) and 3 (bottom-right), but numerical studies of phase space histories reveal a much finer picture. The process of information loss occurs in three phases: local dimensionality reduction, approach to the hydrodynamic attractor loci (red curves in Fig. 1), and evolution toward equilibrium along the attractor. Consider a finite “cloud” of initial states, such as any one of the three colored sets of points shown in Fig. 1. Each cloud contracts and becomes one dimensional. When this happens depends on the initial conditions. For example, the brown cloud in Fig. 1 (the one initialized at smallest value of $\tau_0 T$) loses a dimension quite early and rather far from the attractor, while the other two do this much later.

Quantifying dimensionality reduction.—We have argued that dimensionality reduction in phase space is an important feature of hydrodynamic attractors, but so far we have not provided a working recipe to quantify this process. A promising direction, which we only begin to explore here, follows from recognizing that dimensionality reduction is one of the basic tasks of machine learning. For the simple cases considered here, principal component analysis (PCA) is quite effective (see Refs. [59–63] for other applications of PCA to problems in ultrarelativistic heavy-ion collisions). Intuitively, PCA quantifies the variations of a data set in different directions and associates an explained variance with each of them.

We start by applying PCA to the two-dimensional phase space of MIS-BRSSS models. On the initial time slice we pick a state (T, \dot{T}) and consider a random set of points within a disc around it. For this set of points, the two principal components are approximately equal in magnitude. At each time step we recompute the principal components for the set of states we started with (see Fig. 1) and their evolution in time is shown in Fig. 2.

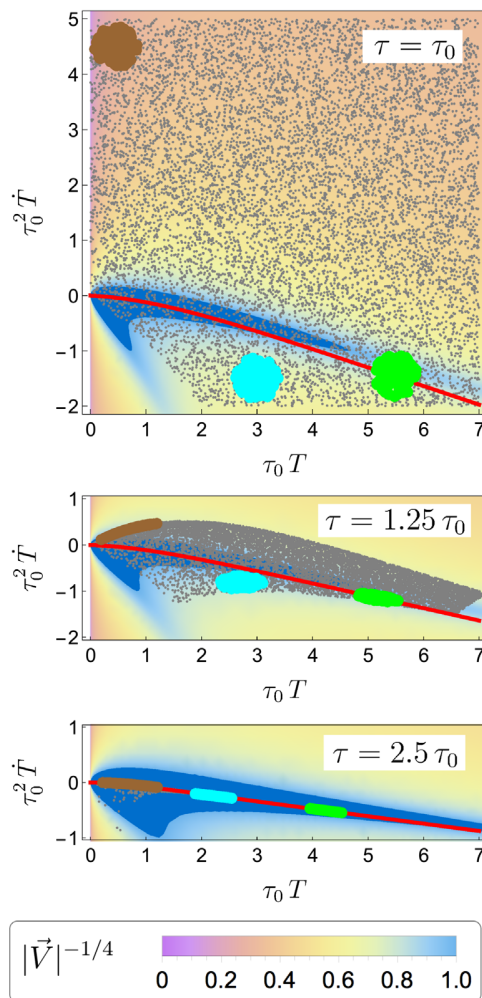


FIG. 1. Three snapshots of evolution in MIS-BRSSS phase space of a cloud of about 10 000 random states in the region determined by the ranges of the top plot. The red curve denotes the family of solutions corresponding to the attractor $\mathcal{A}_*(\tau T)$. The background color represents the speed at which the points move in phase space, with magenta being faster than blue according to the velocity defined in the text. The dark blue denotes the slow region beyond the color coding scale. For the purposes of visualizing local dimensionality reduction, see also Fig. 2, we track three initially spherical regions. The plots were made for $C_\eta = 0.75$ and $C_{\tau_x} = 1$, see Eqs. (3) and (4), and τ_0 denotes initialization time.

Dimensionality reduction is signalled when one of the components is much smaller than the other one.

This analysis extends to phase spaces of arbitrary dimension. An interesting example is provided by the three-dimensional phase space of HJSW. The evolution of principal components is shown in the upper part of Fig. 3. There are three stages of dimensionality reduction. The first, from three to two dimensions, is analogous to the earliest phase of the collapse in MIS-BRSSS models, most likely due to the expansion. The second stage is

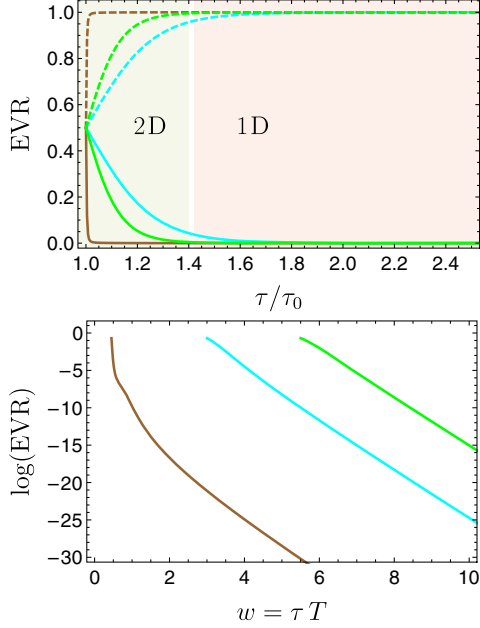


FIG. 2. Top: evolution of explained variance ratio of each principal component in MIS-BRSSS models for circles (radius: 10^{-4}) of initial conditions with centres lying in the middle of initial dots of corresponding color in Fig. 1. Bottom: for large enough values of w there is an exponential decay with a decay rate consistent with twice the transient mode contribution to $\mathcal{A}(w)$. The initial dimensional reduction of the brown region we view as triggered by the expansion rather than by nonhydrodynamic mode decay [22].

characterized by oscillations typical of the nonhydrodynamic sector of a HJSW model. These eventually dissipate resulting in the final stage of one-dimensional evolution.

Slow-roll in phase space.—The basic intuition is that the attractor locus should correspond to a region where the flow in phase space is slowest. One way to motivate why the slow region should behave as an attractor is to use an argument inspired by thermodynamics: a system is likely to be found in a large entropy macrostate because such states cover the majority of phase space. In our setting, the system is likely to be in a slow region because it takes a long time to escape it, while the fast regions can be quickly traversed.

We have found that, in the case of MIS-BRSSS models, this idea correctly identifies the attractor on any given time slice. Let $\vec{X}(\tau) = [\tau_0 T(\tau), \tau_0^2 \dot{T}(\tau)]$ be a point in a slice of phase space at time τ and τ_0 denotes initialization time. This point moves with velocity $\vec{V} = \tau_0 \dot{\vec{X}}(\tau)$. The slow region is defined by its Euclidean norm V , which has a minimum at asymptotically late times when the system approaches local thermal equilibrium. However, the whole region where it is small is of dynamical significance. In Fig. 1, the background color is determined by V , where bluer color implies lower speed. There is a slow region stretching out from local thermal equilibrium, and the attractor $\mathcal{A}_*(w)$ lies

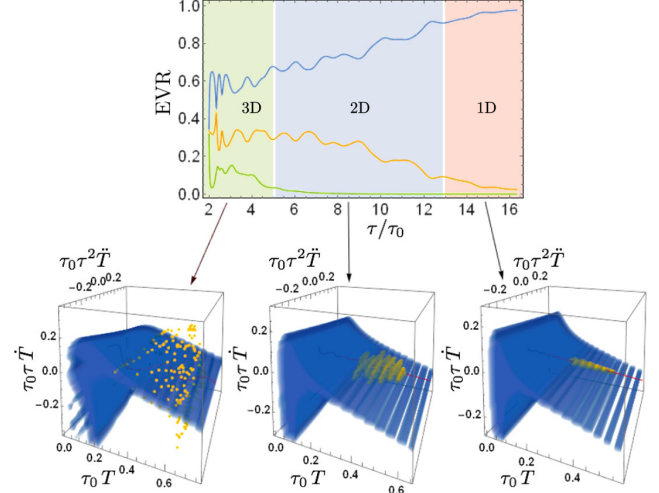


FIG. 3. In HJSW, the evolution of a cloud in phase space can be split into three stages, corresponding to the dimensionality of the cloud. The reduction from three to two dimensions corresponds to a collapse onto the slow region (blue region in plots). The plots were made with $C_\eta = 0.75$, $C_{\tau_x} = 1.16$, and $C_\omega = 9.8$.

along it. It can be approximated by a slow-roll approximation [2] where one neglects \ddot{T} in the equations of motion. This generalizes directly to phase spaces of any dimension. For the case of a HJSW model, the slow regions are shown also in blue in the bottom row of Fig. 3.

In nonautonomous systems, the slow region changes with time. If it were to evolve faster than the solutions do, it would not be useful to characterize the attractor. This is however not the case here: in both Figs. 1 and 3, we observe that once solutions reach the slow region, they stay inside and evolve with it. This is analogous to the adiabatic evolution observed in the case of the Boltzmann equation in the relaxation time approximation considered in Ref. [24].

Multidimensional phase spaces.—In realistic settings, one may not be able to consider the full phase space, but only some finite-dimensional, approximate representation thereof. As an example of such a procedure, we have studied a 16-dimensional subspace of the phase space of the Boltzmann kinetic equation in the relaxation time approximation [64,65]. This subspace is captured by taking the lowest 16 moments of the distribution function and solving the evolution equations as in Ref. [18,19]. We followed the evolution of a set of 240 initial conditions spanning a five-dimensional manifold embedded in the 16-dimensional phase. The results of an exploratory analysis of the resulting dataset using PCA are illustrated by Fig. 4 and described in more detail in the Supplemental Material [66]. This preliminary study supports the viability of the proposed approach in multidimensional phase spaces.

Summary and outlook.—The pressure anisotropy $\mathcal{A}(w)$ has been observed to exhibit universal behavior in various models, characterized by different authors in terms of concepts such as pullback or forward attractors or slow

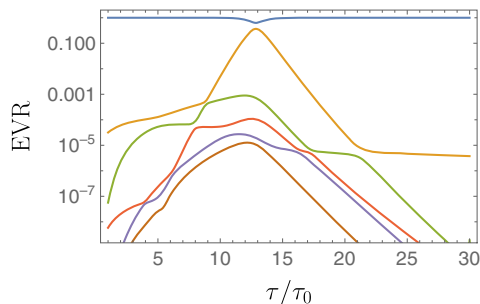


FIG. 4. The six largest principal components and their explained variance ratios as a function of τ . Due to the bias in initial conditions, one component dominates already at the initial time. This direction is not dynamically preferred, as the other components initially grow in importance and only at $\tau \approx 15\tau_0$ we see their expected exponential decay. At $\tau \approx 22\tau_0$, the second principal component stabilizes. This feature may reflect the limitations of PCA to capture effects of curved regions in phase space.

roll, all of which capture some aspects information loss in dissipative systems. In this Letter, we have described hydrodynamic attractors using concepts that allow for generalizations to more realistic settings. We have shown that this can be achieved by considering the phase space of the theory, which alleviates the need to know in advance which particular quantity makes attractor behavior manifest. From this perspective, the hydrodynamic attractor is associated with the more general notion of dimensionality reduction of phase space regions.

We thank J. Carrasquilla, R. Janik, D. Teaney as well as participants of the *XIV Polish Workshop on Relativistic Heavy-Ion Collisions* at AGH, *Initial Stages 2019* at Columbia University and *Foundational Aspects of Relativistic Hydrodynamics* at Banff International Research Station where this work was presented at different stages of development for helpful discussions. The Gravity, Quantum Fields and Information group at A. E. I. is supported by the Alexander von Humboldt Foundation and the Federal Ministry for Education and Research through the Sofja Kovalevskaja Award. M. S. was supported by the Polish National Science Centre Grant No. 2018/29/B/ST2/02457.

*michal.p.heller@aei.mpg.de

†rjefferson@aei.mpg.de

‡michal.spalinski@ncbj.gov.pl

§viktor.svensson@aei.mpg.de

- [1] W. Busza, K. Rajagopal, and W. van der Schee, Heavy ion collisions: The big picture, and the big questions, *Annu. Rev. Nucl. Part. Sci.* **68**, 339 (2018).
 [2] M. P. Heller and M. Spaliński, Hydrodynamics Beyond the Gradient Expansion: Resurgence and Resummation, *Phys. Rev. Lett.* **115**, 072501 (2015).

- [3] G. Başar and G. V. Dunne, Hydrodynamics, resurgence, and transasymptotics, *Phys. Rev. D* **92**, 125011 (2015).
 [4] I. Aniceto and M. Spaliński, Resurgence in extended hydrodynamics, *Phys. Rev. D* **93**, 085008 (2016).
 [5] P. Romatschke, Relativistic Fluid Dynamics Far From Local Equilibrium, *Phys. Rev. Lett.* **120**, 012301 (2018).
 [6] M. Spaliński, On the hydrodynamic attractor of Yang–Mills plasma, *Phys. Lett. B* **776**, 468 (2018).
 [7] M. Strickland, J. Noronha, and G. Denicol, The anisotropic non-equilibrium hydrodynamic attractor, *Phys. Rev. D* **97**, 036020 (2018).
 [8] P. Romatschke, Relativistic hydrodynamic attractors with broken symmetries: Non-conformal and non-homogeneous, *J. High Energy Phys.* **12** (2017) 079.
 [9] G. S. Denicol and J. Noronha, Analytical attractor and the divergence of the slow-roll expansion in relativistic hydrodynamics, *Phys. Rev. D* **97**, 056021 (2018).
 [10] W. Florkowski, E. Maksymiuk, and R. Ryblewski, Coupled kinetic equations for quarks and gluons in the relaxation time approximation, *Phys. Rev. C* **97**, 024915 (2018).
 [11] A. Behtash, C. N. Cruz-Camacho, and M. Martinez, Far-from-equilibrium attractors and nonlinear dynamical systems approach to the Gubser flow, *Phys. Rev. D* **97**, 044041 (2018).
 [12] J. Casalderrey-Solana, N. I. Gushterov, and B. Meiring, Resurgence and hydrodynamic attractors in Gauss-Bonnet holography, *J. High Energy Phys.* **04** (2018) 042.
 [13] J.-P. Blaizot and L. Yan, Fluid dynamics of out of equilibrium boost invariant plasmas, *Phys. Lett. B* **780**, 283 (2018).
 [14] D. Almaalol and M. Strickland, Anisotropic hydrodynamics with a scalar collisional kernel, *Phys. Rev. C* **97**, 044911 (2018).
 [15] G. S. Denicol and J. Noronha, Hydrodynamic attractor and the fate of perturbative expansions in Gubser flow, *Phys. Rev. D* **99**, 116004 (2019).
 [16] A. Behtash, S. Kamata, M. Martinez, and C. N. Cruz-Camacho, Non-perturbative rheological behavior of a far-from-equilibrium expanding plasma, *Phys. Lett. B* **797**, 134914 (2019).
 [17] M. Spaliński, Universal behaviour, transients and attractors in supersymmetric Yang–Mills plasma, *Phys. Lett. B* **784**, 21 (2018).
 [18] M. Strickland, The non-equilibrium attractor for kinetic theory in relaxation time approximation, *J. High Energy Phys.* **12** (2018) 128.
 [19] M. Strickland and U. Tantary, Exact solution for the non-equilibrium attractor in number-conserving relaxation time approximation, *J. High Energy Phys.* **10** (2019) 069.
 [20] J.-P. Blaizot and L. Yan, Emergence of hydrodynamical behavior in expanding quark-gluon plasmas, *Ann. Phys. (Amsterdam)* **412**, 167993 (2020).
 [21] S. Jaiswal, C. Chattopadhyay, A. Jaiswal, S. Pal, and U. Heinz, Exact solutions and attractors of higher-order viscous fluid dynamics for Bjorken flow, *Phys. Rev. C* **100**, 034901 (2019).
 [22] A. Kurkela, W. van der Schee, U. A. Wiedemann, and B. Wu, Early- and Late-Time Behavior of Attractors in Heavy-Ion Collisions, *Phys. Rev. Lett.* **124**, 102301 (2020).

- [23] G. S. Denicol and J. Noronha, Exact Hydrodynamic Attractor of an Ultrarelativistic Gas of Hard Spheres, *Phys. Rev. Lett.* **124**, 152301 (2020).
- [24] J. Brewer, L. Yan, and Y. Yin, Adiabatic hydrodynamization in rapidly-expanding quark-gluon plasma, [arXiv:1910.00021](https://arxiv.org/abs/1910.00021).
- [25] A. Behtash, S. Kamata, M. Martinez, and H. Shi, Global flow structure and exact formal transseries of the Gubser flow in kinetic theory, *J. High Energy Phys.* **07** (2020) 226.
- [26] C. Chattopadhyay and U. W. Heinz, Hydrodynamics from free-streaming to thermalization and back again, *Phys. Lett. B* **801**, 135158 (2020).
- [27] A. Dash and V. Roy, Hydrodynamic attractors for Gubser flow, *Phys. Lett. B* **806**, 135481 (2020).
- [28] M. Shokri and F. Taghinavaz, Bjorken flow in the general frame and its attractor, *Phys. Rev. D* **102**, 036022 (2020).
- [29] D. Almaalol, A. Kurkela, and M. Strickland, following Letter, Non-Equilibrium Attractor in High-Temperature QCD Plasmas, *Phys. Rev. Lett.* **125**, 122302 (2020).
- [30] J.-P. Blaizot and L. Yan, Analytical attractor for Bjorken expansion, [arXiv:2006.08815](https://arxiv.org/abs/2006.08815).
- [31] T. Mitra, S. Mondkar, A. Mukhopadhyay, A. Rebhan, and A. Soloviev, Hydrodynamic attractor of a hybrid viscous fluid in Bjorken flow, [arXiv:2006.09383](https://arxiv.org/abs/2006.09383).
- [32] A. Mazeliauskas and J. Berges, Prescaling and Far-from-Equilibrium Hydrodynamics in the Quark-Gluon Plasma, *Phys. Rev. Lett.* **122**, 122301 (2019).
- [33] J. M. Maldacena, The large N limit of superconformal field theories and supergravity, *Adv. Theor. Math. Phys.* **2**, 231 (1998).
- [34] E. Witten, Anti-de Sitter space and holography, *Adv. Theor. Math. Phys.* **2**, 253 (1998).
- [35] S. Gubser, I. R. Klebanov, and A. M. Polyakov, Gauge theory correlators from noncritical string theory, *Phys. Lett. B* **428**, 105 (1998).
- [36] P. M. Chesler and W. van der Schee, Early thermalization, hydrodynamics and energy loss in AdS/CFT, *Int. J. Mod. Phys. E* **24**, 1530011 (2015).
- [37] J. Berges, M. P. Heller, A. Mazeliauskas, and R. Venugopalan, Thermalization in QCD: Theoretical approaches, phenomenological applications, and interdisciplinary connections, [arXiv:2005.12299](https://arxiv.org/abs/2005.12299).
- [38] P. B. Arnold, G. D. Moore, and L. G. Yaffe, Effective kinetic theory for high temperature gauge theories, *J. High Energy Phys.* **01** (2003) 030.
- [39] S. Schlichting and D. Teaney, The first fm/c of heavy-ion collisions, *Annu. Rev. Nucl. Part. Sci.* **69**, 447 (2019).
- [40] I. Muller, Zum paradoxon der warmeitungstheorie, *Z. Phys.* **198**, 329 (1967).
- [41] W. Israel and J. Stewart, Transient relativistic thermodynamics and kinetic theory, *Ann. Phys. (N.Y.)* **118**, 341 (1979).
- [42] R. Baier, P. Romatschke, D. T. Son, A. O. Starinets, and M. A. Stephanov, Relativistic viscous hydrodynamics, conformal invariance, and holography, *J. High Energy Phys.* **04** (2008) 100.
- [43] A. R. Liddle, P. Parsons, and J. D. Barrow, Formalizing the slow roll approximation in inflation, *Phys. Rev. D* **50**, 7222 (1994).
- [44] M. Spalinski, On the slow roll expansion for brane inflation, *J. Cosmol. Astropart. Phys.* **04** (2007) 018.
- [45] G. Giacalone, A. Mazeliauskas, and S. Schlichting, Hydrodynamic attractors, initial state energy and particle production in relativistic nuclear collisions, *Phys. Rev. Lett.* **123**, 262301 (2019).
- [46] T. Dore, E. McLaughlin, and J. Noronha-Hostler, Far from equilibrium hydrodynamics and the beam energy scan, *J. Phys. Conf. Ser.* **1602**, 012017 (2020).
- [47] A. Behtash, S. Kamata, M. Martinez, and H. Shi, Global flow structure and exact formal transseries of the gubser flow in kinetic theory, *J. High Energy Phys.* **07** (2020) 226.
- [48] J. Bjorken, Highly relativistic nucleus-nucleus collisions: The central rapidity region, *Phys. Rev. D* **27**, 140 (1983).
- [49] R. A. Janik and R. B. Peschanski, Gauge/gravity duality and thermalization of a boost-invariant perfect fluid, *Phys. Rev. D* **74**, 046007 (2006).
- [50] M. P. Heller, R. A. Janik, and P. Witaszczyk, Hydrodynamic Gradient Expansion in Gauge Theory Plasmas, *Phys. Rev. Lett.* **110**, 211602 (2013).
- [51] I. Aniceto, B. Meiring, J. Jankowski, and M. Spaliński, The large proper-time expansion of Yang-Mills plasma as a resurgent transseries, *J. High Energy Phys.* **02** (2019) 073.
- [52] I. Aniceto, G. Başar, and R. Schiappa, A primer on resurgent transseries and their asymptotics, *Phys. Rep.* **809**, 1 (2019).
- [53] W. Florkowski, M. P. Heller, and M. Spaliński, New theories of relativistic hydrodynamics in the LHC era, *Rep. Prog. Phys.* **81**, 046001 (2018).
- [54] R. Loganayagam, Entropy current in conformal hydrodynamics, *J. High Energy Phys.* **05** (2008) 087.
- [55] M. P. Heller, R. A. Janik, M. Spaliński, and P. Witaszczyk, Coupling Hydrodynamics to Nonequilibrium Degrees of Freedom in Strongly Interacting Quark-Gluon Plasma, *Phys. Rev. Lett.* **113**, 261601 (2014).
- [56] J. Noronha and G. S. Denicol, Transient fluid dynamics of the quark-gluon plasma according to AdS/CFT, [arXiv:1104.2415](https://arxiv.org/abs/1104.2415).
- [57] P. K. Kovtun and A. O. Starinets, Quasinormal modes and holography, *Phys. Rev. D* **72**, 086009 (2005).
- [58] P. E. Kloeden and M. Rasmussen, *Nonautonomous Dynamical Systems* (American Mathematical Society, Providence, 2011), Vol. 176.
- [59] R. S. Bhalerao, J.-Y. Ollitrault, S. Pal, and D. Teaney, Principal Component Analysis of Event-By-Event Fluctuations, *Phys. Rev. Lett.* **114**, 152301 (2015).
- [60] A. Mazeliauskas and D. Teaney, Fluctuations of harmonic and radial flow in heavy ion collisions with principal components, *Phys. Rev. C* **93**, 024913 (2016).
- [61] P. Bozek, Principal component analysis of the nonlinear coupling of harmonic modes in heavy-ion collisions, *Phys. Rev. C* **97**, 034905 (2018).
- [62] Z. Liu, W. Zhao, and H. Song, Principal component analysis of collective flow in relativistic heavy-ion collisions, *Eur. Phys. J. C* **79**, 870 (2019).
- [63] F. G. Gardim, F. Grassi, P. Ishida, M. Luzum, and J.-Y. Ollitrault, p_T -dependent particle number fluctuations from principal component analyses in hydrodynamic simulations of heavy-ion collisions, *Phys. Rev. C* **100**, 054905 (2019).
- [64] G. Baym, Thermal Equilibration in Ultrarelativistic Heavy Ion Collisions, *Phys. Lett. B* **138**, 18 (1984).

- [65] W. Florkowski, R. Ryblewski, and M. Strickland, Testing viscous and anisotropic hydrodynamics in an exactly solvable case, *Phys. Rev. C* **88**, 024903 (2013).
- [66] See the Supplemental Material at <http://link.aps.org/supplemental/10.1103/PhysRevLett.125.132301> for more details on dimensionality reduction in kinetic theory, which includes Refs. [67,68].
- [67] M. P. Heller, A. Kurkela, M. Spaliński, and V. Svensson, Hydrodynamization in kinetic theory: Transient modes and the gradient expansion, *Phys. Rev. D* **97**, 091503 (2018).
- [68] M. P. Heller and V. Svensson, How does relativistic kinetic theory remember about initial conditions?, *Phys. Rev. D* **98**, 054016 (2018).

Supplemental Material: Hydrodynamic attractors in phase space

Michal P. Heller,^{1,2,*} Ro Jefferson,^{1,†} Michał Spaliński,^{2,3,‡} and Viktor Svensson^{2,1,§}

¹*Max Planck Institute for Gravitational Physics, Potsdam-Golm, 14476, Germany*

²*National Centre for Nuclear Research, 02-093 Warsaw, Poland*

³*Physics Department, University of Białystok, 15-245 Białystok, Poland*

(Dated: July 3, 2020)

DIMENSIONALITY REDUCTION IN KINETIC THEORY

As a test of our approach in a somewhat more realistic example, we present some details of its application to the dynamics of kinetic theory, specifically the Boltzmann equation in the relaxation time approximation (RTA). This setting was examined in the context of attractors in a number of recent papers [S1–S3]. Most relevant for us is the work of Strickland [S4, S5], who considered the dynamics of the moments of the distribution function and demonstrated that they too show attractor behaviour. In this work we study the same collection of moments but instead of considering each of them separately, we view them as coordinates on a truncated phase space. From this perspective one apply the approach proposed in this Letter to identify correlations between moments and determine the effective dimensionality of a set of solutions as it evolves.

In RTA kinetic theory, in boost-invariant flow, the distribution function satisfies [S6, S7]

$$f(\tau, u, p_T) = D(\tau, \tau_0) f_0(u, p_T) + \int_{\tau_0}^{\tau} \frac{d\tau'}{\tau_{\text{eq}}(\tau')} D(\tau, \tau') f_{\text{eq}}(\tau', u, p_T), \quad (\text{S1})$$

where f_0 defines the initial conditions. u, τ and p_T are boost invariant variables and it is convenient to define $v \equiv \sqrt{u^2 + p_T^2} \tau^2$. The moments of the distribution function are defined by

$$M^{nm}[f] \equiv \int \frac{du}{v} d^2 p_T \left(\frac{v}{\tau}\right)^n \left(\frac{u}{\tau}\right)^m f. \quad (\text{S2})$$

We follow Ref. [S4, S5] closely in solving for the evolution of moments. Each moment satisfies

$$M^{nm}(\tau) = D(\tau, \tau_0) M^{nm}[f_0](\tau) + \int_{\tau_0}^{\tau} \frac{d\tau'}{\tau_{\text{eq}}(\tau')} D(\tau, \tau') M^{nm}[f_{\text{eq}}](\tau'). \quad (\text{S3})$$

For an equilibrium distribution of the Boltzmann form

$$f_{\text{eq}}(\tau, u, p_T) = e^{-\frac{v}{T(\tau)\tau}}, \quad (\text{S4})$$

each $M^{nm}[f_{\text{eq}}]$ can be calculated analytically and are determined by $T(\tau)$. The temperature is related to the energy density by Landau matching and it follows that

the equation for M^{20} translates into a closed equation for the temperature

$$T^4(\tau) = D(\tau, \tau_0) T^4[f_0](\tau) + \int_{\tau_0}^{\tau} \frac{d\tau'}{2\tau_{\text{eq}}(\tau')} D(\tau, \tau') T^4(\tau') H\left(\frac{\tau'}{\tau}\right), \quad (\text{S5})$$

where $H(y) = y^2 + \frac{\tan^{-1}\left(\sqrt{\frac{1}{y^2}-1}\right)}{\sqrt{\frac{1}{y^2}-1}}$. Solving this equation for $T(\tau)$ allows one to calculate every moment $M^{nm}(\tau)$. As in the main text of our Letter, we consider a conformal theory with

$$T\tau_{\text{eq}} = 5\eta/s \quad (\text{S6})$$

and we take $\eta/s = 1/(4\pi)$. The scaled moments

$$\bar{M}^{nm}(\tau) = M^{nm}(\tau)/M_{\text{eq}}^{nm}(\tau), \quad (\text{S7})$$

which all tend to unity at equilibrium, provide a natural setting in which to study phase space dimensionality reduction in this model. This space is infinite-dimensional but as in Refs. [S4, S5] we direct our attention to the 16 moments with n and $m \leq 3$.

At large τ the effective temperature evolves according to the Bjorken asymptotics (see Eq. (1)) up to exponentially decaying corrections which reflect the spectrum of non-hydrodynamic modes [S8, S9]. Given the time evolution of individual moments [S4, S5], within the phase space picture we expect that a single principal component dominates the late time signal, while the rest should decay exponentially.

Defining the dimensionless time variable $w \equiv \tau/\tau_{\text{eq}}$ (the normalization of this variable differs by a constant factor from what is used in the main text), the behaviour is even simpler. The power law piece of different solutions becomes universal and the difference between two solutions at late times is to leading order

$$\delta M^{nm} \sim e^{-\frac{3}{2}w} w^\beta, \quad (\text{S8})$$

where β is a certain set of complex numbers [S9]. Thus, applying PCA to the set of solutions as a function of w , the expectation is that all of them decay exponentially with the same rate asymptotically. Note also that the imaginary part of β leads to oscillations in logarithmic time.

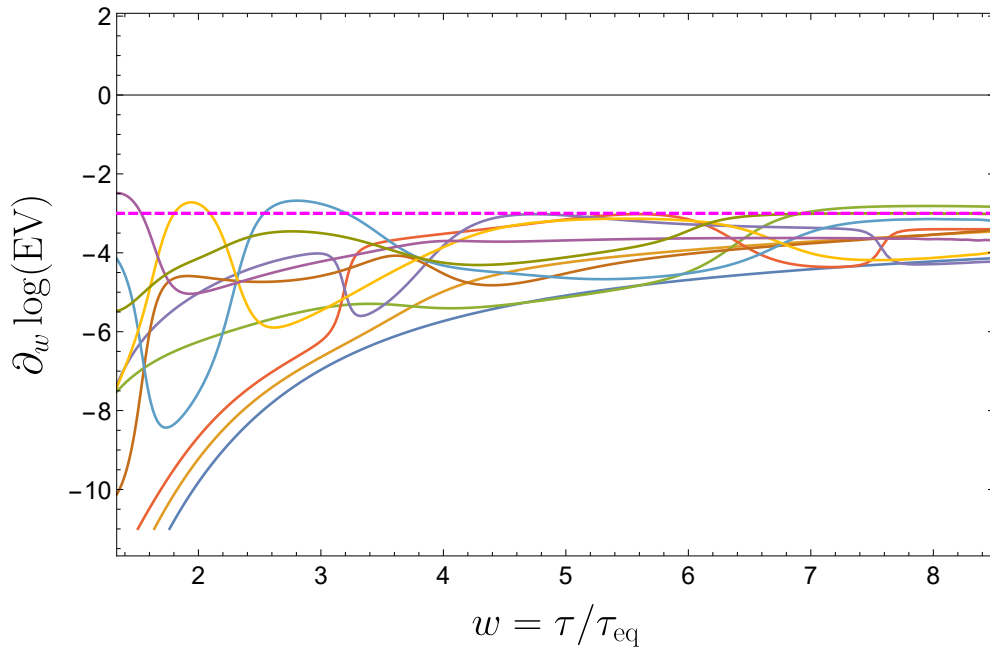


FIG. S1. The derivative of the logarithm of the explained variances seems to approach a constant at large w , indicating an exponential decay. All the components have a similar decay rate, showing that the collapse is somewhat uniform. As was observed in BRSSS (see Fig. 2 in the main text), this decay rate is consistent with twice the decay rate of the non-hydrodynamic modes (dashed magenta line). The oscillations whose frequency decreases at later times is also a feature shared by the non-hydrodynamic modes, see Eq. (S8).

We choose as our family of initial conditions

$$f_0(u, p_T) = A(T_0) e^{-\frac{\sqrt{u^2/\alpha_0^2 + p_T^2 \tau_0^2}}{\Lambda_0 \tau_0}} |u|^{c_u} |p_T|^{c_p}, \quad (\text{S9})$$

where $A(T_0)$ is a normalization factor ensuring that the initial temperature is T_0 . These initial conditions depend on five parameters ($T_0, \Lambda_0, \alpha_0, c_u, c_p$). For these initial conditions, it is easy to evaluate $M^{nm}[f_0]$ to arbitrary precision. This is the reason why they were used earlier in Ref. [S9] to explore hydrodynamization patterns in kinetic theory. Sampling these five parameters at the initial point in time leads to an, at most, five-dimensional manifold embedded in a 16-dimensional space. We sample uniformly in (0.8-1.2 GeV, 0.8-1.2 GeV, 0.5-1.4, -0.5-1, -0.5-1) and take $\tau_0 = 0.1$ fm/c.

In the BRSSS and HJSW models to which most of the main text was devoted, we had much more control over initial conditions and could choose them without bias in any particular direction. The explained variances were initially equal and the hierarchy that developed was purely a result of the dynamics. The present case is more challenging, as the initial conditions we use have a built in bias which translates into a hierarchy of explained variances already at the initial time. Nevertheless, the evolution exhibits the expected characteristics of dimensionality reduction also in this restricted setting. In Fig. 4 in the main text, we plot the explained variance ratio of the six largest principal components as a function of τ .

At early times, the bias in initial conditions is the reason for the large difference in explained variance. As time elapses, the relative importance of the smaller ones grow quickly, showing that the initial situation was not dynamically preferred. At $\tau \approx 15 \tau_0$, dimensionality reduction occurs leaving a single dominant component while the rest decays exponentially. Surprisingly, at $\tau \approx 22 \tau_0$, the second component stabilizes, albeit at a very small value. We conjecture that this is due to the inherent limitations of PCA to capture curved manifolds. If the curve corresponding to the hydrodynamic modes has curvature, more principal components will be needed to describe it, resulting in the behaviour we see in the figure. It would be interesting to apply more sophisticated data analysis methods that can capture such non-linearity, e.g. kernel-PCA.

To characterize the decay rate, we use PCA on the solutions as a function of w . In Fig. S1 we plot the derivative of the logarithm of the explained variances. At large w , they seem to saturate to a constant which is consistent with the twice the decay rate of the non-hydrodynamic modes. In addition, at earlier times we see oscillations, whose frequency seem to decrease at later times. This strengthens the connection to the non-hydrodynamic modes, which exhibit oscillations in logarithmic time.

We have demonstrated that PCA can be used to study the dynamics of dimensionality reduction in theories with

higher dimensional phase spaces. While kinetic theory is in fact infinite-dimensional, all of this information will never be physically relevant and one may truncate the to a finite dimensional space (in this case, the lower moments of the distribution function). At late times, when the dimensionality reduction is governed by interactions, we can interpret the evolution of explained variances in terms of hydrodynamic and non-hydrodynamic modes. At earlier times, when the expansion is dominant, the character of the collapse will be different [S3]. We leave this analysis to future work.

* michal.p.heller@aei.mpg.de
 † rjefferson@aei.mpg.de
 ‡ michal.spalinski@ncbj.gov.pl

- § viktor.svensson@aei.mpg.de
- [S1] P. Romatschke, Phys. Rev. Lett. **120**, 012301 (2018), arXiv:1704.08699 [hep-th].
- [S2] P. Romatschke, JHEP **12**, 079 (2017), arXiv:1710.03234 [hep-th].
- [S3] A. Kurkela, W. van der Schee, U. A. Wiedemann, and B. Wu, Phys. Rev. Lett. **124**, 102301 (2020), arXiv:1907.08101 [hep-ph].
- [S4] M. Strickland, JHEP **12**, 128 (2018), arXiv:1809.01200 [nucl-th].
- [S5] M. Strickland and U. Tantary, (2019), arXiv:1903.03145 [hep-ph].
- [S6] G. Baym, Phys. Lett. **B138**, 18 (1984).
- [S7] W. Florkowski, R. Ryblewski, and M. Strickland, Phys. Rev. **C88**, 024903 (2013), arXiv:1305.7234 [nucl-th].
- [S8] M. P. Heller, A. Kurkela, M. Spaliński, and V. Svensson, Phys. Rev. **D97**, 091503 (2018), arXiv:1609.04803 [nucl-th].
- [S9] M. P. Heller and V. Svensson, Phys. Rev. **D98**, 054016 (2018), arXiv:1802.08225 [nucl-th].

RECEIVED: January 31, 2021

REVISED: March 17, 2021

ACCEPTED: March 25, 2021

PUBLISHED: April 20, 2021

Transseries for causal diffusive systems

Michał P. Heller,^{a,b} Alexandre Serantes,^b Michał Spaliński,^{b,c} Viktor Svensson^{b,a}
and Benjamin Withers^d

^aMax Planck Institute for Gravitational Physics (Albert Einstein Institute),
14476 Potsdam-Golm, Germany

^bNational Centre for Nuclear Research,
02-093 Warsaw, Poland

^cPhysics Department, University of Białystok,
15-245 Białystok, Poland

^dMathematical Sciences and STAG Research Centre, University of Southampton,
Highfield, Southampton SO17 1BJ, U.K.

E-mail: michal.p.heller@aei.mpg.de,
alexandre.serantesrubianes@ncbj.gov.pl,
michal.spalinski@ncbj.gov.pl, viktor.svensson@aei.mpg.de,
b.s.withers@soton.ac.uk

ABSTRACT: The large proper-time behaviour of expanding boost-invariant fluids has provided many crucial insights into quark-gluon plasma dynamics. Here we formulate and explore the late-time behaviour of nonequilibrium dynamics at the level of linearized perturbations of equilibrium, but without any special symmetry assumptions. We introduce a useful quantitative approximation scheme in which hydrodynamic modes appear as perturbative contributions while transients are nonperturbative. In this way, solutions are naturally organized into transseries as they are in the case of boost-invariant flows. We focus our attention on the ubiquitous telegrapher's equation, the simplest example of a causal theory with a hydrodynamic sector. In position space we uncover novel transient contributions as well as Stokes phenomena which change the structure of the transseries based on the spacetime region or the choice of initial data.

KEYWORDS: Holography and condensed matter physics (AdS/CMT), Holography and quark-gluon plasmas

ARXIV EPRINT: [2011.13864](https://arxiv.org/abs/2011.13864)

Contents

1	Introduction	1
2	The momentum-space transseries and its Fourier transform	7
2.1	Constructing the transseries	7
2.2	Large-order behavior	9
3	Saddle point analysis	13
4	Superexponential decay of the nonhydrodynamic saddle points	17
5	Stokes phenomena in spacetime	19
6	Discussion	22
A	Müller-Israel-Stewart in the shear channel	23
B	The causality of the telegrapher's equation	24
C	The large-scale expansion and hydrodynamics	25
D	Applicability of the truncated perturbative series	27
E	Large-order behavior for Gaussian initial data	28
F	Large-order behavior for Lorentzian initial data	30
G	Reconstructing ρ from the transseries: Gaussian initial data case	31
G.1	The perturbative sector	31
G.2	The nonperturbative sector	32

1 Introduction

Understanding nonequilibrium phenomena with hydrodynamic tails has been a very active research direction of the past two decades. One motivation for this quest has been ultra-relativistic heavy-ion collisions at RHIC and LHC and the success of hydrodynamic modelling there [1–4]. Another set of motivations came from condensed matter and quantum-many body physics [5]. There have also been more foundational questions driving this field, such as existence of bounds on transport [6], or the character of the hydrodynamic gradient expansion [7].

One of the driving forces in this endeavour was holography [8–10], in which the nonequilibrium dynamics of a certain class of quantum field theories is represented by

time-dependent geometries involving black holes [11]. Results in this context are often based on numerical solutions of the equations of motion, with analytic or semi-analytic insights limited to basically two cases: linear response theory around equilibrium or highly symmetric dynamics. The former cases are based on Fourier transform techniques while the latter concern situations which can be effectively captured as comoving flows known from cosmology, or from heavy-ion collisions.

Our paper is directly motivated by such a description of ultrarelativistic heavy-ion collisions in terms of a Bjorken flow — one-dimensional expansion of matter, which looks the same in any coordinate frame boosted in the direction of expansion [12]. In the case of conformal models, such dynamics can be expressed as a single function $\mathcal{A}(w)$ which measures deviations away from local equilibrium. w is a dimensionless clock variable and the key motivating point for our paper is that \mathcal{A} has an asymptotic late-time form of a transseries, i.e. a double expansion in powers of $1/w$ and an exponential suppression factor:

$$\mathcal{A} = \sum_{n=1}^{\infty} \mu_n w^{-n} + e^{-\Omega w} w^\gamma \sum_{n=0}^{\infty} \nu_n w^{-n} + \dots \tag{1.1}$$

The ellipsis in the above equation stands for other exponentially suppressed contributions to the sum.

The first sum in (1.1) is the onshell hydrodynamic gradient expansion of the energy-momentum tensor,

$$T^{ab} = \mathcal{E} U^a U^b + \frac{\mathcal{E}}{d-1} (\eta^{ab} + U^a U^b) + \Pi^{ab}, \tag{1.2a}$$

$$\Pi^{ab} = -\eta \sigma^{ab} + \eta \tau \mathcal{D} \sigma^{ab} + \lambda_1 \sigma^{(a} \sigma^{b)c} + \dots, \tag{1.2b}$$

where we focus on conformal theories and the ellipsis denotes three additional nonlinear terms with two derivatives of velocity U^a which are irrelevant for our discussion, as well as higher order contributions, see, for example, [1] for details. In (1.1), the μ_1/w term represents the shear viscosity η contribution and the μ_2/w^2 term represents the combined effect of τ and λ_1 [13]. More generally, each term μ_n/w^n comes from the n^{th} order of the hydrodynamic gradient expansion. The key aspect of [7, 14–17, 17–22] was the ability to explicitly calculate higher order contributions to the sum (1.1) with the conclusion that the gradient expansion evaluated on shell for the Bjorken flow diverges, i.e. $\mu_n \sim n!$ at sufficiently large n (see, however, [23]).

The second contribution in (1.1) is associated with transient, exponentially decaying phenomena known from linear response theory and dressed in the hydrodynamic variables [24, 25], hence the other, also divergent gradient expansion with ν_n/w^n terms. As is the case in the mainstream application area of resurgence in theoretical high-energy physics [26, 27], i.e. coupling constant expansions in interacting quantum mechanical systems, the hydrodynamic sector carries information about transient phenomena through the phenomenon of resurgence.

It is an important open problem to what extent the picture uncovered for Bjorken flow, i.e. divergent hydrodynamic expansion and spatiotemporal dependence as transseries, survives when symmetry assumptions are lifted. New light on this question was shed by our

recent article [28], in which we combined linear response theory with the Fourier transform to investigate convergence of hydrodynamic gradient expansion in linearized conformal hydrodynamics in complete generality.

In linear response theory, a component of conserved currents $\rho(t, \mathbf{x})$ acquires spatiotemporal dependence given by

$$\rho(t, \mathbf{x}) = \int_{\mathbb{R}^d} d^d \mathbf{k} \hat{\rho}(t, \mathbf{k}) e^{i \mathbf{k} \cdot \mathbf{x}}, \quad \hat{\rho}(t, \mathbf{k}) = \sum_{q=0}^N f_q(\mathbf{k}) e^{-i \omega_q(|\mathbf{k}|) t}, \quad (1.3)$$

where $\omega_q(k)$ are dispersion relations for different modes in the system.¹ Hydrodynamic modes are those for which

$$\omega_q(k) = \kappa k^z + \dots, \quad \kappa \in \mathbb{C}, \quad (1.4)$$

with Lifshitz exponent $z > 0$, which guarantees that dissipation accounted for by the imaginary part of κ can be made arbitrary small by giving initial data support at arbitrarily small k . The ellipsis in (1.4) denote terms with higher powers of k , which are a counterpart of the hydrodynamic gradient expansion (1.2). The aforementioned transients are simply contributions to the sum in (1.3) which do not share the property (1.4).

The aim of the present article is to build on [28] to construct a transseries solution describing nonequilibrium processes going beyond the class of comoving flows represented by Bjorken dynamics. Our guiding principle will be to have hydrodynamic phenomena captured by the perturbative part of the transseries with nonperturbative transient phenomena captured by higher transseries sectors — in analogy with Bjorken flow, where the perturbative part is given by the $1/w$ expansion while the transient effects are expressed by terms exponentially suppressed in w . In any given model, there may be many different ways to construct such an expansion, e.g. by treating some microscopic parameter as small. The expansion we use here can be applied to any model.

At the technical level, the key idea is to introduce a formal expansion parameter for the transseries by rescaling space and time coordinates in Minkowski space where a nonequilibrium phenomenon of interest takes place. Since we expect hydrodynamics to be a late time phenomenon, we introduce a formal parameter ϵ through the rescaling

$$t \rightarrow \frac{t}{\epsilon^\alpha}, \quad x \rightarrow \frac{x}{\epsilon}, \quad (1.5)$$

with $\alpha > 0$, and treat ϵ as small. The resultant effect on (1.4), through the corresponding scaling $\omega \rightarrow \epsilon^\alpha \omega, k \rightarrow \epsilon k$, is given by,

$$\omega_q = \kappa \epsilon^{z-\alpha} k^z + \dots \quad (1.6)$$

For a given hydrodynamic sector parameterized by some Lifshitz exponent z , the natural choice is therefore the marginal one, $\alpha = z$, preserving the hydrodynamic scaling (1.4). This choice focuses attention on the sector of interest, whilst not scaling as far as to render it trivial. It also has the desired effect of ensuring that all nonhydrodynamic modes appear

¹This form of $\rho(t, \mathbf{x})$ is appropriate, for example, for holographic systems or in hydrodynamic models. In kinetic theory, the situation is more intricate, see, for example, [29].

nonperturbatively in a small ϵ expansion, since they scale as $\omega = O(\epsilon)^{-z}$. The outcome is that the spectral decomposition (1.3) becomes a transseries in the parameter ϵ with perturbative sectors corresponding to hydrodynamic mode contributions, and nonperturbative sectors corresponding to nonhydrodynamic ones. We emphasise that ϵ is only a formal parameter, and it takes the value $\epsilon = 1$ at the end of the calculation.

For definiteness, in the present work we focus on nonequilibrium phenomena described by the telegrapher's equation

$$\tau \partial_t^2 \rho + \partial_t \rho - D \partial_x^2 \rho = 0, \tag{1.7}$$

which at large distances and long times describes diffusion, or $z = 2$ hydrodynamic scaling (1.4). Later, unless we keep explicitly τ and D , we use their following numerical values

$$\tau = D = \frac{1}{2}. \tag{1.8}$$

The linear partial differential equation (1.7) is well-known in the literature and, as we review in appendix A, it arises as the description of shear channel perturbations in the Müller-Israel-Stewart (MIS) formulation of relativistic hydrodynamics [30].² From a broader perspective, the telegrapher's equation features prominently in the context of quasihydrodynamics [33], where it provides the simplest example of a diffusion-to-sound crossover. Quasihydrodynamics is the natural generalization of standard hydrodynamics in the presence of weakly broken symmetries. Apart from MIS itself, examples of theories featuring a diffusion-to-sound crossover described³ by the telegrapher's equation include quantum fluctuating superconductors [34], systems breaking spatial translations spontaneously in the presence of phase relaxation [35] and, in the AdS/CFT context, probe branes at finite temperature and large baryon density [36–38], models of momentum relaxation [39], higher-derivative gravity [40, 41], and constructions based on generalized global symmetries that describe dynamical electromagnetism in the boundary QFT [42, 43] or viscoelastic media [44].⁴ Furthermore, with a straightforward modification, our methods also apply to the chiral magnetic waves in the presence of axial charge relaxation discussed in [46, 47]. These observations suggest that the results we will derive in this work are potentially relevant for a wide range of distinct physical systems.

After these considerations, let us comment briefly on the mode structure of the telegrapher's equation. We have two modes in the sense of (1.3):

$$\omega_H(k) = \frac{-i + i\Delta(k)}{2\tau}, \quad \omega_{NH}(k) = \frac{-i - i\Delta(k)}{2\tau}, \quad \Delta(k) = \sqrt{1 - 4D\tau k^2}. \tag{1.9}$$

Among these two modes, ω_H is a hydrodynamic diffusion mode

$$\omega_H(k) \rightarrow -iDk^2, \quad k \rightarrow 0, \tag{1.10}$$

²In the AdS/CFT context, the natural counterpart of this problem would be a shear channel fluctuation in all-order hydrodynamics as discussed in [31, 32].

³It is worth remarking that the telegrapher's equation might only emerge in a suitable parametric limit.

⁴See also [45] for an embedding of the telegrapher's equation into a field-theoretic context.

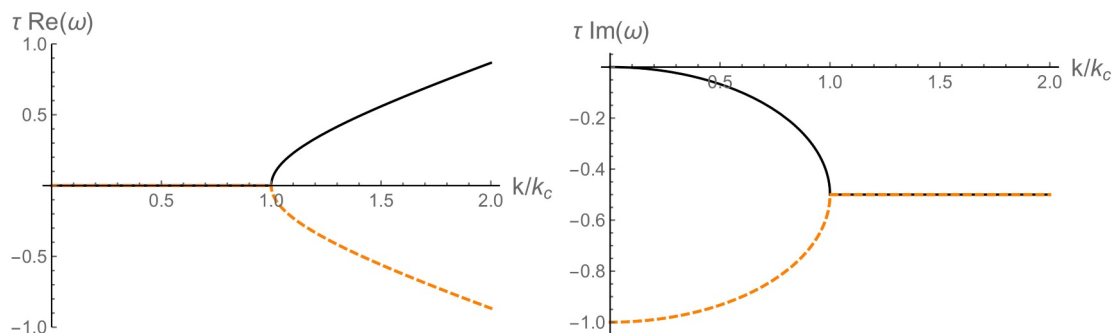


Figure 1. Real (left) and imaginary (right) parts of the hydrodynamic (solid black) and nonhydrodynamic (dashed orange) modes in the shear channel of the Müller-Israel-Stewart theory, as functions of momentum. The modes are given by (1.9).

while ω_{NH} remains gapped in the same limit. As figure 1 illustrates, both modes are nonpropagating and purely decaying below a critical momentum

$$k_c^2 = \frac{1}{4D\tau}, \tag{1.11}$$

which corresponds to a branch point where the hydrodynamic and the nonhydrodynamic modes collide in the sense introduced in [48] and developed in [49–54]. For τ and D given by (1.8), $k_c^2 = 1$. Past the critical momentum, the modes acquire a propagating component. For asymptotically large $|k|$, both modes become purely propagating, with a linear dispersion relation $\omega \rightarrow \pm\sqrt{D/\tau}k$. This should not come as a surprise, since in the end the telegrapher’s equation is nothing but a dissipative wave equation. If one wants to impose relativistic causality with the speed of light set to unity, this requires $D \leq \tau$.⁵

Another illustrative perspective is to view the mode collision represented by the telegrapher’s equation as the simplest incarnation of the so-called k -gap phenomenon, which features widely across physics (see [55] for a review). Apart from the examples mentioned before, the existence of a k -gap in the dispersion relation of the transverse collective excitations is a crucial feature distinguishing liquids and solids [56–58]. Other instances of the k -gap phenomenon in the AdS/CFT context include p -wave superfluids [59] or plasmons [60–62].

In the special case of the telegrapher’s equation, the expansion in powers of ϵ can equally well be regarded as an expansion in powers of the relaxation time τ . In consequence of our choice to seek a perturbative scheme in which hydrodynamic modes appear at leading order while nonhydrodynamic degrees of freedom enter as nonperturbative corrections, we observe that we are expanding around the acausal Navier-Stokes limit, and nonperturbative contributions are necessary to ensure causality. Likewise, physical effects of the propagating modes mentioned above enter only at the nonperturbative level. These observations are illustrated further in appendix D, where we apply our perturbative scheme to a particular example.

⁵In appendix B we discuss the causality properties of the telegrapher’s equation in more detail.

From a more mathematical perspective, we will be studying solutions of a partial differential equation (1.7) in the form of a transseries

$$\hat{\rho}(t, k) = \sum_{n=0}^{\infty} \hat{a}_n(t, k) \epsilon^{2n} + e^{-\frac{t}{\tau \epsilon^2}} \sum_{n=0}^{\infty} \hat{b}_n(t, k) \epsilon^{2n}, \quad (1.12)$$

where the hats indicate momentum space quantities. One of the crucial points of our work will be to make sense of this transseries expression in position space. Similar analyses of other partial differential equations have been carried out before in various contexts, for example in [63–65]. In holography, the large- w expansion of Bjorken flow [7, 20, 21] is also governed by partial differential equations, the fully nonlinear Einstein equations with negative cosmological constant.⁶ One of the interesting conclusions in [63–65] is that the structure of the transseries may be different in different parts of space and time. As we will see, this is also the case in our studies. Furthermore, in our study we want to stress the dependence of the transseries on initial conditions.

Transseries have also been studied in the context of attractors in Bjorken flow [14]. The non-perturbative contributions quickly decay, leaving a universal perturbative piece identified as the attractor. Similarly, in the present context there are many different solutions that differ only by the behaviour of the transients. For that class of solutions, the perturbative part acts as an attractor in the same sense.⁷ However, the Bjorken flow attractor arises from far from equilibrium behaviour involving the fast expansion at early times [66] while in this paper, because of linearity, all dynamics can be understood as small perturbations away from equilibrium. On the other hand, we are able to study more general flows, but leave open the question of what happens when non-linearities are introduced. Note on this front that less symmetric, non-linear flows have been studied numerically in [66–69].

Finally, let us come back to our initial motivation, i.e. the (conformal) Bjorken flow, and discuss the ϵ expansion and (1.12) in relation to w -transseries in (1.1). While the Bjorken flow is a genuinely nonlinear one-dimensional expansion, nothing stops us from applying an ϵ -rescaling (1.5) also to this case. Choosing x to be the expansion direction, the boost-invariance forces the dynamics to depend on proper time $\tau = \sqrt{t^2 - x^2}$ only (not to be confused with the relaxation time τ). As a result, the natural rescaling preserving the character of the proper time is the homogeneous one, i.e. $\alpha = 1$, which simply takes $\tau \rightarrow \tau/\epsilon$. The clock variable is defined as

$$w \equiv \tau T(\tau), \quad (1.13)$$

where $T(\tau)$ is the local effective temperature associated with the local energy density. The homogeneous ϵ expansion forces large proper time expansion of w in powers of $\epsilon^{2/3}/\tau^{2/3}$ starting with the term $(\epsilon^{2/3}/\tau^{2/3})^{-1}$. This reorganizes the transseries (1.1) from a transseries in w , whose each perturbative contribution corresponds to a given order of hydrodynamic gradient expansion evaluated on-shell, to a transseries in $\epsilon^{2/3}/\tau^{2/3}$. In the present work we

⁶When the microscopics is given by kinetic theory models, see [18, 19], the situation is even richer, as the collisional kernel in the Boltzmann equation generically involves integration over momenta.

⁷The series is generically divergent, so it must be properly resummed or optimally truncated.

will be working with the analogue of the latter expansion, whereas the former was discussed in full generality in linearized hydrodynamics in our recent paper [28]. In appendix C we discuss the link between the hydrodynamic gradient expansion and the perturbative part of the ϵ transseries.

2 The momentum-space transseries and its Fourier transform

2.1 Constructing the transseries

In this section we construct transseries solutions to the telegrapher's equation (1.7) in the small formal parameter ϵ as defined in (1.5). Our starting point is thus the following ϵ -rescaled telegrapher's equation,

$$\epsilon^2 \tau \partial_t^2 \rho(t, x) + \partial_t \rho(t, x) - D \partial_x^2 \rho(t, x) = 0, \quad (2.1)$$

with (1.7) and its actual solution recovered by setting $\epsilon = 1$. The point of introducing ϵ is that this is the approach that one can adopt generally, for example in holography or kinetic theory, while the τ -expansion is specific to the telegrapher's equation and related systems.

Due to the spatial translational invariance of (2.1), it is convenient to work in momentum space, where (2.1) reduces to a linear ODE,⁸

$$\epsilon^2 \tau \partial_t^2 \hat{\rho}(t, k) + \partial_t \hat{\rho}(t, k) + D k^2 \hat{\rho}(t, k) = 0. \quad (2.2)$$

One then immediately recognises an appropriate transseries ansatz for $\hat{\rho}(t, k)$ as $\epsilon \rightarrow 0$ as given by (1.12). Plugging it into (2.2) and considering terms order-by-order in ϵ , reveals the following pair of nested ODE systems

$$\partial_t \hat{a}_{n+1}(t, k) + D k^2 \hat{a}_{n+1}(t, k) + \tau \partial_t^2 \hat{a}_n(t, k) = 0, \quad (2.3a)$$

$$\partial_t \hat{b}_{n+1}(t, k) - D k^2 \hat{b}_{n+1}(t, k) - \tau \partial_t^2 \hat{b}_n(t, k) = 0. \quad (2.3b)$$

where we take $\hat{a}_{-1} = \hat{b}_{-1} = 0$. We see that $\hat{a}_{n+1}(t, k)$ obeys a heat equation sourced by the previous order, while $\hat{b}_{n+1}(t, k)$ is governed by the time-reversed equation. At this stage, the two equations are decoupled from one another. In order to solve (2.3), we supplement the equations with initial data at $t = 0$,

$$\rho(0, x) = u(x), \quad \partial_t \rho(0, x) = v(x) \quad (2.4)$$

and denote the corresponding Fourier-transformed functions as $\hat{u}(k), \hat{v}(k)$. For the sake of simplicity of presentation in what follows, we are going to focus on the $u(x) = 0$ case. At the level of the expansion coefficients, this initial condition reduces to $\hat{a}_0(t, k) = \hat{b}_0(t, k) = 0$, $\hat{b}_1(0, k) = -\tau \hat{v}(k)$ and

$$\hat{a}_{n+1}(0, k) + \hat{b}_{n+1}(0, k) = 0, \quad (2.5a)$$

$$\hat{b}_{n+1}(0, k) - \tau (\partial_t \hat{a}_n(0, k) + \partial_t \hat{b}_n(0, k)) = 0, \quad (2.5b)$$

⁸Momentum space quantities are denoted by a hat.

where the last equality applies only for $n > 0$. The initial conditions couple the coefficients arising in the perturbative series to those in the nonperturbative series. Finally, it is possible to find closed-form expressions for $\hat{a}_n(t, k)$ and $\hat{b}_n(t, k)$ that solve (2.3) and obey (2.5). They are given by

$$\hat{a}_{n+1}(t, k) = \frac{2^{2n}\Gamma(n + \frac{1}{2})}{\sqrt{\pi}\Gamma(n + 1)} D^n \tau^{n+1} k^{2n} {}_1F_1\left(2n + 1, n + 1, -Dk^2t\right) \hat{v}(k), \quad (2.6a)$$

$$\hat{b}_{n+1}(t, k) = -\hat{a}_{n+1}(-t, k). \quad (2.6b)$$

Let us now turn our attention to position space. Our guiding principle here will be to define the expansion coefficients of a given sector of the position space transseries as the inverse Fourier transform of the corresponding momentum space coefficients, as long as this inverse Fourier transform exists for positive real t . This is always the case for the perturbative sector of (1.12) (i.e. the \hat{a}_n coefficients). In fact, the perturbative sector proceeds straightforwardly, and we can immediately obtain closed-form results which we present in the remainder of this section. Nonperturbative contributions in position space are both subtle and interesting, and later sections of this paper are devoted to this topic.

The position space coefficient,

$$a_{n+1}(t, x) \equiv \int_{\mathbb{R}} dk \hat{a}_{n+1}(t, k) e^{ikx} \quad (2.7)$$

can be computed in closed form, with the result

$$a_{n+1}(t, x) = \frac{\tau^{n+1}\Gamma(n + \frac{1}{2})^2}{2\pi^{\frac{3}{2}}\sqrt{D}\Gamma(n + 1)t^{n+\frac{1}{2}}} (K_{n+1} * v)(x), \quad (2.8)$$

where $*$ represents a convolution in the spatial coordinate, and the $(n+1)$ -th kernel $K_{n+1}(x)$ is given by

$$K_{n+1}(x) = {}_1F_1\left(\frac{1}{2} + n, \frac{1}{2} - n, -\frac{x^2}{4Dt}\right). \quad (2.9)$$

An alternative representation of the same result is given by

$$a_{n+1}(t, x) = (-1)^n D^n \tau^{n+1} \sum_{q=0}^n \binom{2n}{n-q} \frac{D^q t^q}{q!} \partial_x^{2(n+q)} (G_0 * v), \quad (2.10)$$

where $G_0(t, x)$ is the propagator for the heat equation,

$$G_0(t, x) = \frac{e^{-\frac{x^2}{4Dt}}}{2\sqrt{\pi}\sqrt{Dt}}. \quad (2.11)$$

With $\hat{a}_{n+1}(t, k)$ and $a_{n+1}(t, x)$ now computed, we can arrange them to produce a piece of the full solution for $\hat{\rho}$ and ρ respectively. These we label with a superscript ‘ H ’,

$$\hat{\rho}_\epsilon^{(H)}(t, k) \equiv \sum_{n=0}^{\infty} \hat{a}_{n+1}(t, k) \epsilon^{2n+2}, \quad \rho_\epsilon^{(H)}(t, x) \equiv \sum_{n=0}^{\infty} a_{n+1}(t, x) \epsilon^{2n+2}, \quad (2.12)$$

and since we obtained them by inverse Fourier transform of a series in ϵ we have added a subscript ϵ to denote the fact that they are not exact in ϵ . In the light of (2.10), each term in $\rho_\epsilon^{(H)}(t, x)$ corresponds to a gradient series in ∂_x^2 acting upon a solution of the heat equation that depends on the initial data. In this sense, as advocated in the Introduction and expanded upon in appendix C, $\rho_\epsilon^{(H)}(t, x)$ provides a particular reorganization of a gradient expansion construction of the contribution of the hydrodynamic mode to $\rho(t, x)$, hence the label ‘H’. The convergence of $\rho_\epsilon^{(H)}(t, x)$ will be the focus of the next section, and we refer the reader to appendix D for an analysis of how well $\rho_\epsilon^{(H)}(t, x)$ — when we set $\epsilon = 1$ — reproduces the exact microscopic $\rho(t, x)$ in a particular example.

2.2 Large-order behavior

In this section we analyse the large-order behavior of $\rho_\epsilon^{(H)}(t, x)|_{\epsilon=1}$. We first provide a fully general, model-independent condition for the convergence of this object, which relies only on the support of the initial data in momentum space. Then, we discuss the large-order behavior of the series for initial data where this condition fails.

We begin by splitting the full microscopic $\rho(t, x)$ into hydrodynamic and nonhydrodynamic mode contributions, $\rho(t, x) = \rho^{(H)}(t, x) + \rho^{(NH)}(t, x)$, as defined by individual contributions to the Fourier integral along a path γ ,⁹ where

$$\rho^{(H)}(t, x) \equiv \int_\gamma dk \hat{\rho}^{(H)}(t, k) e^{ikx}, \quad \hat{\rho}^{(H)}(t, k) = f_H(k) e^{-i\frac{\omega_H(\epsilon k)}{\epsilon^2} t}, \quad (2.13)$$

with analogous expressions for the nonhydrodynamic mode, NH . As written, these expressions are exact in ϵ , and notationally this is indicated by the lack of an ϵ subscript. For our choice of initial data ((2.4) with $u = 0$), we have

$$f_H(k) = -f_{NH}(k) = \frac{\epsilon^2 \tau}{\sqrt{1 - 4D\tau\epsilon^2 k^2}} \hat{v}(k). \quad (2.14)$$

By series expanding the exact $\hat{\rho}^{(H)}(t, k)$ around $\epsilon = 0$ we recover the perturbative sector of the momentum space transseries, $\hat{\rho}_\epsilon^{(H)}(t, k)$, computed earlier (2.12). The existence of two branch points in $\omega_H(\epsilon k)$ and $f_H(k)$ at $\epsilon k = \pm |k_c|$ implies that, for $\epsilon |k| > |k_c|$, $\hat{\rho}_\epsilon^{(H)}$ is a divergent series. On the other hand, in defining $\rho_\epsilon^{(H)}$ we assumed that the momentum space integral commutes with the infinite sum in $\hat{\rho}_\epsilon^{(H)}$, in such a way that the individual series expansion coefficients, \hat{a}_n and a_n , were directly related by the Fourier transform. Hence,

$$\rho_\epsilon^{(H)}(t, x) = \int_{\mathbb{R}} dk \hat{\rho}_\epsilon^{(H)}(t, k) e^{ikx}. \quad (2.15)$$

From the expression above it is immediate to see that, unless the momentum space support of the initial data \hat{v} is restricted to¹⁰

$$|k| \leq \frac{|k_c|}{\epsilon}, \quad (2.16)$$

⁹Note that the splitting is only unequivocally defined once a particular integration path γ is specified. While, for entire initial data $\hat{u}(k)$ and $\hat{v}(k)$, $\rho(t, x)$ is the Fourier transform of an entire function, this is not the case for the individual hydrodynamic and nonhydrodynamic contributions as defined in the text, due to the branch points of the mode frequencies at $k^2 = k_c^2$. Each individual contribution is well-defined only after a particular γ to go around the corresponding branch cuts has been provided.

¹⁰Recall that one should set the formal parameter $\epsilon = 1$ at the end of the analysis.

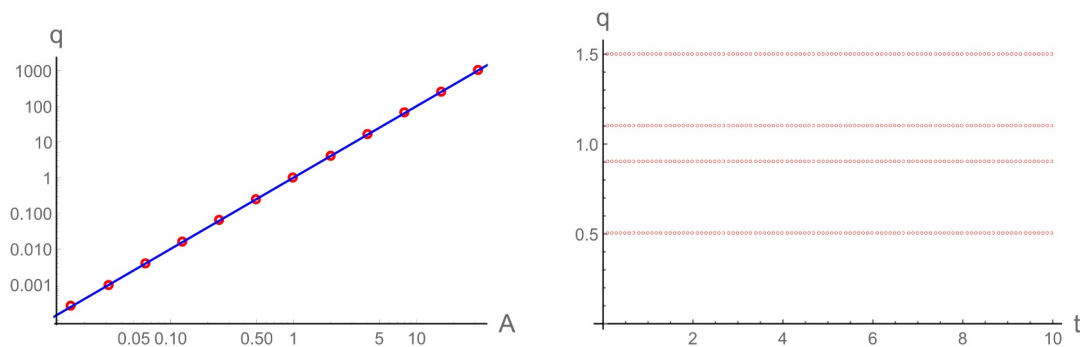


Figure 2. The ratio test for the perturbative sector in position space for initial data (2.17). Left: the ratio q defined in (2.19) vs. maximum support of the initial data in momentum space, A , at $t = 1$. Right: q vs. t for different values of A ; from top to bottom, $A^2 = 1.5, 1.1, 0.9$ and 0.5 .

the integral contains contributions from the momentum space region where $\hat{\rho}_\epsilon^{(H)}$ diverges. Modulo fine-tuned cancellations, the natural expectation to draw from this analysis is that the series $\rho_\epsilon^{(H)}$ does not converge if the initial data does not satisfy the condition (2.16).

It is important to note that, even if we have obtained (2.16) for a particular class of initial data for the telegrapher’s equation, its applicability is not restricted to this example. As long as the hydrodynamic mode frequency $\omega_H(k)$ has a complex singularity at $|k| = |k_c|$ and $f_H(k)$ is analytic for $|k| \leq |k_c|$, equation (2.16) will hold. It can be argued that the existence of this complex singularity in $\omega_H(k)$ is a necessary condition for a microscopic theory to behave causally [28]. From this viewpoint, $\rho_\epsilon^{(H)}$ would be a divergent series in any theory that respects relativistic causality for generic initial data with unrestricted momentum space support.

In order to illustrate how the convergence condition (2.16) applies to our case, we consider compactly supported initial data in momentum space of the form

$$\hat{v}(k) = \frac{1}{2\pi} \Theta(A^2 - k^2), \tag{2.17}$$

where Θ denotes the Heaviside step function. These initial data correspond to a regularized δ -function in position space. For $x = 0$, $a_n(t, 0)$ can be explicitly computed

$$a_{n+1}(t, 0) = \frac{2^{4n} D^n \tau^{n+1} A^{2n+1} \Gamma(n + \frac{1}{2})^2}{\pi^2 \Gamma(2n + 2)} {}_2F_2 \left(2n + 1, r + \frac{1}{2}; n + 1, n + \frac{3}{2}, -A^2 Dt \right). \tag{2.18}$$

To check whether the series expansion defined by the coefficients above is convergent, we use the ratio test and compute numerically

$$q = \lim_{n \rightarrow \infty} q_n, \quad q_n = |a_{n+1}/a_n|. \tag{2.19}$$

A sufficient condition for convergence is that $q < 1$. In figure 2 (left), we plot q as a function of A at $t = 1$. We always find that $q = A^2$ to exceedingly good accuracy. This implies that $\rho_\epsilon^{(H)}(t, x)|_{\epsilon=1}$ only converges for $A < 1$, i.e., for initial data with no support for $|k| > |k_c| = 1$ in k -space. If the support exceeds this bound, we obtain a divergent asymptotic series. This statement is time-independent, as figure 2 (right) shows.

It is worth mentioning that, as long as $|k_c| < A < \infty$, the series divergence is just a geometric one. A factorial growth of the $a_n(t, 0)$ coefficients only appears in the $A \rightarrow \infty$ limit. In this case, $v(x) = \delta(x)$,

$$a_{n+1}(t, 0) = \frac{\tau^{n+1} \Gamma(n + \frac{1}{2})^2}{2\pi^{\frac{3}{2}} \sqrt{D} \Gamma(n+1) t^{n+\frac{1}{2}}}, \quad (2.20)$$

and it follows that the ratio between successive coefficients increases linearly with n ,

$$q_n \sim \frac{\tau}{t} n, \quad (2.21)$$

implying a factorial divergence.

We have found that the correlation between the infinite support of the initial data in k -space and the factorially divergent character of $\rho_\epsilon^{(H)}(t, x)|_{\epsilon=1}$ always extends beyond the particular case of δ -function initial data discussed above. This is the behavior to expect for generic initial data: initial data with a sharp cutoff in momentum space represent fine-tuned states from a position space perspective, in the sense that any modification of the initial data which is localized in position space — for instance, by any Gaussian — would make the momentum space support unbounded.

Let us illustrate further the generic factorial divergence of the perturbative series by focusing on the example provided by Gaussian initial data of the form¹¹

$$v(x) = \frac{e^{-\frac{x^2}{2s^2}}}{\sqrt{2\pi s^2}}, \quad \hat{v}(k) = \frac{1}{2\pi} e^{-\frac{1}{2}s^2 k^2}, \quad (2.22)$$

As it happened with our compactly-supported initial data, this case is also analytically solvable at $x = 0$. We obtain

$$a_{n+1}(t, 0) = \frac{2^{3n} \tau^{n+1} D^n \Gamma(n + \frac{1}{2})^2}{\sqrt{2\pi^{\frac{3}{2}}} s^{2n+1} \Gamma(n+1)} {}_2F_1\left(n + \frac{1}{2}, 2n+1, n+1, -\frac{2Dt}{s^2}\right). \quad (2.23)$$

These coefficients, which diverge factorially as $n \rightarrow \infty$, show a more intricate behavior than their δ -function initial data counterparts. As $n \rightarrow \infty$,

$$q_n \sim r^{-1} n, \quad r = \frac{s^2}{8D\tau} \mu\left(\frac{2Dt}{s^2}\right), \quad (2.24)$$

where the function μ depends only the scaling variable

$$\eta = \frac{t}{t_c}, \quad t_c = \frac{s^2}{2D}, \quad (2.25)$$

and is given by

$$\mu(\eta) = \begin{cases} (1 + \eta)^2, & \eta < 1 \\ 4\eta, & \eta > 1. \end{cases} \quad (2.26)$$

This implies that, for Gaussian initial data, q_n only shows the behavior of δ -function initial data for times greater than a critical time. In figure 3, we plot how r evolves with t for

¹¹See appendix F for initial data of the Lorentzian form, i.e. $v(x) = \frac{\alpha}{\pi(x^2 + \alpha^2)}$.

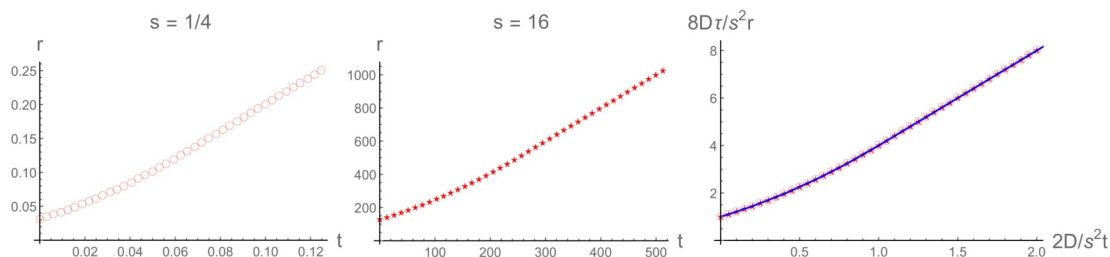


Figure 3. Factorial growth prefactor r defined by (2.24) (left) for Gaussian initial data obtained numerically from (2.23), as a function of time, for $s = 1/4$ (left) and $s = 16$ (middle). Both sets of data collapse on a single universal curve as shown in the right plot, which confirms (2.24) (right).

$s = 1/4$ (left) and $s = 16$ (center). These two curves, when re-scaled by $8D\tau/s^2$ and expressed as functions of $2Dt/s^2$, collapse to a universal function, which agrees with $\mu(\eta)$ (right, in blue).

Let us close this section by mentioning that the r parameter can be equivalently extracted by means of Borel transforms. Given a factorially divergent asymptotic series

$$f(\epsilon^2) = \sum_{n=0}^{\infty} c_n (\epsilon^2)^n, \tag{2.27}$$

its Borel transform $f_B(z)$ given by

$$f_B(z) = \sum_{n=0}^{\infty} \frac{c_n}{n!} z^n, \tag{2.28}$$

and, by definition, has a finite convergence radius in z . This convergence radius is set by the singularity which is closest to the origin in the complex z plane. In general, the analytical continuation of $f_B(z)$ to complex z cannot be computed in closed form and some approximation technique needs to be invoked. A common choice is to use Padé approximants. The (m, n) -Padé approximant of $f_B(z)$ is the unique rational function

$$\mathcal{P}(z) = \frac{\sum_{p=0}^m a_p z^p}{1 + \sum_{p=1}^n b_p z^p} \tag{2.29}$$

such that

$$f_B(z) - \mathcal{P}(z) = O(z^{m+n+1}). \tag{2.30}$$

A well-known property of Padé approximants is that branch cuts in $f_B(z)$ manifest themselves as lines of pole condensation in $\mathcal{P}(z)$. For the Gaussian initial data (2.22), including their δ -function limit $s \rightarrow 0$, we always find a line of pole condensation along the positive z -axis starting at

$$z_c = r, \tag{2.31}$$

where r is given by (2.24). Therefore, we conclude that the exact analytically-continued Borel transform has a branch point at this location, as expected on the basis of the large order behaviour of the series. Note, however, that for Gaussian initial data the location of

the branch point depends on t/t_c , and is given by t/τ only for $t > t_c$. For $t < t_c$ the branch point location also depends on the initial data through its dependence on s . Note that a condensation of poles can hide more than a single branch cut,¹² as happened, for example, in [14]. We will come back to this point in the next section, where we discuss the physical origin of these singularities and their dependence on t .

3 Saddle point analysis

In this section we take a different perspective and address the $\epsilon \rightarrow 0$ limit of the hydrodynamic mode contribution $\rho^{(H)}(t, x)$ by means of a saddle point analysis. As we will show, and as expected on general grounds, this procedure allows us to understand the physical origin of the branch points in the Borel plane.

To start, let us consider a schematic integral

$$I(\lambda) = \int_{\gamma} du G(u) e^{\lambda S(u)}, \tag{3.1}$$

and focus on its behavior for $|\lambda| \rightarrow \infty$. For us, the parameter λ will be simply $\frac{1}{\epsilon^2}$ and we introduce it purely for notational convenience. This behavior can be obtained from a saddle point analysis. The relevant analysis can be decomposed into three subsequent steps. First, one finds the stationary points u_s of the ‘action’ $S(u)$,

$$\left. \frac{d}{du} S(u) \right|_{u=u_s} = 0. \tag{3.2}$$

Second, the steepest descent contours emanating from these saddle points are determined. The steepest descent contour γ_s associated to the u_s saddle point is the path emanating from u_s along which $\text{Re } S(u)$ decreases the fastest. It obeys

$$\text{Im } \lambda S(u(\xi)) = \text{Im } \lambda S(u_s). \tag{3.3}$$

Finally, one decomposes the original integration path γ into steepest descent contours γ_s and calculates the corresponding integrals in a $|\lambda| \rightarrow \infty$ expansion.

The steepest descent path associated to a saddle u_0 can collide with another saddle u_1 when $\arg \lambda$ is such that $\text{Im } \lambda S(u_0) = \text{Im } \lambda S(u_1)$. These saddles are known as adjacent saddles [70] and play a prominent role in controlling the large-order behavior of the $|\lambda| \rightarrow \infty$ expansion around the original u_0 saddle. In particular, when considering the Borel transform of this $|\lambda| \rightarrow \infty$ expansion, adjacent saddles manifest themselves as branch points in the Borel plane [71], located at

$$z_c = -(S_1 - S_0). \tag{3.4}$$

¹²For example, for $f_B(z) = \sqrt{1-z} + \sqrt{2-z}$, the Padé approximation (2.29) is going to display a condensation of poles emanating from 1 towards larger values of z on the real axis. The poles with $1 \leq z < 2$ will correspond to the branch cut associated with $\sqrt{1-z}$ and the poles with $z \geq 2$ will include also contributions from the branch cut associated with $\sqrt{2-z}$.

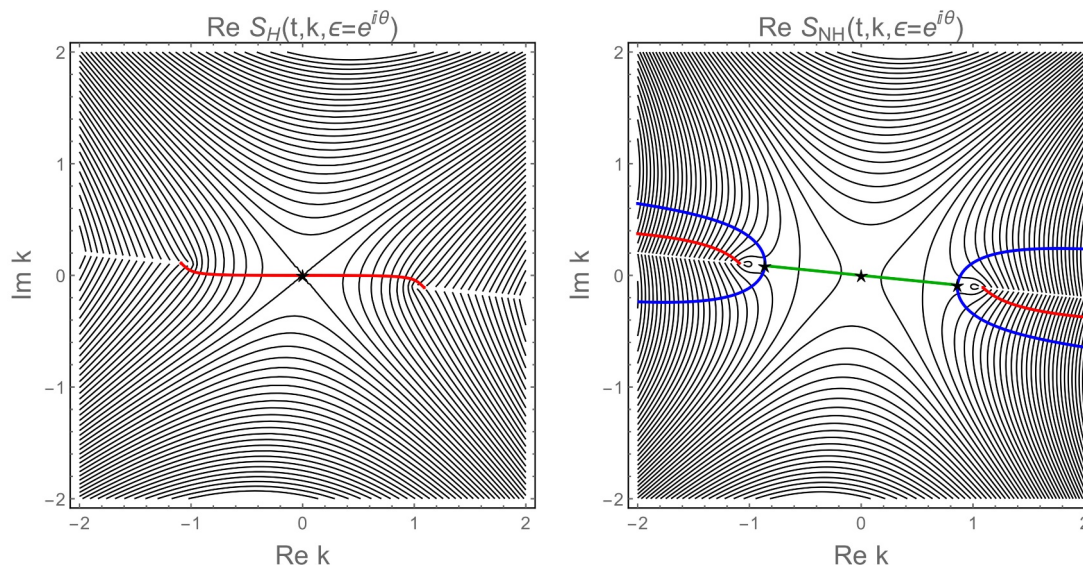


Figure 4. Level plots of the saddle point actions $\text{Re } S_H(t, k)$ (left) and $\text{Re } S_{NH}(t, k)$ (right) for $\epsilon = e^{i\theta}$ for Gaussian initial data (2.22) with $s = 1$, $t = 0.5$ and $\theta = 0.1$. The saddle points are denoted by the black stars and associated steepest descent paths are shown in red ($k = 0$, hydrodynamic), green (k_0 , nonhydrodynamic) and blue (k_{\pm}). The red path crosses the branch cuts (visible as white discontinuities in the plots) and continues on the other sheet, while the green path ends at the k_{\pm} saddles.

Let us apply this line of reasoning to understand the large-order behavior of $\rho_{\epsilon}^{(H)}(t, 0)$ we reported in the previous section for the case of Gaussian initial data (2.22). In this case, we have that

$$\rho^{(H)}(t, x) = \int_{\gamma} dk G_H(k) e^{\frac{S_H(t, x)}{\epsilon^2}}, \quad G_H(k) = \frac{\epsilon^2 \tau}{2\pi \sqrt{1 - 4D\tau\epsilon^2 k^2}}, \quad (3.5)$$

with action

$$S_H(t, x) = -\frac{1}{2}s^2\epsilon^2 k^2 + \frac{(-1 + \sqrt{1 - 4D\tau\epsilon^2 k^2})t}{2\tau} + i\epsilon^2 kx. \quad (3.6)$$

The analogous expressions for $\rho^{(NH)}$, G_{NH} and S_{NH} are obtained by flipping the sign of the square root in (3.6). The most important point to draw from the expression above is that the initial data contribute nontrivially to the relevant action and, as a result, also to its saddle points. Up to this point, our expressions are exact in ϵ .

When $x = 0$, the saddle points of S_H , S_{NH} are as follows. For S_H , we have a single saddle point located at $k = 0$ with vanishing action. On the other hand, S_{NH} has three saddle points. The first one is located at $k = k_0 = 0$ at all times and has action

$$S_0 = -\frac{t}{\tau}. \quad (3.7)$$

The positions of the two remaining ones are time dependent

$$k = k_{\pm} = \pm \sqrt{1 - \left(\frac{t}{t_c}\right)^2} k_c \quad (3.8)$$

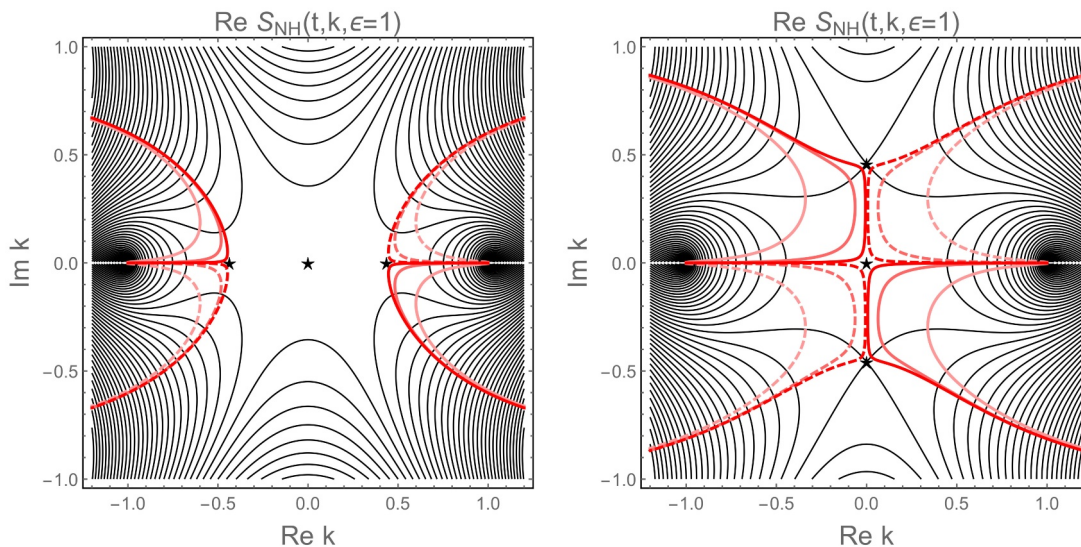


Figure 5. For $s = 1$, level plot of $\text{Re } S_{NH}(t, k)$ for $\epsilon = 1$, superimposed with the steepest descent contours emanating from the $k = 0$ hydrodynamic saddle for different values of $\epsilon = e^{i\theta}$. Solid red lines, from lighter to darker, correspond to $\theta = 2.5 \times 10^{-3}, 2.5 \times 10^{-4}, 2.5 \times 10^{-5}$. Dashed lines represent the negative values of θ , with the same color code. Black stars correspond to saddle point locations. Left: $t = 0.9$. Right: $t = 1.1$

with t_c given by (2.25) and lead to actions

$$S_{\pm} = -\frac{1}{2}s^2 \left(1 + \frac{t}{t_c}\right)^2 k_c^2. \tag{3.9}$$

At $t = 0$, the k_{\pm} saddles start at the critical momenta $\pm k_c$. As t grows, they approach each other along the real k -axis, until colliding with the k_0 saddle at $t = t_c$. Past this time, they recede from the origin in opposite directions along the imaginary k -axis.

The perturbative sector of our transseries, $\rho_{\epsilon}^{(H)}(t, x)$, corresponds to the saddle point expansion around the hydrodynamic saddle.¹³ Crucially, for complex

$$\epsilon = |\epsilon|e^{i\theta}, \tag{3.10}$$

the steepest descent path emanating from this saddle crosses the branch cuts in the hydrodynamic dispersion relation and continues on the nonhydrodynamic sheet. Once there, this path can collide with adjacent nonhydrodynamic saddle points at specific values of θ . An example of this behavior is provided in figure 4, where we also show the steepest descent contours associated to the three nonhydrodynamical saddles.

Figure 5 (left) further illustrates the behavior of the steepest descent path for the hydrodynamic saddle on the nonhydrodynamic sheet as $\theta \rightarrow 0$ for $0 < t \leq t_c$. Solid red lines, from lighter to darker, represent the values $\theta = 2.5 \times 10^{-3}, 2.5 \times 10^{-4}$ and 2.5×10^{-5} , while dashed red lines represent their negatives. As θ approaches zero, the steepest descent path gets progressively closer to the k_{\pm} saddles before veering off to infinity. Furthermore,

¹³See appendix E for further technical details.

$\theta = 0$ marks a discontinuous change in the path behavior, which is the reason why we considered θ as a parameter to vary; for instance, the quadrant in which the red curve extends to infinity undergoes a sudden change. These observations are compatible with the hypothesis that k_{\pm} are the adjacent saddles controlling the divergence of the perturbative series expansion. On the other hand, as illustrated in figure 5 (right), the collision of nonperturbative saddle points at $t = t_c$ causes the nature of the adjacent saddles to change: past t_c , k_0 becomes a new adjacent saddle for the hydrodynamic steepest descent contour.

We can now relate this saddle point analysis to the singularities we observed in the Borel plane in section 2.2. Since for $t > t_c$ we have that $|S_0| < |S_{\pm}|$, the above observations entail that the branch point of the Borel transform which is closest to the origin should go from being located at $z_c = -S_{\pm}$ for $t < t_c$ to being located at $z_c = -S_0$ for $t > t_c$. This prediction matches precisely the behavior of r reported at the end of section 2.2.

Let us emphasize that for $t > t_c$ the branch point associated to the S_{\pm} adjacent saddles, $z_{\pm} = -S_{\pm}$, does not disappear. What actually happens is that, since both $z_0 = -S_0$ and z_{\pm} are real positive quantities with $z_{\pm} > z_0$, the branch cut associated to z_0 superimposes with the branch cuts associated to z_{\pm} , causing the latter to be superficially hidden in the Borel plane (as we illustrated using a simple example in footnote 12).

To expose the hidden z_{\pm} branch points, we proceed along the lines of [72]. We take our original Padé approximant $\mathcal{P}(z)$ and introduce the variable change $z = z(w)$, with $z(w)$ analytic at $w = 0$. Then, we series expand $\mathcal{P}(z = z(w))$ around $w = 0$. Finally, we compute the Padé approximant of the resulting series, $\mathcal{P}(w)$. By a suitable choice of $z(w)$, the images of our original branch points lead to non-superimposing branch cuts in the w Borel plane. A convenient choice of variable change is as follows. Define

$$z(w) = z_c \frac{2w}{1 + w^2} \tag{3.11}$$

with z_c being, as before, the branch point closest to the origin in the z Borel plane. The variable change (3.11) maps a point $z \in (z_c, \infty)$ to two complex conjugated images on the right half of the $|w| = 1$ unit circle, with z_c being mapped to $w = 1$.

For $t < t_c$, the pole structure of $\mathcal{P}(w)$ is as shown in figure 6 (left). We see three lines of pole condensation: two of them are complex conjugated and emanate from the singular points of the map (3.11), located at $w = \pm i$, and are therefore unphysical; the third one starts at $w = 1$ and runs along the positive real axis. This latter line corresponds to the original branch cut starting at $z_c = z_{\pm}$. For $t < t_c$ we see no trace of additional branch points associated to z_0 in the w plane, confirming that for $t < t_c$ k_0 is not an adjacent saddle.

On the other hand, for $t > t_c$, this state of affairs changes. As figure 6 (right) shows, besides the branch point at $w = 1$ corresponding now to $z_c = z_0$, we also find two additional, complex conjugated lines of pole condensation emanating from the unit circle. It is immediate to check that these points are nothing but the images of z_{\pm} under the map (3.11). These images are represented by the upper and lower blue stars in the figure.

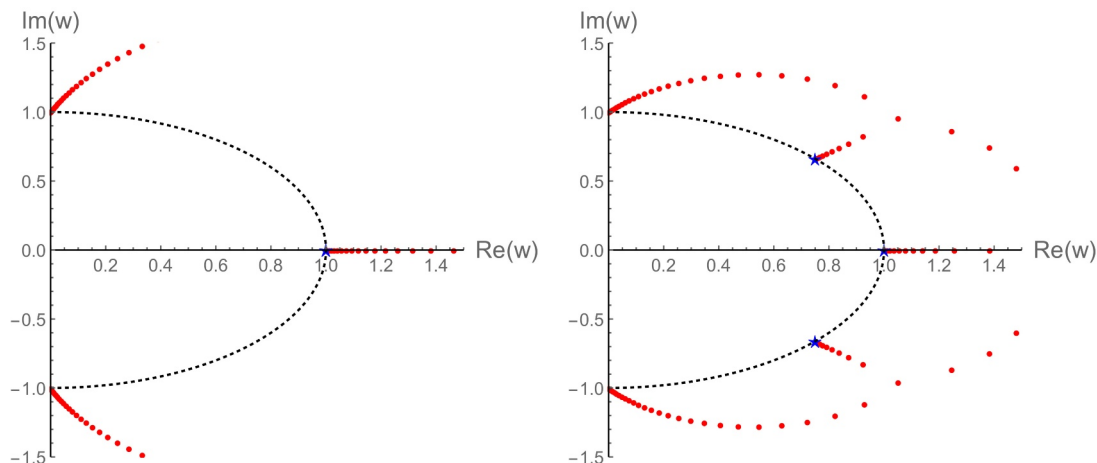


Figure 6. Poles of the Padé approximant $\mathcal{P}(w)$ for $t = 1/2$ (left) and $t = 3$ (right) for Gaussian initial data with $s = 1$. The blue stars signal the images of z_0 and z_{\pm} under the map (3.11), while the dashed black line corresponds to the $|w| = 1$ circle.

4 Superexponential decay of the nonhydrodynamic saddle points

From a physical standpoint, the existence of the k_+ , k_- saddles bears crucial consequences for the late-time behavior of the nonhydrodynamic mode contribution $\rho^{(NH)}$ for the Gaussian initial data, (2.22). To expose these consequences, for the rest of this section we focus on the original $\epsilon = 1$ telegrapher’s equation. We take the integration path γ , used to compute $\rho^{(NH)}$, to lie strictly below the real axis in the complex k -plane. With this choice of path, $\rho^{(NH)}$ is real. Linearity of the telegrapher’s equation means that $\rho^{(NH)}$ is now a fully-fledged solution to the telegrapher’s equation on its own, associated to the initial data,

$$\hat{u}(k) = -\frac{\tau e^{-\frac{1}{2}s^2 k^2}}{2\pi\Delta(k)}, \quad \hat{v}(k) = \frac{e^{-\frac{1}{2}s^2 k^2}(1 + \Delta(k))}{4\pi\Delta(k)}, \quad (4.1)$$

in such a way that $f_H(k) = 0$.¹⁴ In the remaining part of this section, we will denote this solution simply as ρ .

The chosen integration path γ can be deformed into the steepest descent contour associated with the k_- saddle-point (see figure 7). Therefore, the natural expectation is that the late-time behavior of the initial data (4.1) at $x = 0$ is controlled by the S_- action, which predicts a late-time decay *faster than* $e^{-\frac{t}{\tau}}$.

Two questions arise naturally at this point. The first one is whether the faster-than-exponential decay we have uncovered extends to finite x . The second one is whether the existence of these additional saddle points extends to generic initial data with Gaussian asymptotic behavior as $k \rightarrow \infty$.

Both questions can be answered affirmatively by the following argument. For initial data with Gaussian asymptotic behavior, the relevant action to consider in the nonhydro-

¹⁴Since we integrate along a path γ that goes strictly below the real axis, the singularities of Δ do not require attention.

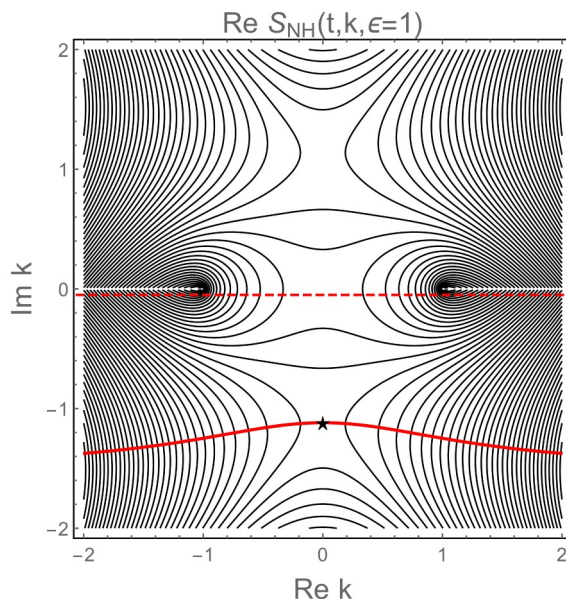


Figure 7. Level plot of $\text{Re } S_{NH}(t, k)$ for Gaussian initial data with $s = 1$ at $t = 3/2$. The dashed red line shows the γ integration contour; the solid red line is the steepest descent path emanating from the k_- saddle.

dynamic sheet at finite x is (we take $\epsilon = 1$ from now on)

$$S_{NH}(t, k) = -\frac{1}{2}s^2k^2 - \frac{1}{2\tau} \left(1 + \sqrt{1 - 4D\tau k^2}\right) + ikx. \quad (4.2)$$

By solving the saddle point equation in a late-time expansion, we find a saddle k_* located in the lower half complex k -plane given by¹⁵

$$k_* = -i\frac{\sqrt{D}}{s^2\sqrt{\tau}}t + i\frac{x}{s^2} + i\frac{s^2}{8D^{\frac{3}{2}}\sqrt{\tau}}\frac{1}{t} + \dots, \quad (4.3)$$

with action

$$S_* = S_{NH}(t, k_*) = -\frac{D}{2\tau s^2}t^2 - \frac{1}{\tau} \left(\frac{1}{2} - \frac{\sqrt{D\tau}}{s^2}x\right)t - \frac{s^4 + 4D\tau x^2}{8D\tau s^2} + \dots \quad (4.4)$$

As the expression above shows, the finiteness of x does not change the leading order late-time behavior of S_* we encountered before for $x = 0$. Moreover, only the asymptotic behavior of the initial data at large k matters in reaching this conclusion.

To test whether the late-time behavior predicted by (4.4) is actually realized, we select the logarithmic derivative $\partial_t \log \rho(t, x)$ as our probe. According to (4.4), we must have that

$$\partial_t \log \rho(t, x) = -\frac{D}{\tau s^2}t - \left(\frac{1}{2\tau} - \frac{\sqrt{D}}{\sqrt{\tau}s^2}x\right) + \dots \quad (4.5)$$

In order to check whether equation (4.5) holds, we restrict ourselves to initial data in which we multiply the Gaussian appearing in (4.1) by a polynomial $P(k)$ (taken to be a function

¹⁵We assume that $x > 0$ in what follows.

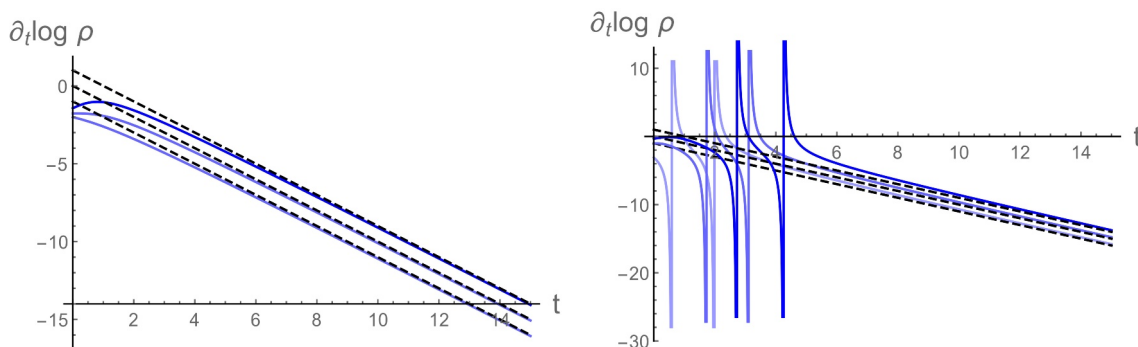


Figure 8. Left: $\partial_t \log \rho$ for $s = 1$ and $P(k) = 1$. Solid blue lines correspond to the numerical integration of the exact expression, dashed black lines to the late-time behavior prediction (4.5). From bottom to top, $x = 0, 1$ and 2 . Right: same as left, now with $P(k)$ given by a even, fourth-order polynomial in k with generated once and for all random coefficients.

of k^2 with real coefficients), fix s , and compute numerically $\partial_t \log \rho(t, x)$ for a range of spatial positions. In figure 8, we show results for $P(k) = 1$ (left) and a fourth-order $P(k)$ with random coefficients drawn from the interval $[-1, 1]$ (right), for $s = 1$ and at $x = 0, 1$ and 2 . These results are in agreement with the hypothesis that the nonhydrodynamic contribution displays a faster-than-exponential decay.

The physical origin of the faster-than-exponential decay is propagation of the data with a Gaussian tail rather than an effect of dissipation governed by the imaginary part of the mode frequency. To see this, note that (4.4) can be suggestively rewritten as

$$S_* = -\frac{s^2}{8D\tau} - \frac{t}{2\tau} - \frac{\left(x - \sqrt{\frac{D}{\tau}}t\right)^2}{2s^2} + \dots \quad (4.6)$$

It is (the tail of) a Gaussian peak propagating in the direction of the positive x with velocity $\sqrt{\frac{D}{\tau}}$ and decay rate $\frac{1}{2\tau}$. These values match the propagating modes at large k seen in figure 1. Figure 9 shows the utility of this line of reasoning. In this figure we plot a dense set of snapshots of ρ — determined by direct numerical integration — as a function of x . We observe that the initial data (4.1) indeed evolve as a propagating wave that recedes from $x = 0$ as time grows. Furthermore, as the argument above suggested this wave gets progressively damped, but just exponentially so.

5 Stokes phenomena in spacetime

For Gaussian initial data, figures 5 and 6 show that both the saddle point structure and the Borel plane structure take a different character depending on whether t is larger or smaller than the critical time $t_c = s^2/2D$. The transseries also undergoes an abrupt change, known as a Stokes phenomenon [27]. It occurs when crossing a point where the imaginary part of the action is the same, i.e.

$$\text{Im}(S_0 - S_{\pm}) = 0. \quad (5.1)$$

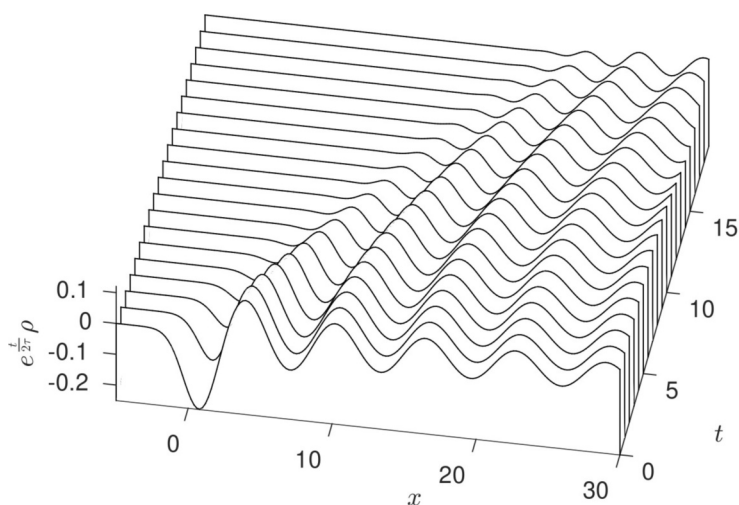


Figure 9. Spacetime evolution of $e^{\frac{t}{2\tau}} \rho(t, x)$ for the initial data (4.1) with $s = 1$. We have multiplied by $e^{\frac{t}{2\tau}}$ to factor out the leading late time decay of the wave (recall that $D = \tau = 1/2$ in our numerical computations).

If we consider the action as a function of complex t , with all other parameters real¹⁶ and $x = 0$, this condition is realized when

$$\text{Im } t = 0 \quad \text{or} \tag{5.2a}$$

$$\text{Re } t = \frac{s^2}{2D}. \tag{5.2b}$$

As the Stokes line at $\frac{s^2}{2D}$ is crossed along the real axis, the contribution of the S_0 saddle is turned off and the contributions of S_- and S_+ are turned on.

In terms of the coefficients $b_n(t, x)$, this is seen as follows. Recall that for Gaussian initial data of the form (2.22), $\hat{b}_n(t, k) = -\hat{a}_n(-t, k)$, where $\hat{a}_n(t, k)$ is given by (2.6a). For $k \in \mathbb{R}$ and as $|k| \rightarrow \infty$, we have that $\hat{b}_{n+1}(t, k)$ behaves as

$$\hat{b}_{n+1} = d_n t^n k^{4n} e^{-D(t_c - t)k^2} + \dots, \quad d_n \in \mathbb{R} \tag{5.3}$$

Therefore, the Fourier integral that computes $b_n(t, x)$ exists for positive real t as long as $t < t_c$. The result is $b_n(t, 0) = -a_n(-t, 0)$ with the latter given by (2.23). This changes dramatically for $t > t_c$, where the Fourier integral diverges along the standard Fourier contour. The contour must be deformed to the k_- saddle point.

For $x = 0$ this series expansion can be computed in closed form, with the end result that

$$\rho_\epsilon^{(NH)}(t, 0) = e^{\frac{s_-}{\epsilon^2}} \sum_{n=0}^{\infty} c_{n+1}(t, 0) \epsilon^{2n+2}, \tag{5.4a}$$

$$c_{n+1}(t, 0) = \frac{(-1)^{n+1} {}_2F_1\left(\frac{1}{2}, -2n, \frac{1}{2} - 2n, \frac{n+1}{n-1}\right)}{2^{n+\frac{3}{2}} t_c^{n+\frac{1}{2}} (\eta+1)^{2n} \sqrt{\eta^2 - 1} \Gamma(n+1) \Gamma(\frac{1}{2} - 2n)}, \tag{5.4b}$$

¹⁶There is no obstruction against considering complex values of s , which give rise to oscillating solutions.

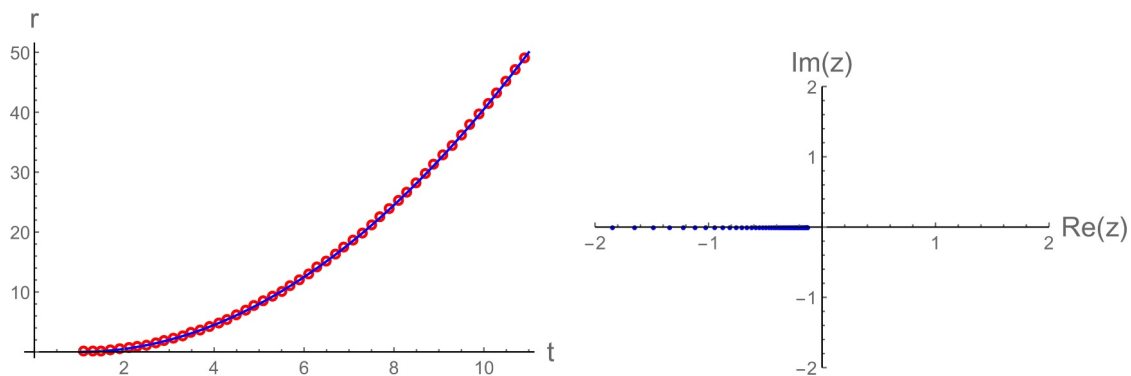


Figure 10. Left: for $s = 1$, r as a function of t as determined directly from the closed-form expression for $c_n(t, 0)$ (open red circles) vs. the function $S_0 - S_-$ (solid blue line). Right: poles of the Padé approximant of $\rho_\epsilon^{(NH)}(t, 0)$ at $t = 3/2$ for $s = 1$.

where $\eta = t/t_c > 1$. This series is factorially divergent. We find that the ratio test behaves as

$$\left| \frac{c_{n+1}(t, 0)}{c_n(t, 0)} \right| \sim \frac{n}{r}, \quad n \rightarrow \infty \tag{5.5}$$

where r is a function given by the difference between the k_0 and k_- saddle point actions,

$$r(t, s) = S_0 - S_- = -\frac{t}{\tau} + \frac{(s^2 + 2Dt)^2}{8D\tau s^2}. \tag{5.6}$$

We provide an example of this behavior in figure 10 (left). In line with this result, the Padé approximant to the Borel transform of the asymptotic expansion (5.4a) displays a line of pole condensation along the negative real axis, starting at $z_c = S_- - S_0$ (see the right plot in figure 10). This location of the branch cut follows from the fact that $k = 0$ is an adjacent saddle for the steepest descent contour emanating from k_- when $\arg \epsilon^2 = \pi$.

To summarize, for these initial data, we take our nonperturbative transseries sector to be defined by

$$\rho_\epsilon^{(NH)}(t, 0) = \begin{cases} e^{\frac{S_0}{\epsilon^2}} \sum_{n=0}^{\infty} b_{n+1}(t, 0) \epsilon^{2n+2}, & t < t_c \\ e^{\frac{S_-}{\epsilon^2}} \sum_{n=0}^{\infty} c_{n+1}(t, 0) \epsilon^{2n+2}, & t > t_c. \end{cases} \tag{5.7}$$

We see that the form of the nonperturbative transseries sector depends on the spacetime location. This is the reason why we started with the transseries in momentum space, see (1.12), which is uniquely defined in terms of the modes in the system.

This kind of Stokes phenomena in spacetime is not unique to this model. It has been investigated previously in, for example, references [63–65]. Those studies show that nonlinearity can also be handled and that a more intricate higher-order Stokes phenomenon can occur.

To close this section, let us emphasize the role that the initial data plays in the spacetime picture. Rather than the Stokes phenomenon occurring as t is varied, one can equivalently regard it as occurring as the initial data is varied. It arises here because the

transseries coefficients depend on the initial data, which we expect is generic and holds also in nonlinear models. If a richer set of initial conditions were considered, a richer set of transseries sectors could be the result. The takeaway lesson here is that both the spacetime location as well as the initial data must be taken into account when formulating the transseries.

Finally, we refer the reader to appendix G, where we employ Borel resummation to illustrate how the exact $\rho^{(H)}(t, 0)$, $\rho^{(NH)}(t, 0)$ — as determined by a numerical integration — can be recovered from the asymptotic expansions $\rho_\epsilon^{(H)}(t, 0)$, $\rho_\epsilon^{(NH)}(t, 0)$.

6 Discussion

The main motivation for our work is understanding nonequilibrium phenomena with a hydrodynamic tail by expressing them as transseries with resurgent relations connecting their various sectors. This point of view originates from the studies of expanding matter in ultrarelativistic heavy-ion collisions described by the paradigmatic example of Bjorken flow. Our work proposes and explores an approach that allows one to frame more general examples of dynamics in the same kind of language. We focus on the linearized regime but, reminiscent of [73], transseries techniques can in principle be applied when deviations from equilibrium are large. It would very interesting to study this question in detail, and to make contact with far from equilibrium attractors, which we leave for future research.

To describe a nonequilibrium process with a transseries one needs to define a small parameter. Guided by results from Bjorken flow, we introduce a formal parameter ϵ based on rescalings of spacetime coordinates (1.5), that organizes the hydrodynamic and nonhydrodynamic contributions into different transseries sectors. While the momentum space picture is straightforward, when passing to coordinate space we see new features which are as yet *unseen* in Bjorken flow and other expanding plasma systems.

In particular, we find that the initial conditions affect the form of nonperturbative contributions in ϵ in the spacetime picture. In our work we focused on a particular simple yet rich and widely encountered equation of motion — the telegrapher’s equation (1.7) — and a few classes of initial conditions. The nonhydrodynamic sector of the transseries took on two different forms. One is as a nonpropagating transient mode evaluated at zero momentum, similar to what was found in the Bjorken flow. However, when the initial conditions produce propagating wave packets, the receding tails of these wave packets gave rise to new transseries sectors. We have seen then that the decay of the nonhydrodynamic data is not only governed by the transient mode at zero momentum, but also by the form of the initial data and the dispersion relations at finite momentum.

While we observed this phenomenon for the telegrapher’s equation, its ingredients seem to originate from the underlying causality of the system. This is necessarily shared by all the models of relativistic matter, in particular holography, which suggests that it is ubiquitous.¹⁷ In studies of the transition to hydrodynamics in relativistic heavy-ion

¹⁷Perhaps similar phenomena can even occur in the holographic Bjorken flow. One can view the gravity dual to the Bjorken flow as a set of nonlinear wave equations with constraints in two variables. This is not too dissimilar from what we considered here if the transseries analysis is extended into the bulk.

collisions using holography, the dominant theme has been the decay of transient modes as the mechanism governing it. Here we see that contributions from the nonhydrodynamic sectors can propagate away from a given spatial location, which effectively may render them zero. It would be very interesting to understand possible phenomenological implications of this observation.

Finally, let us comment on the utility of transseries solutions. The transseries allows one to organize hydrodynamic and nonhydrodynamic phenomena using a unified mathematical language. This is crucial when the hydrodynamic gradient expansion diverges and requires resummation. The transseries provides a framework to resum it yielding a unique answer for a nonequilibrium solution. Furthermore, transseries provides a way to encode different asymptotic behavior in different spacetime regions, or for different initial data. Transitions between these behaviors are described by the Stokes phenomena. In our case, these considerations allowed us to uncover a new interesting physical effect in the context of hydrodynamization.

Acknowledgments

We would like to acknowledge useful exchanges with Inês Aniceto, Matteo Baggioli, Gerald Dunne, Blaise Goutéraux and Daniel Hasenbichler. The Gravity, Quantum Fields and Information group at the Max Planck Institute for Gravitational Physics (Albert Einstein Institute) is supported by the Alexander von Humboldt Foundation and the Federal Ministry for Education and Research through the Sofja Kovalevskaja Award. AS and MS are supported by the Polish National Science Centre grant 2018/29/B/ST2/02457. BW is supported by a Royal Society University Research Fellowship.

A Müller-Israel-Stewart in the shear channel

MIS theory is the simplest phenomenological model of stress-energy tensor equilibration that agrees with relativistic Navier-Stokes hydrodynamics at leading order in the gradient expansion and, at the same time, respects causality.

For a conformal fluid, the construction of MIS theory proceeds as follows. We start from the Landau-frame constitutive relations of first-order viscous relativistic hydrodynamics in d -dimensional Minkowski space (1.2) with the equations of motion of the theory being nothing but the conservation of the full energy-momentum tensor, $\partial_a T^{ab} = 0$. The algebraic relation between Π^{ab} and σ^{ab} implied by (1.2) entails that first-order relativistic viscous hydrodynamics violates causality. In MIS theory, this problem is overcome by promoting Π^{ab} to a set of new independent degrees of freedom that obey a relaxation equation, in such a way that the original constitutive relation (1.2) is recovered at times sufficiently larger than a new time-scale set by a relaxation time τ ,

$$(\tau U^c \mathcal{D}_c + 1)\Pi^{ab} = -\eta\sigma^{ab}. \tag{A.1}$$

The operator \mathcal{D}_a is a Weyl-covariant derivative originally introduced in [74].

In this work, we consider infinitesimal fluctuations of this theory away from thermal equilibrium. We thus write

$$\mathcal{E}(t, \mathbf{x}) = \mathcal{E}_0 + \delta\mathcal{E}(t, \mathbf{x}) \quad U^a = (1, \mathbf{u}(t, \mathbf{x})), \quad (\text{A.2})$$

where \mathcal{E}_0 is the equilibrium energy density, and treat $\delta\mathcal{E}/\mathcal{E}_0$ and \mathbf{u}^2 as infinitesimally small. Moreover, we also make the symmetry assumption that the hydrodynamic variables are independent of x^1, \dots, x^{d-2} . Defining $x^{d-1} \equiv x$, this corresponds to $\delta\mathcal{E} = \delta\mathcal{E}(t, x)$, $u_i = u_i(t, x)$. This ansatz can be viewed as the minimal generalization of a boost-invariant flow, for which the hydrodynamic variables would also be functions of t and x , but only through the combination $\sqrt{t^2 - x^2}$.

As mentioned in the main text, the telegrapher's equation emerges when considering a shear channel fluctuation, for which $\delta\mathcal{E}(t, x) = 0$ and $u_i(t, x) = u_1(t, x)\delta_{i,1}$ with no loss of generality due to rotational invariance. Defining

$$\rho(t, x) \equiv (\mathcal{E}_0 + P(\mathcal{E}_0))u_1(t, x), \quad J(t, x) \equiv \Pi_{1,d-1}(t, x), \quad (\text{A.3})$$

and linearizing in the velocity fluctuation amplitude, the equation for energy-momentum conservation and the dynamical constitutive relation (A.1) can be expressed as

$$\partial_t \rho(t, x) + \partial_x J(t, x) = 0, \quad (\text{A.4})$$

$$\partial_t J(t, x) + \frac{D}{\tau} \partial_x \rho(t, x) = -\frac{1}{\tau} J(t, x). \quad (\text{A.5})$$

where the diffusion constant is $D = \eta/(sT)$. As mentioned in the Introduction, the linear PDE system (A.4)–(A.5) is well-known in the literature [30, 33]. Combining both equations, we recover (1.7).

B The causality of the telegrapher's equation

In this appendix we show that the telegrapher's equation respects causality (see also [30]). The basis of our proof is the following theorem [75].

Theorem (Paley-Wiener). *Let $f(x) \in L^2(\mathbb{R})$ be supported in $x \in [-A, A]$. Then its Fourier transform $\hat{f}(k)$ belongs to $L^2(\mathbb{R})$ and is an entire function of exponential type A .*

We remind the reader that an entire function is a function which is analytic everywhere in the finite complex plane; an entire function of exponential type A is an entire function that obeys the bound

$$|f(z)| \leq C e^{A|z|}, \quad \forall z \in \mathbb{C}. \quad (\text{B.1})$$

with $C \in \mathbb{R}^+$.

Consider the most general solution to the telegrapher's equation, and suppose that the initial data are supported only between $-R$ and R . Causality demands that, at time t , $\rho(t, x)$ is supported at most in the interval $|x| \leq R + t$. Therefore, we have to show that $\hat{\rho}(t, k)$ is an entire function of exponential type at most $R + t$.

The most general square-integrable solution of the telegrapher's equation can be written as

$$\rho(t, x) = \int_{\mathbb{R}} dk \hat{\rho}(t, k) e^{ikx} \tag{B.2}$$

with

$$\hat{\rho}(t, k) = \hat{u}(k) e^{-\frac{t}{2\tau}} \left[\cosh\left(\frac{\Delta t}{2\tau}\right) + \frac{1}{\Delta} \sinh\left(\frac{\Delta t}{2\tau}\right) \right] + \hat{v}(k) e^{-\frac{t}{2\tau}} \frac{2\tau}{\Delta} \sinh\left(\frac{\Delta t}{2\tau}\right). \tag{B.3}$$

We start by noting that an entire function of the square root of a complex number is itself entire if the original function is even. Therefore, both $\cosh\left(\frac{\Delta t}{2\tau}\right)$ and $\frac{1}{\Delta} \sinh\left(\frac{\Delta t}{2\tau}\right)$ are entire functions of k . It then follows that $\hat{\rho}(t, k)$ is entire in k , since \hat{u}, \hat{v} are entire by assumption, and the product of two entire functions, as well as their sum, are themselves entire.

To show that (B.3) is of exponential type at most $R + t$, we proceed as follows. First, we note that both $\cosh\left(\frac{\Delta t}{2\tau}\right)$ and $\frac{1}{\Delta} \sinh\left(\frac{\Delta t}{2\tau}\right)$ are of exponential type $\sqrt{D/\tau}t$. This also applies to their sum. Next, we recall that the product of two functions of exponential types σ_1 and σ_2 is at most exponential type $\sigma_1 + \sigma_2$. Therefore, the type of each term in the sum (B.3) is at most $R + \sqrt{D/\tau}t$. Finally, since the type of the sum of two functions of exponential types σ_1 and σ_2 is smaller or equal than $\max(\sigma_1, \sigma_2)$, it follows that the type of $\rho(t, k)$ is at most $R + \sqrt{D/\tau}t$. As long as $D/\tau \leq 1$, we see that the system respects relativistic causality.

It is worth pointing out that this result conforms with the expectation that, in any local quantum system, causality bounds the diffusion constant in terms of the effective light-cone speed and the local equilibration time [76] (see also [77–79]). In the case at hand, the effective light-cone speed is to be identified with the speed of light, and the local equilibration time with τ .

C The large-scale expansion and hydrodynamics

In our previous work [28], we described the most general construction of linearized hydrodynamics for a neutral conformal fluid in arbitrary number of spacetime dimensions. Specializing to a shear channel fluctuation, the hydrodynamic description of the microscopic field ρ is provided by the conservation equation (A.4) in combination with the purely-spatial gradient expansion of the constitutive relations. For the MIS case, and in the notation of appendix A, the hydrodynamic gradient expansion reads

$$J(t, x) = - \sum_{n=0}^{\infty} c_n \partial_x^{2n+1} \rho(t, x). \tag{C.1}$$

The transport coefficients c_n are extracted from the microscopic shear hydrodynamic mode by a matching computation. In MIS, they are given by

$$c_n = (-1)^n \mathcal{C}_n D^{n+1} \tau^n, \tag{C.2}$$

where \mathcal{C}_n is the n -th Catalan number.

As we have illustrated extensively in the main text, the perturbative series $\rho_\epsilon^{(H)}(t, x)$ corresponds to the hydrodynamic shear mode contribution to the exact $\rho(t, x)$. It is then

natural to ask whether the effective description of MIS theory in terms of classical hydrodynamics contains exactly the same physical information as the perturbative sector of our transseries.

Let us view (C.1) as a formal series, making no assumptions about the relative size of subsequent terms, and perform the rescaling (1.5) both at the level of the gradient expansion (C.1) and the conservation equation. Then, it turns out that the perturbative sector of our transseries, $\rho_\epsilon^{(H)}(t, x)$, solves the resulting system order-by-order in an expansion around $\epsilon = 0$. Equivalently, if we ignored the specific values of the transport coefficients c_n but somebody handed to us $\rho_\epsilon^{(H)}(t, x)$, we could fix the former by demanding that the latter is a solution order-by-order in an expansion around $\epsilon = 0$. This procedure could then be viewed as the position space counterpart of the matching computation performed in [28].

It should be noted that while $\rho_\epsilon^{(H)}(t, x)$ is a solution, the initial conditions we imposed on the $a_n(t, x)$ coefficients in the main text are completely unnatural from the perspective of the hydrodynamic description of the system. These boundary conditions relied on the existence of the nonperturbative sector of the momentum space transseries, which allowed us to enforce simultaneously that $\hat{\rho}(0, k) = \hat{u}(k)$, $\partial_t \hat{\rho}(0, k) = \hat{v}(k)$. This nonperturbative sector is absent now, reflecting the fact that the algebraic relation between $J(t, x)$ and $\rho(t, x)$ in the hydrodynamic description implies the loss of the nonhydrodynamic degree of freedom.

We now proceed to explain the natural choice of initial conditions from the perspective of the hydrodynamic description. After the spacetime rescaling, our equations of motion are given by

$$\epsilon^2 \partial_t \rho(t, x) + \epsilon \partial_x J(t, x) = 0, \quad J(t, x) = - \sum_{n=0}^{\infty} c_n \epsilon^{2n+1} \partial_x^{2n+1} \rho(t, x). \quad (\text{C.3})$$

The ansatz

$$\rho(t, x) = \sum_{n=0}^{\infty} a_n(t, x) \epsilon^n \quad (\text{C.4})$$

results in the following nested ODE system

$$(\partial_t - D \partial_x^2) a_{2n}(t, x) = \sum_{q=1}^n c_q \partial_x^{2(q+1)} a_{2(n-q)}(t, x) \quad (\text{C.5})$$

with an equivalent expression for the odd coefficients. Again, the n -th term in the series expansion (C.4) is a solution of the heat equation sourced by the $n - 1$ previous orders.

Let us assume that, at a time slice $t = t_0$, $\rho(t_0, x) = \rho_0(x)$ is known. In this situation, the natural boundary conditions to impose on (C.4) are that, at $t = t_0$, the leading-order term $a_0(t_0, x)$ agrees with $\rho_0(x)$, with the remaining higher-order terms vanishing. Due to the structure of (C.5), these boundary conditions result in the vanishing of the odd order terms in (C.4) for all times.

With this choice of boundary conditions, (C.5) can be explicitly solved in closed-form. In Fourier space, we find that¹⁸

$$\hat{a}_{2n}(t, k) = \delta_{n,0} \hat{\rho}_0(k) - (-1)^n c_n t k^{2(n+1)} {}_1F_1(1 - n, 2 + n, Dk^2 t) e^{-Dk^2 t} \hat{\rho}_0(k). \quad (\text{C.6})$$

¹⁸Since the nested ODE system (C.5) is time-translation invariant, we set $t_0 = 0$ with no loss of generality.

The expansion coefficients can be explicitly computed in position space. The zeroth-order one is the solution of the heat equation given by $a_0(t, x) = (G_0 * \rho_0)(t, x)$, where G_0 is given in equation (2.11). The remaining ones are

$$a_{2n}(t, x) = c_n \sum_{q=0}^{n-1} \frac{\Gamma(n)\Gamma(n+2)}{\Gamma(n-q)\Gamma(n+2+q)\Gamma(q+1)} D^q t^{q+1} \partial_x^{2(n+q+1)} a_0(t, x). \quad (\text{C.7})$$

As it happened with our previous choice of initial conditions, each term is a gradient series in ∂_x^2 acting on a particular solution of the heat equation.

D Applicability of the truncated perturbative series

The practical usefulness of the perturbative piece of the asymptotic expansion developed in the previous section is that, when truncated to low order, it provides a good description of the exact velocity field ρ in some spacetime regions. Owing to our general discussion in the Introduction, where we introduced our large-scale expansion, we expect that these regions correspond to those in which the nonhydrodynamic mode contribution has significantly decayed.

Let us illustrate this by considering the time evolution of δ -function initial data of the form $u(x) = 0, v(x) = \delta(x)$. In this case, $\rho(t, x)$ corresponds to the propagator of the telegrapher's equation [30],

$$G(t, x) = \Theta(t)\Theta\left(\frac{D}{\tau}t^2 - x^2\right) \frac{1}{\sqrt{4D\tau}} e^{-\frac{t}{2\tau}} I_0\left(\sqrt{\frac{t^2}{4\tau^2} - \frac{x^2}{4D\tau}}\right). \quad (\text{D.1})$$

The expression above clearly demonstrate that the telegrapher's equation is causal: for any $t > 0$, $\rho(t, x)$ vanishes if $|x| > \sqrt{\frac{D}{\tau}}t$.

We compare the exact $\rho(t, x)$ above with the with the perturbative expansion $\rho_\epsilon^{(H)}|_{\epsilon=1}$ obtained by means of equation (2.10) truncated to first and third nontrivial order. The results can be found in figure 11.

We clearly see that, for any x , $\rho_\epsilon^{(H)}|_{\epsilon=1}$ never provides an accurate description of ρ at early times. This is due to the fact that, in this regime, the nonhydrodynamic mode contribution, which is necessary to enforce the initial condition $\rho(0, x) = 0$ we chose, is still sizable. This state of affairs changes at later times. In particular, focusing on a fixed x as t grows, we eventually observe a very good agreement between ρ and the low-order truncated $\rho_\epsilon^{(H)}|_{\epsilon=1}$.

Another important point to be drawn from figure 11 is that $\rho_\epsilon^{(H)}|_{\epsilon=1}$ is never a good approximation of the exact microscopic ρ outside the causal cone of the system. While the exact ρ vanishes there, $\rho_\epsilon^{(H)}|_{\epsilon=1}$ does not. The reason behind this difference is that $\rho^{(H)}$ is solely built out of the hydrodynamic shear mode, and is therefore blind to the nonhydrodynamic contribution needed to enforce the causal response of the system. This fact provides a nice illustration of the general lesson that the nonhydrodynamic sector is essential to guarantee causality [1].

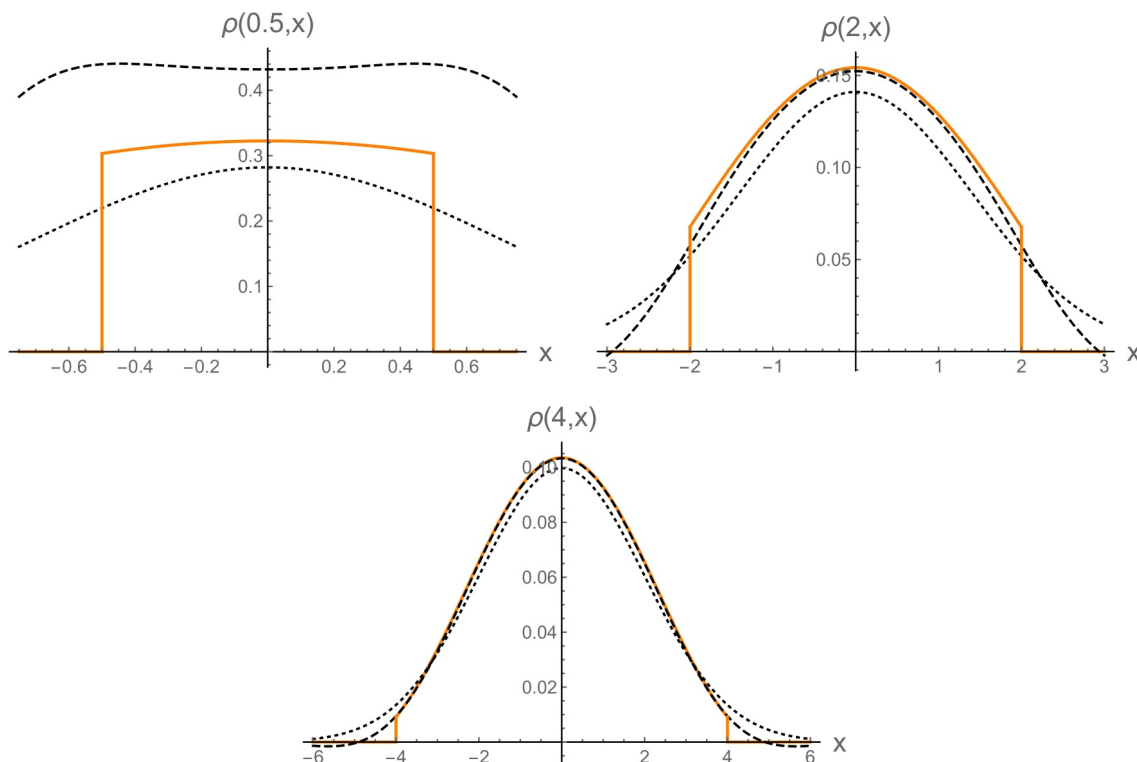


Figure 11. Comparison between the exact ρ corresponding to δ -function initial data (solid orange) and the $\rho_\epsilon^{(H)}|_{\epsilon=1}$ expansion truncated to first (dotted black) and third order (dashed black).

E Large-order behavior for Gaussian initial data

In the main text, we showed that the large-order behavior of the perturbative series is controlled by the adjacent nonperturbative saddle points. In this appendix, we elaborate further on this connection for the case of Gaussian initial data.

Following Berry and Howls [70], we can express the $a_{n+1}(t, 0)$ coefficient of the perturbative series expansion as the following contour integral,

$$a_{n+1}(t, 0) = \Gamma\left(n + \frac{1}{2}\right) \frac{1}{2\pi i} \oint_{\Gamma} dk \frac{\tau}{2\pi\sqrt{1 - 4D\tau k^2}} \left(\frac{k^2}{-S_H(k)}\right)^{n+\frac{1}{2}} k^{-(2n+1)}, \quad (\text{E.1})$$

$$S_H(k) = -\frac{1}{2}s^2 k^2 + (-1 + \sqrt{1 - 4D\tau k^2}) \frac{t}{2\tau} \quad (\text{E.2})$$

with Γ a positively-oriented path enclosing $k = 0$ in the hydrodynamic sheet.

It can be demonstrated that (E.1) can be alternatively expressed as a contour integral in the nonhydrodynamic sheet,

$$a_{n+1}(t, 0) = \Gamma\left(n + \frac{1}{2}\right) \frac{1}{\pi i} \int_{\Gamma'} dk \frac{\tau}{2\pi\sqrt{1 - 4D\tau k^2}} \frac{1}{(-S_{NH}(k))^{n+\frac{1}{2}}}, \quad (\text{E.3})$$

$$S_{NH}(k) = -\frac{1}{2}s^2 k^2 - \left(1 + \sqrt{1 - 4D\tau k^2}\right) \frac{t}{2\tau}, \quad (\text{E.4})$$

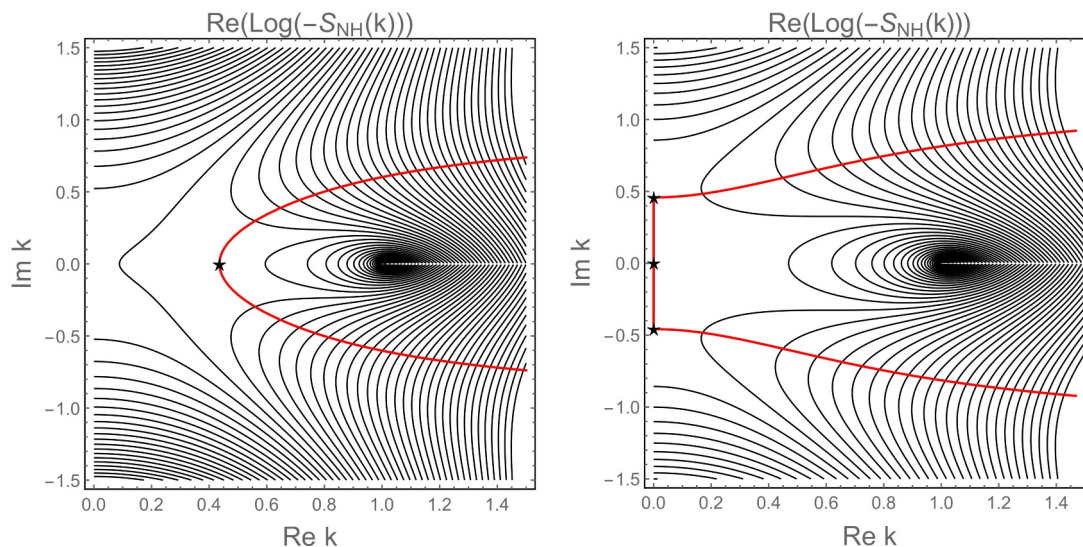


Figure 12. Relevant steepest descent contours to perform the large- n saddle point analysis (solid red), along with the adjacent saddles (black stars), for $s = 1$. Left: $t = 0.9$. Right: $t = 1.1$.

where Γ' is a path starting at $\infty - i0$ below the right branch cut, going around the right branch point, and ending at $\infty + i0$ above the right branch cut.¹⁹

In order to analyze the behavior of (E.3) when $n \rightarrow \infty$, it is natural to decompose Γ' into the steepest descent contours associated to the adjacent saddles discussed in the main text, and employ a saddle point approximation afterward.²⁰ The relevant steepest descent contours involved in computing (E.3) in a large n asymptotic expansion are depicted in figure 12.

For $t < t_c$, only the k_+ saddle contributes to $a_n(t, 0)$. On the other hand, for $t > t_c$, we have contributions both from k_+ , k_- and k_0 .

Let us focus on the former case first. At leading order, it is immediate to show that

$$a_{n+1}(t, 0) = \frac{\Gamma(n)}{(-S_+)^n} \left[G(k_+) \sqrt{-\frac{2}{\pi S''_{NH}(k_+)}} + O\left(\frac{1}{n}\right) \right], \quad (\text{E.5})$$

from which it follows that $r = \lim_{n \rightarrow \infty} n a_n(t, 0)/a_{n+1}(t, 0) = -S_+$, as reported in the main text. A plot of the deviation of the ratio

$$r_{n+1} = \frac{a_{n+1}^{\text{exact}}(t, 0)}{a_{n+1}^{\text{s.p.}}(t, 0)}, \quad (\text{E.6})$$

from one, where a_{n+1}^{exact} is given by (2.23) and $a_{n+1}^{\text{s.p.}}$ by (E.5), can be found in figure 13 (left). We have considered several different times before t_c . It is readily seen that, as $n \rightarrow \infty$, $r_n \rightarrow 1$ plus a $O(1/n)$ correction, confirming the validity of equation (E.5).

¹⁹In writing (E.3), we have taken into account that left and right branch cuts contribute equally to the total result.

²⁰Since at $k_* = k_+, k_-$ or k_0 we have that $S'_{NH}(k_*) = 0$, but $S_{NH}(k_*) \neq 0$, these saddles are also stationary points of $\log(-S_{NH}(k))$.

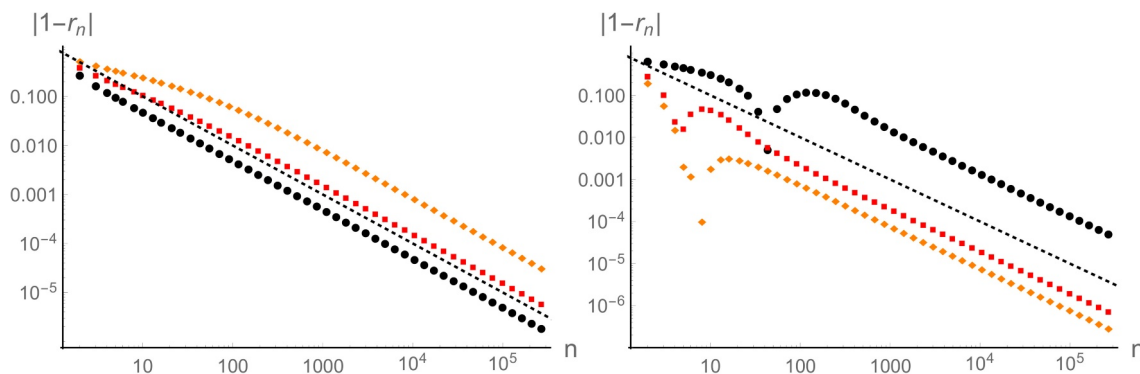


Figure 13. Deviation ratio (E.6) between the exact $a_n(t, 0)$ coefficients and the large-order prediction of the saddle point analysis, for Gaussian initial data with $s = 1$. Left: $t = 0.25$ (black), $t = 0.5$ (red), $t = 0.75$ (orange). Right: $t = 1.25$ (black), $t = 3$ (red), $t = 5$ (orange). The dotted black line is a plot of the function $1/n$ to guide the reader’s eye.

On the other hand, for $t > t_c$, we have three separate contributions to consider. We find that at leading order the k_0 saddle contributes as

$$\frac{\Gamma(n)}{(-S_0)^n} \left[G(k_0) \sqrt{-\frac{2}{\pi S''_{NH}(k_0)}} + O\left(\frac{1}{n}\right) \right] \quad (\text{E.7})$$

while the first nontrivial term of the combined contribution of the k_+ , k_- saddles is given by

$$\frac{\Gamma\left(n + \frac{1}{2}\right)}{(-S_+)^{n+\frac{1}{2}}} \frac{2}{i\pi} \left(G'(k_+) - \frac{S'''_{NH}(k_+)}{3S''_{NH}(k_+)} G(k_+) \right) \frac{(-S_+)}{\left(n + \frac{1}{2}\right) S''_{NH}(k_+)} + \dots \quad (\text{E.8})$$

Since $|S_0| < |S_+|$, the k_{\pm} contribution is exponentially suppressed with respect to the k_0 one,²¹ which now governs the divergence of the perturbative series expansion. The behavior of r_n for $t > t_c$ with $a_n^{\text{s.p.}}(t, 0)$ given by (E.7) is illustrated by figure 13 (right).

F Large-order behavior for Lorentzian initial data

Another family of initial data that allows to compute in closed-form the coefficients of the perturbative expansion at $x = 0$ is that of Lorentzian initial data,

$$v(x) = \frac{\alpha}{\pi(x^2 + \alpha^2)}, \quad \hat{v}(k) = \frac{1}{2\pi} e^{-\alpha|k|}, \quad (\text{F.1})$$

where we find

$$a_{n+1}(t, 0) = \frac{\alpha^{2n+1} \tau^{n+1}}{4\pi^2 D^{n+1} t^{2n+1}} \Gamma\left(n + \frac{1}{2}\right)^2 U\left(2n + 1, n + \frac{3}{2}, \frac{\alpha^2}{4Dt}\right). \quad (\text{F.2})$$

²¹Despite this, in the main text we show that Borel transform techniques were capable of unveiling it.

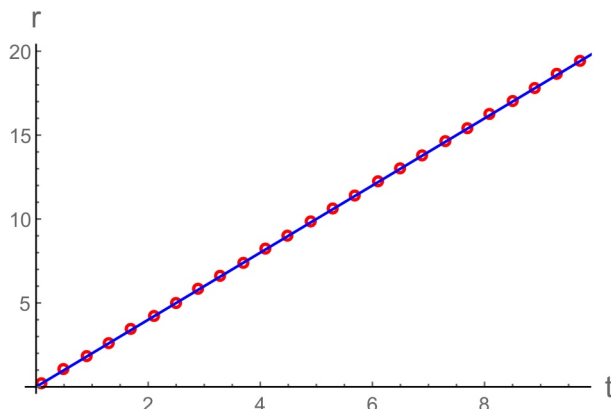


Figure 14. Lorentzian initial data exhibits factorial growth for the series coefficients. Here we show r as defined in (F.3) vs. t for $\alpha = 1$.

As it happened for Gaussian initial data, we find that, for $n \rightarrow \infty$, $q_n = \lim_{n \rightarrow \infty} \left| \frac{a_{n+1}(t,0)}{a_n(t,0)} \right|$ is linear in n , implying that the series is factorially divergent. The large n behavior determined numerically is compatible with

$$q_n \sim \frac{1}{r}n, \quad r \equiv \frac{t}{\tau}, \tag{F.3}$$

irrespectively of the value of α . See figure 14 for an example of this asymptotic behavior in the case $\alpha = 1$.

G Reconstructing ρ from the transseries: Gaussian initial data case

In this appendix we illustrate how Borel resummation can be employed to reconstruct the exact $\rho(t, x)$ from the different transseries at our disposal. The agreement between the Borel resummation and the exact solution determined by direct numerical integration provides a nontrivial consistency check of the results presented in the main text. For the sake of brevity, we focus on Gaussian initial data of the form (2.22).

Before starting, let us recall that the splitting of $\rho(t, x)$ into hydrodynamic and nonhydrodynamic contributions is only unequivocally defined once a particular integration path γ is provided, due to the branch points of $\Delta(k)$.²² To keep track of which integration path we are employing, we will denote by $\gamma_{(+,-)}$ the equivalence class of integration paths starting at $-\infty + i0^+$ above the left branch cut and ending at $\infty - i0^+$ below the right one, with an analogous interpretation for $\gamma_{(-,+)$, $\gamma_{(-,-)}$ and $\gamma_{(+,+)$.

G.1 The perturbative sector

As mentioned before, the Padé approximant of the Borel-transformed asymptotic series displays a line of pole condensation along the positive real z -axis starting at $z_c = -S_-$ and, as a consequence, we have to resort to lateral Borel resummations. It turns out

²²We choose the principal branch for $\Delta(k)$.

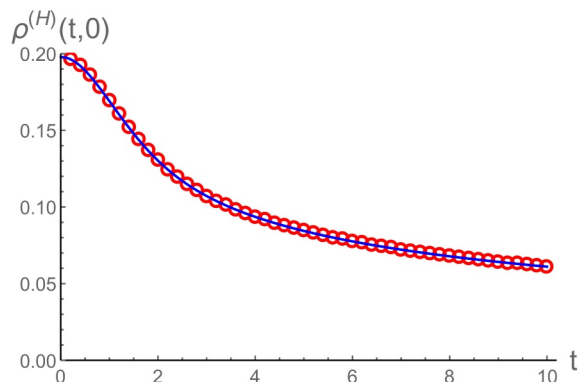


Figure 15. Average of the lateral Borel resummations of $\rho_\epsilon^{(H)}(t, x)|_{\epsilon=1}$ (open red circles) for Gaussian initial data with $s = 1$ compared with the $\rho^{(H)}(t, 0)$ determined directly by a numerical integration along the $\gamma_{(-,-)}$ contour (solid blue curve).

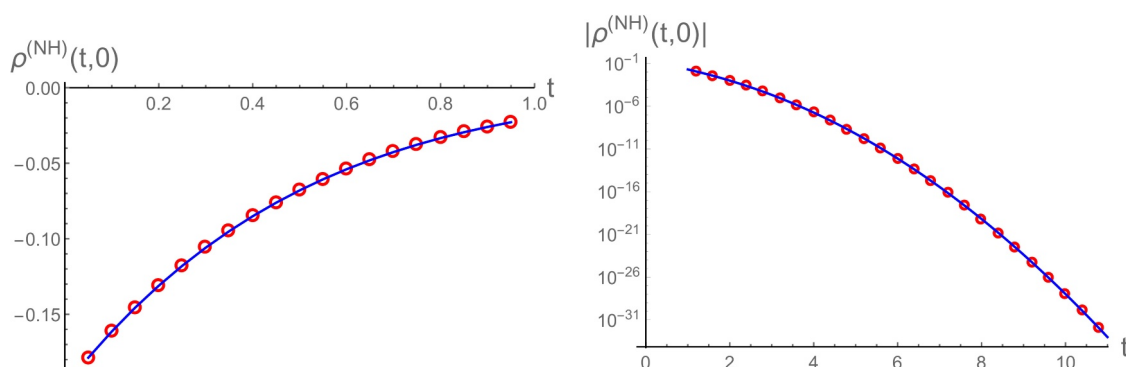


Figure 16. Left: same as figure 15, but now for the nonperturbative series at $t < t_c$. Right: result of the Borel resummation of the nonperturbative series for $t > t_c$ (open circles) compared with the $\rho^{(NH)}(t, 0)$ determined by a numerical integration along $\gamma_{(-,-)}$ (solid blue curve).

that the negative (positive) lateral Borel resummation corresponds to the choice of $\gamma_{(+,-)}$ ($\gamma_{(-,+)}$) integration contour in the original integral, with the average of both corresponding to the $\gamma_{(-,-)}, \gamma_{(+,+)}$ integration paths. We plot an example of this agreement in figure 15.

G.2 The nonperturbative sector

For the nonperturbative sector, we have a discontinuous change in the nonperturbative series when $t = t_c$; correspondingly, we discuss the $t < t_c$ and $t > t_c$ cases separately:

- $t < t_c$. In this regime, the Fourier integral defining $b_n(t, x)$ in terms of $b_n(t, k)$ converges. Therefore, $b_n(t, 0) = -a_n(-t, 0)$, with $a_n(t, 0)$ given by (2.23). The relation between the lateral Borel resummations and the γ integration contours is the same as for the perturbative series, with the real result being given by the average of both lateral resummations. We plot this average in figure 16 (left), where we compare it with the $\rho^{(NH)}(t, 0)$ determined by a direct numerical integration, finding very good agreement between both quantities.

- $t > t_c$. In this regime, the nonperturbative sector of our transseries is given by (5.4a)–(5.4b). The absence of singularities on the positive real axis in the Borel plane implies that the Borel transform of $\rho_\epsilon^{(NH)}(t, 0)$ is Borel resummable; hence the integration along the real axis agrees trivially with the average of the lateral resummations. In figure 16 (right), we compare the $\rho^{(NH)}(t, 0)$ determined by a direct numerical integration with the resummation result, finding again excellent agreement.

Open Access. This article is distributed under the terms of the Creative Commons Attribution License ([CC-BY 4.0](https://creativecommons.org/licenses/by/4.0/)), which permits any use, distribution and reproduction in any medium, provided the original author(s) and source are credited.

References

- [1] W. Florkowski, M.P. Heller and M. Spalinski, *New theories of relativistic hydrodynamics in the LHC era*, *Rept. Prog. Phys.* **81** (2018) 046001 [[arXiv:1707.02282](https://arxiv.org/abs/1707.02282)] [[INSPIRE](#)].
- [2] P. Romatschke and U. Romatschke, *Relativistic fluid dynamics in and out of equilibrium*, Cambridge Monographs on Mathematical Physics, Cambridge University Press, U.K. (2019).
- [3] W. Busza, K. Rajagopal and W. van der Schee, *Heavy ion collisions: the big picture, and the big questions*, *Ann. Rev. Nucl. Part. Sci.* **68** (2018) 339 [[arXiv:1802.04801](https://arxiv.org/abs/1802.04801)] [[INSPIRE](#)].
- [4] C. Shen and L. Yan, *Recent development of hydrodynamic modeling in heavy-ion collisions*, *Nucl. Sci. Tech.* **31** (2020) 122 [[arXiv:2010.12377](https://arxiv.org/abs/2010.12377)] [[INSPIRE](#)].
- [5] S.A. Hartnoll, A. Lucas and S. Sachdev, *Holographic quantum matter*, [arXiv:1612.07324](https://arxiv.org/abs/1612.07324) [[INSPIRE](#)].
- [6] P. Kovtun, D.T. Son and A.O. Starinets, *Viscosity in strongly interacting quantum field theories from black hole physics*, *Phys. Rev. Lett.* **94** (2005) 111601 [[hep-th/0405231](https://arxiv.org/abs/hep-th/0405231)] [[INSPIRE](#)].
- [7] M.P. Heller, R.A. Janik and P. Witaszczyk, *Hydrodynamic gradient expansion in gauge theory plasmas*, *Phys. Rev. Lett.* **110** (2013) 211602 [[arXiv:1302.0697](https://arxiv.org/abs/1302.0697)] [[INSPIRE](#)].
- [8] J.M. Maldacena, *The large N limit of superconformal field theories and supergravity*, *Int. J. Theor. Phys.* **38** (1999) 1113 [*Adv. Theor. Math. Phys.* **2** (1998) 231] [[hep-th/9711200](https://arxiv.org/abs/hep-th/9711200)] [[INSPIRE](#)].
- [9] E. Witten, *Anti-de Sitter space and holography*, *Adv. Theor. Math. Phys.* **2** (1998) 253 [[hep-th/9802150](https://arxiv.org/abs/hep-th/9802150)] [[INSPIRE](#)].
- [10] S.S. Gubser, I.R. Klebanov and A.M. Polyakov, *Gauge theory correlators from noncritical string theory*, *Phys. Lett. B* **428** (1998) 105 [[hep-th/9802109](https://arxiv.org/abs/hep-th/9802109)] [[INSPIRE](#)].
- [11] V.E. Hubeny and M. Rangamani, *A holographic view on physics out of equilibrium*, *Adv. High Energy Phys.* **2010** (2010) 297916 [[arXiv:1006.3675](https://arxiv.org/abs/1006.3675)] [[INSPIRE](#)].
- [12] J.D. Bjorken, *Highly relativistic nucleus-nucleus collisions: the central rapidity region*, *Phys. Rev. D* **27** (1983) 140 [[INSPIRE](#)].
- [13] R. Baier, P. Romatschke, D.T. Son, A.O. Starinets and M.A. Stephanov, *Relativistic viscous hydrodynamics, conformal invariance, and holography*, *JHEP* **04** (2008) 100 [[arXiv:0712.2451](https://arxiv.org/abs/0712.2451)] [[INSPIRE](#)].

- [14] M.P. Heller and M. Spaliński, *Hydrodynamics beyond the gradient expansion: resurgence and resummation*, *Phys. Rev. Lett.* **115** (2015) 072501 [[arXiv:1503.07514](#)] [[INSPIRE](#)].
- [15] G. Basar and G.V. Dunne, *Hydrodynamics, resurgence, and transasymptotics*, *Phys. Rev. D* **92** (2015) 125011 [[arXiv:1509.05046](#)] [[INSPIRE](#)].
- [16] I. Aniceto and M. Spaliński, *Resurgence in extended hydrodynamics*, *Phys. Rev. D* **93** (2016) 085008 [[arXiv:1511.06358](#)] [[INSPIRE](#)].
- [17] W. Florkowski, R. Ryblewski and M. Spaliński, *Gradient expansion for anisotropic hydrodynamics*, *Phys. Rev. D* **94** (2016) 114025 [[arXiv:1608.07558](#)] [[INSPIRE](#)].
- [18] M.P. Heller, A. Kurkela, M. Spaliński and V. Svensson, *Hydrodynamization in kinetic theory: Transient modes and the gradient expansion*, *Phys. Rev. D* **97** (2018) 091503 [[arXiv:1609.04803](#)] [[INSPIRE](#)].
- [19] M.P. Heller and V. Svensson, *How does relativistic kinetic theory remember about initial conditions?*, *Phys. Rev. D* **98** (2018) 054016 [[arXiv:1802.08225](#)] [[INSPIRE](#)].
- [20] J. Casalderrey-Solana, N.I. Gushterov and B. Meiring, *Resurgence and hydrodynamic attractors in Gauss-Bonnet holography*, *JHEP* **04** (2018) 042 [[arXiv:1712.02772](#)] [[INSPIRE](#)].
- [21] I. Aniceto, B. Meiring, J. Jankowski and M. Spaliński, *The large proper-time expansion of Yang-Mills plasma as a resurgent transseries*, *JHEP* **02** (2019) 073 [[arXiv:1810.07130](#)] [[INSPIRE](#)].
- [22] A. Behtash, S. Kamata, M. Martinez, T. Schäfer and V. Skokov, *Transasymptotics and hydrodynamization of the Fokker-Planck equation for gluons*, *Phys. Rev. D* **103** (2021) 056010 [[arXiv:2011.08235](#)] [[INSPIRE](#)].
- [23] G.S. Denicol and J. Noronha, *Exact hydrodynamic attractor of an ultrarelativistic gas of hard spheres*, *Phys. Rev. Lett.* **124** (2020) 152301 [[arXiv:1908.09957](#)] [[INSPIRE](#)].
- [24] R.A. Janik and R.B. Peschanski, *Gauge/gravity duality and thermalization of a boost-invariant perfect fluid*, *Phys. Rev. D* **74** (2006) 046007 [[hep-th/0606149](#)] [[INSPIRE](#)].
- [25] M.P. Heller, R.A. Janik, M. Spaliński and P. Witaszczyk, *Coupling hydrodynamics to nonequilibrium degrees of freedom in strongly interacting quark-gluon plasma*, *Phys. Rev. Lett.* **113** (2014) 261601 [[arXiv:1409.5087](#)] [[INSPIRE](#)].
- [26] D. Dorigoni, *An introduction to resurgence, trans-series and alien calculus*, *Annals Phys.* **409** (2019) 167914 [[arXiv:1411.3585](#)] [[INSPIRE](#)].
- [27] I. Aniceto, G. Basar and R. Schiappa, *A primer on resurgent transseries and their asymptotics*, *Phys. Rept.* **809** (2019) 1 [[arXiv:1802.10441](#)] [[INSPIRE](#)].
- [28] M.P. Heller, A. Serantes, M. Spaliński, V. Svensson and B. Withers, *The hydrodynamic gradient expansion in linear response theory*, [arXiv:2007.05524](#) [[INSPIRE](#)].
- [29] P. Romatschke, *Retarded correlators in kinetic theory: branch cuts, poles and hydrodynamic onset transitions*, *Eur. Phys. J. C* **76** (2016) 352 [[arXiv:1512.02641](#)] [[INSPIRE](#)].
- [30] P. Romatschke, *New developments in relativistic viscous hydrodynamics*, *Int. J. Mod. Phys. E* **19** (2010) 1 [[arXiv:0902.3663](#)] [[INSPIRE](#)].
- [31] Y. Bu and M. Lublinsky, *All order linearized hydrodynamics from fluid-gravity correspondence*, *Phys. Rev. D* **90** (2014) 086003 [[arXiv:1406.7222](#)] [[INSPIRE](#)].
- [32] Y. Bu and M. Lublinsky, *Linearized fluid/gravity correspondence: from shear viscosity to all order hydrodynamics*, *JHEP* **11** (2014) 064 [[arXiv:1409.3095](#)] [[INSPIRE](#)].

- [33] S. Grozdanov, A. Lucas and N. Poovuttikul, *Holography and hydrodynamics with weakly broken symmetries*, *Phys. Rev. D* **99** (2019) 086012 [[arXiv:1810.10016](#)] [[INSPIRE](#)].
- [34] R.A. Davison, L.V. Delacrétaz, B. Goutéraux and S.A. Hartnoll, *Hydrodynamic theory of quantum fluctuating superconductivity*, *Phys. Rev. B* **94** (2016) 054502 [*Erratum ibid.* **96** (2017) 059902] [[arXiv:1602.08171](#)] [[INSPIRE](#)].
- [35] L.V. Delacrétaz, B. Goutéraux, S.A. Hartnoll and A. Karlsson, *Theory of hydrodynamic transport in fluctuating electronic charge density wave states*, *Phys. Rev. B* **96** (2017) 195128 [[arXiv:1702.05104](#)] [[INSPIRE](#)].
- [36] M. Kaminski, K. Landsteiner, J. Mas, J.P. Shock and J. Tarrio, *Holographic operator mixing and quasinormal modes on the brane*, *JHEP* **02** (2010) 021 [[arXiv:0911.3610](#)] [[INSPIRE](#)].
- [37] R.A. Davison and A.O. Starinets, *Holographic zero sound at finite temperature*, *Phys. Rev. D* **85** (2012) 026004 [[arXiv:1109.6343](#)] [[INSPIRE](#)].
- [38] C.-F. Chen and A. Lucas, *Origin of the Drude peak and of zero sound in probe brane holography*, *Phys. Lett. B* **774** (2017) 569 [[arXiv:1709.01520](#)] [[INSPIRE](#)].
- [39] R.A. Davison and B. Goutéraux, *Momentum dissipation and effective theories of coherent and incoherent transport*, *JHEP* **01** (2015) 039 [[arXiv:1411.1062](#)] [[INSPIRE](#)].
- [40] S. Grozdanov, N. Kaplis and A.O. Starinets, *From strong to weak coupling in holographic models of thermalization*, *JHEP* **07** (2016) 151 [[arXiv:1605.02173](#)] [[INSPIRE](#)].
- [41] S. Grozdanov and A.O. Starinets, *Second-order transport, quasinormal modes and zero-viscosity limit in the Gauss-Bonnet holographic fluid*, *JHEP* **03** (2017) 166 [[arXiv:1611.07053](#)] [[INSPIRE](#)].
- [42] S. Grozdanov and N. Poovuttikul, *Generalised global symmetries in holography: magnetohydrodynamic waves in a strongly interacting plasma*, *JHEP* **04** (2019) 141 [[arXiv:1707.04182](#)] [[INSPIRE](#)].
- [43] D.M. Hofman and N. Iqbal, *Generalized global symmetries and holography*, *SciPost Phys.* **4** (2018) 005 [[arXiv:1707.08577](#)] [[INSPIRE](#)].
- [44] S. Grozdanov and N. Poovuttikul, *Generalized global symmetries in states with dynamical defects: The case of the transverse sound in field theory and holography*, *Phys. Rev. D* **97** (2018) 106005 [[arXiv:1801.03199](#)] [[INSPIRE](#)].
- [45] M. Baggioli, M. Vasin, V.V. Brazhkin and K. Trachenko, *Field theory of dissipative systems with gapped momentum states*, *Phys. Rev. D* **102** (2020) 025012 [[arXiv:2004.13613](#)] [[INSPIRE](#)].
- [46] A. Jimenez-Alba, K. Landsteiner and L. Melgar, *Anomalous magnetoresponse and the Stückelberg axion in holography*, *Phys. Rev. D* **90** (2014) 126004 [[arXiv:1407.8162](#)] [[INSPIRE](#)].
- [47] M. Stephanov, H.-U. Yee and Y. Yin, *Collective modes of chiral kinetic theory in a magnetic field*, *Phys. Rev. D* **91** (2015) 125014 [[arXiv:1501.00222](#)] [[INSPIRE](#)].
- [48] B. Withers, *Short-lived modes from hydrodynamic dispersion relations*, *JHEP* **06** (2018) 059 [[arXiv:1803.08058](#)] [[INSPIRE](#)].
- [49] S. Grozdanov, P.K. Kovtun, A.O. Starinets and P. Tadić, *Convergence of the gradient expansion in hydrodynamics*, *Phys. Rev. Lett.* **122** (2019) 251601 [[arXiv:1904.01018](#)] [[INSPIRE](#)].

- [50] S. Grozdanov, P.K. Kovtun, A.O. Starinets and P. Tadić, *The complex life of hydrodynamic modes*, *JHEP* **11** (2019) 097 [[arXiv:1904.12862](#)] [[INSPIRE](#)].
- [51] N. Abbasi and S. Tahery, *Complexified quasinormal modes and the pole-skipping in a holographic system at finite chemical potential*, *JHEP* **10** (2020) 076 [[arXiv:2007.10024](#)] [[INSPIRE](#)].
- [52] A. Jansen and C. Pantelidou, *Quasinormal modes in charged fluids at complex momentum*, *JHEP* **10** (2020) 121 [[arXiv:2007.14418](#)] [[INSPIRE](#)].
- [53] C. Choi, M. Mezei and G. Sárosi, *Pole skipping away from maximal chaos*, [arXiv:2010.08558](#) [[INSPIRE](#)].
- [54] D. Arean, R.A. Davison, B. Goutéraux and K. Suzuki, *Hydrodynamic diffusion and its breakdown near AdS_2 fixed points*, [arXiv:2011.12301](#) [[INSPIRE](#)].
- [55] M. Baggioli, M. Vasin, V.V. Brazhkin and K. Trachenko, *Gapped momentum states*, *Phys. Rept.* **865** (2020) 1 [[arXiv:1904.01419](#)] [[INSPIRE](#)].
- [56] M. Baggioli and K. Trachenko, *Low frequency propagating shear waves in holographic liquids*, *JHEP* **03** (2019) 093 [[arXiv:1807.10530](#)] [[INSPIRE](#)].
- [57] M. Baggioli and K. Trachenko, *Maxwell interpolation and close similarities between liquids and holographic models*, *Phys. Rev. D* **99** (2019) 106002 [[arXiv:1808.05391](#)] [[INSPIRE](#)].
- [58] M. Baggioli, *How small hydrodynamics can go*, *Phys. Rev. D* **103** (2021) 086001 [[arXiv:2010.05916](#)] [[INSPIRE](#)].
- [59] R.E. Arias and I.S. Landea, *Hydrodynamic Modes of a holographic p-wave superfluid*, *JHEP* **11** (2014) 047 [[arXiv:1409.6357](#)] [[INSPIRE](#)].
- [60] U. Gran, M. Tornsö and T. Zingg, *Exotic holographic dispersion*, *JHEP* **02** (2019) 032 [[arXiv:1808.05867](#)] [[INSPIRE](#)].
- [61] M. Baggioli, U. Gran, A.J. Alba, M. Tornsö and T. Zingg, *Holographic plasmon relaxation with and without broken translations*, *JHEP* **09** (2019) 013 [[arXiv:1905.00804](#)] [[INSPIRE](#)].
- [62] M. Baggioli, U. Gran and M. Tornsö, *Transverse collective modes in interacting holographic plasmas*, *JHEP* **04** (2020) 106 [[arXiv:1912.07321](#)] [[INSPIRE](#)].
- [63] S.J. Chapman and D.B. Mortimer, *Exponential asymptotics and stokes lines in a partial differential equation*, *Proc. Roy. Soc. London A* **461** (2005) 2385.
- [64] S. Chapman, C. Howls, J. King and A. O. Daalhuis, *Why is a shock not a caustic? the higher-order stokes phenomenon and smoothed shock formation*, *Nonlinearity* **20** (2007) 2425.
- [65] C. Howls, P. Langman and A. Olde Daalhuis, *On the higher-order stokes phenomenon*, *Proc. Roy. Soc. London A* **460** (2004) 2285.
- [66] A. Kurkela, W. van der Schee, U.A. Wiedemann and B. Wu, *Early- and Late-Time Behavior of Attractors in Heavy-Ion Collisions*, *Phys. Rev. Lett.* **124** (2020) 102301 [[arXiv:1907.08101](#)] [[INSPIRE](#)].
- [67] P. Romatschke, *Relativistic hydrodynamic attractors with broken symmetries: non-conformal and non-homogeneous*, *JHEP* **12** (2017) 079 [[arXiv:1710.03234](#)] [[INSPIRE](#)].
- [68] A. Kurkela, S.F. Taghavi, U.A. Wiedemann and B. Wu, *Hydrodynamization in systems with detailed transverse profiles*, *Phys. Lett. B* **811** (2020) 135901 [[arXiv:2007.06851](#)] [[INSPIRE](#)].

- [69] V.E. Ambrus, S. Busuioc, J.A. Fotakis, K. Gallmeister and C. Greiner, *Bjorken flow attractors with transverse dynamics*, [arXiv:2102.11785](#) [INSPIRE].
- [70] M.V. Berry and C.J. Howls, *Hyperasymptotics for integrals with saddles*, *Proc. Roy. Soc. London A* **434** (1991) 657.
- [71] M. Serone, G. Spada and G. Villadoro, *The power of perturbation theory*, *JHEP* **05** (2017) 056 [[arXiv:1702.04148](#)] [INSPIRE].
- [72] O. Costin and G.V. Dunne, *Resurgent extrapolation: rebuilding a function from asymptotic data. Painlevé I*, *J. Phys. A* **52** (2019) 445205 [[arXiv:1904.11593](#)] [INSPIRE].
- [73] S. Bhattacharyya, V.E. Hubeny, S. Minwalla and M. Rangamani, *Nonlinear fluid dynamics from gravity*, *JHEP* **02** (2008) 045 [[arXiv:0712.2456](#)] [INSPIRE].
- [74] R. Loganayagam, *Entropy current in conformal hydrodynamics*, *JHEP* **05** (2008) 087 [[arXiv:0801.3701](#)] [INSPIRE].
- [75] R.S. Strichartz, *A guide to distribution theory and Fourier transforms*, World Scientific, Singapore (2003).
- [76] T. Hartman, S.A. Hartnoll and R. Mahajan, *Upper bound on diffusivity*, *Phys. Rev. Lett.* **119** (2017) 141601 [[arXiv:1706.00019](#)] [INSPIRE].
- [77] R.A. Davison, S.A. Gentle and B. Goutéraux, *Slow relaxation and diffusion in holographic quantum critical phases*, *Phys. Rev. Lett.* **123** (2019) 141601 [[arXiv:1808.05659](#)] [INSPIRE].
- [78] R.A. Davison, S.A. Gentle and B. Goutéraux, *Impact of irrelevant deformations on thermodynamics and transport in holographic quantum critical states*, *Phys. Rev. D* **100** (2019) 086020 [[arXiv:1812.11060](#)] [INSPIRE].
- [79] M. Baggioli and W.-J. Li, *Universal bounds on transport in holographic systems with broken translations*, *SciPost Phys.* **9** (2020) 007 [[arXiv:2005.06482](#)] [INSPIRE].

Convergence of hydrodynamic modes: insights from kinetic theory and holography

Michał P. Heller^{1,2*}, Alexandre Serantes^{2†}, Michał Spaliński^{2,3‡},
Viktor Svensson^{1,2°} and Benjamin Withers^{4§}

1 Max Planck Institute for Gravitational Physics (Albert Einstein Institute),
14476 Potsdam-Golm, Germany

2 National Centre for Nuclear Research, 02-093 Warsaw, Poland

3 Physics Department, University of Białystok, 15-245 Białystok, Poland

4 Mathematical Sciences and STAG Research Centre, University of Southampton,
Highfield, Southampton SO17 1BJ, UK

* michal.p.heller@aei.mpg.de, † alexandre.serantesrubianes@ncbj.gov.pl,
‡ michal.spalinski@ncbj.gov.pl, ° viktor.svensson@aei.mpg.de,
§ b.s.withers@soton.ac.uk

Abstract

We study the mechanisms setting the radius of convergence of hydrodynamic dispersion relations in kinetic theory in the relaxation time approximation. This introduces a qualitatively new feature with respect to holography: a nonhydrodynamic sector represented by a branch cut in the retarded Green's function. In contrast with existing holographic examples, we find that the radius of convergence in the shear channel is set by a collision of the hydrodynamic pole with a branch point. In the sound channel it is set by a pole-pole collision on a non-principal sheet of the Green's function. More generally, we examine the consequences of the Implicit Function Theorem in hydrodynamics and give a prescription to determine a set of points that necessarily includes all complex singularities of the dispersion relation. This may be used as a practical tool to assist in determining the radius of convergence of hydrodynamic dispersion relations.



Copyright M. P. Heller *et al.*

This work is licensed under the Creative Commons

[Attribution 4.0 International License](https://creativecommons.org/licenses/by/4.0/).

Published by the SciPost Foundation.

Received 04-02-2021

Accepted 26-05-2021

Published 01-06-2021

doi:[10.21468/SciPostPhys.10.6.123](https://doi.org/10.21468/SciPostPhys.10.6.123)



Check for
updates

Contents

1	Introduction	2
2	The shear channel	5
3	The sound channel	10
4	A prescription for finding the radius of convergence	14
4.1	Polynomial P	15
4.2	Non-polynomial P and case studies	16
4.2.1	Single mode	16

4.2.2	RTA kinetic theory: shear channel	16
4.2.3	RTA kinetic theory: sound channel	17
5	Summary	17
A	The points $k = \pm \frac{3}{4}i$ in the sound channel	19
	References	21

1 Introduction

Understanding the foundations of relativistic hydrodynamics as a description of nonequilibrium physics has been an important research theme of the past decade. The experimental motivation behind it comes from the field of ultrarelativistic heavy-ion collisions, where relativistic hydrodynamics is the framework successfully used to connect the early time physics of quantum chromodynamics (QCD) with the properties of the particle spectrum in the detectors [1, 2]. On the theoretical side, how the hydrodynamic regime emerges from QCD in particular and quantum field theories in general has turned out to be a subject ripe for discoveries.

Our work is motivated by three interrelated lines of theoretical physics research. The first one concerns microscopically accurate descriptions of strongly-coupled quantum field theories with large number of degrees of freedom in terms of their classical gravity duals [3]. The second one concerns partial differential equations that embed relativistic hydrodynamics in a form of well-behaved and numerically tractable equations of motion for relativistic matter. We will refer to such frameworks as MIS-type models [4]. The last one concerns relativistic kinetic theory, which may arise as an effective description of QCD, or as a standalone model. The common feature among them is the absence of stochastic effects.

Broadly speaking, there are two main strategies to explore the transition to hydrodynamics in these different frameworks. The first involves studying highly symmetric flows, with the boost-invariant (Bjorken) flow being a widely used model of expanding matter in ultrarelativistic heavy-ion collisions [5]. The second utilizes linear response theory studies of singularities of retarded two-point functions G_R in the complex frequency plane at a fixed spatial momentum. In our work we will be mostly concerned with the latter situation and we will return to expanding plasma systems only in the summary.

The key observation of holography is that in a class of quantum field theories, the retarded two-point functions of the stress tensor in equilibrium have singularities in the form of infinitely many single poles [6]. Each pole gives rise to a decaying and oscillating contribution upon inverting the Fourier transform. A similar story holds in MIS-type models, in which the number of such singularities is finite and small. As a result, some features encountered in holography can also be understood in these settings where they are often analytically tractable.

Among such poles, there are two special ones, which are arbitrarily long-lived upon making spatial momentum sufficiently small. These are the hydrodynamic shear and sound modes characterized by gapless dispersion relations of the respective form,

$$\omega_{\perp} = -i \frac{\eta}{sT} k^2 + \mathcal{O}(k^4) \quad \text{and} \quad \omega_{\parallel}^{\pm} = \pm \frac{1}{\sqrt{3}} k - i \frac{2}{3} \frac{\eta}{sT} k^2 + \mathcal{O}(k^3), \quad (1)$$

where η/s is the ratio of shear viscosity to entropy density and T is the equilibrium temperature. The small- k expansion is a direct momentum space manifestation of the hydrodynamic

gradient expansion and in (1) we dropped contributions from terms having two and more derivatives of fluid variables. The other modes are exponentially decaying in time and correspond to transient effects when perturbing equilibrium by a small amount. For holographic models, hydrodynamic and transient excitations are nothing else than quasinormal modes of anti-de Sitter black holes with planar horizons [7].

In the context of the aforementioned foundational aspects, the question that rose to prominence in the past two years, see [8–16], is what is the radius of convergence of the hydrodynamic dispersion relations when expanded around $k = 0$ and, if finite, what sets it.

It turns out that in the holographic quantum field theories studied to date starting with [8], as well as in the MIS-type models analyzed so far [12], the radius of convergence, $|k^*|$, is finite and the critical momentum it corresponds to, k^* , is set by a branch point singularity of the hydrodynamic dispersion relation. This branch point is the result of a collision between the hydrodynamic mode in question and one of the transient modes in a complexified spatial momentum plane. By this we mean that the single pole singularities of the retarded correlator move in the complex frequency plane as a function of momentum and for some momenta they degenerate (collide).

Note that in linear response theory it is sufficient to study only the radius of convergence of the small- k expansion of the dispersion relations. This is because this radius also dictates the radius of convergence of the position-space gradient expansion of the hydrodynamic constitutive relations as shown in [12], when supplemented with a choice of initial data.

Holography is a framework dealing with strongly-coupled quantum field theories and a natural question that arises is how the story of modes and their collisions generalizes to weakly-coupled situations. This is addressed in our present work. The starting point for our considerations is relativistic kinetic theory

$$p^\mu \partial_\mu f = \mathcal{C}[f], \tag{2}$$

where f is a one-particle distribution function, that depends on spacetime coordinates and the particle momenta p^μ , and \mathcal{C} is a collision kernel that defines the model and encodes interactions between particles.¹

Kinetic theory can act as an effective description of processes in weakly-coupled quantum field theories when interference effects can be neglected [17, 18]. In particular, the effective kinetic theory of QCD [19–21] has recently become a framework of significant theoretical and phenomenological interest in the context of ultrarelativistic heavy-ion collisions [22–31].

In general, little is known about the inner workings of retarded correlators in kinetic theories with nontrivial collision terms (see, however, [32]). In the present work we will specialize to a particularly simple and, therefore, widely employed collision kernel that encodes exponential relaxation to the equilibrium distribution function

$$\mathcal{C}[f] = p_\mu u^\mu \frac{f(x, p) - f_0(x, p)}{\tau}, \tag{3}$$

where u^μ is the comoving velocity vector, τ is the relaxation time and we take $f_0(x, p)$ to be given by a Boltzmann distribution

$$f_0(x, p) = \frac{1}{(2\pi)^3} e^{\frac{p_\mu u^\mu}{T}}. \tag{4}$$

For this so-called relaxation time approximation (RTA) kinetic theory [33] and for massless particles, the retarded correlators were computed in closed-form in [34] (see also [35]). If

¹Throughout the text we assume mostly plus metric sign convention.

x^0 denotes time and k is the Fourier transform momentum component along the x^3 direction, then the retarded correlator in the shear channel takes the form

$$\frac{G_{R,\perp}^{01,01}(\omega, k)}{-(\mathcal{E} + \mathcal{P})} = \frac{2k\tau(2k^2\tau^2 + 3(1 - i\tau\omega)^2) + 3i(1 - i\tau\omega)(k^2\tau^2 + (1 - i\tau\omega)^2)L}{2k\tau(3 + 2k^2\tau^2 - 3i\tau\omega) + 3i(k^2\tau^2 + (1 - i\tau\omega)^2)L}, \quad (5)$$

whereas in the sound channel one gets

$$\frac{G_{R,\parallel}^{03,03}(\omega, k)}{-3(\mathcal{E} + \mathcal{P})} = \frac{1}{3} + \omega^2\tau \frac{2k\tau + i(1 - i\tau\omega)L}{2k\tau(k^2\tau + 3i\omega) + i(k^2\tau + 3\omega(i + \tau\omega))L}, \quad (6)$$

with L denoting the logarithmic term

$$L = \log\left(\frac{\omega - k + \frac{i}{\tau}}{\omega + k + \frac{i}{\tau}}\right). \quad (7)$$

In the above equations \mathcal{E} and \mathcal{P} are equilibrium energy density and pressure. The remaining nontrivial components can be obtained using tracelessness and conservation of the stress tensor. In the rest of the text, if not explicitly stated, we will set $\tau = 1$ without loss of generality.

While, unsurprisingly, one finds that there exist shear and sound mode frequencies arising as single pole singularities of respectively (5) and (6), the correlators also contain logarithmic branch point non-analyticities. The corresponding branch cuts emanate from $\omega = -\frac{i}{\tau} \pm k$ and, therefore, represent a transient sector whose real-time imprint is an exponential decay supplemented with oscillations and power-law corrections [4].

Following [35], one can understand the branch cuts as originating from the free propagation of particles whose interactions with the background equilibrated medium are captured by their finite lifetime set by τ . The branch cut arises because perturbations of the stress tensor at a given spatial point receive contributions from particles moving with the speed of light and coming in from various directions. The latter are single pole contributions that the integration over angles converts to the logarithm (7). Because one deals with a correlator of a conserved quantity, the contribution of the decaying particles to the stress-energy tensor cannot be lost and needs to be transferred to other degrees of freedom – the hydrodynamic shear and sound waves.

The aim of our study of kinetic theory is to understand the interplay between the hydrodynamic modes – described by single poles which, at low k , are localized close to the origin in the complex ω -plane – and the branch cut transient sector (7). In particular, we want to understand what kind of phenomena set the radius of convergence for the hydrodynamic dispersion relations in this setup. In [34, 35] it was noticed that since the correlator (5)-(6) contains a branch cut, the hydrodynamic poles can move to a non-principal sheet as a function of (in these works, real) momentum, labelled as the ‘hydrodynamic onset transition’. However, since the position of branch cuts is largely a matter of choice, we do not anticipate that this transition is related to the radius of convergence of the hydrodynamic expansion, and indeed it is not.

Starting from the explicit expressions of the retarded thermal two-point functions contained in equations (5)-(6), we will provide substantial numerical evidence supporting the fact that, in RTA kinetic theory, the mechanism determining the critical momentum k^* is different from holography. Our main findings are the following:

1. In the shear channel, the radius $|k_\perp^*|$ is set by a collision between the hydrodynamic pole $\omega_\perp(k)$ and a nonhydrodynamic branch point $\omega_{bp}(k)$. This corresponds to a logarithmic branch point singularity of $\omega_\perp(k)$. We find $|k_\perp^*| = 3/(2\tau)$.
2. In the sound channel, the radius $|k_\parallel^*|$ corresponds to a collision between the hydrodynamic pole $\omega_\parallel^\pm(k)$ and another *gapless* pole that originates in a non-principal sheet of

the retarded correlator. The collision itself takes place on a non-principal sheet of the correlator, and corresponds to a branch point singularity of $\omega_{\parallel}^{\pm}(k)$. We find numerically $|k_{\parallel}^*| \simeq 0.7410387/\tau$.

With the mechanisms in both RTA kinetic theory and holography established, we turn our attention to general lessons. We use the Implicit Function Theorem to place constraints on the singularities of the dispersion relation $\omega(k)$ in any theory where they can be defined by an equation of the form $P(\omega, k) = 0$. Both the location of the singularities and the type of singularity can be constrained by the form of P .

The structure of the paper is as follows. The shear and the sound channel dispersion relations in RTA kinetic theory are respectively discussed in sections 2 and 3. Afterward, in section 4 we comment on our results in light of the Implicit Function Theorem, where we also provide a general prescription for determining the radius of convergence of the hydrodynamic modes. We close the paper with a summary in section 5.

2 The shear channel

In the shear channel, the poles of the retarded thermal two-point function (5) correspond to the solutions of

$$P_{\perp}(\omega, k) = 2k(3 + 2k^2 - 3i\omega) + 3i(k^2 + (1 - i\omega)^2)L = 0. \tag{8}$$

For future reference, we define $A(\omega, k) = 2k(3 + 2k^2 - 3i\omega)$ and $B(\omega, k) = 3i(k^2 + (1 - i\omega)^2)$. Apart from the hydrodynamic mode $\omega_{\perp}(k)$, that behaves as

$$\omega_{\perp}(k) = -\frac{i}{5}k^2 + \dots, \tag{9}$$

when $k \rightarrow 0$, (5) is endowed with two nonhydrodynamic branch points located at

$$\omega_{bp}^{\pm}(k) = \pm k - i. \tag{10}$$

Our main focus is the large-order behavior of the series expansion (9). Introducing the ansatz

$$\omega_{\perp}(k) = \sum_{q=1}^{\infty} c_q k^{2q} \tag{11}$$

into (8), expanding around $k = 0$, and demanding that the resulting series vanishes order-by-order, we can find the c_q coefficients straightforwardly. We have carried out this procedure up to $q = q_{max} = 500$. The results of applying the ratio test to the sequence $\{c_q, q \in \mathbb{N}\}$ are plotted in figure 1 (left). We find that the norm of the critical momentum in the shear channel, which must satisfy

$$\lim_{q \rightarrow \infty} \left| \frac{c_{q+1}}{c_q} \right| = |k_{\perp}^*|^{-2}, \tag{12}$$

is compatible with the value

$$|k_{\perp}^*| = \frac{3}{2}. \tag{13}$$

This is illustrated in the left plot in figure 1 by a dashed blue line corresponding to $|k_{\perp}^*|^{-2} = \frac{4}{9}$, as well as in the right plot, where we show that the difference between $\left| \frac{c_{q+1}}{c_q} \right|$ and $|k_{\perp}^*|^{-2}$ indeed goes to zero as $q \rightarrow \infty$. In order to cross-check this result, we analytically continue the series expansion (11) into the complex k -plane by means of symmetric Padé approximants,

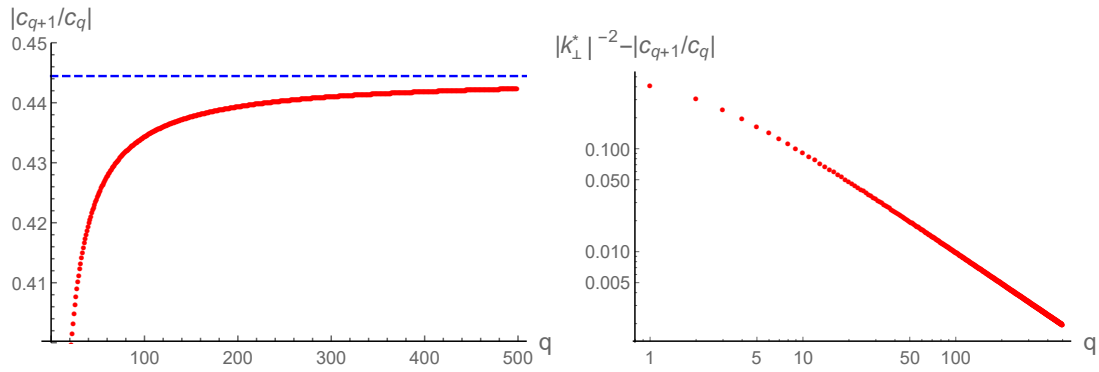


Figure 1: Left: ratio test applied to the sequence $\{c_q, q \in \mathbb{N}\}$. As q increases, the quantity $\left| \frac{c_{q+1}}{c_q} \right|$ approaches a constant. The conjectured limit as $q \rightarrow \infty$, $|k_{\perp}^*|^{-2} = 4/9$, is represented by the dashed blue line in the plot. Right: difference between $|k_{\perp}^*|^{-2}$ and $\left| \frac{c_{q+1}}{c_q} \right|$ as $q \rightarrow \infty$. We clearly see that this difference tends to zero as a power-law.

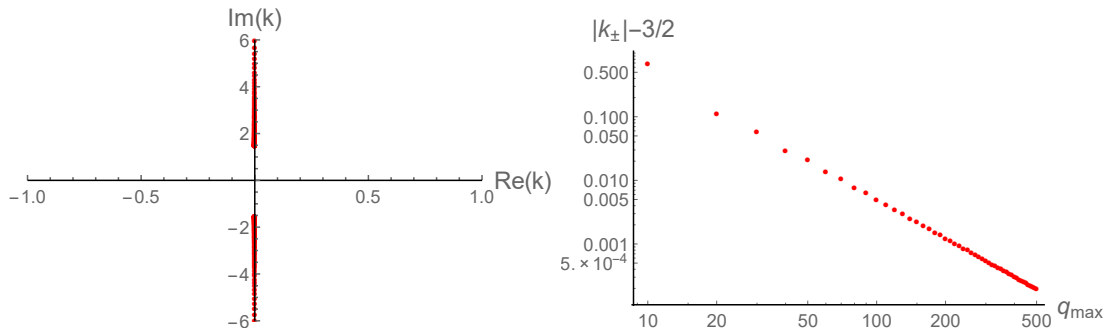


Figure 2: Left: location of the poles of the symmetric Padé approximant of order 250 in the complex k -plane. Two lines of pole condensation along the imaginary k -axis are clearly visible. For the resolution employed here, these lines start at $k = \pm 1.50020004i$. These values are compatible with $|k_{\perp}^*| = \frac{3}{2}$. Right: difference between $|k_{\pm}|$ and $|k_{\perp}^*|$ as the order of the symmetric Padé approximant, $\frac{q_{max}}{2}$, is increased.

and determine the single poles of the resulting rational function. In this approach, a branch point singularity of the exact $\omega_{\perp}(k)$ manifests itself as a line of pole condensation. The results of this procedure, for a symmetric Padé approximant of order 250, are shown in figure 2 (left). We find two lines of pole condensation along the imaginary k -axis, starting at

$$k = k_{\pm} = \pm 1.50020004i, \tag{14}$$

in very good agreement with the observations performed above. Furthermore, upon increasing the order of the symmetric Padé approximant, the difference between $|k_{\pm}|$ and $|k_{\perp}^*| = \frac{3}{2}$ decreases monotonically in a power-law fashion, as can be seen in figure 2 (right).

In the light of the results presented so far, it is natural to conjecture that the series expansion of $\omega_{\perp}(k)$ around $k = 0$ stops converging due to the presence of two branch point singularities located at $k = \pm \frac{3}{2}i$.

It can be checked directly that (8) vanishes at $k = \pm \frac{3}{2}i$, $\omega = \frac{i}{2}$, since the divergence of the logarithmic term as $\omega \rightarrow \frac{i}{2}$ is suppressed by its $\omega - \frac{i}{2}$ prefactor. Hence, the points $(k = \pm \frac{3}{2}i, \omega = \frac{i}{2})$ are valid solutions of $P_{\perp} = 0$. These points are special from several viewpoints. First, when $k = \pm \frac{3}{2}i$, the nonhydrodynamic branch point ω_{bp}^{\pm} is located at $\frac{i}{2}$, which

implies that at $k = \pm \frac{3}{2}i$ the hydrodynamic pole collides with a nonhydrodynamic branch point, as claimed in the Introduction. Second, since these points can also be found by demanding that

$$A(\omega, k) = B(\omega, k) = 0, \tag{15}$$

at nonzero k , they also correspond to the only finite momentum solutions at which the coefficient of the logarithmic branch point present in (8) disappears.

Let us illustrate the first point mention above. We will do this by computing numerically ω_{\perp} along the ray $k = k_{\theta} \equiv |k|e^{i\theta}$, calculating its distance to the ω_{bp}^+ branch point, and showing that this distance vanishes as $\theta \rightarrow \frac{\pi}{2}$.

Before presenting our results, let us emphasize an important observation that needs to be taken into account in order to carry out this computation. As originally found in reference [34] for the real k case, ω_{\perp} can cross the branch cut joining ω_{bp}^+ and ω_{bp}^- .² This crossing does not entail that ω_{\perp} ceases to exist [35]; it just means that ω_{\perp} migrates to a different sheet of the retarded two-point function defined by analytical continuation. While this branch cut crossing does not pose any obstruction to the convergence of the series expansion of ω_{\perp} around $k = 0$, it has to be taken into account when obtaining ω_{\perp} numerically.

There are essentially two different ways to achieve this. The first one is to trade (8) for an ODE for ω_{\perp} ; the second, to analytically continue L to a non-principal branch once the branch cut crossing has taken place. In particular, to go the n -th sheet of P_{\perp} , one just has to replace L as given in (7) by

$$L_n = \log\left(\frac{\omega - k + i}{\omega + k + i}\right) + 2\pi i n. \tag{16}$$

We have verified explicitly that both approaches are compatible with one another.

To get the ODE, we calculate

$$\frac{d}{dk}P_{\perp}(\omega_{\perp}(k), k) = \partial_{\omega}P_{\perp}(\omega_{\perp}(k), k)\omega'_{\perp}(k) + \partial_k P_{\perp}(\omega_{\perp}(k), k) = 0, \tag{17}$$

and employ (8) to replace the logarithmic term in (17).³ The final result is that

$$k(i - 2\omega_{\perp})\omega'_{\perp} + 3\omega_{\perp}(i + \omega_{\perp}) - k^2 = 0. \tag{18}$$

This equation is to be solved with initial conditions given by the hydrodynamic shear mode small- k expansion. Some results for $|\omega_{\perp}(k_{\theta}) - \omega_{bp}^+(k_{\theta})|$ when $\theta = \frac{\pi}{2} - \delta\theta$, $\delta\theta > 0$ are shown in figure 3. Our findings confirm our expectations: in the limit $\delta\theta \rightarrow 0$, the hydrodynamic pole and the branch point collide at $|k| = \frac{3}{2}$.⁴ An equivalent plot can be obtained by monitoring the distance between ω_{\perp} and ω_{bp}^- along the ray defined by $\theta = -\frac{\pi}{2} + \delta\theta$.

We would also like to offer an alternative way of picturing the branch point, hydrodynamic pole collision, more in line with the observations around equation (15). This alternative picture builds upon the crucial fact that the structure of the solutions of (8) can change qualitatively if we analytically continue P_{\perp} to other sheets. For instance, gapless solutions require $n = 0$ and hence do not exist in the non-principal sheets; at the same time, while gapped solutions are absent in the principal sheet, they do appear when $n \neq 0$.

Let us focus on these gapped solutions. By performing the replacement $L \rightarrow L_n$ in P_{\perp} (as mentioned in equation (16)) it is possible to obtain them as the following series expansion around $k = 0$,

$$\omega_{\perp}^{(NH,n)}(k) = -i + \alpha k + \frac{1}{3}i(\alpha^2 - 1)k^2 + \frac{1}{81}i(\alpha^2 - 1)^2k^4 + \frac{1}{243}\alpha(\alpha^2 - 1)^2k^5 + \dots, \tag{19}$$

²Unless stated otherwise, we will always consider that the log function is evaluated on the principal branch.

³The sequence of steps involved in obtaining the equation breaks down right at the point where the hydrodynamic mode collides with the branch point; we are not interested in this precise point, only in its vicinity.

⁴Choosing $\delta\theta$ to be negative but of the same magnitude gives the same results.

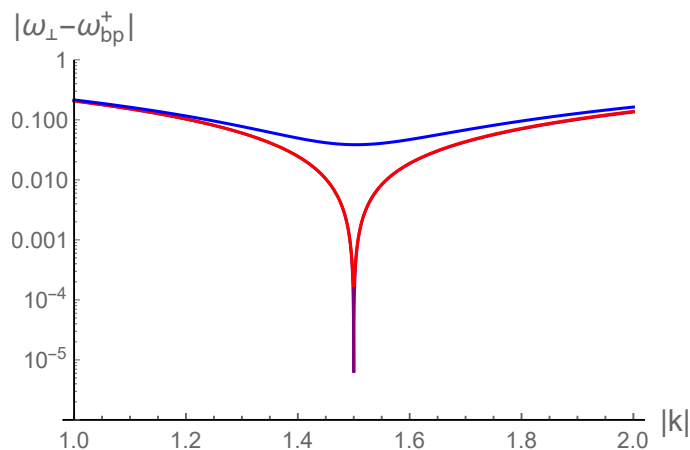


Figure 3: Distance in the complex ω -plane between the hydrodynamic pole ω_{\perp} and the branch point ω_{bp}^+ as k varies along the ray $k_{\theta} = |k|e^{i\theta}$, for $\theta = \frac{\pi}{2} - 10^{-1}$ (blue), $\frac{\pi}{2} - 10^{-3}$ (red) and $\frac{\pi}{2} - 10^{-6}$ (purple). As $\frac{\pi}{2} - \theta \rightarrow 0$, the distance reaches a minimum at $|k| = \frac{3}{2}$.

where the parameter α is constrained to obey the transcendental equation

$$(\alpha^2 - 1) \left(2\pi n - i \log \frac{\alpha - 1}{\alpha + 1} \right) - 2i\alpha = 0. \tag{20}$$

The important point to keep in mind is that $(k = \pm \frac{3}{2}i, \omega = \frac{i}{2})$ are still valid solutions in any non-principal sheet, since the replacement $L \rightarrow L_n$ leaves the conditions (15) invariant. In this sense, at $(k = \pm \frac{3}{2}i, \omega = \frac{i}{2})$ the complex curve equation $P_{\perp} = 0$ goes from having an infinite number of solutions to having just one. It is natural to guess that, for each $n \neq 0$, there is going to be at least one $\omega_{\perp}^{(NH,n)}$ passing precisely through this point. Our numerical computations support this hypothesis. In figure 4, we plot the trajectories followed by a subset of the $\omega_{\perp}^{(NH,n)}$ poles as k varies from 0 to $\frac{3}{2}i$ along the imaginary axis. We clearly see that, at $k = \frac{3}{2}i$, the poles degenerate. The relevant $\omega_{\perp}^{(NH,n)}$ have $\text{Re}(\alpha) > 0$ and $\text{Im}(\alpha) < 0$ (> 0) for $n < 0$ (> 0). An analogous situation takes place if we consider that k ranges from 0 to $-\frac{3}{2}i$ instead; in this latter case, the $\omega_{\perp}^{(NH,n)}$ poles that become degenerate have the opposite value of $\text{Re}(\alpha)$.

To conclude this section, we discuss the behavior of both ω_{\perp} and the correlator (5) in the vicinity of $k = \frac{3}{2}i$. Let us start with the former object, and define

$$k = \frac{3i}{2} - i\delta, \quad \omega = \frac{i}{2} - i\delta - i\epsilon, \tag{21}$$

in such a way that $|\epsilon|$ measures the distance between ω_{\perp} and the branch point ω_{bp}^+ . A numerical analysis shows that, in the $\delta \rightarrow 0$ limit, ϵ behaves as

$$\epsilon \sim \frac{\delta}{-\log(\delta)}, \tag{22}$$

implying that $k = \frac{3}{2}i$ corresponds to a logarithmic branch point of ω_{\perp} . We illustrate the behavior represented by equation (22) in figure 5 – where we consider that $\delta \in \mathbb{R}, \delta > 0$, in such a way that we approach $k = \frac{3}{2}i$ from below along the imaginary axis – and figure 6, where we provide the results for another two, different directions.

Regarding the correlator (5), it is natural to wonder the effect that the branch point-hydrodynamic pole collision we have found has on its residue at the pole. In particular, for

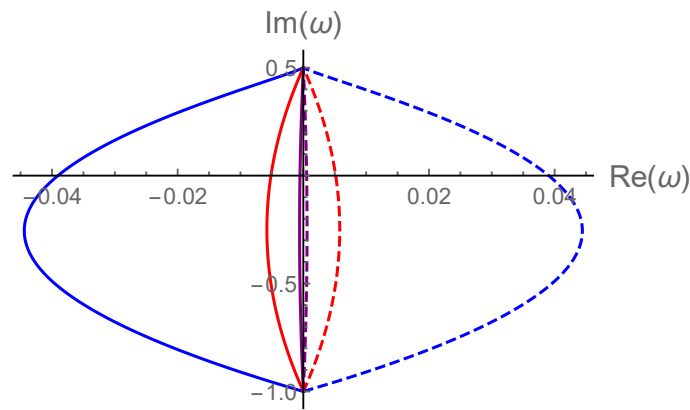


Figure 4: As k goes from 0 to $\frac{3}{2}i$, the gapped poles in the non-principal sheets start at $\omega = -i$ (on their respective sheet) and degenerate at the branch point. We plot the trajectories followed by the poles with $|n| = 1$ (blue), $|n| = 10$ (red) and $|n| = 100$ (purple) with solid (dashed) curves corresponding to positive (negative) n .

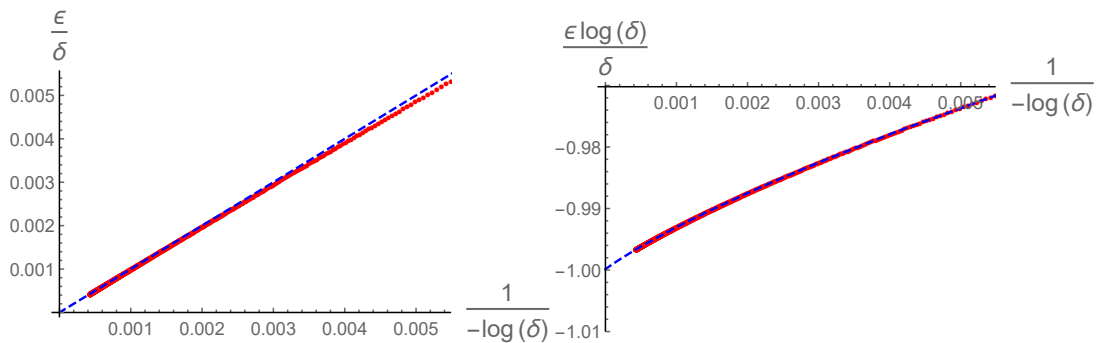


Figure 5: Left: numerically determined ratio $\frac{\epsilon}{\delta}$ as a function of $\frac{1}{-\log(\delta)}$ (red dots) together with the function $\frac{1}{-\log(\delta)}$ (dashed blue line). Right: numerically determined ratio $\frac{\epsilon \log(\delta)}{\delta}$ as a function of $\frac{1}{-\log(\delta)}$ (red dots), and corresponding interpolating function (solid blue). The values below $\frac{1}{-\log(\delta)} = 4.34294 \times 10^{-4}$ in the dashed blue curve have been obtained by an extrapolation. For $\delta = 0$, this extrapolated curve hits -0.99985 , in very good agreement with equation (22).

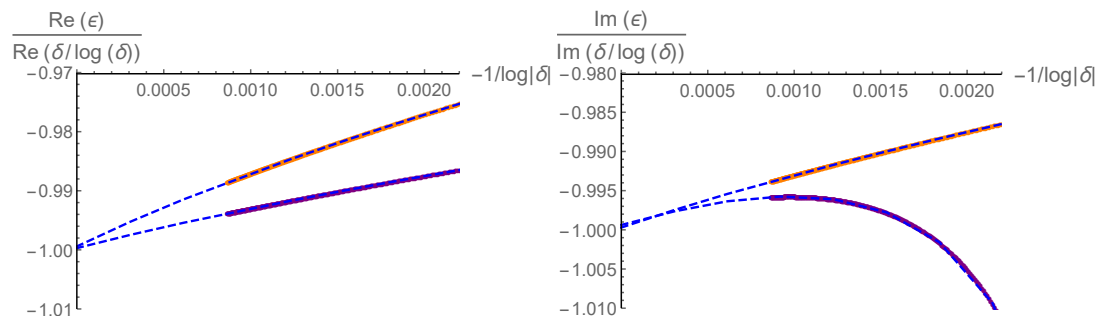


Figure 6: Check that the expression (22) holds when approaching $k = \frac{3}{2}i$ along the rays $k = \frac{3}{2}i + \xi e^{i(\frac{\pi}{2} - \frac{1}{100})}$ (purple) and $k = \frac{3}{2}i + \xi$ (orange), with $\xi \in \mathbb{R}^+$. The dashed blue curves correspond to interpolating functions, whose extrapolation to $\delta = 0$ results in values compatible with -1 . Left: check of the real part of (22). Right: check of the imaginary part.

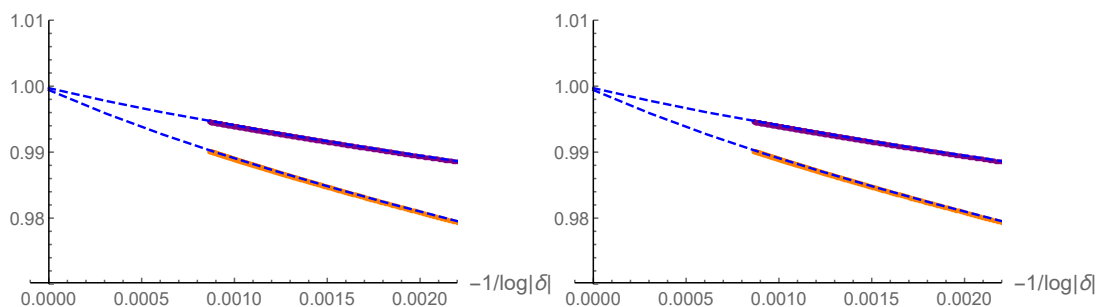


Figure 7: Ratios $\frac{\text{Re}(R_{\perp}^{01,01})}{\text{Re}(3i/41/\log \delta)}$ (orange dots) and $\frac{\text{Im}(R_{\perp}^{01,01})}{\text{Im}(3i/41/\log \delta)}$ (purple dots) when approaching $k = \frac{3}{2}i$ along the ray $k = \frac{3}{2}i + \xi e^{i\theta}$, with $\xi \in \mathbb{R}^+$. The dashed blue lines correspond to interpolating functions that, when extrapolated to $\delta = 0$, are compatible with one. Left: $\theta = \frac{\pi}{2} - \frac{1}{100}$. Right: $\theta = -\frac{\pi}{2} + \frac{1}{100}$.

the picture presented so far to be internally consistent, this residue would need to vanish right at the critical momentum where the collision takes place. As we illustrate in figure 7, this is precisely what happens. We considered the quantity

$$R_{\perp}^{01,01} = \text{Res}_{\omega=\omega_{\perp}(k)} \left(\frac{G_{R,\perp}^{01,01}(\omega, k)}{-(\mathcal{E} + \mathcal{P})} \right), \tag{23}$$

and explored its behavior as a function of k when approaching $k = \frac{3}{2}i$ from different directions. Our observations are compatible with the functional form

$$R_{\perp}^{01,01} \sim \frac{3i}{4} \frac{1}{\log(\delta)}, \tag{24}$$

as $|\delta| \rightarrow 0$. The behavior of ω_{\perp} and $R_{\perp}^{01,01}$ around $k = -\frac{3}{2}i$ also follows (22) and (24) respectively, provided one replaces $k \rightarrow -k$ in the definitions of δ and ϵ .

3 The sound channel

In the sound channel (6), the hydrodynamic mode frequencies $\omega_{\parallel}^{\pm}(k)$ are given by

$$P_{\parallel}(\omega, k) = 2k(k^2 + 3i\omega) + i(k^2 + 3\omega(i + \omega))L = 0, \tag{25}$$

where L is defined as in equation (7). As before, P_{\parallel} has two branch points located at $\omega_{bp}^{\pm}(k)$. The hydrodynamic mode frequencies $\omega_{\parallel}^{\pm}(k)$ behave as

$$\omega_{\parallel}^{\pm}(k) = \pm \frac{k}{\sqrt{3}} - i \frac{2}{15} k^2 + \dots \tag{26}$$

The complete series expansion of $\omega_{p,arallel}^{\pm}$ around $k = 0$ has the form

$$\omega_{\parallel}^{\pm}(k) = \pm \frac{k}{\sqrt{3}} + \sum_{q=2}^{\infty} c_q^{\pm} k^q, \tag{27}$$

with $c_{2q+1}^{-} = -c_{2q+1}^{+}$ and $c_{2q}^{-} = c_{2q}^{+}$, due to the the fact that the hydrodynamic sound modes are symmetric with respect to the imaginary ω -axis for real k , $\omega_{\parallel}^{-}(k) = -\omega_{\parallel}^{+}(k)^*$. In the following, we will focus on the ω_{\parallel}^{-} hydrodynamic mode.

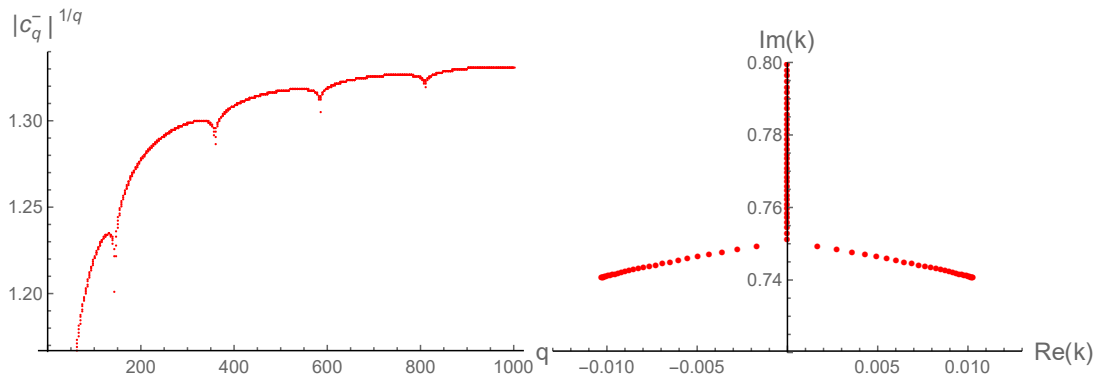


Figure 8: Left: root test applied to the c_q^- coefficients of the series expansion of ω_{\parallel}^- around $k = 0$. The resulting sequence seems to saturate to a finite value as $q \rightarrow \infty$ in a non-monotonic fashion. Left: location in the complex k -plane of the poles of the symmetric Padé approximant (order 500) to the series expansion of ω_{\parallel}^- around $k = 0$ (truncated at order 1000). Three lines of pole condensation are clearly visible.

Plugging (27) into (25), series expanding around $k = 0$ and demanding that the resulting expression vanishes order-by-order allows us to determine the c_q^- coefficients. We have carried out this procedure up to a maximum order $q = q_{max} = 10^3$. The result of applying the root test to the coefficient sequence can be found in figure 8 (left). We observe that $|c_q^-|^{1/q}$ saturates to a finite value in a non-monotonic fashion. In order to find the location of the singularities of $\omega_{\parallel}^-(k)$ in the complex k -plane, we first continue analytically the sum (27) – truncated to order q_{max} – by means of a symmetric Padé approximant of order $\frac{q_{max}}{2}$, and then determine the locations of the poles of the resulting rational function. The three lines of pole condensation which are closest to $k = 0$ are depicted in figure 8 (right). One extends along the positive imaginary axis and emanates from the point

$$k_0 = 0.7513375i. \tag{28}$$

The other two are symmetric with respect to the imaginary axis, and start from the points

$$k_{\pm} = \pm 0.0102799 + 0.7409764i. \tag{29}$$

Since $|k_{\pm}| = 0.7410477 < |k_0|$, the symmetric points k_{\pm} seem to be the ones setting the

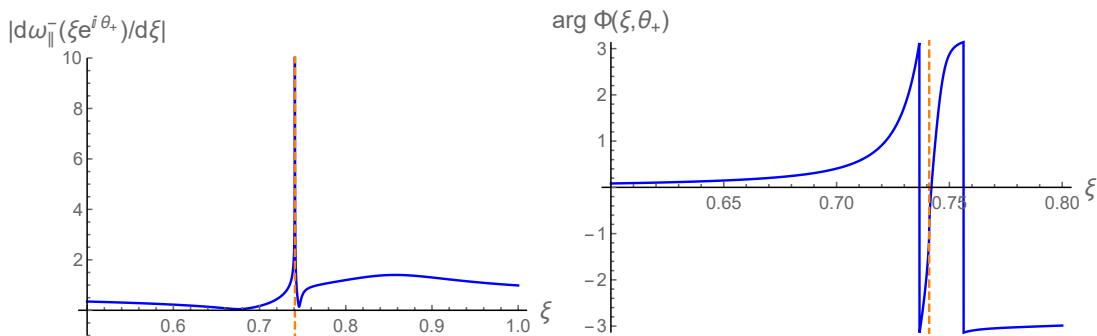


Figure 9: For the hydrodynamic mode frequency ω_{\parallel}^- , computed along the ray $k = \xi e^{i\theta_+}$, norm of the first derivative with respect to ξ (left plot) and argument of L along the corresponding path in the complex k -plane (right plot). The point $\xi = |k_{\pm}|$ has been signalled by the dashed orange vertical line in both plots.

convergence radius of the series expansion of $\omega_{\parallel}^{-}(k)$ around $k = 0$.

In order to understand what these symmetric poles correspond to, we transform the original complex curve equation $P_{\parallel}(\omega_{\parallel}(k), k) = 0$ into an ODE for $\omega_{\parallel}(k)$, just as we described in the previous section for the shear channel. This ODE reads

$$C(\omega_{\parallel}(k), k)\omega'_{\parallel}(k) - D(\omega_{\parallel}(k), k) = 0, \tag{30}$$

$$C(\omega, k) = ik^2 + 6k^3\omega + 3ik\omega^2 - 6k\omega^3, \tag{31}$$

$$D(\omega, k) = k^4 + 5ik^2\omega + 8k^2\omega^2 - 9i\omega^3 - 9\omega^4. \tag{32}$$

Solving this ODE along the ray $k = \xi e^{i\theta_+}$, where $\theta_+ = \arg k_+$ and $\xi \in \mathbb{R}^+$, we find the results displayed in figure 9. In the left plot, we observe that at, $\xi = |k_+|$,

$$\left| \frac{d}{d\xi} \omega_{\parallel}^{-}(\xi e^{i\theta_+}) \right|$$

peaks. Hence, k_+ is close to a point in which $\omega_{\parallel}^{-}(k)$ has a divergent first derivative. In the right plot, we show the phase of the argument of L , $\Phi = \frac{\omega - k + i}{\omega + k + i}$, evaluated along our path. We see that the point $k = k_+$ is reached after $\omega_{\parallel}^{-}(k)$ has crossed the branch cut and entered into the $n = 1$ sheet.⁵

In order to find the critical momentum at which $\omega_{\parallel}^{-}(k)$ diverges, we take advantage of the fact that $\omega'_{\parallel}(k)$ obeys

$$\partial_{\omega} P_{\parallel}(\omega_{\parallel}(k), k)\omega'_{\parallel}(k) + \partial_k P_{\parallel}(\omega_{\parallel}(k), k) = 0, \tag{33}$$

and, as a consequence, points for which

$$P_{\parallel}(\omega, k) = \partial_{\omega} P_{\parallel}(\omega, k) = 0, \quad 0 < |\partial_k P_{\parallel}(\omega, k)| < \infty, \tag{34}$$

have a divergent $\omega_{\parallel}^{\pm}(k)$. A crucial observation is that, since the point we are after lies on the $n = 1$ sheet, we need to first analytically continue $L \rightarrow L_{n=1}$ as described in the previous section. In the end, a numerical computation reveals that the momentum $k_{c,n=1}$ at which conditions (34) hold is given by

$$k_{c,n=1} = 0.0102873 + 0.7409673i. \tag{35}$$

The distance between $k_{c,n=1}$ and k_+ is 1.17×10^{-5} . This confirms that the right point of pole accumulation observed in the Padé approximant is actually associated with a point in which $\omega_{\parallel}^{-}(k)$ diverges. Analogous arguments can be employed to demonstrate that k_- is associated to a divergent $\omega_{\parallel}^{-}(k)$ in the $n = -1$ sheet.

It is natural to wonder whether points in which $\omega_{\parallel}^{-}(k)$ diverges are restricted to the $n = \pm 1$ sheets. The answer is negative: for every nonzero $n \in \mathbb{Z}$, there exists a point $k_{c,n}$ of this kind, which can be found by solving (34) on the n -th sheet. Since, numerically, we find that $k_{c,-|n|} = -k_{c,|n|}^*$, we only discuss the $n > 0$ case in the following. The behavior of $k_{c,n}$ is illustrated in figure 10. We find that $\text{Re}(k_{c,n})$ decreases monotonically with n , approaching zero as $n \rightarrow \infty$. On the other hand, both $\text{Im}(k_{c,n})$ and $|k_{c,n}|$ increase monotonically, tending to $\frac{3}{4}$ in the $n \rightarrow \infty$ limit. Hence, the singularities of $\omega_{\parallel}^{-}(k)$ which are closest to the origin correspond to $k_{c,\pm 1}$: these are the singularities that set the convergence radius of the series expansion of ω_{\parallel}^{-} around $k = 0$.

⁵This observation follows from the fact that $\arg \Phi$ flips from $+\pi$ to $-\pi$.

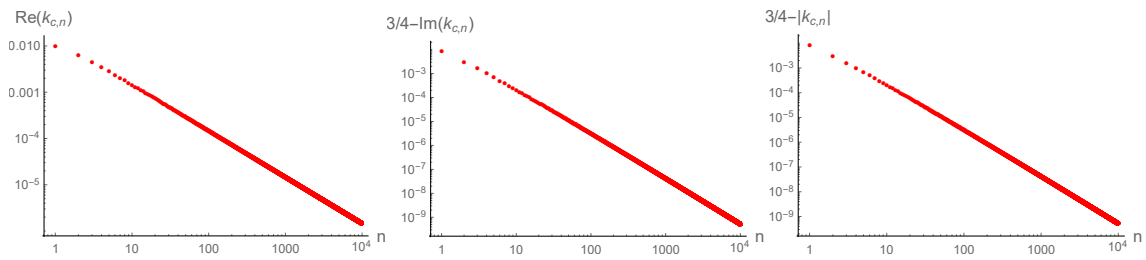


Figure 10: Numerically determined values of the points $k_{c,n}$ (for $n > 0$) where the relations (34) are obeyed in the upper-half of the complex k -plane close to the imaginary axis. At these points, $\omega_{\parallel}^{-}(k)$ diverges. We plot their real part (left plot), their imaginary part (middle plot) and their norm (right plot).

An immediate consequence of the results presented above is that the point $k = \frac{3}{4}i$ acts as an accumulation point of two infinite sequences of branch points, one coming in from the right, associated with positive n , and another coming in from the left, associated with negative n .⁶ Furthermore, the point $k = \frac{3}{4}i$ seems to correspond to the first purely imaginary pole of our original Padé approximant (cf. equation (28)). As we argue in appendix A, despite being associated to the starting point of a line of pole condensation of a Padé approximant, $k = \frac{3}{4}i$ does not correspond to a branch point of ω_{\parallel}^{-} , but rather to an essential singularity.⁷

To conclude this section, we will show that the critical momenta $k_{c,n}$ can be understood as arising from a pole collision. As for the shear channel case, the solutions of the complex curve equation $P_{\parallel} = 0$ on the non-principal sheets play a prominent role in our analysis. In the case at hand, the solutions of interest are the non-principal gapless poles,⁸ whose series expansion around $k = 0$ is given by

$$\omega_{\parallel}^{(H,n)}(k) = \frac{i}{3}k^2 - \frac{i}{9}k^4 - \frac{i}{9\pi n}k^5 + \frac{2i}{27}k^6 + \frac{4i}{27n\pi}k^7 + \dots \tag{36}$$

Our main claim is that the critical momenta $k_{c,n}$ correspond to branch point singularities at which the hydrodynamic ω_{\parallel}^{-} mode collides with $\omega_{\parallel}^{(H,n)}$ on the n -th sheet of P_{\parallel} .

In order to illustrate this statement, let us consider the behavior of $\omega_{\parallel}^{(H,1)}$ and ω_{\parallel}^{-} in the complex ω -plane as we vary k along the ray $k = |k|e^{i\theta}$. In figure 11 we plot the trajectories of ω_{\parallel}^{-} (solid) and $\omega_{\parallel}^{(H,1)}$ (dashed) for $\theta - \arg k_{c,1} = -10^{-2}$ (brown), -10^{-3} (red), -10^{-4} (blue) and -10^{-5} (purple). As $\theta - \arg k_{c,1} \rightarrow 0$, both ω_{\parallel}^{-} and $\omega_{\parallel}^{(H,1)}$ approach the point

$$\omega_{\parallel}^{-}(k_{c,1}) = 0.0142827 - 0.2563247i, \tag{37}$$

more closely. This point, which has been determined independently by solving the conditions (34) for $n = 1$, corresponds to the green star in the figure. The behavior we observe is precisely the one to expect if there is indeed a mode collision at $\omega = \omega_{\parallel}^{-}(k_{c,1})$.

Regarding the $\omega_{\parallel}^{+}(k)$ hydrodynamic mode, an analysis analogous to the one presented so far shows that the complex singularities closest to the origin correspond to two branch points located at $k = k_{c,\pm 1}^*$, which can again be interpreted as collisions between $\omega_{\parallel}^{+}(k)$ and $\omega_{\parallel}^{(H,\pm 1)}$ on non-principal sheets.

⁶A direct numerical analysis shows that $\arg(\frac{3}{4}i - k_{c,n}) \rightarrow \pi$ as $n \rightarrow \infty$, i.e., the curves along which the branch points condense are parallel to the real k -axis in the $n \rightarrow \infty$ limit

⁷Some authors require an essential singularity to be isolated, but we do not.

⁸There are also non-principal gapped poles, with series expansion $\omega_{\parallel}^{(NH,n)} = -i + \alpha k + \frac{1}{3}i(\alpha^2 - 1)k^2 + \dots$, where α obeys a transcendental equation. For $n = 0$, this equation has no solutions; for $n \neq 0$, we find purely imaginary solutions – with positive imaginary part for $n > 0$ – that the change $n \rightarrow -n$ conjugates.

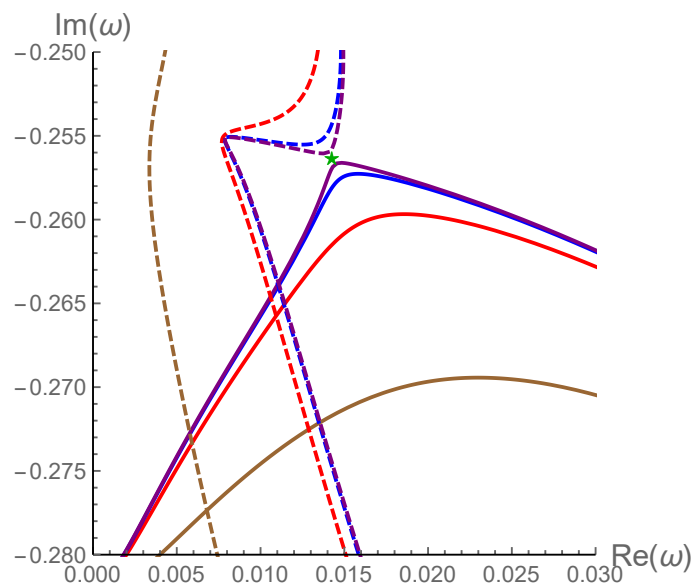


Figure 11: Trajectories followed by ω_{\parallel}^- (solid curves) and $\omega^{(H,n=1)}$ (dashed curves) in the complex ω -plane, as k varies along the ray $k = |k|e^{i\theta}$ for $\theta - \arg k_{c,1} = -10^{-2}$ (brown), -10^{-3} (red), -10^{-4} (blue) and -10^{-5} (purple). As $\theta - \arg k_{c,1}$ decreases, the corresponding trajectories become closer to each other, until colliding at the point $\omega = 0.0142827 - 0.2563247i$ (green star). This point has been determined independently by solving equations (34) for $n = 1$.

Taking stock, the main conclusion of the analysis presented in this section is that the convergence radius of the series expansion of $\omega_{\parallel}^{\pm}(k)$ around $k = 0$ is given by

$$|k_{\parallel}^*| = |k_{c,1}| = 0.7410387, \tag{38}$$

and set by mode collisions between $\omega_{\parallel}^{\pm}(k)$ and $\omega_{\parallel}^{(H,\pm 1)}$ on non-principal sheets.

4 A prescription for finding the radius of convergence

In the preceding sections our analysis of RTA kinetic theory has revealed novel obstructions to the convergence of the hydrodynamic series. In light of this, it is worth revisiting the basics surrounding convergence of the function $\omega(k)$ expanded as a series in small k . The radius of convergence of $\omega(k)$ expanded around any value of k (which we will mostly take to be $k = 0$, relevant to the hydrodynamic expansion) is determined by the closest singularity of $\omega(k)$ to that point in the complex k -plane.⁹ Often, $\omega(k)$ is implicitly defined by a complex curve given by

$$P(\omega, k) = 0, \tag{39}$$

which may correspond to the determinant of a fluctuation mode matrix or, with care, the inverse of an appropriate Green’s function or simply its denominator. These elementary observations have previously been used to determine the radius of convergence of the hydrodynamic gradient expansion for holographic theories [8–10, 13, 14, 16] as well as MIS theory [12]. In

⁹If $\omega(k)$ is defined on a multi-sheeted Riemann surface, one must also ensure the singularity is on the correct sheet of ω .

the preceding sections of this paper we have employed this procedure to compute this radius of convergence for RTA kinetic theory.

A natural question is given $P(\omega, k)$, is there a shortcut to determining the singularities of $\omega(k)$? In this section we examine this question in the light of the Implicit Function Theorem. In doing so, we arrive at a prescription for a set of points that includes all singularities of $\omega(k)$. For previous related work on a similar question we direct the reader to [9, 10], although we note our prescription differs in some key mathematical aspects.

Let us first recall the Implicit Function Theorem (taken from [36])

Implicit Function Theorem. Let $P(\omega, k)$ be analytic in ω, k near $\omega = k = 0$. Assuming $P(0, 0) = 0$ and $\partial_\omega P(0, 0) \neq 0$ then there exists a unique function $\omega(k)$ analytic in some neighbourhood $|k| < k_*$ of $k = 0$ such that $\omega(0) = 0$ and $P(\omega(k), k) = 0$.

Conversely, the following set of points $\omega, k \in \mathbb{C}$,

$$\{(\omega, k) | P = \partial_\omega P = 0\} \cup \{(\omega, k) | P = 0 \wedge (P \text{ is not analytic})\}, \tag{40}$$

includes the locations of all singularities of $\omega(k)$, since these are the only possible points of $P = 0$ where the function $\omega(k)$ may itself fail to be analytic by the Implicit Function Theorem.¹⁰ Crucially however, note that the set (40) can include points where there are no singularities of $\omega(k)$. Thus, given the set (40), to determine the radius of convergence each point should be further examined in order to find out which, if any, is the closest singularity to the point around which one is expanding (which is $\omega = k = 0$ for the hydrodynamic expansion).

In the remainder of this section we illustrate these observations with a set of examples, beginning with the relatively simple case where P is a polynomial in section 4.1, before discussing our main results on RTA kinetic theory and how they fit into this picture, for which P is not a polynomial, in section 4.2.

4.1 Polynomial P

Here we collect some known results from [36]. Suppose P can be written as a polynomial in ω and k as follows

$$P(\omega, k) = \sum_{i=0}^N c_i(k) \omega^i. \tag{41}$$

In this case $\omega(k)$ is said to be an algebraic function. The candidate singularities (40) thus either correspond to those points where $P = \partial_\omega P = 0$, in which case multiple branches degenerate, or where P is non-analytic. Since P is polynomial, if k is finite, this latter case only happens when $\omega = \infty$. This occurs only when the coefficient of the highest order term in ω vanishes, $c_N(k) = 0$. In this case, the number of roots of the resulting polynomial in ω is reduced.

We can also illustrate a case where a point in the set (40) does not correspond to a singularity of $\omega(k)$. This occurs whenever two branches of $\omega(k)$ happen to take on the same value at some $k \in \mathbb{C}$, with each branch remaining analytic around this point. The canonical example is the Lemniscate of Bernoulli [37] where, at the origin of the ‘figure-of-eight’-shaped curve obeying $P = \partial_\omega P = 0$, two branches cross but remain analytic there.¹¹

The type of singularities that algebraic functions can have is constrained by the Newton-Puiseux theorem. If P has r degenerate roots at a point, the theorem says that this singularity is a branch point of order r . Furthermore, around this point, $\omega(k)$ can be expanded as a

¹⁰In [9, 10] P was labelled a ‘spectral curve’ and focus placed on points for which $P = \partial_\omega P = 0$, labelled ‘critical points’.

¹¹A similar phenomenon occurs in holography, where branches of the scalar quasinormal mode spectrum for the BTZ black hole [38, 39], $\omega_n(k)$, cross at finite $k \in \mathbb{C}$, but with no corresponding singularity of $\omega_n(k)$.

convergent series in powers of $k^{1/r}$.¹² In the next section we show that this is no longer the case for non-polynomial P .

4.2 Non-polynomial P and case studies

We now turn to the instances where $P(\omega, k)$ is not a polynomial. This may be the case when it arises as an all-orders gradient expansion, or includes functions like the logarithm as in RTA kinetic theory above. Then P can fail to be analytic in more ways than a polynomial is allowed to. For example, there can be points where P does not converge (as it happens in the case of the gradient expansion), or where some of its pieces are non-analytic. Again, we stress that these conditions do not imply that there is necessarily a singularity there, only that they are permitted.

4.2.1 Single mode

To examine this case in the simplest way possible, consider a theory with a single mode,

$$P(\omega, k) = \omega - \omega_1(k). \tag{42}$$

We give a physical example below. Regarding the set (40), there are no points for (42) where $\partial_\omega P = 0$. However, the set of potential singularities (40) need not be empty, since $\omega_1(k)$ itself can contain singularities. These are then inherited by $\omega(k)$.

This scenario occurs in the following physical example: relativistic hydrodynamics, defined perturbatively in gradients. Without loss of generality, the gradient-expanded constitutive relations can be put in the Landau frame, and when evaluated on the hydrodynamic fluctuations can be reorganized using the equations of motion such that they contain no time derivatives [12, 40]. The equations of motion for a shear channel fluctuation therefore contain one and only one time derivative, which acts on the ideal part of the current. The resulting $P(\omega, k)$ is necessarily of the form (42) with $\omega_1(k)$ expressed as an infinite series in k . As an illustrative concrete example, the hydrodynamic limit of MIS theory in the shear channel has a P of the form (42) where [12],

$$\omega_1(k) = -i \sum_{n=0}^{\infty} C_n D^{n+1} \tau^n k^{2n+2}, \tag{43}$$

where C_n are the Catalan numbers, and D, τ are respectively the diffusion constant and relaxation time. Note that the series (43) has a finite radius of convergence, and correspondingly summing (43) gives the exact expression for $\omega_1(k)$ which contains a branch point singularity.

4.2.2 RTA kinetic theory: shear channel

The case studied in this paper, RTA kinetic theory, offers several new interesting elements. These arise from the multi-sheeted structure of the logarithmic function which enters into P . We find that the singularities of $\omega(k)$ can be much richer and moreover can no longer be described by Puiseux series.

The singularity of $\omega_\perp(k)$ which is closest to the origin and that sets the radius of convergence occurs when the hydrodynamic pole collides with the logarithmic branch point. In fact, an infinite number of gapped poles located on the other non-principal sheets also collide with the branch point. Referring to the set of points (40), this point does not satisfy the condition $\partial_\omega P = 0$, rather, it is a point where P is non-analytic. This occurs at finite ω and k , which is impossible in the polynomial case.

¹²If the singularity is located at $\omega = \infty$, this holds for ω^{-1} instead.

One may think of this singularity as an infinite-dimensional generalization of what happens when the highest order term vanishes for a polynomial. Indeed, at this point, the coefficient of the logarithm in P vanishes, reducing the number of branches from an infinite number to a finite number. On the other hand, around this point there are an infinite number of branches in $\omega_{\perp}(k)$; if one expresses $\omega_{\perp}(k)$ as a series around this point, it does not take the form of a Puiseux series, since a Puiseux series can only describe a finite number of branches. Instead of fractional powers, the numerical evidence at our disposal indicates that the series includes logarithms (see equation (22)).

4.2.3 RTA kinetic theory: sound channel

In the sound channel, the multivaluedness of the logarithm also plays an interesting role. Surprisingly, each sheet of the analytically continued Green's function contains an additional gapless pole.

It is unclear whether these additional poles have any significant role to play in terms of physical excitations of the system; nevertheless, their mathematical role in our current analysis is clear. They give rise to singularities in $\omega_{\parallel}(k)$ at the values of k where they collide with the physical hydrodynamic pole. This happens for each of the non-principal poles at a sequence of k accumulating at an essential singularity of $\omega_{\parallel}(k)$. The radius of convergence of $\omega_{\parallel}(k)$ around $k = 0$ is given by singularities coming from the collision with $\omega_{\parallel}^{(H,n=\pm 1)}$. At this point, the analytic continuation of P has a degeneracy as diagnosed by the $P = \partial_{\omega}P = 0$ condition in (40).

The essential singularity at the accumulation point in $\omega_{\parallel}(k)$ is a new feature not possible for algebraic curves. Around this point, a Puiseux series does not capture the behaviour of $\omega_{\parallel}(k)$. In appendix A, we show that the expansion includes exponentially small contributions, taking the form of a transseries.

5 Summary

The physics of nonequilibrium systems has benefited enormously from studies of model systems in which the approach to equilibrium and the emergence of hydrodynamic behaviour could be investigated. Until the advent of holography, the most prominent approach was to use kinetic theory, whose applicability rests upon the notion of well-defined particles (or quasi-particles) and the weak-coupling regime. In contrast, the AdS/CFT correspondence is used at infinitely strong coupling.

Microscopic models formulated in the language of holography or kinetic theory both lead to hydrodynamic behaviour close to equilibrium in a sense which can be made precise at the linearized level: the system has modes whose frequencies vanish at long wavelength. There is however a significant qualitative difference in the remaining features of the analytic structure of retarded correlators. While the singularities of strongly coupled theories as well as MIS-type models take the form of isolated poles, the retarded Green's function of kinetic theory in the relaxation time approximation has both poles and branch points. This implies that the natural object to deal with is the analytically continued Green's function, which can be viewed as defined on a multi-sheeted Riemann surface.

The analytically continued Green's function in RTA kinetic theory has an infinite number of poles. In the shear channel, there is a single hydrodynamic pole on the physical sheet, and an infinite number of nonhydrodynamic poles on the non-principal ones. The radius of convergence of the hydrodynamic series is set by a collision of the hydrodynamic pole and a branch point. In the sound channel, the radius of convergence of the hydrodynamic series is

set by the collision of the hydrodynamic pole with a gapless pole on a non-principal sheet. Note that in order to understand the emergence of the finite radius of convergence in terms of singularity collisions, it is essential to continue beyond the principal branch of the logarithm appearing in the original Green's function.

It is worth pointing out that the structure of gapped poles in kinetic theory found here is consistent with studies of boost-invariant flow in RTA kinetic theory. Calculations of the late proper time expansion in $\mathcal{N} = 4$ SYM reveal that its large-order behaviour contains detailed information about the rich nonhydrodynamic spectrum of this theory, which is completely consistent with what is known from linear response [41, 42]. Analogous calculations in MIS-type models [43, 44] show a similar consistency. Calculations of the late proper time expansion in RTA kinetic theory [45] point to the conclusion that the nonhydrodynamic sector consists of an infinite number of nonhydrodynamic modes whose frequencies coincide at vanishing momentum [46]. The analysis of analytically continued retarded correlation functions described here reveals such a set of gapped poles. Whether these objects can be mapped to each other remains an open problem.

More generally, our analysis has not addressed the question of whether the poles of the analytically continued Green's function in the non-principal sheets are endowed with any physical significance. While we don't have an answer to this question, we would like to point out that similar situations are not unprecedented. For instance, in the context of hadronic scattering, resonances appear as poles of the scattering amplitude in non-principal sheets [47]. Perhaps closer to the present context, poles in non-principal sheets are also relevant for the phenomenon of Landau damping in scalar quantum electrodynamics [48].

Whenever the dispersion relations are defined by a complex curve $P(\omega, k) = 0$, the Implicit Function Theorem implies that singularities are allowed (but not necessary) only at points where either P is non-analytic or $\partial_\omega P = 0$. Both conditions must be taken into account. When P is polynomial, the latter condition plays an important role since it can indicate a branch point singularity (but not always), and the former condition can indicate poles. In RTA kinetic theory, we have found that the former condition plays a significant role. In theories where P is a polynomial, the behavior can be described by a Puiseux series with a non-zero radius of convergence. In theories where P is not a polynomial, such as RTA kinetic theory, the singularity can be of other types and it is not known if the series expansion around these singularities is convergent or not. In holography, while the singularities of $\omega(k)$ which set the radius of convergence are known to be square-root type branch points in the examples studied to date,¹³ the analytic structure of $P(\omega, k)$ in general remains an open question.

Acknowledgements

We would like to thank R. A. Davison, B. Goutéraux and C. Pantelidou for valuable discussions. We would also like to thank the organisers and participants of the online seminar series HoloTube [49] for their hospitality. The Gravity, Quantum Fields and Information group at the Max Planck Institute for Gravitational Physics (Albert Einstein Institute) is supported by the Alexander von Humboldt Foundation and the Federal Ministry for Education and Research through the Sofja Kovalevskaja Award. AS and MS are supported by the Polish National Science Centre grant 2018/29/B/ST2/02457. BW is supported by a Royal Society University Research Fellowship.

¹³Potentially quartic roots are seen in special cases [14].

A The points $k = \pm \frac{3}{4}i$ in the sound channel

In this appendix we address the behavior of $\omega_{\parallel}^{\pm}(k)$ along the imaginary k -axis. The analysis presented here reveals the existence of essential singularities in the sound channel dispersion relations, although we would like to emphasize that these essential singularities occur outside the radius of convergence of the small- k expansion of $\omega_{\parallel}^{\pm}(k)$.

We study $\omega_{\parallel}^{-}(k)$ first, and start by solving the equation of motion (30) around $k = \frac{3}{4}i$ in a series expansion, i.e., we define $k = i(\frac{3}{4} - \delta)$, $\delta \in \mathbb{R}$, $\delta > 0$ and consider the ansatz

$$\omega_{\parallel}^{-}(k) = iw_0 + i \sum_{q=1}^{\infty} w_q \delta^q. \tag{44}$$

At zeroth order, this results in four roots –with one degenerate root–, $w_0 = -\frac{1}{4}, \frac{1}{4}$ and $\frac{3}{4}$, of which the first one is singled out by a direct comparison with the numerical solution. The remaining expansion coefficients can be determined recursively, with the result that $w_1 = -1$ and the rest vanish: the behavior of $\omega_{\parallel}^{-}(k)$ as $k \rightarrow \frac{3}{4}i$ from below along the imaginary axis cannot be reproduced by a power series ansatz. To see this, let us linearize around the power series solution we just found. We consider

$$\omega_{\parallel}^{-}(k) = -\frac{1}{4}i - i\delta + \sum_{q=1}^{\infty} \chi_q(\delta) \eta^q, \tag{45}$$

where η is a fictitious parameter, and solve (30) recursively in a $\eta \rightarrow 0$ expansion. In the end, we find that

$$\chi_1(\delta) = \alpha e^{-\frac{3}{32\delta}} e^{\frac{\delta}{2}} (3 - 4\delta), \tag{46}$$

$$\chi_2(\delta) = i\alpha^2 e^{-\frac{3}{16\delta}} e^{\delta} (3 - 4\delta) \frac{9 - 108\delta - 656\delta^2 + 192\delta^3}{64\delta^2}, \tag{47}$$

etc., with the overall conclusion that $\chi_q(\delta) = O(e^{-\frac{3}{32\delta}q})$. Hence, there is an essential singularity at $\delta = 0$. Said otherwise, the distance between $\omega_{\parallel}^{-}(k)$ and the branch point at $\omega_{bp}^{+}(k) = k - i = -i\frac{1}{4} - i\delta$ is nonperturbatively small in δ as $\delta \rightarrow 0$. In the light of these results, we can set $\eta = 1$ in (45) and view the result as a transseries expansion in δ .

The only point that this analysis cannot address is the value of the coefficient α . To fix it, we need to plug the transseries expansion (45) back into $P_{\parallel}(\omega, k)$, expand around $\delta = 0$, and demand that we have a solution. The end result of this procedure is that

$$\alpha = \frac{i}{2} e^{-\frac{9}{4}}. \tag{48}$$

As a final consistency check, we compare our transseries expansion truncated to order $q = q_{max}$ with the ω_{\parallel}^{-} we have determined numerically. It is convenient to plot the ratio

$$r_{q_{max}}^{-} = \frac{\omega_{\parallel}^{-}(k) - \omega_{bp}^{+}(k)}{\sum_{q=1}^{q_{max}} \chi_q(\delta = \frac{3}{4} + ik)}. \tag{49}$$

Examples for $q_{max} = 1, 4$ and 8 can be found in figure 12 (right). We see that $r_{q_{max}}^{-} \rightarrow 1$ as $k \rightarrow \frac{3}{4}i$; furthermore, as q_{max} increases, the agreement away from $k = \frac{3}{4}i$ improves significantly. This confirms that our analysis is correct. The distance between ω_{\parallel}^{-} and the branch point ω_{bp}^{+} can be found in the left plot of figure 12.

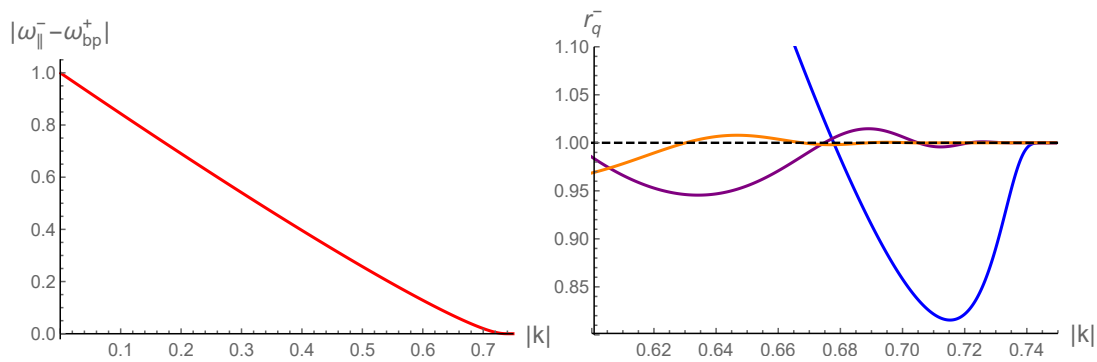


Figure 12: Left: distance between the hydrodynamic mode frequency ω_{\parallel}^- and the branch point ω_{bp}^+ , as k goes from 0 to $\frac{3}{4}i$ along the imaginary axis. This distance decreases monotonically and vanishes as $k \rightarrow \frac{3}{4}i$. Right: comparison between the distance $|\omega_{\parallel}^- - \omega_{bp}^+|$ and the analytic prediction (45) for $k \rightarrow \frac{3}{4}i$ along the imaginary k -axis from below, as quantified by the ratio r_q^- defined in equation (49). We have considered $q = 1$ (blue), $q = 4$ (purple) and $q = 8$ (orange). As q increases, the agreement gets progressively better, as seen by the progressively closer approach of the different curves to the value $r_q^- = 1$ (dashed black line).

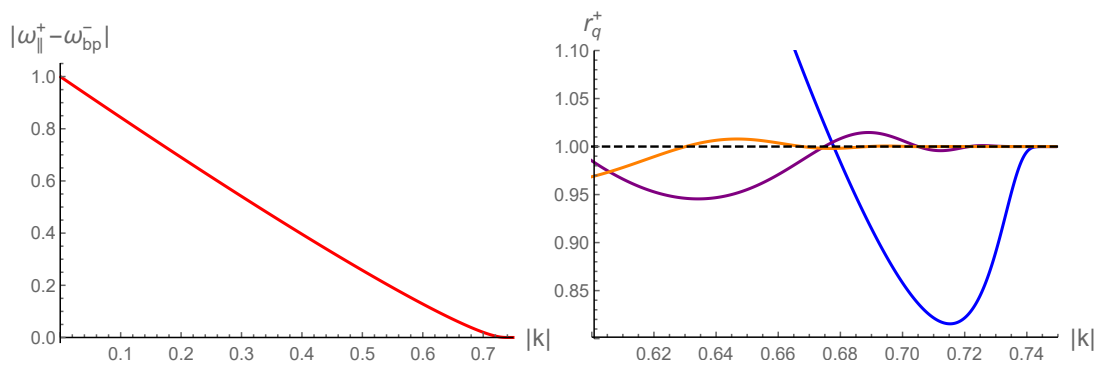


Figure 13: Same as figure 12, but now for the hydrodynamic mode frequency ω_{\parallel}^+ and the branch point ω_{bp}^- . The relevant modifications that need to be performed to obtain this figure are described in the text.

An analysis analogous to the one presented above can be carried out for ω_{\parallel}^+ . In this case, we find that this mode collides with the ω_{bp}^- branch point at $k = -\frac{3}{4}i$. Defining δ by the relation $k = -\frac{3}{4}i + \delta i$, ω_{\parallel}^+ can also be represented as a transseries in δ as $\delta \rightarrow 0$,

$$\omega_{\parallel}^+ = -\frac{i}{4} - i\delta + \sum_{q=1}^{\infty} \chi_q(\delta), \tag{50}$$

with $\chi_q(\delta)$ given by the same expressions as above. We check the relation (50) –truncated at orders $q_{max} = 1, 4$ and 8 – in figure 13 (right), where we plot the ratio

$$r_{q_{max}}^+ = \frac{\omega_{\parallel}^+(k) - \omega_{bp}^-(k)}{\sum_{q=1}^{q_{max}} \chi_q\left(\delta = \frac{3}{4} - ik\right)}. \tag{51}$$

To summarize, in this appendix we have demonstrated that:

- $\omega_{\parallel}^{\pm}(k)$ present essential singularities at $k = \mp \frac{3}{4}i$.
- These essential singularities appear when the ω_{\parallel}^{\pm} pole collides with the ω_{bp}^{\mp} logarithmic branch point.

As discussed in the main body of the text, this phenomenon has no counterpart for algebraic functions.

References

- [1] W. Busza, K. Rajagopal and W. van der Schee, *Heavy ion collisions: The big picture and the big questions*, Annu. Rev. Nucl. Part. Sci. **68**, 339 (2018), doi:[10.1146/annurev-nucl-101917-020852](https://doi.org/10.1146/annurev-nucl-101917-020852).
- [2] C. Shen and L. Yan, *Recent development of hydrodynamic modeling in heavy-ion collisions*, Nucl. Sci. Tech. **31**, 122 (2020), doi:[10.1007/s41365-020-00829-z](https://doi.org/10.1007/s41365-020-00829-z).
- [3] J. Casalderrey-Solana, H. Liu, D. Mateos, K. Rajagopal and U. A. Wiedemann, *Gauge/string duality, hot QCD and heavy ion collisions*, (2011), [arXiv:1101.0618](https://arxiv.org/abs/1101.0618).
- [4] W. Florkowski, M. P. Heller and M. Spaliński, *New theories of relativistic hydrodynamics in the LHC era*, Rep. Prog. Phys. **81**, 046001 (2018), doi:[10.1088/1361-6633/aaa091](https://doi.org/10.1088/1361-6633/aaa091).
- [5] J. D. Bjorken, *Highly relativistic nucleus-nucleus collisions: The central rapidity region*, Phys. Rev. D **27**, 140 (1983), doi:[10.1103/PhysRevD.27.140](https://doi.org/10.1103/PhysRevD.27.140).
- [6] P. K. Kovtun and A. O. Starinets, *Quasinormal modes and holography*, Phys. Rev. D **72**, 086009 (2005), doi:[10.1103/PhysRevD.72.086009](https://doi.org/10.1103/PhysRevD.72.086009).
- [7] E. Berti, V. Cardoso and A. O. Starinets, *Quasinormal modes of black holes and black branes*, Class. Quantum Grav. **26**, 163001 (2009), doi:[10.1088/0264-9381/26/16/163001](https://doi.org/10.1088/0264-9381/26/16/163001).
- [8] B. Withers, *Short-lived modes from hydrodynamic dispersion relations*, J. High Energ. Phys. **06**, 059 (2018), doi:[10.1007/JHEP06\(2018\)059](https://doi.org/10.1007/JHEP06(2018)059).
- [9] S. Grozdanov, P. K. Kovtun, A. O. Starinets and P. Tadić, *Convergence of the gradient expansion in hydrodynamics*, Phys. Rev. Lett. **122**, 251601 (2019), doi:[10.1103/PhysRevLett.122.251601](https://doi.org/10.1103/PhysRevLett.122.251601).
- [10] S. Grozdanov, P. K. Kovtun, A. O. Starinets and P. Tadić, *The complex life of hydrodynamic modes*, J. High Energ. Phys. **11**, 097 (2019), doi:[10.1007/JHEP11\(2019\)097](https://doi.org/10.1007/JHEP11(2019)097).
- [11] A. Amoretti, D. Areán, B. Goutéraux and D. Musso, *Gapless and gapped holographic phonons*, J. High Energ. Phys. **01**, 058 (2020), doi:[10.1007/JHEP01\(2020\)058](https://doi.org/10.1007/JHEP01(2020)058).
- [12] M. P. Heller, A. Serantes, M. Spaliński, V. Svensson and B. Withers, *The hydrodynamic gradient expansion in linear response theory*, (2020), [arXiv:2007.05524](https://arxiv.org/abs/2007.05524).
- [13] N. Abbasi and S. Tahery, *Complexified quasinormal modes and the pole-skipping in a holographic system at finite chemical potential*, J. High Energ. Phys. **10**, 076 (2020), doi:[10.1007/JHEP10\(2020\)076](https://doi.org/10.1007/JHEP10(2020)076).
- [14] A. Jansen and C. Pantelidou, *Quasinormal modes in charged fluids at complex momentum*, J. High Energ. Phys. **10**, 121 (2020), doi:[10.1007/JHEP10\(2020\)121](https://doi.org/10.1007/JHEP10(2020)121).

- [15] M. Baggioli, *How small hydrodynamics can go*, Phys. Rev. D **103**, 086001 (2021), doi:[10.1103/PhysRevD.103.086001](https://doi.org/10.1103/PhysRevD.103.086001).
- [16] D. Arean, R. A. Davison, B. Goutéraux and K. Suzuki, *Hydrodynamic diffusion and its breakdown near AdS_2 fixed points*, (2020), [arXiv:2011.12301](https://arxiv.org/abs/2011.12301).
- [17] P. Arnold and L. G. Yaffe, *Effective theories for real-time correlations in hot plasmas*, Phys. Rev. D **57**, 1178 (1998), doi:[10.1103/PhysRevD.57.1178](https://doi.org/10.1103/PhysRevD.57.1178).
- [18] J. Berges, M. P. Heller, A. Mazeliauskas and R. Venugopalan, *Thermalization in QCD: theoretical approaches, phenomenological applications, and interdisciplinary connections*, (2020), [arXiv:2005.12299](https://arxiv.org/abs/2005.12299).
- [19] P. Arnold, G. David Moore and L. G. Yaffe, *Transport coefficients in high temperature gauge theories. 1. Leading log results*, J. High Energ. Phys. **11**, 001 (2000), doi:[10.1088/1126-6708/2000/11/001](https://doi.org/10.1088/1126-6708/2000/11/001).
- [20] P. B. Arnold, G. D. Moore and L. G. Yaffe, *Effective kinetic theory for high temperature gauge theories*, J. High Energ. Phys. **01**, 030 (2003), doi:[10.1088/1126-6708/2003/01/030](https://doi.org/10.1088/1126-6708/2003/01/030).
- [21] P. Arnold, G. D. Moore and L. G. Yaffe, *Transport coefficients in high temperature gauge theories, 2. Beyond leading log*, J. High Energ. Phys. **05**, 051 (2003), doi:[10.1088/1126-6708/2003/05/051](https://doi.org/10.1088/1126-6708/2003/05/051).
- [22] A. Kurkela and Y. Zhu, *Isotropization and hydrodynamization in weakly coupled heavy-ion collisions*, Phys. Rev. Lett. **115**, 182301 (2015), doi:[10.1103/PhysRevLett.115.182301](https://doi.org/10.1103/PhysRevLett.115.182301).
- [23] L. Keegan, A. Kurkela, A. Mazeliauskas and D. Teaney, *Initial conditions for hydrodynamics from weakly coupled pre-equilibrium evolution*, J. High Energ. Phys. **08**, 171 (2016), doi:[10.1007/JHEP08\(2016\)171](https://doi.org/10.1007/JHEP08(2016)171).
- [24] A. Mazeliauskas and J. Berges, *Prescaling and far-from-equilibrium hydrodynamics in the quark-gluon plasma*, Phys. Rev. Lett. **122**, 122301 (2019), doi:[10.1103/PhysRevLett.122.122301](https://doi.org/10.1103/PhysRevLett.122.122301).
- [25] A. Kurkela, A. Mazeliauskas, J.-F. Paquet, S. Schlichting and D. Teaney, *Effective kinetic description of event-by-event pre-equilibrium dynamics in high-energy heavy-ion collisions*, Phys. Rev. C **99**, 034910 (2019), doi:[10.1103/PhysRevC.99.034910](https://doi.org/10.1103/PhysRevC.99.034910).
- [26] A. Kurkela, A. Mazeliauskas, J.-F. Paquet, S. Schlichting and D. Teaney, *Matching the nonequilibrium initial stage of heavy ion collisions to hydrodynamics with QCD kinetic theory*, Phys. Rev. Lett. **122**, 122302 (2019), doi:[10.1103/PhysRevLett.122.122302](https://doi.org/10.1103/PhysRevLett.122.122302).
- [27] A. Kurkela and A. Mazeliauskas, *Chemical equilibration in weakly coupled QCD*, Phys. Rev. D **99**, 054018 (2019), doi:[10.1103/PhysRevD.99.054018](https://doi.org/10.1103/PhysRevD.99.054018).
- [28] A. Kurkela and A. Mazeliauskas, *Chemical equilibration in hadronic collisions*, Phys. Rev. Lett. **122**, 142301 (2019), doi:[10.1103/PhysRevLett.122.142301](https://doi.org/10.1103/PhysRevLett.122.142301).
- [29] D. Almaalol, A. Kurkela and M. Strickland, *Nonequilibrium attractor in high-temperature QCD plasmas*, Phys. Rev. Lett. **125**, 122302 (2020), doi:[10.1103/PhysRevLett.125.122302](https://doi.org/10.1103/PhysRevLett.125.122302).
- [30] X. Du and S. Schlichting, *Equilibration of the Quark-Gluon Plasma at finite net-baryon density in QCD kinetic theory*, (2020), [arXiv:2012.09068](https://arxiv.org/abs/2012.09068).

- [31] X. Du and S. Schlichting, *Equilibration of weakly coupled QCD plasmas*, (2020), [arXiv:2012.09079](https://arxiv.org/abs/2012.09079).
- [32] G. D. Moore, *Stress-stress correlator in ϕ^4 theory: poles or a cut?*, J. High Energ. Phys. **05**, 084 (2018), doi:[10.1007/JHEP05\(2018\)084](https://doi.org/10.1007/JHEP05(2018)084).
- [33] J. L. Anderson and H. R. Witting, *A relativistic relaxation-time model for the Boltzmann equation*, Physica **74**, 466 (1974), doi:[10.1016/0031-8914\(74\)90355-3](https://doi.org/10.1016/0031-8914(74)90355-3).
- [34] P. Romatschke, *Retarded correlators in kinetic theory: branch cuts, poles and hydrodynamic onset transitions*, Eur. Phys. J. C **76**, 352 (2016), doi:[10.1140/epjc/s10052-016-4169-7](https://doi.org/10.1140/epjc/s10052-016-4169-7).
- [35] A. Kurkela and U. Achim Wiedemann, *Analytic structure of nonhydrodynamic modes in kinetic theory*, Eur. Phys. J. C **79**, 776 (2019), doi:[10.1140/epjc/s10052-019-7271-9](https://doi.org/10.1140/epjc/s10052-019-7271-9).
- [36] P. Flajolet and R. Sedgewick, *Analytic Combinatorics*, Cambridge University Press, Cambridge, ISBN 9780511801655 (2009), doi:[10.1017/CBO9780511801655](https://doi.org/10.1017/CBO9780511801655).
- [37] J. Bernoulli, *Solutio constructio curvæ accessus & recessu æquabilis, ope rectificationionis curvæ cujusdam algebraicæ: Addenda nuperæ solutioni mensis junii*, Acta Eruditorum, 336 (1694).
- [38] D. Birmingham, I. Sachs and S. N. Solodukhin, *Conformal field theory interpretation of black hole quasinormal modes*, Phys. Rev. Lett. **88**, 151301 (2002), doi:[10.1103/PhysRevLett.88.151301](https://doi.org/10.1103/PhysRevLett.88.151301).
- [39] D. T. Son and A. O. Starinets, *Minkowski-space correlators in AdS/CFT correspondence: recipe and applications*, J. High Energ. Phys. **09**, 042 (2002), doi:[10.1088/1126-6708/2002/09/042](https://doi.org/10.1088/1126-6708/2002/09/042).
- [40] S. Grozdanov and N. Kaplis, *Constructing higher-order hydrodynamics: The third order*, Phys. Rev. D **93**, 066012 (2016), doi:[10.1103/PhysRevD.93.066012](https://doi.org/10.1103/PhysRevD.93.066012).
- [41] M. P. Heller, R. A. Janik and P. Witaszczyk, *Hydrodynamic gradient expansion in gauge theory plasmas*, Phys. Rev. Lett. **110**, 211602 (2013), doi:[10.1103/PhysRevLett.110.211602](https://doi.org/10.1103/PhysRevLett.110.211602).
- [42] I. Aniceto, J. Jankowski, B. Meiring and M. Spaliński, *The large proper-time expansion of Yang-Mills plasma as a resurgent transseries*, J. High Energ. Phys. **02**, 073 (2019), doi:[10.1007/JHEP02\(2019\)073](https://doi.org/10.1007/JHEP02(2019)073).
- [43] M. P. Heller and M. Spaliński, *Hydrodynamics beyond the gradient expansion: Resurgence and resummation*, Phys. Rev. Lett. **115**, 072501 (2015), doi:[10.1103/PhysRevLett.115.072501](https://doi.org/10.1103/PhysRevLett.115.072501).
- [44] I. Aniceto and M. Spaliński, *Resurgence in extended hydrodynamics*, Phys. Rev. D **93**, 085008 (2016), doi:[10.1103/PhysRevD.93.085008](https://doi.org/10.1103/PhysRevD.93.085008).
- [45] M. P. Heller, A. Kurkela, M. Spaliński and V. Svensson, *Hydrodynamization in kinetic theory: Transient modes and the gradient expansion*, Phys. Rev. D **97**, 091503 (2018), doi:[10.1103/PhysRevD.97.091503](https://doi.org/10.1103/PhysRevD.97.091503).
- [46] M. P. Heller and V. Svensson, *How does relativistic kinetic theory remember about initial conditions?*, Phys. Rev. D **98**, 054016 (2018), doi:[10.1103/PhysRevD.98.054016](https://doi.org/10.1103/PhysRevD.98.054016).

- [47] J. R. Peláez, *From controversy to precision on the sigma meson: a review on the status of the non-ordinary $f_0(500)$ resonance*, Phys. Rep. **658**, 1 (2016), doi:[10.1016/j.physrep.2016.09.001](https://doi.org/10.1016/j.physrep.2016.09.001).
- [48] A. Rajantie and M. Hindmarsh, *Simulating hot Abelian gauge dynamics*, Phys. Rev. D **60**, 096001 (1999), doi:[10.1103/PhysRevD.60.096001](https://doi.org/10.1103/PhysRevD.60.096001).
- [49] Holographists, *Holotube*, <https://projects.ift.uam-csic.es/holotube>

The hydrodynamic gradient expansion in linear response theory

Michał P. Heller,^{1,2,*} Alexandre Serantes,^{2,†} Michał Spaliński,^{2,3,‡}
Viktor Svensson,^{2,1,§} and Benjamin Withers^{4,¶}

¹*Max Planck Institute for Gravitational Physics (Albert Einstein Institute), 14476 Potsdam-Golm, Germany*

²*National Centre for Nuclear Research, 02-093 Warsaw, Poland*

³*Physics Department, University of Białystok, 15-245 Białystok, Poland*

⁴*Mathematical Sciences and STAG Research Centre,
University of Southampton, Highfield, Southampton SO17 1BJ, UK*

One of the foundational questions in relativistic fluid mechanics concerns the properties of the hydrodynamic gradient expansion at large orders. Studies of expanding systems arising in heavy-ion collisions and cosmology show that the expansion in real space gradients is divergent. On the other hand, expansions of dispersion relations of hydrodynamic modes in powers of momenta have a non-vanishing radius of convergence. We resolve this apparent tension finding a beautifully simple and universal result: the real space hydrodynamic gradient expansion diverges if initial data have support in momentum space exceeding a critical value, and converges otherwise. This critical value is an intrinsic property of the microscopic theory, and corresponds to a branch point of the spectrum where hydrodynamic and nonhydrodynamic modes first collide.

Introduction– The goal of relativistic hydrodynamics is to provide an effective description of long-lived, long wavelength degrees of freedom – hydrodynamic modes – which are generally expected to dominate nonequilibrium dynamics of collective states of quantum field theories at macroscopic scales and sufficiently late times [1]. Understanding what exact scales and times these are has been a very active field of research of the past decade in connection with studies of collective phases of strong interactions in relativistic heavy-ion collisions at RHIC and LHC [2, 3]. In these settings, relativistic hydrodynamics is the framework translating between the spectrum of low-energy particles observed in detectors and microscopic features such as information about initial state, equation of state and interaction strength [4, 5]. Related recent developments in relativistic hydrodynamics go well beyond the realm of nuclear physics and extend also to astrophysics [6–8], as well as to studies of strong gravity [9, 10].

Much progress on the emergence of relativistic hydrodynamics has occurred recently thanks to, on one hand, viewing hydrodynamics as an effective field theory formulated in a spacetime derivative expansion [11] and, on the other, using insights from linear response theory [12].

The effective field theory approach expresses expectation values of conserved currents in terms of derivatives of local classical fields. For the energy-momentum tensor $\langle T^{\mu\nu} \rangle$ these can be chosen as the energy density \mathcal{E} and a normalized fluid velocity U^μ . The energy momentum tensor is represented as a sum of all possible terms graded by the number of derivatives, starting with the perfect fluid contribution. The foundational importance of this expansion is that at a formal level it is unique and well defined in any system which is known to equilibrate. By comparing this formal series to the analogous gradient expansion calculated in a microscopic theory one can express the parameters appearing in the hydrodynamic

series – transport coefficients – in terms of microscopic quantities. Interestingly, the gradient series evaluated on a solution of the evolution equations can have a vanishing radius of convergence at least in the case of highly-symmetric flows describing rapidly expanding matter, as was discovered in AdS/CFT calculations [13–15], hydrodynamic models [16–18] and kinetic theory [19, 20].

In linear response theory [21], the response of the system is governed by sums of harmonic contributions with complex frequencies which encode Fourier space singularities of retarded correlators [22]. Imaginary parts of these frequencies capture effects of dissipation. Terms associated with frequencies which vanish at small momentum correspond to shear and sound mode hydrodynamic excitations, while the rest represents transient phenomena [2]. The gradient expansion of the hydrodynamic constitutive relations translates here into series in spatial momentum for shear and sound mode frequencies. In Ref. [23] and later in Refs. [24, 25] it was observed that such a series has a finite non-zero radius of convergence, which is governed by the presence of nonhydrodynamic modes. This parallels the fact that the Borel transform of the gradient expansion in an expanding plasma similarly reveals information about the nonhydrodynamic sectors. These transient excitations are present in all relativistic models which do not violate causality.

The present Letter combines these two lines of research [26] in a novel way, which allows us to make for the first time rather generic statements about the convergence of the hydrodynamic gradient expansion across microscopic theories and models. In particular, we show that the convergence of the real space gradient expansion of the constitutive relations in the linearized regime is governed by the same mechanism that yields a finite radius of convergence of series expansions of hydrodynamic mode frequencies at small momentum.

Hydrodynamics– The expectation value of the conserved energy-momentum tensor can be expressed as the perfect-fluid part plus corrections $\Pi^{\mu\nu}$

$$\langle T^{\mu\nu} \rangle = (\mathcal{E} + \mathcal{P}) U^\mu U^\nu + \mathcal{P} g^{\mu\nu} + \Pi^{\mu\nu}. \quad (1)$$

In hydrodynamics, $\Pi^{\mu\nu}$ is represented in terms of derivatives of the hydrodynamic fields which we take as the energy density \mathcal{E} and flow velocity U^μ with $U \cdot U = -1$. The pressure \mathcal{P} is related to \mathcal{E} via an equation of state [2, 3].

We consider flat d -dimensional spacetime and use the Landau frame where $U_\mu \Pi^{\mu\nu} = 0$. We focus on conformal and parity-invariant theories. Conformal symmetry forces $\Pi^\mu{}_\mu = 0$ and $\mathcal{P} = \mathcal{E}/(d-1)$. Under these conditions, the most general hydrodynamic $\Pi^{\mu\nu}$ takes the form [27, 28]

$$\begin{aligned} \Pi^{\mu\nu} = & -\eta \sigma^{\mu\nu} + \tau_\pi \eta \mathcal{D} \sigma^{\mu\nu} - \\ & - \frac{1}{2} \theta_1 \mathcal{D}_\alpha \mathcal{D}^\alpha \sigma^{\mu\nu} - \theta_2 \mathcal{D}^{(\mu} \mathcal{D}^{\nu)} \mathcal{D}_\alpha U^\alpha + \dots, \end{aligned} \quad (2)$$

where the ellipsis denotes terms higher than third order in derivatives and we display only terms which contribute at the linearized level. The angle-brackets in Eq. (2) denote the tensors made symmetric, transverse and traceless, $\mathcal{D} = U^\mu \partial_\mu$ and $\mathcal{D}^\mu = (g^{\mu\nu} + U^\mu U^\nu) \partial_\nu$ are respectively a comoving and a transverse derivative, $\sigma^{\mu\nu} = 2\mathcal{D}^{(\mu} U^{\nu)}$ denotes the shear tensor and η is the shear viscosity, τ_π the Israel-Stewart relaxation time and θ_1, θ_2 are third order transport coefficients.

We focus on small perturbations away from thermal equilibrium, i.e., we consider

$$U^\mu = (1, \mathbf{u})^\mu \quad \text{and} \quad \mathcal{E} = \mathcal{E}_0 + \epsilon \quad (3)$$

with $|\epsilon/\mathcal{E}_0|, |u_i u^i| \ll 1$. We denote spatial indices with Latin letters and spatial vectors with bold font. It is useful to work in Fourier space with a plane-wave Ansatz

$$u^i(t, \mathbf{x}) = \hat{u}^i(\mathbf{k}) e^{-i\omega t + i\mathbf{k} \cdot \mathbf{x}}, \quad \epsilon(t, \mathbf{x}) = \hat{\epsilon}(\mathbf{k}) e^{-i\omega t + i\mathbf{k} \cdot \mathbf{x}}. \quad (4)$$

The perturbations can be decomposed into shear and sound channel components [1], labelled here by \perp and \parallel subscripts. They are given by

$$\hat{\mathbf{u}}_\parallel = \frac{\mathbf{k} \cdot \hat{\mathbf{u}}}{k^2} \mathbf{k}, \quad \hat{\mathbf{u}}_\perp = \hat{\mathbf{u}} - \hat{\mathbf{u}}_\parallel. \quad (5)$$

with $\hat{\epsilon} = 0$ vanishing in the shear channel. With no loss of generality, due to rotational invariance, we take

$$\mathbf{k} = (0, \dots, 0, k). \quad (6)$$

Conservation of the energy-momentum tensor together with the hydrodynamic constitutive relation (2) determines the frequencies ω appearing in Eq. (4) as functions of k . The dispersion relations take the form [27, 28]

$$\begin{aligned} \tilde{\omega}_\perp = & -i \frac{\eta}{sT} k^2 - i \left(\frac{\eta^2 \tau_\pi}{s^2 T^2} - \frac{\theta_1}{2sT} \right) k^4 + \dots, \\ \tilde{\omega}_\parallel^\pm = & \pm c_s k - i\Gamma k^2 \mp \frac{\Gamma}{2c_s} (\Gamma - 2c_s^2 \tau_\pi) k^3 - \\ & i \left(2\Gamma^2 \tau_\pi - \frac{(d-2)(\theta_1 + \theta_2)}{2(d-1)sT} \right) k^4 + \dots, \end{aligned} \quad (7)$$

where the tilde means that these are frequencies in the hydrodynamic theory rather than in a microscopic theory. In the above equation, T and s are the temperature and entropy density associated with \mathcal{E}_0 , $c_s = 1/\sqrt{(d-1)}$ is the speed of sound, and $\Gamma = (d-2)/(d-1)\eta/(sT)$. As is clear from these expressions, hydrodynamic excitations of arbitrarily small momentum are arbitrarily long-lived.

Calculations in holography [23–25] reveal that the series (7) have a finite and non-zero radius of convergence, with evidence that goes back to the studies of causal second order hydrodynamics in Ref. [11]. In physically interesting cases, linear response theory shows that apart from the hydrodynamic modes, there are additional excitations that are short-lived, i.e. whose complex frequency $\omega(k)$ has a non-vanishing imaginary part even as $k \rightarrow 0$ [11, 12, 29, 30]. Explicit calculations in several representative cases show that the radius of convergence of hydrodynamic dispersion relations is set by the magnitude k_* of a (possibly complex) momentum for which the frequency of a hydrodynamic mode coincides with that of a nonhydrodynamic one at a branch point of $\omega(k)$ [23–25].

Constitutive relations– Our goal is to understand the properties of the gradient expansion (2) in linearized hydrodynamics in real space that would facilitate comparison with earlier studies of nonlinear evolution in expanding plasma systems. To this end, we propose a novel way of parametrizing $\Pi^{\mu\nu}$, involving only spatial derivatives. We find that the most general form of $\Pi^{\mu\nu}$ in this setting can be constructed from three elementary tensorial structures that are first, second and third order in gradients and linear in the hydrodynamic fluctuations. These are respectively

$$\sigma_{jl} = \left(\partial_j u_l + \partial_l u_j - \frac{2}{d-1} \delta_{jl} \partial_r u^r \right), \quad (8)$$

$$\pi_{jl}^\epsilon = \left(\partial_j \partial_l - \frac{1}{d-1} \delta_{jl} \partial^2 \right) \epsilon, \quad (9)$$

$$\pi_{jl}^u = \left(\partial_j \partial_l - \frac{1}{d-1} \delta_{jl} \partial^2 \right) \partial_r u^r. \quad (10)$$

With no loss of generality we write the constitutive relations in the form

$$\Pi_{jl} = -A(\partial^2) \sigma_{jl} - B(\partial^2) \pi_{jl}^u - C(\partial^2) \pi_{jl}^\epsilon, \quad (11)$$

where A, B and C are infinite series in spatial Laplacians,

$$A = \sum_{n=0}^{\infty} a_n (-\partial^2)^n, \quad (12)$$

and the a_n are transport coefficients, with similar expressions for B and C involving transport coefficients b_n and c_n . The remaining components are $\Pi_{tt} = \Pi_{ti} = 0$ by the Landau frame condition. In principle, A, B and C could also depend on ∂_t , but in the hydrodynamic gradient expansion one can use the conservation equations to

replace temporal derivatives by spatial ones in a systematic way [31].

It follows from Eq. (11) that each even order in gradients introduces one new transport coefficient, while each odd order higher than one introduces two. We find it remarkable that such a simple argument implies that the number of independent transport coefficients at a given order in the gradient expansion of linearized hydrodynamics does not grow with the order, but is limited.

An analogous situation occurs in the series expansions of ω_\perp , ω_\parallel^\pm around $k = 0$. Since ω_\parallel^+ , ω_\parallel^- obey the relation $\omega_\parallel^+(k) = -\omega_\parallel^-(k)^*$, their series coefficients are not independent. These coefficients are real for odd powers of k , and purely imaginary for even powers of k . ω_\perp is given by a series expansion in k^2 with purely imaginary coefficients. Therefore, each even order in Eq. (7) introduces two new real parameters, while each odd order introduces just one. This counting matches the number of independent transport coefficients in Eq. (11), and suggests that it is possible to express a_n , b_n and c_n , see Eq. (12), in terms of the hydrodynamic dispersion relations (7).

Matching– We now show explicitly that there is a direct relation between A , B and C defined in Eq. (11) and the hydrodynamic dispersion relations (7). Any observable can be used to perform matching, and here we choose to match to the microscopic shear and sound mode dispersion relations, in turn.

For the shear mode, with the wave vector choice we made in (6), the only non-zero components of σ_{jl} are

$$\sigma_{1,d-1} = \sigma_{d-1,1} = i k u_1 \quad (13)$$

where we have taken $\mathbf{u} = (u_1, 0, \dots, 0)$ with no loss of generality due to rotational invariance. π_{jl}^u and π_{jl}^ϵ vanish identically for this mode since $\partial_i u^i = \epsilon = 0$.

The conservation of the energy-momentum tensor (1), in combination with the hydrodynamic constitutive relation (11), predicts the following dispersion relation

$$\tilde{\omega}_\perp(k) = -i \frac{1}{sT} \sum_{n=0}^{\infty} a_n k^{2n+2}. \quad (14)$$

Demanding that $\tilde{\omega}_\perp(k)$ agrees with the microscopic shear hydrodynamic mode ω_\perp at every order in an expansion around $k^2 = 0$ fixes the a_n coefficients to be

$$a_n = [k^{2n+2}] (i s T \omega_\perp), \quad (15)$$

where the notation $[k^p](f)$ denotes the coefficient of k^p in the series expansion of f around $k = 0$.

With $A(\partial^2)$ fixed, we determine $B(\partial^2)$ and $C(\partial^2)$ by considering the sound mode. Now $\mathbf{u} = (0, \dots, 0, u_{d-1})$, $\epsilon \neq 0$ and

$$\pi_{jl}^u = -\frac{1}{2} k^2 \sigma_{jl}. \quad (16)$$

Furthermore, the only non-zero components of σ_{jl} and π_{jl}^ϵ are

$$\sigma_{jj} = -\frac{2}{d-1} i k u_{d-1}, \quad j = 1 \dots d-2, \quad (17a)$$

$$\sigma_{d-1,d-1} = \frac{2(d-2)}{d-1} i k u_{d-1} \quad (17b)$$

$$\pi_{jj}^\epsilon = \frac{1}{d-1} k^2 \epsilon, \quad j = 1 \dots d-2, \quad (17c)$$

$$\pi_{d-1,d-1}^\epsilon = -\frac{d-2}{d-1} k^2 \epsilon. \quad (17d)$$

In the end, the conservation equations reduce to

$$-i \omega \epsilon + i k s T u_{d-1} = 0, \quad (18a)$$

$$\begin{aligned} & -i \omega s T u_{d-1} + \frac{1}{d-1} i k \epsilon + \\ & + \frac{d-2}{d-1} \sum_{n=0}^{\infty} (2a_n - b_{n-1}) k^{2n+2} u_{d-1} + \\ & + \frac{d-2}{d-1} \sum_{n=0}^{\infty} i c_n k^{2n+3} \epsilon = 0, \end{aligned} \quad (18b)$$

where we have introduced $b_{-1} \equiv 0$ for brevity. Note that the conservation equation (18a) does not depend on transport coefficients as a result of our frame choice. Eqs. (18) has two solutions, $\tilde{\omega}_\parallel^+(k)$ and $\tilde{\omega}_\parallel^-(k)$, given as series expansions around $k = 0$, whose coefficients depend on a_n , b_n and c_n . Demanding that these quantities agree with the microscopic sound modes $\omega_\parallel^+(k)$ and $\omega_\parallel^-(k)$, the matching conditions for b_n and c_n are

$$b_n = [k^{2n+4}] \left(-i \frac{d-1}{d-2} s T (\omega_\parallel^+ + \omega_\parallel^-) + 2 i s T \omega_\perp \right), \quad (19a)$$

$$c_n = [k^{2n+4}] \left(-\frac{k^2}{d-2} - \frac{d-1}{d-2} \omega_\parallel^+ \omega_\parallel^- \right). \quad (19b)$$

The coefficients a_n , b_n and c_n are directly related to the transport coefficients defined in the standard way. Up to third order in gradients one has

$$\begin{aligned} a_0 &= \eta, \quad a_1 = \frac{\eta^2 \tau_\pi}{sT} - \frac{1}{2} \theta_1, \quad c_0 = \frac{2 \eta \tau_\pi}{(d-1) sT}, \\ b_0 &= \theta_2 - \frac{2(d-3) \eta^2 \tau_\pi}{(d-1) sT}. \end{aligned} \quad (20)$$

The explicit relation between hydrodynamic dispersion relations (7) and hydrodynamic constitutive relations as encapsulated by Eqs. (15) and (19) is our main result. Its importance stems from the fact that it connects well-studied hydrodynamic dispersion relations as series in small k with real space hydrodynamic constitutive relations which previously have only been tested at large orders for expanding plasma systems. In the rest of the paper, we explore the implications of this relation on the radius of convergence of the hydrodynamic gradient expansion in real space.

Large order behaviour– The analytic properties of the dispersion relations can be used to constrain the growth of transport coefficients. We expect that in a microscopic theory which respects relativistic causality, the hydrodynamic dispersion relations $\omega_{\perp}(k)$ and $\omega_{\parallel}^{\pm}(k)$ have at least one branch-point singularity in the complex k -plane. One justification for this expectation is of empirical nature, as it is realized in theories of causal hydrodynamics and holography. In the Supplemental Material we provide an additional argument in favour of it. Importantly, it implies that $\omega_{\perp}(k)$ and $\omega_{\parallel}(k)$ cannot be polynomials in k , so the hydrodynamic gradient expansion (11) following from the matching conditions (15) and (19) must contain an infinite number of terms. Moreover, the transport coefficients a_n, b_n and c_n grow geometrically in a manner controlled by the position of the branch points closest to $k = 0$ [32]

$$\lim_{n \rightarrow \infty} |a_n|^{1/n} = |k_*^{(A)}|^{-2}, \quad (21)$$

where $|k_*^{(A)}|$ denotes the modulus of the branch point location, and analogous expressions hold for b_n and c_n . Note that $|k_*^{(A)}|, |k_*^{(B)}|, |k_*^{(C)}|$ correspond to the closest branch point between ω_{\perp} and ω_{\parallel} as dictated by Eqs. (15) and (19). The power appearing on the right hand side of Eq. (21) is due to the fact that the transport coefficients are coefficients of a Taylor series in k^2 .

Convergence– The convergence properties of the series (11) depend on the behavior of the transport coefficients a_n, b_n and c_n as well as on the particular solution ϵ and \mathbf{u} . In this Section we show that the support in momentum space of the latter plays a crucial role in determining the radius of convergence of the gradient expansion. We will focus on square-integrable functions, thus excluding trivial cases for which the gradient expansion truncates at a finite order.

We start by assuming that the flow is homogeneous in the x^1, \dots, x^{d-2} directions, and define $x \equiv x^{d-1}$. Furthermore, we take the Fourier transforms of $\epsilon(t, x)$ and $u^i(t, x)$, $\hat{\epsilon}(t, k)$ and $\hat{u}^i(t, k)$, to vanish for $|k| > |k_{max}|$. In the linearized regime, the support is time-independent and thus this condition is a restriction on the support of the initial data.

According to the Paley-Wiener theorem [33], the Fourier transform of a square-integrable function $\hat{f}(k)$ supported in $|k| \leq |k_{max}|$ is an entire function of exponential type $|k_{max}|$ [34]. In particular, it follows that

$$\limsup_{n \rightarrow \infty} |f^{(n)}(x)|^{1/n} = |k_{max}|. \quad (22)$$

Let us consider now the A -contribution to (11). For a compactly-supported \hat{u}^i , $\sigma_{jl}(t, x)$ will be of exponential type $|k_{max}|$ for all times. Hence,

$$\limsup_{n \rightarrow \infty} |\partial_x^{2n} \sigma_{jl}(t, x)|^{1/n} = |k_{max}|^2. \quad (23)$$

Applying the root test results in the following convergence criterium for the A -contribution to (11)

$$\limsup_{n \rightarrow \infty} |a_n \partial_x^{2n} \sigma_{jl}(t, x)|^{1/n} = \frac{|k_{max}|^2}{|k_*^{(A)}|^2} < 1. \quad (24)$$

Analogous arguments apply to the remaining pieces of (11), with the conclusion that the gradient expansion of the constitutive relations will be a convergent series if and only if the support of the hydrodynamic perturbations and their time-derivatives at $t = 0$ does not exceed the smallest of $|k_*^{(A)}|, |k_*^{(B)}|$ and $|k_*^{(C)}|$.

The condition for the convergence of the gradient expansion spelled out above applies to arbitrary longitudinal fluid flows. Note that previous real space statements about the convergence or divergence of the hydrodynamic expansion were based on case studies of comoving flows in simple expanding spacetimes. Our analysis here covers a large class of models and does not make any simplifying symmetry assumptions about the longitudinal spacetime dependence.

Even if divergent, the partial sums of the gradient expansion only grow geometrically as long as the support of the initial data in k -space does not extend to infinity. If it does, this geometric divergence is enhanced to the factorial one known from the studies of expanding geometries [13, 16–20, 35]. The ambiguity of the sum is then related to the multi-sheeted structure of the dispersion relations $\omega(k)$ for $|k| > |k_*|$ [23–25] and requires contributions from nonhydrodynamic modes to be resolved.

For a flow without any symmetry restrictions, we can argue heuristically that the same convergence conditions hold. Let us focus again on the A -contribution to (11). Truncating the series to N -th order results in

$$- \int_{\mathbb{R}^{d-1}} d^{d-1} \mathbf{k} \left[\sum_{n=0}^N a_n (\mathbf{k}^2)^n \right] \hat{\sigma}_{ij}(t, \mathbf{k}) e^{i \mathbf{k} \cdot \mathbf{x}}, \quad (25)$$

where we have interchanged the order of summation and integration. According to Eq. (21), the partial sums appearing in Eq. (25) are convergent as $N \rightarrow \infty$, provided that they are evaluated at $|\mathbf{k}| < |k_*^{(A)}|$. Outside this $(d-1)$ -dimensional sphere we get a non-convergent series. Hence, it seems natural to assume that the condition for Eq. (25) to converge as $N \rightarrow \infty$ is that the hydrodynamic variable $\hat{\mathbf{u}}$ does not have support past $|k_*^{(A)}|$. Analogous arguments would hold also for the B - and C -pieces, supporting the fact that the convergence criterion spelled out before is fully general.

An illustrative example– For illustration, we now consider a shear channel perturbation in the Müller-Israel-Stewart (MIS) theory of hydrodynamics [36–38],

$$\epsilon = 0, \quad \mathbf{u} = (u_1(t, x), 0, \dots, 0). \quad (26)$$

The only tensor structure contributing to Eq. (11) is the shear tensor and the only nontrivial independent component of the constitutive relations is

$$\Pi_{1,d-1}(t, x) = - \sum_{n=0}^{\infty} a_n (-1)^n \partial_x^{2n+1} u_1(t, x). \quad (27)$$

The a_n transport coefficients can be computed in closed form, since the shear hydrodynamic mode is known exactly [11],

$$\omega_{\perp}(k) = i \frac{-1 + \sqrt{1 - 4D\tau_{\pi}k^2}}{2\tau_{\pi}}, \quad (28)$$

where $D \equiv \eta/(sT) = (d-1)/(d-2)\Gamma$ is the diffusion constant. MIS contains also a single nonhydrodynamic shear mode which differs from Eq. (28) by the sign of the square root. The final result for the a_n coefficients is

$$a_n = sT C_n D^{n+1} \tau_{\pi}^n, \quad (29)$$

where C_n are the Catalan numbers. Therefore,

$$|k_*^{(A)}| = \left(\limsup_{n \rightarrow \infty} |a_n|^{1/n} \right)^{-1/2} = 1/\sqrt{4D\tau_{\pi}}, \quad (30)$$

which is also the location of the branch points of Eq. (28), where the hydrodynamic and the nonhydrodynamic mode collide.

The initial state of the system is fully specified by $u_1(0, x)$ and $\partial_t u_1(0, x)$. We take $u_1(0, x) = 0$ and

$$\partial_t \hat{u}_1(0, k) = \frac{1}{2\pi} e^{-\frac{1}{2}\gamma^2 k^2} \Theta(k_{max}^2 - k^2), \quad (31)$$

where Θ is the Heaviside step function. As seen in Fig. 1, the real space gradient expansion is convergent for $k_{max}^2 < 1/(4D\tau_{\pi})$, geometrically divergent for $1/(4D\tau_{\pi}) \leq k_{max}^2 < \infty$, and factorially divergent for $k_{max} \rightarrow \infty$. This is exactly what is expected on the basis of our general analysis.

Discussion and outlook– We have shown that the radius of convergence of the real space hydrodynamic gradient expansion evaluated on a solution of the evolution equations is determined by the momentum space support of the initial data. This represents a major step forward beyond earlier studies of expanding systems. Any statement about the convergence of the derivative series should thus be viewed as pertaining to the asymptotics of specific solutions and does not impact the definition of hydrodynamics which rests on its ability to match these asymptotics to those of underlying microscopic theories.

The applicability of hydrodynamics is connected with the radius of convergence of the gradient expansion only in the sense that both issues reflect the presence of a regulator sector consisting of transient, nonhydrodynamic modes required by causality. The regime of applicability of hydrodynamics is determined by the scale where

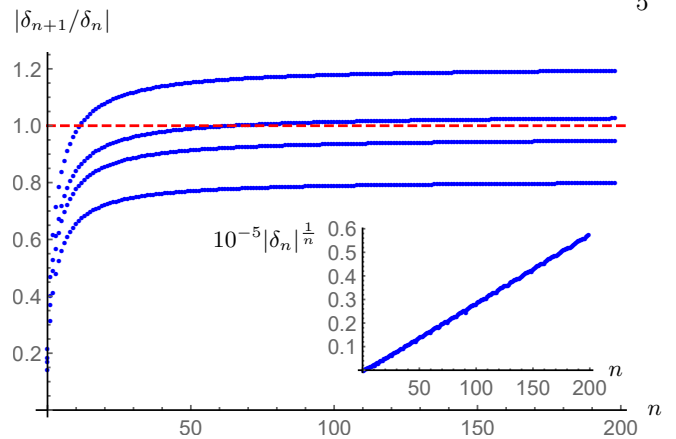


FIG. 1. Main plot: Ratio test applied to the gradient expansion (27), where δ_n denotes the n -th contribution. We use $\gamma = 0.1$ and consider $t = 1$, $x = 0.5$ with $s = T = \eta = \tau_{\pi} = 1$, in such a way that $|k_*^{(A)}| = 0.5$. From top to bottom, $k_{max} = 0.55, 0.51, 0.49, 0.45$. The gradient expansion is convergent for $k_{max} < |k_*^{(A)}|$ and geometrically divergent otherwise, as expected. Inset: root test applied to δ_n when $k_{max} \rightarrow \infty$. The geometric divergence of the gradient expansion is enhanced to a factorial one, manifest here in the asymptotic linear growth of $|\delta_n|^{1/n}$ with n .

specific calculations begin to be sensitive to the nonhydrodynamic mode spectrum [39].

It is very important that complete information about the nonhydrodynamic sector is encoded in the gradient series itself. In the case of an expanding plasma this is very beautifully expressed by the phenomenon of resurgence [40], which makes it possible to extract the form of the full solution from the asymptotic series [16, 18, 41]. The integration constants necessary to describe any complete solution enter that procedure as transseries parameters. An analogous encoding of nonhydrodynamic data in the hydrodynamic sector is seen in the analytic continuation of dispersion relations [23]. Generalizations of these ideas based on developments reported in this Letter are the subject of ongoing research [42].

Acknowledgements– We would like to thank G. Dunne, as well as participants of the workshop *Foundational Aspects of Relativistic Hydrodynamics* at Banff International Research Station where this work was presented for the first time for helpful discussions. The Gravity, Quantum Fields and Information group at AEI is supported by the Alexander von Humboldt Foundation and the Federal Ministry for Education and Research through the Sofja Kovalevskaja Award. AS and MS are supported by the Polish National Science Centre grant 2018/29/B/ST2/02457. BW is supported by a Royal Society University Research Fellowship.

-
- * michal.p.heller@aei.mpg.de
† alexandre.serantesrubianes@ncbj.gov.pl
‡ michal.spalinski@ncbj.gov.pl
§ viktor.svensson@aei.mpg.de
¶ b.s.withers@soton.ac.uk
- [1] P. Kovtun, *Lectures on hydrodynamic fluctuations in relativistic theories*, J. Phys. A **45** (2012) 473001 [arXiv:1205.5040].
- [2] W. Florkowski, M. P. Heller and M. Spaliński, *New theories of relativistic hydrodynamics in the LHC era*, Rept. Prog. Phys. **81** (2018), no. 4 046001 [arXiv:1707.02282].
- [3] P. Romatschke and U. Romatschke, *Relativistic Fluid Dynamics In and Out of Equilibrium*. Cambridge Monographs on Mathematical Physics. Cambridge University Press, 5, 2019.
- [4] U. Heinz and R. Snellings, *Collective flow and viscosity in relativistic heavy-ion collisions*, Ann. Rev. Nucl. Part. Sci. **63** (2013) 123–151 [arXiv:1301.2826].
- [5] W. Busza, K. Rajagopal and W. van der Schee, *Heavy Ion Collisions: The Big Picture, and the Big Questions*, Ann. Rev. Nucl. Part. Sci. **68** (2018) 339–376 [arXiv:1802.04801].
- [6] M. Shibata, K. Kiuchi and Y.-i. Sekiguchi, *General relativistic viscous hydrodynamics of differentially rotating neutron stars*, Phys. Rev. D **95** (2017), no. 8 083005 [arXiv:1703.10303].
- [7] M. G. Alford, L. Bovard, M. Hanauske, L. Rezzolla and K. Schwenzer, *Viscous Dissipation and Heat Conduction in Binary Neutron-Star Mergers*, Phys. Rev. Lett. **120** (2018), no. 4 041101 [arXiv:1707.09475].
- [8] F. S. Bemfica, M. M. Disconzi and J. Noronha, *Causality of the Einstein-Israel-Stewart Theory with Bulk Viscosity*, Phys. Rev. Lett. **122** (2019), no. 22 221602 [arXiv:1901.06701].
- [9] M. M. Caldarelli, O. J. Dias, R. Emparan and D. Klemm, *Black Holes as Lumps of Fluid*, JHEP **04** (2009) 024 [arXiv:0811.2381].
- [10] S. R. Green, F. Carrasco and L. Lehner, *Holographic Path to the Turbulent Side of Gravity*, Phys. Rev. X **4** (2014), no. 1 011001 [arXiv:1309.7940].
- [11] R. Baier, P. Romatschke, D. T. Son, A. O. Starinets and M. A. Stephanov, *Relativistic viscous hydrodynamics, conformal invariance, and holography*, JHEP **04** (2008) 100 [arXiv:0712.2451].
- [12] P. K. Kovtun and A. O. Starinets, *Quasinormal modes and holography*, Phys.Rev. **D72** (2005) 086009 [arXiv:hep-th/0506184].
- [13] M. P. Heller, R. A. Janik and P. Witaszczyk, *Hydrodynamic Gradient Expansion in Gauge Theory Plasmas*, Phys.Rev.Lett. **110** (2013), no. 21 211602 [arXiv:1302.0697].
- [14] A. Buchel, M. P. Heller and J. Noronha, *Beyond adiabatic approximation in Big Bang Cosmology: hydrodynamics, resurgence and entropy production in the Universe*, arXiv:1603.05344.
- [15] M. Baggioli and A. Buchel, *Holographic Viscoelastic Hydrodynamics*, JHEP **03** (2019) 146 [arXiv:1805.06756].
- [16] M. P. Heller and M. Spaliński, *Hydrodynamics Beyond the Gradient Expansion: Resurgence and Resummation*, Phys. Rev. Lett. **115** (2015), no. 7 072501 [arXiv:1503.07514].
- [17] G. V. Dunne and M. Ünsal, *What is QFT? Resurgent trans-series, Lefschetz thimbles, and new exact saddles*, PoS **LATTICE2015** (2016) 010 [arXiv:1511.05977].
- [18] I. Aniceto and M. Spaliński, *Resurgence in Extended Hydrodynamics*, Phys. Rev. **D93** (2016), no. 8 085008 [arXiv:1511.06358].
- [19] M. P. Heller, A. Kurkela, M. Spaliński and V. Svensson, *Hydrodynamization in kinetic theory: Transient modes and the gradient expansion*, Phys. Rev. **D97** (2018), no. 9 091503 [arXiv:1609.04803].
- [20] M. P. Heller and V. Svensson, *How does relativistic kinetic theory remember about initial conditions?*, Phys. Rev. **D98** (2018), no. 5 054016 [arXiv:1802.08225].
- [21] L. P. Kadanoff and P. C. Martin, *Hydrodynamic equations and correlation functions*, Annals of Physics **24** (Oct., 1963) 419–469.
- [22] See also the supplemental material.
- [23] B. Withers, *Short-lived modes from hydrodynamic dispersion relations*, JHEP **06** (2018) 059 [arXiv:1803.08058].
- [24] S. Grozdanov, P. K. Kovtun, A. O. Starinets and P. Tadić, *Convergence of the Gradient Expansion in Hydrodynamics*, Phys. Rev. Lett. **122** (2019), no. 25 251601 [arXiv:1904.01018].
- [25] S. Grozdanov, P. K. Kovtun, A. O. Starinets and P. Tadić, *The complex life of hydrodynamic modes*, JHEP **11** (2019) 097 [arXiv:1904.12862].
- [26] See Refs. [43–47] for an earlier work where different aspects of linearized hydrodynamics are considered in the context of AdS/CFT.
- [27] S. Grozdanov and N. Kaplis, *Constructing higher-order hydrodynamics: The third order*, Phys. Rev. D **93** (2016), no. 6 066012 [arXiv:1507.02461].
- [28] S. M. Diles, L. A. Mamani, A. S. Miranda and V. T. Zanchin, *Third-order relativistic hydrodynamics: dispersion relations and transport coefficients of a dual plasma*, JHEP **05** (2020) 019 [arXiv:1909.05199].
- [29] P. Romatschke, *Retarded correlators in kinetic theory: branch cuts, poles and hydrodynamic onset transitions*, Eur. Phys. J. **C76** (2016), no. 6 352 [arXiv:1512.02641].
- [30] S. Grozdanov, N. Kaplis and A. O. Starinets, *From strong to weak coupling in holographic models of thermalization*, JHEP **07** (2016) 151 [arXiv:1605.02173].
- [31] See appendix A of [27].
- [32] H. S. Wilf, *generatingfunctionology. ak peters*, 2005.
- [33] R. S. Strichartz, *A guide to distribution theory and Fourier transforms*. World Scientific Publishing Company, 2003.
- [34] See the Supplementary Material for the relevant mathematical background.
- [35] M. P. Heller, *Holography, Hydrodynamization and Heavy-Ion Collisions*, Acta Phys. Polon. **B47** (2016) 2581 [arXiv:1610.02023].
- [36] I. Müller, *Zum Paradoxon der Wärmeleitungstheorie*, Z.Phys. **198** (1967) 329–344.
- [37] W. Israel, *Nonstationary irreversible thermodynamics: a causal relativistic theory*, Annals of Physics **100** (1976), no. 1-2 310–331.
- [38] W. Israel and J. Stewart, *Transient relativistic thermodynamics and kinetic theory*, Annals Phys. **118** (1979) 341–372.

- [39] M. Spaliński, *Small systems and regulator dependence in relativistic hydrodynamics*, Phys. Rev. **D94** (2016), no. 8 085002 [arXiv:1607.06381].
- [40] I. Aniceto, G. Basar and R. Schiappa, *A Primer on Resurgent Transseries and Their Asymptotics*, Phys. Rept. **809** (2019) 1–135 [arXiv:1802.10441].
- [41] I. Aniceto, B. Meiring, J. Jankowski and M. Spaliński, *The large proper-time expansion of Yang-Mills plasma as a resurgent transseries*, JHEP **02** (2019) 073 [arXiv:1810.07130].
- [42] M. P. Heller, A. Serantes, M. Spalinski, V. Svensson and B. Withers, *To appear*, .
- [43] M. Lublinsky and E. Shuryak, *Improved Hydrodynamics from the AdS/CFT*, Phys. Rev. D **80** (2009) 065026 [arXiv:0905.4069].
- [44] Y. Bu and M. Lublinsky, *All order linearized hydrodynamics from fluid-gravity correspondence*, Phys.Rev. **D90** (2014), no. 8 086003 [arXiv:1406.7222].
- [45] Y. Bu and M. Lublinsky, *Linearized fluid/gravity correspondence: from shear viscosity to all order hydrodynamics*, JHEP **11** (2014) 064 [arXiv:1409.3095].
- [46] Y. Bu and M. Lublinsky, *Linearly resummed hydrodynamics in a weakly curved spacetime*, JHEP **04** (2015) 136 [arXiv:1502.08044].
- [47] Y. Bu, M. Lublinsky and A. Sharon, *Hydrodynamics dual to Einstein-Gauss-Bonnet gravity: all-order gradient resummation*, JHEP **06** (2015) 162 [arXiv:1504.01370].
- [48] See [12] for a detailed discussion of how rotational invariance constrains the form of the retarded correlator.
- [49] E. Krotscheck and W. Kundt, *Causality criteria*, Communications in Mathematical Physics **60** (1978), no. 2 171–180.

Supplementary material

Our main objective in this appendix is to provide additional arguments in favor of the two hypothesis regarding the behavior of the hydrodynamic dispersion relations put forward in the main text:

1. $\omega(k)$ has at least one singularity in the complex k -plane.
2. This singularity is a branch point.

We start by recalling that, under a metric fluctuation $\eta^{\mu\nu} \rightarrow \eta^{\mu\nu} + h^{\mu\nu}$, the response of the energy-momentum tensor expectation value in the thermal state is controlled by the retarded two-point function

$$G^{\mu\nu,\alpha\beta}(t, \mathbf{x}) = -i\Theta(t)\langle [T^{\mu,\nu}(t, \mathbf{x}), T^{\alpha\beta}(0, 0)] \rangle \quad (\text{A.32})$$

as

$$\begin{aligned} \delta\langle T^{\mu\nu}(t, \mathbf{x}) \rangle &= \\ &= -\frac{1}{2} \int_{\mathbb{R}^{1,d-1}} dt' d^d \mathbf{x}' G^{\mu\nu,\alpha\beta}(t-t', \mathbf{x}-\mathbf{x}') h_{\alpha\beta}(t', \mathbf{x}'). \end{aligned}$$

The expectation values are taken in the background thermal state. Defining

$$G^{\mu\nu,\alpha\beta}(t, \mathbf{x}) = \int_{\mathbb{R}^{1,d-1}} d\omega d^{d-1} \mathbf{k} e^{-i\omega t + i\mathbf{k}\cdot\mathbf{x}} \hat{G}^{\mu\nu,\alpha\beta}(\omega, \mathbf{k}), \quad (\text{A.33})$$

and similarly for $h^{\mu\nu}$, Eq. (A.33) can be written as

$$\begin{aligned} 2(2\pi)^{-d} \delta\langle T^{\mu\nu}(t, \mathbf{x}) \rangle &= \\ &= - \int_{\mathbb{R}^{1,d-1}} d\omega d^{d-1} \mathbf{k} e^{-i\omega t + i\mathbf{k}\cdot\mathbf{x}} \hat{G}^{\mu\nu,\alpha\beta}(\omega, \mathbf{k}) \hat{h}_{\alpha\beta}(\omega, \mathbf{k}). \end{aligned}$$

Hydrodynamic and nonhydrodynamic frequencies appear as poles of $\hat{G}^{\mu\nu,\alpha\beta}(\omega, \mathbf{k})$ which, due to rotational invariance, only depend on \mathbf{k}^2 [48]. To discuss the interplay between relativistic causality and the analyticity properties of these frequencies, we consider the following setup: we imagine that our metric fluctuation is only active at $t = 0$ and, furthermore, we also assume that it only depends on $x^{d-1} \equiv x$,

$$h^{\mu\nu}(t, \mathbf{x}) = \delta(t) f^{\mu\nu}(x). \quad (\text{A.34})$$

In momentum space,

$$\hat{h}^{\mu\nu}(\omega, \mathbf{k}) = \frac{1}{2\pi} \delta(k_1) \dots \delta(k_{d-2}) \hat{f}^{\mu\nu}(k), \quad (\text{A.35})$$

where we have also defined $k \equiv k_{d-1}$. Hence,

$$\begin{aligned} 2(2\pi)^{1-d} \delta\langle T^{\mu\nu}(t, x) \rangle &= \\ &= - \int_{\mathbb{R}^{1,1}} d\omega dk e^{-i\omega t + ikx} \hat{G}^{\mu\nu,\alpha\beta}(\omega, 0, \dots, 0, k) \hat{f}_{\alpha\beta}(k). \end{aligned}$$

Performing the integral with respect to ω , we obtain

$$\begin{aligned} \delta\langle \hat{T}^{\mu\nu}(t, k) \rangle &= \sum_{q=0}^{N_H} \xi_q^{\mu\nu}(k) e^{-i\omega_q(k)t} + \\ &+ \sum_{q=0}^{N_{NH}} \Xi_q^{\mu\nu}(k) e^{-i\Omega_q(k)t} + \text{b.c.} \end{aligned} \quad (\text{A.36})$$

In writing the spectral decomposition (A.36), we have deformed our original integration contour along the real ω -axis to isolate the contributions coming from the singularities of $\hat{G}^{\mu\nu,\alpha\beta}(\omega, k)$ in the lower half of the complex ω -plane. N_H, N_{NH} refer respectively to the number of hydrodynamic ω_q and nonhydrodynamic Ω_q modes excited by the metric fluctuation, while the excitation coefficients $\xi_q^{\mu\nu}$ and $\Xi_q^{\mu\nu}$ are determined by the residues of the retarded correlator at its poles and the initial data. Finally, b.c. denotes the continuous contributions coming from the branch cuts that might be present. These contributions are absent in theories of causal relativistic hydrodynamics and AdS/CFT in the semiclassical limit, but do appear in kinetic theory.

As a final comment about Eq. (A.36), note that we have also assumed that any remaining contribution coming from an integral around infinity can be neglected. This is justified in the case in which our microscopic theory is a CFT and $t > 0$: for $|\omega| \rightarrow \infty$ the retarded correlator should reduce to the vacuum result, which does not grow exponentially fast in the same limit.

Imagine now that $f^{\mu\nu}(x)$ is a square-integrable function supported only for $|x| \leq R$. Relativistic causality demands that, at $t > 0$, the support of $\delta\langle T^{\mu\nu}(t, x) \rangle$ is at most $R + t$. Let us assume that $\delta\langle T^{\mu\nu}(t, x) \rangle$ is also square-integrable at all times. Then, the Paley-Wiener theorem [33] tells us that the spatial Fourier transform of $\delta\langle T^{\mu\nu}(t, x) \rangle$, $\delta\langle T^{\mu\nu}(t, k) \rangle$, is an entire function of exponential type at most $R + t$, also square-integrable along the real k -axis. We remind the reader that an entire function $f(z)$ is a function analytic everywhere in the complex z -plane, and that an entire function of exponential type σ is an entire function obeying the bound

$$|f(z)| \leq C e^{\sigma|z|}, \quad \forall z \in \mathbb{C}, \quad C \in \mathbb{R}^+. \quad (\text{A.37})$$

In the light of the Paley-Wiener theorem, and when the spectral decomposition (A.36) holds, property 1 follows by contradiction: if the frequency $\omega(k)$ were entire, its Laurent series expansion

$$\omega(k) = \sum_{n=1}^{\infty} w_n k^n \quad (\text{A.38})$$

would be convergent $\forall k \in \mathbb{C}$, and the bound (A.37), as applied to $\delta\langle T^{\mu\nu}(t, k) \rangle$, would be violated. This result is in line with the conclusions of Ref. [49]. Since ω_{\perp} is given by a Taylor series in k^2 , while ω_{\parallel}^{\pm} are series in k , the only

possible exception to this behavior would be the case in which $\omega_{\perp} = 0$, $|\omega_{\parallel}^{\pm}| \propto |k|$, which corresponds precisely to ideal hydrodynamics.

On the other hand, property 2 can be justified as follows: if $\omega(k)$ had a pole, $\delta\langle T^{\mu\nu}(t, k) \rangle$ would develop an essential singularity at the pole location, thus failing to be entire. Furthermore, as argued in Ref. [49], for systems with a finite number of modes a pole in some dispersion relation entails that the initial value problem does

not have a unique solution.

A final consequence of property 2 is that nonhydrodynamic modes must exist in a theory that respects relativistic causality. These modes, which in principle could be absent if the singularities in the hydrodynamic dispersion relations were poles, appear naturally when analytically continuing these functions past the branch cuts that are actually present.

dr hab. Michal P. Heller
Max Planck Institute for Gravitational Physics
and
National Centre for Nuclear Research
email: michal.p.heller@aei.mpg.de
web: aei.mpg.de/GQFI

Statement of contributions

In regards to the publication

Heller, M. P., Kurkela, A., Spaliński, M., & Svensson, V. (2018). Hydrodynamization in kinetic theory: Transient modes and the gradient expansion. Physical Review D, 97(9), 091503. doi: 10.1103/PhysRevD.97.091503

my contributions were:

Participation in discussions, writing the first version of our code deriving large order gradient expansion, contribution to data analysis, contribution to understanding off-real axis singularities in the Borel plane, writing parts of the paper.

-

In regards to the publication

Heller, M. P., & Svensson, V. (2018). How does relativistic kinetic theory remember about initial conditions? Phys.Rev.D, 98(5). doi: 10.1103/PhysRevD.98.054016

my contributions were:

Suggesting the problem to Viktor, participation in discussions, coding the first version of a very accurate time evolution algorithm, proposing to search for a control parameter (which led to the Δ parameter), writing parts of the paper.

-

In regards to the publication

Heller, M. P., Jefferson, R., Spaliński, M., & Svensson, V. (2020). Hydrodynamic Attractors in Phase Space. Physical Review Letters, 125(13), 132301. doi: 10.1103/PhysRevLett.125.132301

my contributions were:

Suggesting to "machine learn" attractors, participation in discussions, partial data analysis using PCA, proposing RTA kinetic theory as an interesting application of our framework, writing parts of the paper.

-

In regards to the publication

Heller, M. P., Serantes, A., Spaliński, M., Svensson, V., & Withers, B. (2020). The hydrodynamic gradient expansion in linear response theory. ArXiv e-prints, 2007.05524

my contributions were:

Identifying the problem, participation in discussions, explorations of possibilities for hydrodynamic constitutive relations in linearized hydrodynamics, writing parts of the paper.

-

In regards to the publication

Heller, M. P., Serantes, A., Spaliński, M., Svensson, V., & Withers, B. (2021). Transseries for causal diffusive systems. Journal of High Energy Physics, 2021(4), 192–38. doi: 10.1007/JHEP04(2021)192

my contributions were:

Participation in discussions, writing parts of the paper.

-

In regards to the publication

Heller, M. P., Serantes, A., Spaliński, M., Svensson, V., & Withers, B. (2020). Convergence of hydrodynamic modes: insights from kinetic theory and holography. ArXiv e-prints, 2012.15393. Accepted for publication in SciPost Physics.

my contributions were:

Suggesting kinetic theory as an interesting model to explore radius of convergence of hydrodynamic dispersion relations, participation in discussions, writing parts of the paper.

Sincerely,



Michal P. Heller,
Potsdam (Germany), June 4, 2021

Michał Spaliński
Narodowe Centrum Badań Jądrowych & Uniwersytet w Białymstoku

Statement of contributions

In regards to the publication

Heller, M. P., Kurkela, A., Spaliński, M., & Svensson, V. (2018). Hydrodynamization in kinetic theory: Transient modes and the gradient expansion. Physical Review D, 97(9), 091503. doi: 10.1103/PhysRevD.97.091503

my contributions were:

Parts of: calculations of the gradient expansion, Pade-Borel analysis, writing the paper.

In regards to the publication

Heller, M. P., Jefferson, R., Spaliński, M., & Svensson, V. (2020). Hydrodynamic Attractors in Phase Space. Physical Review Letters, 125(13), 132301. doi: 10.1103/PhysRevLett.125.132301

my contributions were:

Parts of: numerical solutions in BRS3 and HJSW, PCA analysis, writing the paper.

In regards to the publication

Heller, M. P., Serantes, A., Spaliński, M., Svensson, V., & Withers, B. (2020). The hydrodynamic gradient expansion in linear response theory. ArXiv e-prints, 2007.05524

my contributions were:

Parts of: matching calculation, writing the paper.

In regards to the publication

Heller, M. P., Serantes, A., Spaliński, M., Svensson, V., & Withers, B. (2021). Transseries for causal diffusive systems. Journal of High Energy Physics, 2021(4), 192–38. doi: 10.1007/JHEP04(2021)192

my contributions were:

Parts of: perturbation expansions for the telegraphers' equation, writing the paper.

In regards to the publication

Heller, M. P., Serantes, A., Spaliński, M., Svensson, V., & Withers, B. (2020). Convergence of hydrodynamic modes: insights from kinetic theory and holography. ArXiv e-prints, 2012.15393. Accepted for publication in SciPost Physics.

my contributions were:

Parts of: analysis of singularities of the retarded Green's function, writing the paper.

Sincerely,

A handwritten signature in black ink, appearing to read "M. Spaliński". The signature is written in a cursive style with a large, sweeping initial "M".

Michal Spaliński,
Warszawa, June 9, 2021

Benjamin Withers
University of Southampton,
Southampton, SO17 1BJ,
United Kingdom

Statement of contributions

In regards to the publication

Heller, M. P., Serantes, A., Spaliski, M., Svensson, V., & Withers, B. (2020). The hydrodynamic gradient expansion in linear response theory. ArXiv e-prints, 2007.05524

my contributions were:

Partial contribution to: the development of the spatial gradient expansion, its connection to branch points of dispersion relations, the role of the compact support and the Paley-Wiener theorem, writing the article.

—

In regards to the publication

Heller, M. P., Serantes, A., Spaliski, M., Svensson, V., & Withers, B. (2021). Transseries for causal diffusive systems. Journal of High Energy Physics, 2021(4), 19238. doi: 10.1007/JHEP04(2021)192

my contributions were:

Partial contribution to: using the formal parameter epsilon as a tool to organise the series for diffusion, explicit computation of large order expansions for Gaussian and Lorentzian initial data, numerics in section 4 for figure 9, writing the article.

—

In regards to the publication

Heller, M. P., Serantes, A., Spaliski, M., Svensson, V., & Withers, B. (2020). Convergence of hydrodynamic modes: insights from kinetic theory and holography. ArXiv e-prints, 2012.15393. Accepted for publication in SciPost Physics.

my contributions were:

Partial contribution to: numerically analysing the radius of convergence in Kinetic theory, the relation between radius of convergence and complex curves

through analytic examples, writing the article.

Sincerely,

A handwritten signature in black ink, appearing to be 'B. Withers', written in a cursive style.

Benjamin Withers,
United Kingdom, May 27, 2021

Alexandre Serantes,
National Center for Nuclear Research,
02-093 Warsaw, Poland

Statement of contributions

In regards to the publication

Heller, M. P., Serantes, A., Spaliski, M., Svensson, V., & Withers, B. (2020). The hydrodynamic gradient expansion in linear response theory. ArXiv e-prints, 2007.05524

I contributed to:

the development of the purely spatial formulation of the gradient expansion, the matching computation, the argument relating the singularity structure of the hydrodynamic dispersion relations to relativistic causality, the analysis of the large-order behavior of the transport coefficients, the analysis of the large-order behavior of the derivative operators acting on the initial data, the final convergence criterion, writing the paper.

In regards to the publication

Heller, M. P., Serantes, A., Spaliski, M., Svensson, V., & Withers, B. (2021). Transseries for causal diffusive systems. Journal of High Energy Physics, 2021(4), 19238. doi: 10.1007/JHEP04(2021)192

I contributed to:

the closed-form computation of the perturbative part of the transseries presented in Section 2.1, the convergence criterion and the analysis of the large-order behavior of the perturbative part of the transseries presented in Section 2.2, the saddle point analysis exposing the relation between the large-order behavior of the perturbative part of the transseries for Gaussian initial and the adjacent saddle points presented in Section 3 and Appendix E, the numerical computations presented in Section 4, the closed-form computation of the non-perturbative transseries sector appearing in Section 5, the novel results presented in appendices B, C, D, F, G, writing the article.

In regards to the publication

Heller, M. P., Serantes, A., Spaliski, M., Svensson, V., & Withers, B. (2020). Convergence of hydrodynamic modes: insights from kinetic theory and holography. ArXiv e-prints, 2012.15393. Accepted for publication in SciPost Physics.

I contributed to:

the elucidation of the mechanism setting the convergence radius of the shear channel hydrodynamic mode and the numerical computations supporting this result (Section 2), the elucidation of the mechanism setting the convergence ra-

dius of the sound channel hydrodynamic mode and the numerical computations supporting this result (Section 3), the computation of the transseries presented in Appendix A, writing the article.

Sincerely,

Alexandre Serantes,
Warsaw, May 31, 2021

Ro Jefferson
Nordita
Hannes Alfvéns väg 12
106 91 Stockholm, Sweden

Statement of contributions

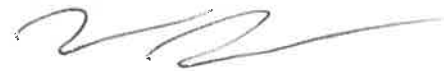
In regards to the publication

Heller, M. P., Jefferson, R., Spaliński, M., & Svensson, V. (2020). Hydrodynamic Attractors in Phase Space. Physical Review Letters, 125(13), 132301. doi: 10.1103/PhysRevLett.125.132301

my contributions were:

Developing code in Python to perform PCA analysis, and to explore the feasibility of variational auto-encoders for manifold learning. Participated in analyzing results and group discussions. Minor role in writing/editing the article.

Sincerely,



Ro Jefferson,
Stockholm, May 15, 2021

Statement of contributions

In regards to the publication

Heller, M. P., Kurkela, A., Spaliński, M., & Svensson, V. (2018). Hydrodynamization in kinetic theory: Transient modes and the gradient expansion. Physical Review D, 97(9), 091503. doi: 10.1103/PhysRevD.97.091503

my contributions were:

To participate in the calculation of the perturbative expansion and participate in writing the article.

Sincerely,

A handwritten signature in black ink, appearing to read 'Aleks Kurkela', with a long horizontal flourish extending to the right.

Name,

Location, June 3, 2021

Aleksi Kurkela

Stavanger, June 6th, 2021